



**A Transferable Infochemical for Multiple Crustaceans and
Mechanistic Assessment of its pH Dependency**

This thesis is submitted for the degree of Doctor of Philosophy,
School of Natural Sciences
University of Hull, United Kingdom

by

Paula Schirmmacher

B.Sc. (Hons), University of Göttingen, Germany

M.Sc., Goethe University Frankfurt, Germany

Supervised by:

Jörg D. Hardege

Christina C. Roggatz

May 2023

The important thing is not to shout at this point, Vimes told himself. Do not ... what do they call it ... go postal? Treat this as a learning exercise.

Find out why the world is not as you thought it was. Assemble the facts, digest the information, consider the implications. THEN go postal. But with precision.

- Terry Pratchett, Thud! -

Parts of this PhD Thesis have already been published:

P. Schirmacher, C.C. Roggatz, D.M. Benoit and J.D. Hardege.
Ocean acidification amplifies the olfactory response to 2-phenylethylamine:
Altered cue reception as a mechanistic pathway?
J Chem Ecol, 47(10), 859-876. 2021.

C.C. Roggatz, M. Saha, S. Blanchard, P. Schirmacher, P. Fink, F. Verheggen
and J.D. Hardege. Becoming nose-blind – Climate change impacts on
chemical communication. *Glob Chang Biol*, 2022.

Acknowledgments

First, I would like to thank my supervisors Dr. Jörg D. Hardege and Dr. Christina C. Roggatz. I also acknowledge the support of Dr. David Benoit who co-supervised the first half of my PhD. Furthermore, I thank the Viper High Performance Computing facility of the University of Hull and its support team. This thesis was funded by a PhD Scholarship from the University of Hull as part of the PhD project cluster MolStressH2O.

Special thanks goes to Amber Jones, fellow PhD student in the ChemEcolHull research group, for motivating and inspiring me and her help with data collection and sex determination for chapter 2 and 3 of this thesis. I would also like to thank Adam Bates, fellow PhD student, for being my office buddy and finding creative solutions to all sorts of little problems. Finally, I am infinitely grateful for the support I received from my family and specifically my husband Dai Tombs. This PhD thesis would not have been possible without you.

Note to Reader

To improve readability, this thesis has been hyperlinked: Every figure, table, equation and chapter reference is a link that leads to the respective item. Additionally, the page numbers in the table of content, list of figures and list of tables are hyperlinked to allow the reader to easily move between sections. Citations lead the reader to the bibliography. Wherever available, references in the bibliography contain (active) DOIs, leading directly to the cited paper online. Finally, the numbers at the end of each reference refer to the pages in the text containing the citation. This allows the reader to jump back to their previous position in the document after following a reference.

Abstract

Many organisms rely on their sense of smell to explore and interact with their environment. Meeting another organism, infochemicals help them decide whether to eat it, flee, fight or mate with it. The infochemical 2-phenylethylamine (PEA) has previously been associated with predator avoidance in mammals and feeding deterrence in algae. This thesis explores the hypothesis that PEA also induces a comparable avoidance behaviour in crustaceans. In behaviour assays with shore crabs and hermit crabs, movement patterns and behavioural displays were explored in current average marine pH conditions and end-of-the-century average pH, as associated with climate change. Furthermore, using liquid chromatography with tandem mass-spectrometry, shore crab urine was analysed for PEA. Results indicate that PEA attracts both species in reduced pH conditions, rather than deterring them as expected for a predator cue. Agonistic displays in response to PEA and evidence for PEA in shore crab urine suggest that PEA mediates agonistic interactions in crustaceans. Excreted with urine, PEA elicits the full behavioural response in crustaceans only in decreased pH conditions. Therefore, this thesis tested the hypothesis that the pH-dependent response hinges on pH-dependent changes to the infochemical itself. Quantum chemical computations validated by nuclear magnetic resonance (NMR) spectroscopy allowed calculating PEA's different protonation states, and its interaction with a model receptor in different protonation states. Results confirm that the pH-dependent response to PEA could be attributed to changes in charge distribution in the infochemical, potentially leading to altered receptor-ligand affinity. A comparison with the neurotransmitter dopamine reveals that the exact chemical structure and charge distribution of PEA matters for its biological function. Although dopamine and PEA are broadly chemically similar, their biological role for crustaceans appears different. In summary, PEA is an infochemical mediating agonistic interactions in crustaceans in a pH-dependent manner.

Table of Contents

1	Introduction	1
1.1	Chemically Mediated Information	1
1.2	Transferable Infochemicals	3
1.3	Climate Change and Ocean Acidification	6
1.4	Infodisruption: Interference with Chemically Mediated Information	7
1.4.1	The Reproducibility Crisis in Marine Infodisruption Research	8
1.4.2	Mechanisms of Infodisruption	9
1.4.3	Acidification Changes Chemicals	11
1.5	Research Approach	17
2	The Ecological Role of 2-Phenylethylamine (PEA) for Hermit Crabs	20
2.1	Introduction	20
2.1.1	The Infochemical 2-Phenylethylamine	20
2.1.2	Hermit Crabs as Model Species	21
2.1.3	Research Approach and Hypotheses	23
2.2	Materials and Methods	24
2.2.1	Hermit Crab Collection and Husbandry	25
2.2.2	Behavioural Choice Experiments	28
2.2.3	Sex and Weight Determination of Hermit Crabs	35
2.2.4	Data Analysis and Statistics	37
2.3	Results	41
2.3.1	First Insights	41
2.3.2	Behaviour Tracking and Sex-specific Effects	43
2.3.3	Choice Experiments in Flume	46
2.3.4	Seasonality	51

2.3.5	Weight-dependent vs. Sex-dependent Effects	52
2.3.6	pH-dependent Behavioural Effect Size Compared to Changes in Biologically Active Compound	54
2.4	Discussion	57
2.5	Conclusion	66
3	Is PEA a Transferable Infochemical?	67
3.1	Introduction	67
3.1.1	PEA Mediated Behaviours	67
3.1.2	Shore Crabs and their Chemosensory Behaviours	68
3.1.3	Research Approach and Hypotheses	71
3.2	Materials and Methods	72
3.2.1	Shore Crab Collection and Husbandry	72
3.2.2	Behavioural Choice Experiments with Shore Crabs	73
3.2.3	Data Gathering	75
3.2.4	Data Analysis and Statistics	77
3.2.5	Urine Extraction and Chemical Preparation of PEA	78
3.2.6	Liquid Chromatography and Tandem Mass Spectrometry of PEA	79
3.3	Results	80
3.3.1	Sex-specific Differences in Shore Crabs	80
3.3.2	Movement of Shore Crabs in Response to PEA	81
3.3.3	Behavioural Response of Shore Crabs to PEA	84
3.3.4	PEA in Shore Crab Urine	88
3.4	Discussion	90
3.5	Conclusion	97
4	Mechanistic Assessment of the pH-dependent Response to PEA	98
4.1	Introduction	98
4.1.1	Computational Chemistry in Chemical Ecological Research Questions	99
4.1.2	Quantum Chemistry	100

4.1.3	The Conformation of PEA	105
4.1.4	Chemoreception in Crustaceans	106
4.1.5	Potential Receptors for PEA and their pH Dependency	107
4.1.6	Research Approach and Hypotheses	109
4.2	Materials and Methods	111
4.2.1	Computations of PEA in Water	111
4.2.2	Nuclear Magnetic Resonance Spectroscopy of PEA for Model Validation	113
4.2.3	Computations of Receptor Binding	114
4.2.4	Computations of Protonated Receptor Binding	117
4.2.5	Reality Check: Salinity and Temperature Conditions in Field and Model	118
4.3	Results	121
4.3.1	Conformational Preference and Charge Distribution of Different Protonation States of PEA	121
4.3.2	Computational Model Validation	128
4.3.3	An Increased PEA Dipole Increases Receptor-Ligand Binding	134
4.3.4	A Protonated Receptor Binding Pocket Residue Decreases Receptor-Ligand Binding	137
4.3.5	Reality Check: Salinity and Temperature Conditions in Field and Model	140
4.4	Discussion	143
4.5	Conclusion	149
5	Similar Chemistry - Same Function?	150
5.1	Introduction	150
5.1.1	The Similarity Concept in Chemistry	151
5.1.2	Characteristics and Reactivity of Dopamine in Water compared to PEA	152
5.1.3	The Role of Dopamine in Crustacean Behaviour	156
5.1.4	Research Approach and Hypotheses	158
5.2	Materials and Methods	159

5.2.1	Determination of Relevant Protonation States of Dopamine	159
5.2.2	Computations of Dopamine	160
5.2.3	NMR Spectroscopy of Dopamine	162
5.2.4	Behavioural Choice Experiments with Hermit Crabs	162
5.2.5	Data Analysis and Statistics	164
5.3	Results	165
5.3.1	Protonation States of Dopamine	165
5.3.2	Conformational Preference and Charge Distribution of Different Protonation States of Dopamine	167
5.3.3	Computational Model Validation	172
5.3.4	Behavioural Response of Hermit Crabs to Dopamine	174
5.4	Discussion	177
5.5	Conclusion	182
6	Summary and Discussion	184
7	Conclusion	189
	References	190
	Supplementary	233

List of Figures

1.1	Potential Pathways by which Acidification Affects the Behaviour.	10
1.2	Example pH-Abundance Curve.	13
2.1	Set-up of the Behavioural Choice Experiment.	30
2.2	Technical Drawing of the Flume for Choice Experiments.	33
2.3	Picture of Flume Showing Laminar Flow with Dye.	34
2.4	Hermit Crab Sex Differences.	36
2.5	First Insight of Behavioural Response of Hermit Crabs to PEA at pH 8.1 and pH 7.7.	42
2.6	Attraction and Repulsion of Female and Male Hermit Crabs in Response to PEA.	44
2.7	Average Distance of Male and Female Hermit Crabs to PEA Source.	45
2.8	Choice of Flume Side for Female and Male Hermit Crabs.	47
2.9	Cumulative Probability of Decision in Flume.	49
2.10	The Decision Probability of Hermit Crabs for Different Concentrations of PEA in the Flume at pH 7.7.	51
2.11	Weight Difference between Female and Male Hermit Crabs.	53
2.12	Correlation between the Attraction to PEA and the Weight of the Hermit Crab.	54
2.13	Comparison of the Effect Size of the pH Changing Hermit Crab Behaviour and the Protonation State of PEA Respectively.	56
3.1	Claw Measurements in Shore Crabs.	73
3.2	Schematic Illustration of Cheliped Display.	76
3.3	Sex-specific Measurements of Shore Crabs.	80
3.4	Weight and Claw Size-dependent Response of Shore Crabs to PEA.	83
3.5	Probability of Cheliped Display in Response to PEA depending on Weight to Claw Length Ratio of Shore Crabs.	85

3.6	Probability of Escape Behaviour Display in Shore Crabs in Response to PEA.	86
3.7	Active Percentage of Bioassay Time for Shore Crabs in Response to PEA.	87
3.8	Shore Crabs Probing or Grabbing Filter Paper.	88
3.9	Chromatograms of PEA Fragments for a PEA Standard, a PEA Extraction Standard and a Shore Crab Urine Sample.	90
4.1	Conformations of PEA.	105
4.2	Secondary Structure of the TAAR1 Receptor Marking the Position of the Binding Pocket.	115
4.3	Temperature and Salinity-dependency of the Dielectric Constant.	119
4.4	Energy Scan of PEA and PEAH ⁺ in Different Environments to Identify Stable Conformations.	122
4.5	Charge Distribution and Dipole Moment of PEA and PEAH ⁺	127
4.6	Structure and Naming of Carbons in PEA/PEAH ⁺	129
4.7	Calculated Nuclear Proton Shieldings Compared to Experimental NMR Shifts.	130
4.8	Conformation of PEA inside the TAAR1 Receptor Pocket.	135
4.9	Conformation of PEA inside the TAAR1 Receptor Pocket with protonated histidine.	138
4.10	Changes to the Conformational Stability of PEA with the Dielectric Constant.	141
4.11	The Binding Energy of TAAR1-PEA/PEAH ⁺ in Different Dielectric Environments.	143
5.1	Chemical Structure of PEA and Dopamine.	150
5.2	Deprotonation Scheme of Dopamine.	154
5.3	Simplified Pathway of Dopamine Oxidation	155
5.4	Visualisation of the Terminology for Dopamine Conformations.	161
5.5	pH-dependent Abundance of Dopamine in Different Protonation States	166
5.6	Neutral and Zwitterionic Dopamine Preferred Conformation	170
5.7	Dipoles of Dopamine in Protonated, Neutral and the Two Zwitterionic Forms.	171

5.8	¹ H NMR Spectrum of Protonated Dopamine and Regression Analysis of Experimental Shifts with Calculated Shieldings.	173
5.9	Average Distance of Male and Female Hermit Crabs to Dopamine Source.	175
S1	Heatmaps of Combined Spatial Response of Hermit Crabs to PEA at pH 8.1.	234
S2	Heatmaps of Combined Spatial Response of Hermit Crabs to PEA at pH 7.7.	236
S3	Distance Travelled by Hermit Crabs in Response to PEA.	238
S4	Average Acceleration of Hermit Crabs in Response to PEA.	238
S5	Activity of Hermit Crabs in Response to PEA.	239
S6	Heatmaps of Combined Spatial Response of Shore Crabs to PEA at pH 8.1.	240
S7	Heatmaps of Combined Spatial Response of Shore Crabs to PEA at pH 7.7.	242
S8	Weight and Claw Length in Female and Male Shore Crabs.	244
S9	Heatmaps of Combined Spatial Response of Hermit Crabs to Dopamine at pH 8.1.	245
S10	Heatmaps of Combined Spatial Response of Hermit Crabs to Dopamine at pH 7.7.	247
S11	Distance Travelled by Hermit Crabs in Response to Dopamine.	249
S12	Average Acceleration of Hermit Crabs in Response to Dopamine.	249
S13	Activity of Hermit Crabs in Response to Dopamine.	250

List of Tables

1.1	Examples of Infochemicals from aquatic environments.	14
4.1	The Energetically Favoured Conformations of PEA and PEAH ⁺	126
4.2	Comparison of Experimental ¹ H NMR Shifts with Calculated Shifts of Protonated and Neutral PEA in Water.	133
5.1	Energetically Favoured Conformations of Protonated and Neutral/Zwitterionic Dopamine in Implicit Solvation Model.	167
5.2	Energetically Favoured Conformations of Protonated and Neutral/Zwitterionic Dopamine in More Realistic (Hybrid) Solvation Model.	168
5.3	Torsion Angles of Amino Side Chain for Protonated and Neutral/Zwitterionic Dopamine.	169
5.4	Linear Mixed Effect Analysis of the Spatial Response of Hermit Crabs to Dopamine.	176

CHAPTER 1

Introduction

1.1 Chemically Mediated Information

We humans focus on seeing and hearing the world around us; we go to art galleries and concerts, but ‘smell performances’ are rather uncommon. Although our active perception often excludes the olfactory sense, the perfume industry makes billions¹ by capitalising our unconscious bias for pleasant scents. In the course of the recent pandemic, (temporary) loss of olfaction through COVID-19 infection² made us further appreciate our sense of smell.³

Many other species, however, actively rely on their sense of smell to find their way around the world, guided by rich cocktails of chemicals. Encountering another organism, their sense of smell helps to decide whether to eat it, flee, fight, or mate with it.^{4,5} Chemistry is hence the universal language of life on earth.⁴ Chemicals that mediate information are termed ‘infochemicals’.⁶ Thereby, the response that the infochemical elicits can be to the benefit or detriment of the organism.⁶

The use of chemicals to convey information might have evolved from ‘leaking’ hormones, excreted metabolites or compounds used for defence and is arguably the oldest and most versatile form of communication.⁵ It is a common misconception, however, that infochemicals, which are sometimes called semiochemicals,⁷ are designed and synthesised for the sole purpose of communication. This would be energetically expensive and only necessary when privacy is paramount in communication, e.g. under selection pressure

from sexual selection and speciation.⁴ Rather than specifically synthesised chemicals, most infochemicals are secondary metabolites, used primarily for other purposes in the body.⁴ Hence, in aquatic organisms, for example, infochemicals are often excreted with other metabolic waste products via gills.

As chemical diffusion in water can be a slow process, directional distribution of infochemicals is often paramount. Crustaceans, for example, are known to be able to shoot their urine, containing various information-rich metabolites, several body lengths towards their fight opponent, making this an effective communication strategy to deter and mark their territory.⁸ Whilst volatility is key for infochemicals with a large operating range in air, aquatic infochemicals are more diverse, belonging to a variety of substance classes, such as peptides, fatty acids or small polar and non-polar molecules.^{9,10} Depending on the role of the infochemical in the communication process, its solubility, size and functional groups can be vastly different (see also Table 1.1).⁹

However, searching for a single chemical compound that elicits a specific behaviour is a simplified view of chemical ecology, that does not reflect the complexity of chemical bouquets, which are used widely in communication systems.¹⁰ Mixtures of infochemicals are often remnants of the biosynthetic pathway for their production but can also have important ecological functions.⁷ Using chemical bouquets as infochemicals allows related species (that share biochemical pathways) to develop species-specific pheromones.⁷ In moths, for example, blends of chemical compounds with distinctly different ratios are known to function as species- and even population-specific sex pheromones.^{11–13} Similarly, shore crabs (*Carcinus maenas*) are known to use a pheromone bouquet.^{14,15} Thereby, the different components of the compound blend control different aspects of the behavioural cascade.¹⁵ Compound blends are known to mediate a variety of behaviours in crustaceans, such as reproduction, feeding, settlement and dominance, making it a core concept in chemical ecology.⁸

1.2 Transferable Infochemicals

Infochemicals can be categorised based on their functioning for different organisms and whether their perception is beneficial for the sender or receiver.⁵ Infochemicals that evolved for a specific purpose are actively released and likely to be beneficial for the sender. These infochemicals are called 'signals', whilst the term 'cue' refers to infochemicals that are released incidentally and are hence not moulded by natural selection.⁵ However, this cue-signal duality does not capture the full breadth of chemically mediated information and should rather be seen as a continuum.¹⁶

Furthermore, the term 'pheromone' refers to intra-specific signals.⁴ It is interesting to note that animals from different species tend to not be able to perceive each other's pheromones.⁷

Whilst pheromones evolved for intra-specific chemical signalling, infochemicals can also mediate information between species ('allelochemicals'). In many instances, smelling infochemicals from other species can be an advantage for the emitter or the receiver of the allelochemical. Chemical deception, for example, can benefit the emitter of the odour ('allomone').⁶ The earwig (*Labidura riparia*) produces allomones that mimic the smell of carrion, which discourages a wide array of predators.¹⁷ Furthermore, allomones can be used for sit-and-wait foraging strategies of predators:⁷ The web silk of spiders from the genus *Argiope* and *Nephila* contains putrescine, which attracts flies (*Diptera*), the spiders' prey.¹⁸ Additionally, eavesdropping on infochemicals from different species can be beneficial in predator-prey interactions. Prey can smell an approaching predator ('kairomone'), allowing for an early escape without relying on visual contact.⁷ Yet predators can also locate their prey through scent.⁷ Finally, smelling injury-released chemical alarm cues from other species of the same prey guild can give individuals in mixed-species aggregations the crucial advantage to escape their predators.¹⁹

Even species that do not co-occur spatially and temporally can use the same chemical cues. Applying to a wide array of species, I suggest calling these compounds ‘transferable infochemical’. Thereby, different species use the same transferable infochemical to mediate information in comparable situations. In several ostariophysan fishes, for example, the same compound mix of chondroitin sulfates, has been identified as a component of the injury-released chemical alarm cue. Zebrafish, *Danio rerio*, the northern studfish, *Fundulus catenatus*, and the fathead minnow, *Pimephales promelas*, all show avoidance behaviour in response to synthetic chondroitin sulfates.^{20,21} It is important to note, however, that in minnows and zebrafish the full behavioural response was only evoked by conspecific skin extract, indicating that, beside the transferable infochemical chondroitin sulfate, other species-specific compounds contribute to the alarm cue bouquet^{20,21} (see page 2 for introduction of chemical bouquets). Similarly, feeding behaviour can be triggered by transferable infochemicals: Several naive fish species increased locomotion activity and displayed feeding-related search behaviours in response to cysteine;²² and water fleas (*Daphnia magna*) increase mandible movements in response to cysteine.²³ Another example of the use of the same chemical compound across different species is 2-phenylethylamine, which has been detected in the urine of 38 different mammalian species, with levels >3000-fold higher in numerous carnivores as compared to herbivores.²⁴ Rodents²⁴ as well as sea lampreys²⁵ are known to avoid the dietary predator odour 2-phenylethylamine.

Chondroitin sulfates, cysteine and 2-phenylethylamine are all used as infochemicals for many different species. But why are some chemical compounds universally used, whilst other infochemicals are highly specific? Prevalent chemicals in a certain context (injury, feeding, fear etc.) might simply be readily available chemical indicators, leading to their use as an infochemicals. The rupture of epidermal club cells, which are an integral part of the ostariophysan immune system, release chondroitin sulfates.²⁶ Cysteine can be

found in many different food sources^{27,28} and the metabolisation of animal tissue leads to the formation of 2-phenylethylamine, which might explain its presence in carnivore urine.²⁴ Hence, in all above cases, there is a potential link between the release of the infochemical and a fundamental property of the signal source.

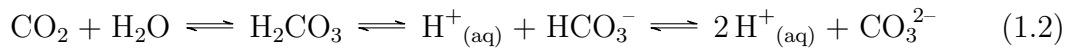
This mechanistic link between signal intensity and a characteristic of the signal sender is also key to the definition of ‘index signals’.⁷ Because of their mechanistic link index signals have an inherent honesty (see Maynard Smith and Harper (2003)²⁹ for the origins of the honest signal theory): The signal cannot be faked. Male blennies (*Salaria pavo* & *Salaria fluviatilis*), for example, advertise their parental care qualities with a pheromone that is produced by the glands that are also responsible for protective protein secretion for eggs.³⁰ Higher pheromone levels correlate with more protein secretion.³⁰ The mechanistic link between protective protein secretion and the pheromone ensures the honesty of the signal.

The link between the release of a compound and a fundamental (physiological) property of the sender applies to both, index signals and transferable infochemicals. Hence, their definitions seem to overlap. However, transferable infochemicals are not limited to chemical signals, as they are not necessarily actively released and their role has not evolved for a specific purpose (see definition of ‘signal’ above), as shown by the above examples of a transferable feeding cue and chemical alarm cue. Furthermore, whilst the definition of index signals focuses on describing honest chemical signalling, the term ‘transferable infochemical’ sets the focus of its definition on the prevalent use of an infochemical across different species.

1.3 Climate Change and Ocean Acidification

The earth is undergoing long term changes. Increasing atmospheric carbon dioxide (CO_2) levels drive global warming.³¹ It is less widely known, however, that about 30% of our emitted anthropogenic carbon is absorbed by the oceans, with wide-ranging consequences for its chemical equilibria.³¹

Firstly, the increased CO_2 concentration in the water changes the water chemistry by shifting the equilibrium towards higher bicarbonate (HCO_3^-) rather than carbonate (CO_3^{2-}) levels³² (see eq. 1.1). Furthermore, CO_2 and water form carbonic acid (H_2CO_3), which partially dissociates into bicarbonate anions (HCO_3^-) and hydrogen ions/protons (H^+).³² Further partial dissociation forms more H^+ and carbonate anions (CO_3^{2-}) (see equation 1.2).³²



The increased H^+ level (due to increased CO_2 levels) increases the acidity of the water. The acidity/alkalinity of a solution can be described using the pH scale. As the pH is defined as the negative decadic logarithm of the H^+ concentration (equation 1.3), high acidity (high concentration of protons, $[\text{H}^+]$) is recorded as low pH.³³

$$\text{pH} = -\log_{10}[\text{H}^+] \quad (1.3)$$

At 25°C , a neutral solution has a pH of 7, whilst a pH below 7 indicates acidic, and above 7 alkaline conditions.³³ In general, the pH is logged from 0 to 14, ranging from acidic

(low pH) to alkaline (high pH). However, the pH can exceed this range in both directions, depending on the concentration and strength of the acid/base. It is important to note that, as the pH is recorded on a logarithmic scale, small changes in the pH can correspond to large changes in acidity: Decreasing the ocean's pH by 0.1 unit corresponds to a 30% increase in the concentration of H^+ in seawater (assuming constant alkalinity and temperature).³⁴

As a consequence of anthropogenic CO_2 emissions, ocean surface pH has declined from pH 8.15 in 1980 by 0.06-0.09 pH units until today and is predicted to drop further to pH 7.65 by the end of the century (business-as-usual scenario RCP8.5).^{31,35} This process, known as ocean acidification, has detrimental effects on calcifying organisms such as corals and some plankton as they rely on calcium carbonate ($CaCO_3$) availability in the oceans.³⁶ As the increased CO_2 levels decrease CO_3^{2-} availability (eq. 1.1), calcifying organisms struggle to maintain their external skeleton.³⁶ Other effects of ocean acidification, however, for example on (chemically mediated) animal behaviours are sometimes overlooked.³⁷

1.4 Infodisruption: Interference with Chemically Mediated Information

Chemical communication often seems to be the natural choice of sensory channel in aquatic environments as aquatic organisms are enveloped in a solution of infochemicals, with every organism around them contributing to the 'smellscape'.³⁸ Furthermore, in aquatic conditions, chemical communication is generally thought to be more reliable than visual signals,³⁹ as in turbid or deep water light conditions might be suboptimal for visual communication.³⁹

However, infochemicals are not always stable over time and not necessarily consistently available across different environmental conditions. Indeed, many chemically mediated behaviours are known to be sensitive to divergence from optimal environmental conditions.⁴⁰ Furthermore, chemicals in water as well as in air can degrade when exposed to heat or pollutants and the acidity of the water can affect their charge.³⁷ Chemical ecologists only recently discovered that infochemicals are no exception.⁴¹ The disturbance of infochemical-mediated biotic interactions is called ‘infodisruption’.⁴² Thereby, the term does not exclusively refer to negative effects on chemical communication processes. Instead, infodisruption describes the disruption of the chemical communication process, potentially amplifying or hampering chemically mediated behaviours.³⁷ Whilst ocean acidification has been shown to amplify the bioavailability of the feeding deterrents saxitoxin and tetrodotoxin,⁴³ for example, several amino acids, bile fluid, and intestinal fluid invoked a reduced olfactory response in gilthead seabream in comparable conditions.⁴⁴ Although the direction of the effect is different in the above examples, the ‘normal’ transfer of chemically mediated information is disrupted in both cases.

1.4.1 The Reproducibility Crisis in Marine Infodisruption Research

In marine chemical ecology, infodisruption through ocean acidification has been a research focus for about a decade. However, early and highly publicized studies reporting radical changes in the behavioural response of clownfish larvae to predator odours under elevated CO₂ conditions^{45,46} are now hotly debated.^{47–49} Since then, numerous independent studies found that, depending on the species and chosen behaviour, high CO₂ levels can have positive, negative and no effect on marine animal behaviour (reviewed by Clements and Hunt, 2015⁵⁰).

The documented behavioural effects of ocean acidification range from impaired learning ability⁵¹ and decision-making⁴⁶ to changes in olfactory-mediated behaviours.⁴¹ However, a meta-analysis showed that the estimated effect size of ocean acidification impacts on fish behaviour has been declining since this phenomenon has first been observed.⁵² Furthermore, recent efforts to replicate the effect of ocean acidification on avoidance behaviour of coral reef fishes (the above mentioned highly publicized studies)^{45,46} have been unsuccessful,⁴⁷ which sparked a debate on reproducible methods and transparent data analysis.^{48,49}

This debate motivated me to search for robust methods in the course of my PhD, to produce consistent reliable results. Firstly, I chose to work with known chemicals rather than ‘conditioned water’, which contains unknown amounts of unknown infochemicals secreted by an organism. Choosing a known chemical excludes potentially complex interactive effects of chemical mixtures in the conditioned water and enabled me to determine and work at threshold concentration. Secondly, I repeated my behavioural experiment to ensure reproducibility of my results and used behaviour tracking software rather than solely relying on visual observations, to exclude observer bias (chapter 2 & 3). Lastly, a main goal of my PhD was the pursuit of a holistic mechanistic understanding of how acidified conditions can affect different steps along the signalling cascade (chapter 4 & 5), whilst previous studies have mostly focused on a single potential mechanism to explain ocean acidification effects on animal behaviour.

1.4.2 Mechanisms of Infodisruption

Ocean acidification is the combined effect of elevated CO₂ and decreased pH. Fig. 1.1 maps five potential mechanisms (described below) by which ocean acidification can alter animal behaviour to the signalling cascade of chemically mediated behaviour. The

signalling cascade starts with a signal source (for example an organism, habitat, food) producing/releasing infochemicals, which are transported through the medium and bind to a receptor. The signal is then transmitted and translated internally to evoke a behaviour. Changes in individual animal behaviour can then in turn alter intra- and inter-specific interactions, potentially with population or community-wide implications.⁵³

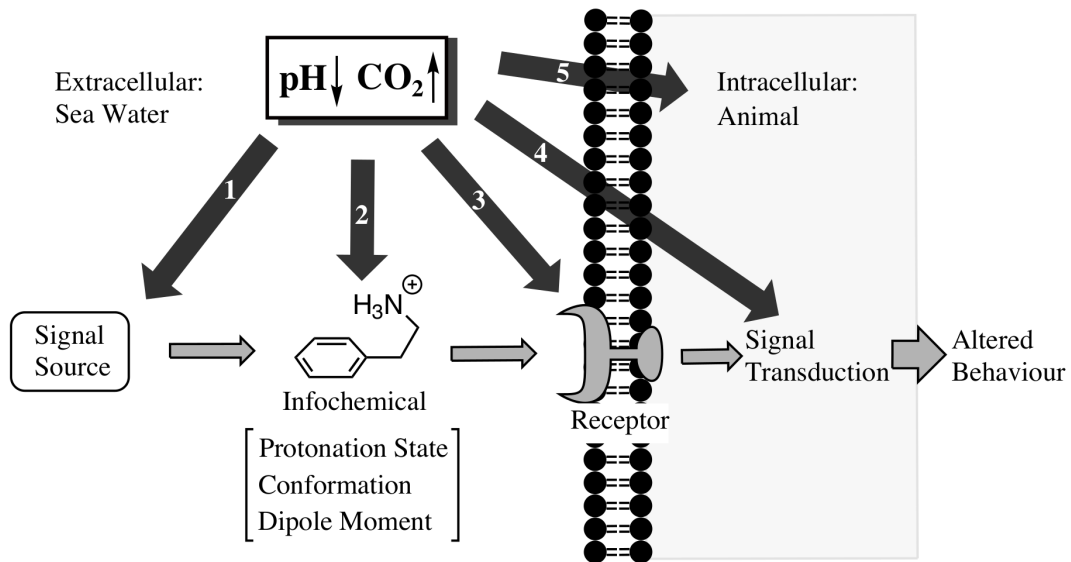


Fig. 1.1: Visualisation of the possible mechanisms by which decreased pH or increased CO_2 levels can alter animal behaviour. The signalling cascade from source to behaviour is shown with light grey arrows. The potential effects of acidification interfering with this pathway are shown in dark gray and numbered. Thereby, the stressors can affect the signal source (1), the infochemical (2), the receptor or its interaction with the ligand (3), the signal transduction (4) and the physiology or fitness of an animal (5).

Fig. 1.1 shows that, firstly, elevated CO_2 / decreased pH conditions can affect the signal source. In terrestrial environments, aphid alarm pheromone, for example, is reduced in quality and quantity when animals are exposed to elevated CO_2 conditions.^{54,55} Although, to the best of my knowledge there are no studies on the effects of ocean acidification on biosynthesis and chemical composition of infochemicals in marine environments, similar patterns are conceivable for signalling cascades in aquatic conditions. Secondly, infochemicals are known to potentially change their conformation and charge distri-

bution in low pH conditions, which in turn can change chemoreception.^{41,56} Changes to chemoreception have also been observed in electrophysiological and transcriptomic measurements, showing that elevated CO₂ impairs the olfactory response of sea bass⁵⁷ and sea bream⁴⁴ to feeding cues (third potential pathway, Fig. 1.1). Conversely, Nilsson et al. 2012⁵⁸ proposed that elevated CO₂ interferes with signal transduction by altering the GABA_A (γ -aminobutyric acid) neurotransmitter system in the fish brain, which is shown as pathway four in Fig. 1.1. Finally, although many aquatic animals are known to be able to compensate for acid-base disturbances,^{59,60} the fifth potential mechanisms suggests that ocean acidification can elevate their metabolic load, potentially affecting the behavioural response to infochemicals.⁶¹

1.4.3 Acidification Changes Chemicals

The first three pathways in Fig. 1.1 (at least partially) build on the notion that pH can change chemicals. To improve our understanding of how chemicals in water can be affected by changing pH conditions, the definition of the term ‘acid’ provides some clarity. According to Brønsted-Lowry’s acid-base theory, an acid (HA) is any chemical compound capable of donating a proton (H⁺).^{62,63} By donating a proton, the acid dissociates into its conjugate base in an equilibrium reaction that is described by the acid dissociation constant K_a (eq. 1.4 and 1.5).⁶⁴ A molecule can have several acid dissociation constants, depending on the number of protons it can give up. Stronger acids have larger dissociation constants, whilst weaker acids have smaller dissociation constants.



$$K_a = \frac{[\text{H}^+][\text{A}^-]}{[\text{HA}]} \quad (1.5)$$

Alternatively to the K_a , its negative decadic logarithm pK_a is often used to simplify mathematical expressions. Additionally, as previously defined (eq. 1.3), the negative decadic logarithm of the proton concentration defines the pH of a solution. Re-arranging eq. 1.5 accordingly results in the Henderson-Hasselbalch equation (eq. 1.7), which connects the acid dissociation constant K_a and the ratio of acid/conjugate base to the pH of the solution.^{64,65}

$$pK_a = -\log_{10}K_a = \log_{10}\frac{[\text{HA}]}{[\text{H}^+][\text{A}^-]} \quad (1.6)$$

$$\text{pH} = pK_a + \log_{10}\left(\frac{[\text{A}^-]}{[\text{HA}]}\right) \quad (1.7)$$

From this follows that the protonation state of any compound with ionisable groups is susceptible to changes in environmental pH conditions, whereby the dissociation constant K_a (or pK_a) describes the degree of susceptibility of a compound to pH changes. Plotting the pH against $[\text{HA}]$ (eq. 1.7), Fig. 1.2 illustrates that with increasing pH, a compound that can donate a proton (HA, here with $pK_a=7.8$) dissociates whereby its abundance drops. The correlation follows a non-linear curve due to the logarithmic relationship. The point of inflection marks the pK_a value of the acid, which, for mono-protonic acids, equates to 50% of HA in the protonated and 50% in the deprotonated state (A^- , not shown in Fig. 1.2).

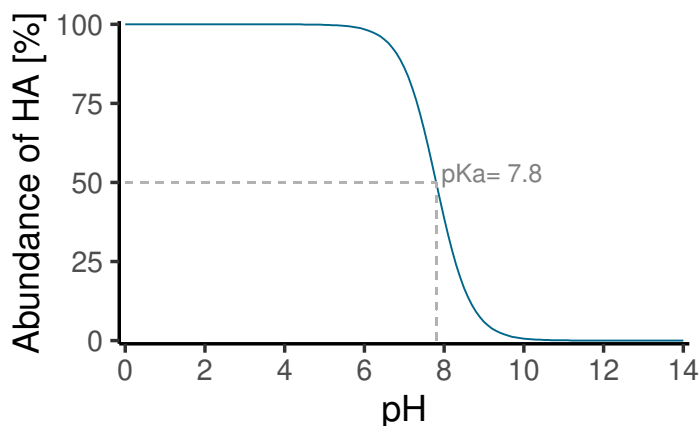


Fig. 1.2: pH-dependent abundance curve for an example compound HA with an ionisable group at $pK_a=7.8$. With increasing pH, the abundance drops in a non-linear way. The point of inflection marks the pK_a value, which equates to 50% of HA in the protonated and 50% in the deprotonated state for monoprotic acids. Whilst the abundance of HA decreases, the abundance of the conjugated base A^- increases respectively (curve not shown).

Applying these fundamental chemical principles to the reality of aquatic chemical communication demonstrates that any compound with ionisable groups is an acid or base and hence might be susceptible to pH change. The pK_a value is a direct measure of the pH range in which an ionisable functional group of a molecule can be protonated. When the pH of the environment approaches the pK_a value of a functional group, a proportion of the chemical compound changes its protonation state (protonated or deprotonated, depending on the direction of the pH change, see Fig 1.2). Given the pH, the abundance ratio of protonation states can be determined with the Henderson-Hasselbalch equation (eq. 1.7).

To determine how this applies to aquatic infochemicals, we must examine the diversity of functional groups in infochemicals. Aquatic infochemicals contain a wide variety of functional groups, many of which can donate a proton within environmentally relevant

pH ranges. To illustrate the variety of infochemical functional groups, some examples are collated in Table 1.1.

Table 1.1: Examples of infochemicals from aquatic environments.

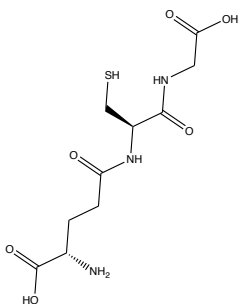
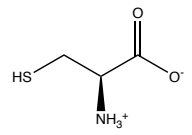
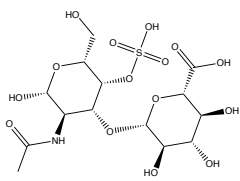
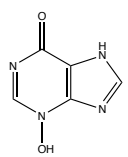
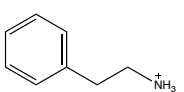
Structural class	Ecological Role	Example	Reference
Peptide	Larval settlement, reproduction, foraging, antimicrobial defence		[66,67]
Amino acid	Foraging, reproduction		[22,66]
Saccharide	Alarm conspecifics, mate recognition		[20,68]
Purine	Alarm conspecifics, larval settlement		[69–71]
Biogenic amine	Predator avoidance, foraging for scavengers		[25,72,73]

Table 1.1 shows that infochemicals can include a wide variety of different functional groups, e.g. amino ($\text{NH}_3^+/\text{NH}_2$), carboxy (COOH/COO^-) and thiol groups (SH/S^-), many of which are susceptible to pH changes.

However, as deduced above (section 1.4.2), the infochemical is just one component of the signalling cascade. In its essence, chemoreception is the interaction of a protein receptor and its ligand. As proteins comprise of long chains of amino acid residues, which are often pH sensitive,⁷⁴ pH-dependent changes in even a few amino acid residues can lead to fundamental changes in the 3D conformation of the receptor and its ligand affinity.⁷⁵⁻⁷⁷ Hence, both ligand and receptor are potentially pH-dependent. This creates a multifaceted problem, whereby small changes in pH can potentially change the charge distribution of the protein receptor or the infochemical. Additionally, changes in the charge may in turn affect the conformation of either of the two. All four mechanisms have the potential to disrupt chemoreception.

From a chemist's perspective it is puzzling that the first mechanisms that were proposed for marine infodisruption (and predominated the debate until recently) are based on internal physiological processes (effects of ocean acidification on the GABA_A neurotransmitter system):^{58,78} Even though infochemicals and olfactory receptors are directly exposed to the changing environmental conditions, chemical ecologists have focused on internal neurotransmitter functioning to explain the changes in chemical communication due to ocean acidification. This thesis attempts to approach the topic of pH-dependent chemical communication from a chemistry rather than physiological perspective.

Although in the context of climate change, the two stressors elevated CO₂ and decreased pH are coupled, they can have independent effects on chemically mediated behaviours.⁷⁹ To promote the understanding of the underlying mechanisms of ocean acidification effects on chemoreception, this study attempts to disentangle the effects of decreasing pH and increasing CO₂ on chemically mediated behaviour. As elevated CO₂ levels can have wide-ranging physiological effects (pathway 5 in Fig. 1.1), which are not subject of this study, I chose to manipulate only the pH, leaving the carbonate chemistry of the water relatively unchanged.

Finally, it is important to note that environmental conditions are seldom stable. Infodisruption might already occur on a regular basis, depending on the stability of the infochemical and the respective ecosystem. In many aquatic ecosystems, diurnal and seasonal fluctuations in pH, temperature and light levels expose infochemicals and organisms to ever changing conditions.^{80,81} In coastal environments, these changes are particularly pronounced due to tidal cycles and photosynthesis/respiration.⁸² Whilst organisms are known to rely on metabolic compensations to maintain acid-base balance in intertidal environments,⁸³ mechanisms for the compensation or adaptation of chemosensory systems are poorly understood.³⁷

Similar to the cyclic changes of light conditions (sun/moon) that affect visual communication⁸⁴ or even offset physiological processes,⁸⁵ variable pH conditions characterise today's oceans, and coastal environments in particular.^{80,82,86} Current daily pH fluctuations often even exceed average pH changes of surface ocean water as expected in the face of ocean acidification by the end of the century.^{80,81} Similar to e.g. visual foraging strategies being adapted to day/night cycles in light conditions, it seems likely that behavioural coping mechanisms allow organisms to handle current daily/seasonal pH fluctuation, for example by timing chemically mediated behaviours that are sensitive to pH change to optimal environmental conditions.

Although current fluctuations in environmental conditions often exceed average long-term changes due to climate change by the end of the century,^{80,81} ocean acidification shifts the range of pH fluctuations and even increases its amplitude.^{81,87} Hence, whilst the phenomenon of infodisruption is not tied to average changes owing to climate change (as natural fluctuations in environmental conditions can also create suboptimal sensory conditions), climate change can exacerbate the effects of infodisruption in naturally fluctuating environments. Thereby, intertidal organisms may be exposed to critical environmental thresholds earlier.

1.5 Research Approach

Many studies have adopted an ecological perspective on infochemicals or else explored the chemical basis of ecological interactions. This work attempts a true interdisciplinary approach, combining behavioural ecology with computational and analytical chemistry to improve our understanding of the mechanisms underlying pH-dependency of chemically mediated information, based on the example of the transferable infochemical 2-phenylethylamine (PEA, see also section 1.2).

I choose to work with PEA, which is known to act as a dietary predator odour for many species.²⁴ Thereby, PEA excretion levels are suspected to be defined by the metabolism of animal tissue.²⁴ Being particularly interested in a mechanistic understanding of chemical ecological processes, the potential link between the signal intensity (PEA level in urine) and a characteristic of the signal sender (its feeding strategy) is intriguing (see also section 1.2). As several species have been shown to avoid and/or excrete PEA,^{24,25} its role is potentially transferable to other (aquatic) species. The avoidance response to PEA of as distantly related species as rodents²⁴ and sea lampreys²⁵ has been hypothesised to be explained by increased levels of PEA in carnivore urine, potentially alerting prey of the presence of a predator.²⁴ However, it is unclear how scavengers could fit into this predator-prey rationale, as they potentially consume equally high amounts of animal tissue without being predators. The literature on 2-phenylethylamine as an infochemical is being covered in more detail in section 2.1.

This PhD thesis is structured into four data chapters, which each contain a background introduction (including a section on specific research questions), a description of the methods and results, and their discussion. The results obtained in the separate chapters are then compared and discussed together, also addressing future perspective and

implications of the presented work. The focus of each of the data chapters is outlined below.

The first data chapter, chapter 2, focuses on the behaviour of hermit crabs in response to the infochemical PEA in different pH conditions, to deduce its role for chemical communication in hermit crabs. To characterise the chemically mediated response, its seasonality, weight- and sex-dependency are assessed.

In the second data chapter, chapter 3, I explore whether the observed behavioural response to PEA is specific to hermit crabs, by repeating some of the behavioural experiments from chapter 2 with shore crabs. Furthermore, mass spectrometric analysis of shore crab urine allow for conclusions on the origin of PEA in marine environments.

The third data chapter, chapter 4, assesses the potential mechanisms underlying the observed pH dependency of the behavioural response of hermit crabs and shore crabs to PEA. Using quantum chemical methods and nuclear magnetic resonance spectroscopy, changes in the structure and charge of the infochemical in response to changes in pH are assessed. As (charge-dependent) electrostatic interactions are a crucial aspect for receptor-ligand interactions, I also study the binding properties of PEA with a model receptor in proof-of-concept computational experiments. Thereby, pH-dependent changes in the infochemical as well as the receptor are considered. Living in variable environmental conditions, hermit crabs and shore crabs are exposed to fluctuations in salinity and temperature in addition to changes in pH. Therefore, I also assess the vulnerability of my computational model of the infochemical in water and receptor-ligand interaction to changes in salinity and temperature.

The final data chapter, chapter 5, explores the possibility that the chemically mediated response to PEA is the result of chemical mimicry, whereby the infochemical binds to a non-target receptor. Repeating some of the previous behavioural and computational

experiments, I explore structural and mechanistic similarities of PEA to the neurotransmitter dopamine and assess whether dopamine evokes comparable behavioural responses to PEA, as shown in chapter 2.

The aim of this thesis is to explore the ecological role of PEA for multiple crustaceans and to assess the potential mechanisms underlying the pH dependency of the behavioural response.

CHAPTER 2

The Ecological Role of 2-Phenylethylamine (PEA) for Hermit Crabs

2.1 Introduction

Infochemicals structure communities and shape trophic cascades⁸⁸⁻⁹⁰ and yet the chemical compounds underlying these crucial interactions are rarely known in marine environments. This hampers our understanding of chemical communication processes and its susceptibility to changing environments.³⁷

2.1.1 The Infochemical 2-Phenylethylamine

To expand upon our knowledge of chemical communication processes in marine environments and their pH dependency, I draw an example from the terrestrial environment and choose to work with 2-phenylethylamine (PEA), a known dietary predator odour that is detected in the urine of many mammals²⁴ (see also section 1.2). Carnivorous mammals have been found to have up to >3000-fold higher PEA levels in their urine than herbivores; and rodents innately avoid the smell of PEA whilst displaying a stereotyped fear response to this interspecies odour.²⁴ Ferrero et al. (2011)²⁴ identified the chemosensory receptor TAAR4 as the primary target for PEA detection in rodents.

In aquatic environments, sea lampreys are known to avoid the smell of PEA^{25,91} and PEA has hence been suggested for pest control measures of invasive sea lampreys.⁹² Di Rocco et al. (2016)⁹¹ argue that their response to PEA might be explained by sea lampreys avoiding the smell of their (terrestrial) predators, such as raccoons, which are known to excrete PEA with their urine.²⁴

Furthermore, PEA is known to be present in a variety of plants, including algae, where it has been hypothesised to function as a feeding deterrent.⁹³ PEA has been detected in brown and red marine algae in Germany and Turkey.^{94,95} As PEA is known to function as a dietary predator cue for different species^{24,25} and known to be present in marine environments,⁹⁴ its ecological role for marine organisms needs to be further explored.

2.1.2 Hermit Crabs as Model Species

I chose to work with the common marine hermit crab (*Pagurus bernhardus*) to promote our understanding of the ecological role of PEA in marine environments. Almost 800 species of hermit crabs (anomuran decapod crustaceans) inhabit a variety of marine environments.⁹⁶ In British coastal environments, *Pagurus bernhardus* is the most common hermit crab.⁹⁷ Hermit crabs are generalist carrion scavengers, fulfilling a crucial ecosystem role in intertidal tide pools.^{98,99} The lack of calcification of their abdominal exoskeleton requires hermit crabs to occupy foreign shelter.^{96,97} Choosing empty snail shells as mobile shelters both protects their soft abdomen and creates a refuge from attack whereby the animal fully retracts into its shell.⁹⁶

Olfaction is a dominant sensory channel in hermit crabs, although behavioural responses are often enhanced by combining visual and olfactory stimuli.¹⁰⁰ As hermit crabs are known to display a variety of chemically mediated behaviours, most notably regarding shell choice,¹⁰¹ they are considered a model species in chemical ecology.^{8,102,103}

Furthermore, hermit crabs are known to respond to predator odours by altering their behaviour,¹⁰⁴ and their social interactions, shell selection and foraging rely on chemical signalling.¹⁰³ This makes them an excellent study species to determine the ecological role of the infochemical PEA in marine environments.

Due to the fluctuating environmental conditions in intertidal environments (the natural habitat of hermit crabs) studying the response of hermit crabs to PEA in average pH condition alone, risks missing any pH-dependent functionality. Ocean acidification is known to change marine environments,³¹ with potentially detrimental effects on chemical communication^{41,57} (see also section 1.4). Although the average annual changes in ocean acidity due to climate change are small considering the short life span of hermit crabs, they also routinely experience fluctuations in pH, salinity and temperature in their environmental conditions: Living in intertidal zones, hermit crabs inhabit environments of extremes.⁸²

Due to the tidal cycle and day-night rhythms pH fluctuations vary locally, but they often exceed the average expected pH shift due to ocean acidification⁸⁰⁻⁸² - pH 8.1 to pH 7.7 by the end of the century.³¹ In the low-intertidal, the most common habitat of hermit crabs, the pH has been shown to fluctuate between pH 7.83 and pH 8.30 (mean pH 8.09) due to the tidal cycle (data from southeast Australia).⁸² This pH difference of 0.47 over a single day is similar in size to the projected average ocean acidification of ΔpH 0.4 by the end of the century.

With ocean acidification shifting the current diurnal pH range and increasing its amplitude,⁸¹ intertidal organisms such as hermit crabs might be exposed to critical threshold pH conditions in the near future. It is hence crucial to improve our understanding of the pH-dependency of infochemicals to identify vulnerable chemically mediated behaviours.

The infochemical 2-phenylethylamine, which is the focus for this thesis, has an amino group with $pK_a=9.83$,¹⁰⁵ showing that the molecule is pH-dependent. The chosen pH range 8.1-7.7 in this study represents average ocean acidification by the end of the century,³¹ which improves comparability with other studies.^{41,47,79} However, the pH range that is relevant for current and future intertidal environments might exceed this pH range.

2.1.3 Research Approach and Hypotheses

This chapter focuses on exploring the ecological role of PEA for hermit crabs. To approach this research question, I tested the response of individual animals to PEA, giving them the opportunity to retreat or investigate the odour source.

Although evidence of PEA functioning as a deterrent (predator odour²⁴ or feeding deterrent⁹³) predominate, its potential attractiveness to scavenging organisms should be considered when formulating hypotheses on the behavioural response to PEA: Bacteria biosynthesise PEA from organic detritus by decarboxylating the essential amino acid phenylalanine.¹⁰⁶ As omnivorous opportunistic scavengers,^{97,107} the appetite of hermit crabs is versatile. Scavengers such as hermit crabs could associate the smell of PEA with decay and it might therefore be an attractive feeding cue rather than a deterrent. I therefore hypothesise that PEA acts as a feeding cue for hermit crabs. I hence expect hermit crabs to be attracted to PEA. Repeating my own experiments with various methods ensures the reproducibility of the results.

Furthermore, observing weight and sex-dependent patterns in the behavioural response allows for further insights into the ecological role of PEA. If PEA acts as a feeding cue rather than a deterrent for hermit crabs, in the absence of competition, the weight and sex of the animal should not affect its attraction to the odour. Although within a group,

competition might induce some weight/sex-dependent effects in response to a feeding cue,⁹⁹ I expect *individual* animals (as in my experimental set-up) to be attracted to PEA irrespective of their weight or sex.

Finally, as reduced seawater pH is known to disrupt the olfactory response to food cues¹⁰² and shell choice¹⁰⁸ in hermit crabs, I hypothesise that reducing the pH to end-of-the-century average conditions (pH 7.7) disrupts the behavioural response to PEA. Hence, I expect hermit crabs to be neither attracted to nor repulsed by PEA at pH 7.7. As PEA has an amino group with $pK_a=9.83$,¹⁰⁵ I hypothesise that changes in the infochemical might be responsible for pH-dependent changes in chemically mediated behaviour. Hence, I expect that changes in the protonation state of the infochemical ('chemical effect size') are in the same order of magnitude as changes in the chemically mediated behaviour ('biological effect size').

Over the course of my PhD, I studied the response of hermit crabs to PEA in several separate experiments. As my knowledge of the subject grew, my hypotheses were adjusted and my methods refined. Hence, wherever applicable, the methods and results sections are divided into three subsections to allow the reader to follow the development of the methods: first insights, behaviour tracking and sex-specific effects, and choice experiments in flume.

2.2 Materials and Methods

I chose two different set-ups to observe attraction/repulsion of hermit crabs in response to PEA in choice experiments:

1. The odour is added as a point source to static water conditions.
2. The response to an in-flow concentration of PEA is tested in a flume.

Whilst experiments testing the response to a point source represent more realistic conditions for a feeding cue (i.e. an animal follows an odour trail to the source of food), this set-up has the drawback that due to the unknown diffusion properties of PEA and variable diffusion conditions in the static water tank, the actual concentration that is detected by the animal is unknown. When referring to the conditions in the static water tank experiments, I therefore refer to the concentration of the point source, although, due to diffusion, the actual concentration perceived by the animal is much lower. The flume experiments address this knowledge gap by exposing hermit crabs to known in-flow concentrations of PEA.

2.2.1 Hermit Crab Collection and Husbandry

Hermit crabs (*Pagurus bernhardus*) were collected by hand at low tide from the rocky shore near Scarborough, UK. For each of the three experiments, hermit crabs were collected anew and kept at the aquaria facilities of the University of Hull.

First Insights

The first behavioural experiment (section 2.3.1) was carried out with *Pagurus bernhardus* collected from Boggle Hole (54°25'19.6"N 0°31'43.6"W) in November 2018. At the aquaria facilities of the University of Hull, 70 hermit crabs were kept in 100 L tanks at a density of about 25 animals per tank and a light/dark cycle of 12 h/12 h. Of the 4 husbandry tanks available for this set of experiments, one was initially left empty, allowing for a rotating husbandry system that ensured hermit crabs were only used in one set of experiments: Animals that had been exposed to PEA were moved to the empty tank. Moving hermit crabs to the initially empty 4th tank emptied a husbandry tank, which was subsequently used to house only hermit crabs after their exposure to

PEA. The husbandry tanks were connected by a 1600 L circulating artificial seawater system with pH 8.1 ± 0.1 , $15.8 \pm 0.2^\circ\text{C}$ and salinity 35.9 ± 0.2 PSU. Hermit crabs were acclimatised to a twice weekly feeding rhythm with commercially available cooked blue mussels and were not fed for 5-7 days prior to the experiments to standardise appetite levels.

Behaviour Tracking and Sex-specific Effects

To further explore sex-, pH- and weight-specific differences in the response of hermit crabs to PEA (section 2.3.2), hermit crabs were collected in February 2021 at low tide from Filey Brigg ($54^\circ 13' 02.0''\text{N}$ $0^\circ 16' 29.3''\text{W}$) near Scarborough, UK. On the collection day the seawater was 6°C , had a salinity of 32 PSU and the pH was 8.15.

After collection from the wild, the animals were transferred to the aquaria facilities of the University of Hull. 100 hermit crabs were held in 4 100 L tanks at a density of 20-26 animals per tank with a 12 h/12 h light/dark cycle. The tanks were supplied by a 1600 L circulating artificial seawater system, adjusted to 35 ± 1 PSU, pH 8.1 ± 0.1 and $15.6 \pm 0.4^\circ\text{C}$ (mean \pm standard deviation). Nitrate levels and carbonate hardness were checked weekly using aquaria test kits (Marine Lab, Nitrate Test, NTLab and KH/Alk Profi Test, Salifert) and were within 5-10 mg/L and 9.0-9.4 dKH respectively. Additionally, the total alkalinity of the husbandry water was determined using a titrator (HI-84531-02 total alkalinity mini titrator for water analysis, Hanna instruments) in weekly intervals. The total alkalinity in the husbandry tanks was 132.5 ± 3.2 mg/L (as CaCO_3 , mean \pm standard deviation). After 3 weeks of acclimatisation to the husbandry conditions and a twice-weekly feeding rhythm with commercially available cooked blue mussels, the animals were not fed for 5-7 days prior to the behaviour assays to gain tight control on their appetite levels and ensure a response to a potential feeding cue.

For up to 3 weeks after the collection, copulatory-type behaviour was observed (0-3 pairs per tank). Thereby, one hermit crab firmly holds the shell of another¹⁰⁹ and doesn't release it when fed. The latter is typically placed 'upside-down', with the top of the shell on the sediment. Copulatory-type behaviour occurred decreasingly over time and was not observed any more when data collection started.

After being exposed to PEA, hermit crabs were housed in small individual containers within their housing tanks. Containers were crafted from empty pipette tip boxes (11 cm × 7 cm × 6 cm) and filled with 0.5 cm sediment. To ensure good water circulation, each container had a total of ten small holes around the sides and a large hole in the lid, covered with mesh. Each container was labelled with a number, allowing for the identification of hermit crabs without marking their body.

Choice Experiments in Flume

For the third set of behavioural assays, hermit crabs were again collected from Filey Brigg near Scarborough, UK, on 27th of August 2021 at low tide. In the collection tide pools the temperature was 17°C, the pH was 8.21, the salinity 32 PSU and the alkalinity 138.6 mg/L as CaCO₃ (Hanna Instrument, HI-84531-02 Total Alkalinity mini titrator for water analysis).

120 animals were transferred to 2 200 L tanks at the aquaria facilities at Hull University at a density of 60 animals per tank and kept at $15.3 \pm 0.2^\circ\text{C}$ and salinity 35 ± 1 PSU (mean ± standard deviation) in artificial seawater. The water was constantly aerated and filtered (Superfish AquaFlow 200). Additionally, 15% of the water was changed 1-2 times per week. Ammonia, nitrite, and nitrate levels were closely monitored and did not exceed 0.2 mg/L, 0.25 mg/L and 10 mg/L respectively. The pH was 8.01 ± 0.1 (mean ± standard deviation) and the alkalinity was 107.8 ± 2.4 mg/L as CaCO₃ (mean

\pm standard deviation; Hanna Instrument, HI-84531-02 Total Alkalinity mini titrator for water analysis). The hermit crabs were acclimatised for three weeks to a twice weekly feeding rhythm with cooked blue mussel and light/dark periods of 12h/12h prior to the start of the experiment. To standardise appetite levels, animals were not fed for 7 days before the experiment. No copulatory-type behaviour was observed.

As previously, after being exposed to PEA, hermit crabs were housed in small individual containers within their housing tanks. Containers were crafted from empty pipette tip boxes (11 cm \times 7 cm \times 6 cm) and filled with 0.5 cm sediment. To ensure good water circulation, each container had a total of ten small holes around the sides and a large hole in the lid, covered with mesh. Each container was labelled with a number, allowing for the identification of hermit crabs without marking their body.

2.2.2 Behavioural Choice Experiments

First Insights

To gain first insights into the reaction of hermit crabs to PEA at different pH conditions, the animals (n=20 per pH condition) were randomly allocated to be tested in pH condition 7.7 and 8.1. For the experiments in pH 7.7, the pH of the artificial seawater was adjusted in batches of 4 L to pH 7.7 ± 0.05 , using 1 molar hydrochloric acid (diluted from 37% hydrochloric acid, Fisher Scientific). (For justification of the choice of pH manipulation see section 1.5.)

The first behavioural experiments were carried out in the laboratory (3rd floor), which required the transport of hermit crabs in batches of 5 from the ground floor aquaria facilities. Hermit crabs were allowed to recover from transport for at least 20 min before experiments. The light was dimmed to reduce the impact of visual stimuli. After being acclimatised to the pH of the new environment for 2 min in a separate

tank, each individual was tested for its undisturbed movement pattern in the tank (control) and its reaction to PEA (2-phenylethylamine hydrochloride, Sigma-Aldrich, 98%). Therefore, PEA solutions were prepared with artificial seawater adjusted to the same pH as the bioassay tank water. The control and three PEA concentrations were tested subsequently with 2 min acclimation time in a separate tank between the assays. Hence, every animal was exposed to 4 subsequent experiments, allowing for 2 min rest in between exposures. After experiments, animals were kept separately to PEA-naive animals to ensure that no animal was reused (see section 2.2.1).

The assay tank (28 cm × 18 cm) contained 1 L of artificial seawater with pH 7.7 ± 0.05 or pH 8.1 ± 0.05 . Hermit crabs were individually caged with a plastic cylinder in the middle of the tank and filter papers (1 cm², Whatman No. 3) were dropped on either side of the tank. In the control experiment, both filter papers were blank. In the three PEA conditions, the filter paper contained 200 μL of the respective PEA concentration ($3 \cdot 10^{-6}$ mol/L, $3 \cdot 10^{-5}$ mol/L and $3 \cdot 10^{-4}$ mol/L) on one side, whilst it was left empty on the other side of the tank (internal control). The side of the PEA filter paper was randomised for each individual. After allowing the cue to diffuse for 20 s, the hermit crab was released by lifting the plastic cylinder and observed for 2 min. For the data analysis, the tank was virtually divided into thirds (see Fig. 2.1) and the time spent in each of the three areas was recorded manually or via video to ensure consistency.

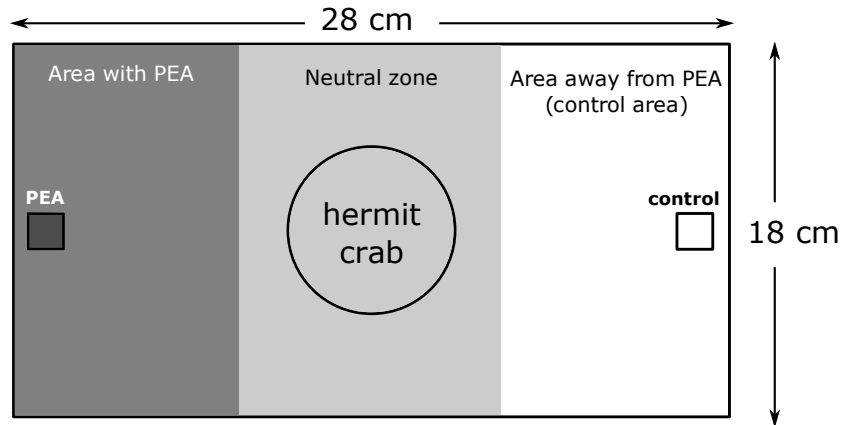


Fig. 2.1: Set-up of the behavioural choice experiment. The hermit crab was caged with a plastic cylinder in the middle of the neutral zone whilst filter papers containing the cue were dropped on either side of the tank (squares). After 20 s of diffusion time, the cylinder was lifted, and the movement pattern of the hermit crab was observed and recorded by video for 2 min. For data analysis, the time spent in the three areas (dark gray, gray, white) of the tank was measured.

Behaviour Tracking and Sex-specific Effects

To better understand the response of hermit crabs to PEA, the previous experiment was repeated, whereby the number of animals tested was more than doubled (46 animals tested), the sex and weight of each animal was determined after the experiment and the animals' movement patterns were tracked using software to exclude potential observer bias.

Unlike in the initial set of experiments (see above), this set of behaviour assays was carried out within the husbandry room to reduce potential confounding factors of transport upon the behavioural response of hermit crabs. During behaviour assays the light level was low (around 45 lux, Mini Light Meter DT-86, CEM instruments) to reduce the impact of visual stimuli. For the experiments in pH 7.7, the pH of the artificial seawater was adjusted in batches of 10 L to 7.7 ± 0.05 , using 1 molar hydrochloric acid (diluted from 37% hydrochloric acid, Fisher Scientific). The total alkalinity of the artificial sea-

water was determined in weekly random samples and averaged at 116.4 ± 8.9 mg/L for pH 8.1 and 100.6 ± 3.4 mg/L for pH 7.7 (as CaCO_3 , average \pm standard deviation).

A hermit crab was placed in artificial seawater ($18 \pm 1^\circ\text{C}$, 35 ± 1 PSU, pH 8.1 or 7.7) and allowed to acclimatise to the experimental conditions for 3 min in a separate container. After acclimatisation, the animal was transferred to the middle of the bioassay tank ($28 \text{ cm} \times 18 \text{ cm}$), filled with 1 L artificial seawater of the respective pH, and left to acclimatise to the tank conditions for 30 s, whilst being caged in the center of the tank. This was long enough for most of the animals to emerge from their shell. Then, a filter paper (1 cm^2 , Whatman No. 3) was introduced on either end of the tank. On one side, the filter paper contained 200 μL PEA at $3 \cdot 10^{-5}$ mol/L, $3 \cdot 10^{-4}$ mol/L or $3 \cdot 10^{-3}$ mol/L or was left blank for a negative control experiment. As experiments were fully paired (within pH condition and PEA concentration), every animal was exposed to 8 experimental conditions, allowing for 3 min rest in between experiments and 1 h after a set of 4 experiments. After experiments, animals were kept separately to PEA-naive animals to ensure that no animal was reused (see section 2.2.1).

The concentration of PEA on the filter paper was increased 10-fold as the results from the first insight experiment suggested further information on pH-dependent effects could be gained at higher concentrations. The filter paper on the other side was left blank as internal control. As before, the test solutions were prepared with PEA (2-phenylethylamine hydrochloride, Sigma-Aldrich, 98 %) in artificial seawater of the respective experimental pH. The order of the experiments was randomised and the cue side was randomised for each individual.

After the cue on the filter paper was allowed to diffuse for 20 s, the cage was lifted and the movement of the animal was recorded on video for 2 min. Animals that stayed hidden in their shell for 3 consecutive negative control experiments were deemed unfit and

excluded from the experiment. The sex and weight of the hermit crabs was determined after the behavioural experiments (see section 2.2.3).

All videos were analysed blindly using the behaviour tracking software LoliTrack (version 5.1.1, Loligo Systems, Denmark). Blind analysis involved trimming all videos to exclude the first frames, where a summary sheet with the experimental conditions was presented to the camera. As I would not have been able to deduce the experimental conditions of the experiment from the trimmed video, this removed all potential unconscious bias from the analysis. After finishing the analysis, information about the experimental conditions were retrieved from the untrimmed videos and analysis results and information on the experimental conditions were merged.

Choice Experiments in Flume

The reaction of 30 hermit crabs to 6 concentrations of PEA (10^{-10} mol/L, 10^{-9} mol/L, 10^{-8} mol/L, 10^{-7} mol/L, 10^{-6} mol/L, 10^{-5} mol/L) as well as an artificial seawater control was tested in current average pH 8.1 and end-of-the-century level pH 7.7 in a custom-made flume, built from black acrylic (see Fig. 2.2). The flume was set up in the husbandry room to reduce potential confounding factors of transport upon the behavioural response of hermit crabs.

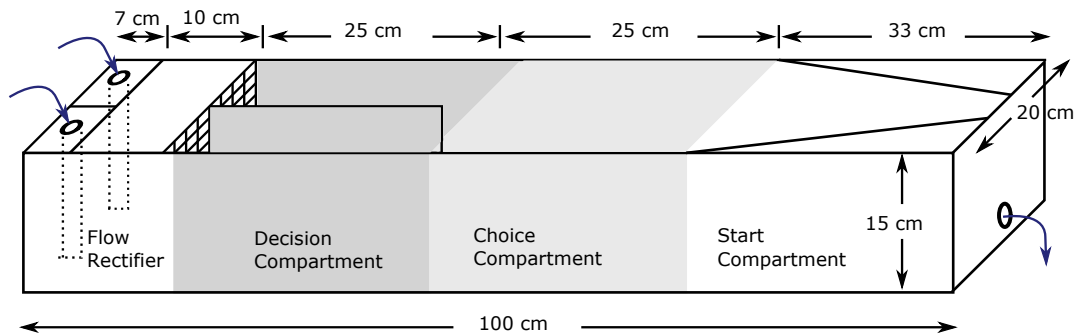


Fig. 2.2: Set-up of the flume to determine the reaction of hermit crabs to in-flow concentrations of PEA. The cue enters the flume vertically at about 0.8 L/min per side and passes a flow rectifier, ensuring laminar flow for the entire length of the flume. The hermit crab is placed in the centre of the start compartment, allowing it to explore the odour plumes in the choice compartment. The time is measured until the animal crosses the decision line (halfway mark of decision compartment).

The pH was adjusted using 1 mol/L hydrochloric acid (diluted from 37% hydrochloric acid, Fisher Scientific). The flow of artificial seawater inside the flume was adjusted to 1.6 L/min (0.8 L/min per inflow side, 20 cm/min). The alkalinity of the flume water was 115.1 ± 2.2 mg/L as CaCO_3 for pH 8.1 and 85.4 ± 9.4 mg/L as CaCO_3 for pH 7.7 (mean \pm standard deviation; Hanna Instrument, HI-84531-02 Total Alkalinity mini titrator for water analysis). 3D-printed flow rectifiers (10 cm long lattice of 80 mm square tubes, made from polylactic acid) ensure laminar flow, which was verified using fluorescent dye (see Fig. 2.3).

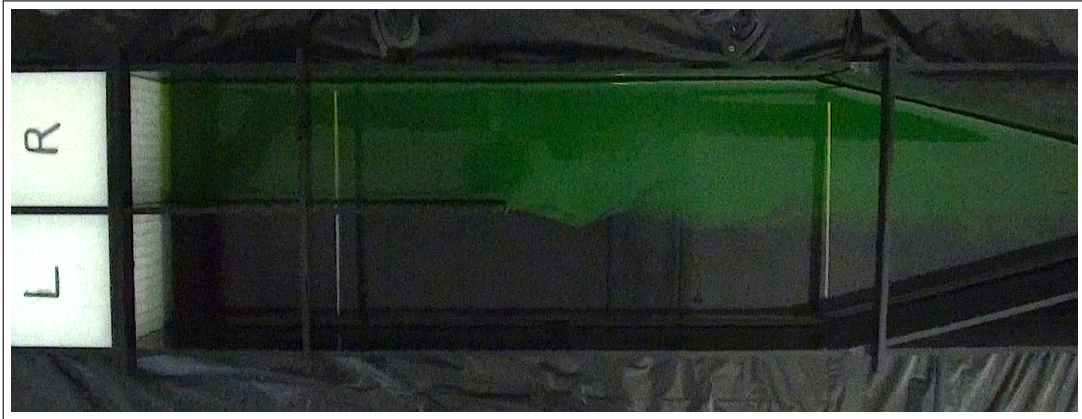


Fig. 2.3: Top view of the flume with fluorescent dye added to right inflow (fluorescein in artificial seawater) to show the laminar flow in the start, choice and decision compartment. Artificial seawater was added to the left inflow. White lines mark the start of the choice compartment (start line, right) and the middle of the decision compartment (decision line, left). Crossing the decision line defines the end point of the experiment. Two brackets support the structural integrity of the tank (not depicted in technical drawing Fig. 2.2).

The cue was added to the inflow tubes using a peristaltic pump at 11.1 mL/min per side. This corresponds to a 72-fold dilution of the cue when added to the inflow of the flume. Hence the start solutions were 72-times more concentrated than the target solutions of 10^{-10} mol/L - 10^{-5} mol/L PEA in the flume. To reduce water usage, the artificial seawater from the outflow of the flume was filtered (Superfish AquaFlow 200) with foam, carbon and ceramic filtration steps for at least 1 h and reused up to 2 times in the flume.

Before each set of bioassays, the flume was rinsed for at least 5 min with artificial seawater. Additionally, before each individual bioassay, the flume was rinsed with artificial seawater for 1 min and the odour plumes were allowed to establish for 3 min before the animal was placed in the centre of the start compartment (see Fig. 2.2 for compartments). Then, the hermit crab was allowed to explore the odours inside the choice compartment. Crossing the half-way mark of the decision compartment defined the

endpoint of the assay (see also top view of tank Fig. 2.3). The distance between the beginning of the choice compartment and the decision line was 38 cm. If no decision was made after 10 min, the experiment was aborted. However, the data was not discarded, but included in the data set as 'censored' data. In statistics, censoring means that the value of an observation is only partially known. In this case the time is >600 s but the decision is unknown.

Each animal was tested for their response to increasing concentrations (including control) in one pH condition and tested for the other pH condition the following day. Hence, every animal was exposed to a total of 14 experiments, with 5 min rest in between experiments and 24 h rest after a set of 7 experiments. The cue side was randomised for different individuals. After the hermit crabs were tested in both pH conditions its sex and weight was determined (see section 2.2.3).

2.2.3 Sex and Weight Determination of Hermit Crabs

Hermit crabs occupy empty mollusc shells to protect their fragile abdomen.⁹⁷ Hence, crucial parts of their anatomy are hidden within the shell, and males and females can only be distinguished after its removal (see Fig. 2.4A).

The shell was cracked carefully using a small bench vice (Stanley Multi Angle Vice × 70 mm). Then, the animal was left to free itself from the shell fragments and placed on its back for sexing under a microscope (Leica DFC290). Female hermit crabs have four appendages (pleopods) on the left side of the abdomen, whilst males have only three.⁹⁷ Unlike in males, pleopods in females divide into two branches and have long setae to hold eggs⁹⁷ (see Fig. 2.4C& D). Furthermore, a pair of gonopores can be found at the base of their 3rd leg pair (pereiopods) (Fig. 2.4C), whilst gonopores in males are found at the base of the 5th pereiopods ⁹⁷ (Fig. 2.4B). Male gonopores, however are

only about half the size of female gonopores and, unlike in females, the hole is partially covered (confirmed with SEM, not shown here), making them harder to identify.

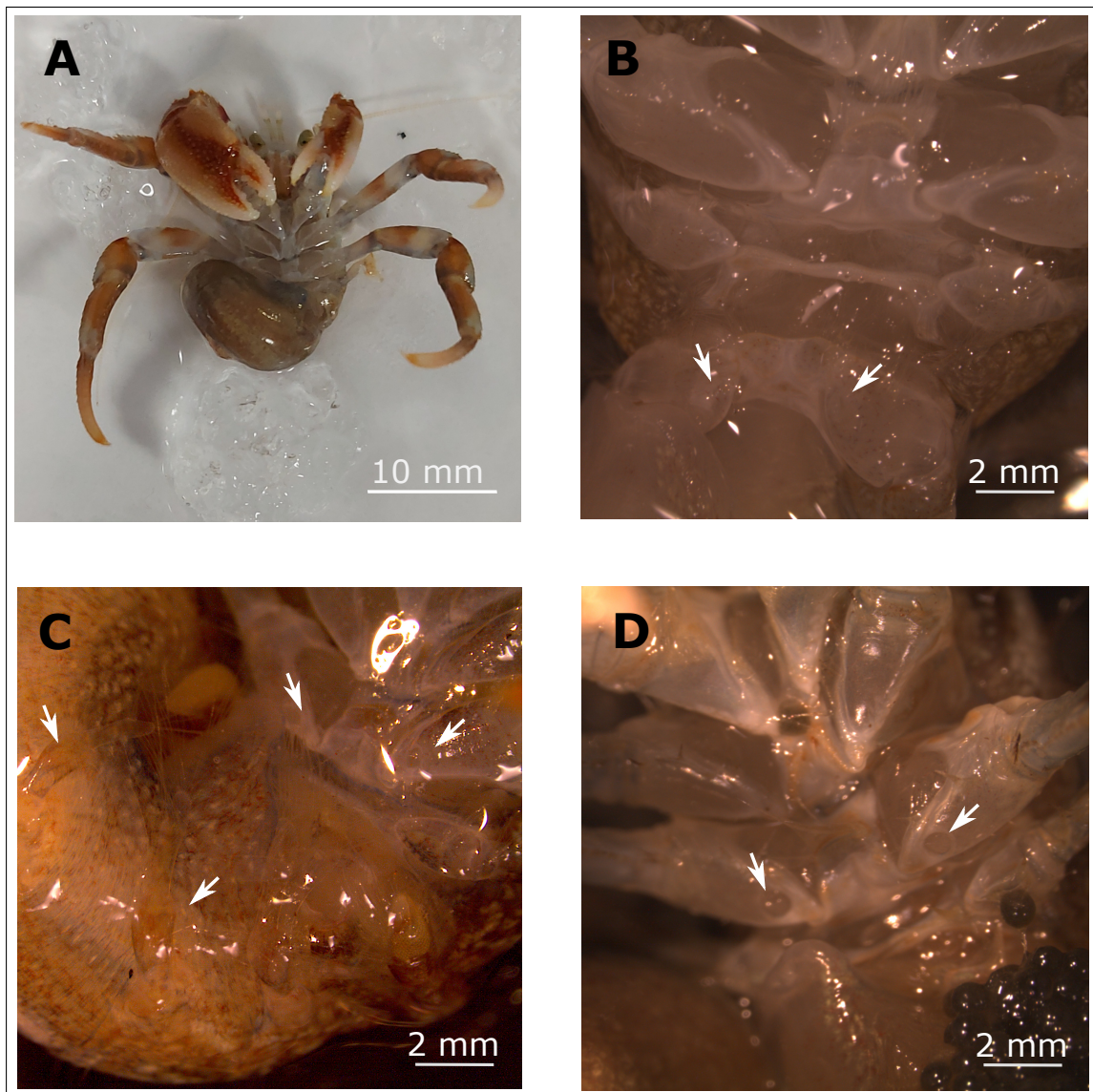


Fig. 2.4: *Pagurus bernhardus* without its shell to distinguish between the sexes (ventral view). (A) shows a male hermit crab without its shell, exposing its soft abdomen. (B) shows the basal segment of the 2-5th pereopod of a male individual, where the gonopores open on the coxae of the 5th pereopods (white arrows). In (C) a female hermit crab with gonopores on the 3rd pereopod (white arrows) and the top pleopods (white arrows), branched and with long setae, is shown. (D) shows a female with eggs. White arrows point towards the gonopores on the coxae of the 3rd pereopod.

After sex determination, the hermit crab was carefully dried on a paper towel and weighed without its shell. Ovigerous females were weighed with their clutch of eggs. As Lancaster (1990)¹⁰⁹ had found the smallest ovigerous female to weigh only 0.13 g, the minimum weight for this study was set to 0.3 g to ensure mature animals. Then, the animal was placed into a small container, filled with artificial seawater and containing a selection of suitable shells. The containers were crafted from empty pipette tip boxes (11 cm × 7 cm × 6 cm), filled with 0.5 cm sediment and placed within the housing tanks. To ensure good water circulation, each container had a total of ten small holes around the sides and a large hole in the lid, covered with mesh. After at least 24 h recovery, hermit crabs were placed back into the main tank. Sex determination and weighing was carried out with the help of Amber Jones, fellow PhD student in the ChemEcolHull research group.

2.2.4 Data Analysis and Statistics

All statistics were carried out with R (version 4.0.2).¹¹⁰ For data visualisation, I used the package ‘ggplot2’.¹¹¹ The behaviour assays in static tanks, as described above, have a paired structure within the level of the individual animal as the same hermit crab was tested multiple times (negative control, three or more PEA concentrations). Using mixed effect models (‘lme4’ R package),¹¹² allows me to account for this paired structure by treating the identity of the individual animal as a random effect. The term ‘mixed effect’ refers to the mixture of ‘random’ and ‘fixed’ effects. Whilst fixed effects (such as sex, pH or concentration) explain consistent trends in a dataset, random effects (such as the identity of the animal or the experimental day) account for the variation across the whole dataset.

I chose to analyse my data using mixed effect models rather than repeated measures ANOVA or even paired non-parametric tests with adjustments for multiple testing, as mixed effect models better reflect the complexity of my experimental set-up, with multiple (interacting) fixed factors, and are better at handling missing data.¹¹³ Furthermore, ANOVAs assume that the dependent variable is continuous and independent variables are categorical;¹¹³ experiments in which one of the fixed factors is continuous (such as weight) cannot be analysed with an ANOVA. Mixed effect models, on the other hand, offer more flexibility in modelling an array of data types and can deal with both nominal and continuous independent variables, making it an increasingly common approach in ecological data analysis.¹¹⁴

In addition to these overarching mixed effect models, smaller non-parametric tests (e.g. Wilcoxon test) were used for hypothesis-driven comparison of specific groups of interest.

To explore significant effects in mixed effect models, Tukey's test was used for multiple comparisons, using the 'multcomp' package¹¹⁵ or, for larger numbers of fixed effects, the estimated marginal means (also called least-square means, package 'emmeans'¹¹⁶) with Sidak adjustment method for the p-values.

First Insights

Before video tracking software was used, the time the hermit crab spent near the PEA point source (see dark gray zone in Fig. 2.1) was used as the outcome (dependent) variable. Using linear mixed effect models, allowed me to adjust for the repeated measures with each individual, analysing the attraction of hermit crabs to PEA at three different concentrations and at pH 8.1 and 7.7. To check for any variance in the experimental procedure, the effect size of the experimental data was also examined in a separate model.

Behaviour Tracking and Sex-specific Effects

Using the behaviour tracking software LoliTrack (version 5.1.1, Loligo Systems, Denmark), allowed me to export several locomotion-related parameters from the videos of the behaviour assays, such as distance travelled, acceleration, percentage of time active and the average position inside the tank. The latter was used to visualise the attractive/repulsive effect of PEA on hermit crabs using heatmaps of the tank (based on `drawcontours.R`, written by J.D. Forester¹¹⁷) for each condition and sex. To account for the randomised side (left or right) of the cue, the x-axis displays the distance from the cue source side rather than the length of the tank. The average distance from the PEA source side (x-axis in heatmaps) was then further analysed in linear mixed effect models (package ‘`lme4`’¹¹² in R), considering fixed additive and/or interactive effects of sex, concentration, and pH and random effects on the individual level.

Additionally, the continuous data was reduced to binomial data, to focus on the overall choice of hermit crabs (attraction vs. repulsion) in response to different concentrations of PEA. To establish the threshold of attraction/repulsion, I determined the average position in the tank during all control experiments (control filter paper on both sides). In the control experiments, hermit crabs positioned themselves on average 13.4 cm from the PEA source side. With a tank length of 28 cm, this is very close to the centre of the tank (see also Fig. 2.1 for tank set-up). Animals that were on average closer to the PEA source than 13.4 cm were deemed ‘attracted’, whilst a ‘repulsion’ was defined as an average distance from the PEA source > 13.4 cm. The binomial data of attraction/repulsion was explored using generalised mixed effect models (binomial distribution with a logit link) to study the fixed additive and/or interactive effects of sex, concentration, and pH on the overall preference of hermit crabs in response to PEA, whilst accounting for the paired study design using random effects.

Choice Experiments in Flume

The flume data was analysed using time-to-event analysis (also called survival analysis, R packages ‘survival’,^{118,119} ‘survminer’¹²⁰ and ‘cmprsk’¹²¹). Time-to-event analysis investigates the probability that an event occurs and models the probability of a change in state over time.¹²² The outcome variable hence depends on the time until the event as well as its frequency over the observed timespan.¹²¹ Here, the hermit crab crossing a line in the decision compartment of the flume (‘decision line’) was defined as the endpoint of the experiment. Furthermore, time-to-event analysis also allows for the inclusion of assays where the animal didn’t reach a decision (i.e. didn’t cross the decision line within 10 min). These datapoints which are only partially known, are called ‘censored data’: The hermit crab explored the tank for the duration of the assay (600s) but its final decision remains unknown.

I chose to use time-to event analysis to analyse the data collected in the flume as it allows me to consider not only whether an event occurred, but also when it occurred, in a combined dependent variable.¹²² Other data analysis methods could have only analysed either the binary choice of the animal or the time until decision. Furthermore, time-to-event analysis allows me to account for censored data appropriately.¹²² Using more ‘traditional’ statistical methods, for example ANOVA (for continuous time data) or Chi-squared tests (for choice data), would have required the exclusion of all censored data points, leading to reduced sample size and an underestimation of the true time until decision.

A mixed-effect approach (‘random’ and ‘fixed’ effects, see above) can be incorporated into time-to event analysis using Cox proportional hazards models¹²³ (R package ‘coxme’¹²⁴). Cox proportional hazards models were fitted to determine the effect of the concentration of PEA, the sex, the weight of the individual and the pH of the water

(fixed effects), whilst accounting for the variation of the response on the individual level (random effect). A Cox regression model is a semi-parametric model that computes the instantaneous rate at which events occur (hazard).¹²² As Cox models make no assumption of the baseline hazard rate, the quantity of interest from a Cox regression model is the hazard ratio, which represents the ratio of hazards between two groups.¹²³

In addition to time-to-event analysis, general sex-specific differences in the number of animals that explored the tank (crossed the start line) and reached a decision (crossed the decision line), across all conditions, were explored using Pearson's Chi-squared tests. As the Chi-square distribution is continuous, the Yates correction is applied to adjust for the assumption of discrete occurrences in the contingency table.¹²⁵

2.3 Results

2.3.1 First Insights

The initial choice experiment with hermit crabs reveals that PEA can be an attractant for hermit crabs. In pH 8.1, 12 out of 20 hermit crabs spent more time in the area with the cue ($3 \cdot 10^{-4}$ mol/L on filter paper) than during the respective negative control experiment and 14 out of 20 hermit crabs preferred the area with PEA in pH 7.7. Fig. 2.5 suggests that whilst the time spent in the third of the tank furthest away from the cue appears to decrease in a dose-dependent manner (Fig. 2.5B), the time spent in the area with PEA increases subsequently (Fig. 2.5A).

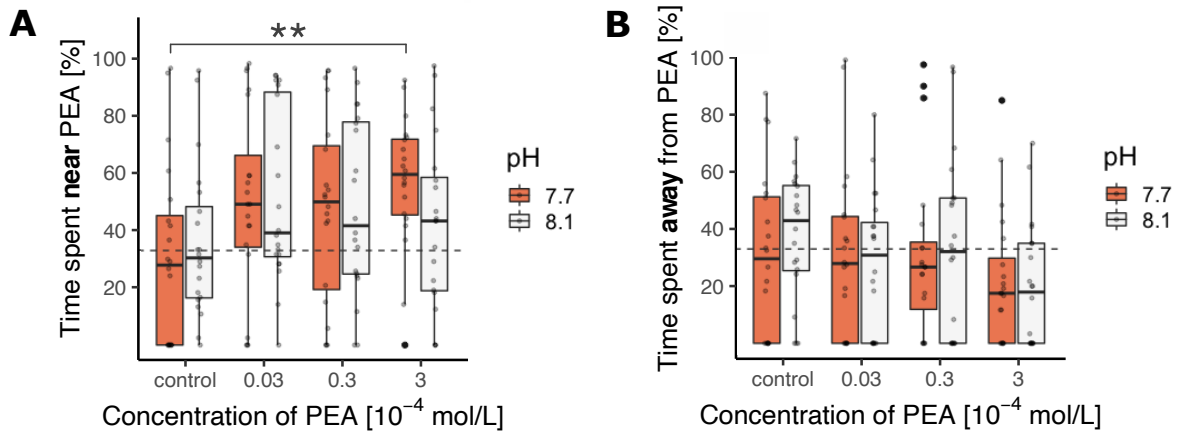


Fig. 2.5: Behavioural response of hermit crabs ($N=20$) to PEA at current pH (8.1) and end-of-the-century level (7.7). Percentage of time spent in the third of the tank with the PEA source (A) and furthest away from it (B) at different PEA concentrations. The dashed gray line indicates a third of the time, (33%). At pH 7.7 (orange), hermit crabs spend significantly more time near the highest dose (A, $p^{**}<0.01$, Tukey's post-hoc test, indicated by bracket with asterisks), whilst there was no significant difference at pH 8.1 (white). The boxplots depict the median with first and third quartile of the distribution. Whiskers extend to 1.5 the interquartile range; data beyond that range are defined as outliers and plotted individually. The boxplots are overlaid by the actual data points in semi-transparent.

The response of hermit crabs in the control experiments is comparable (i.e. not significantly different) in both pH conditions, indicating that the decreased pH in the absence of a signalling cue has no measurable effect on their general movement pattern. However, the attractive effect of PEA is stronger at low pH. [There is clear evidence for a concentration-dependent effect at pH 7.7 \(Likelihood ratio test on linear mixed effect model, \$LRT=9.64\$, \$n=3\$, \$p^*=0.02\$ \)](#). In particular, hermit crabs spend significantly more time in the area with PEA during the highest exposure experiment ($3 \cdot 10^{-4}$ mol/L) than during the negative control experiment (Tukey's post-hoc test, $p^{**}=0.0096$, on average 27%). On the other hand, there is no evidence for a dose-dependent response to PEA at pH 8.1 (Likelihood-ratio test, $LRT=3.78$, $n=3$, $p=0.29$). The date of the experiment has no significant effect on the models, testifying the rigorousness of the procedure.

2.3.2 Behaviour Tracking and Sex-specific Effects

To further explore the increased potency of PEA at low pH, the previous experiment was repeated with improved methods. The PEA concentrations were increased 10-fold to gain more information on the role of PEA in current average pH condition (pH 8.1), the experimental design was fully paired (as opposed to paired within the pH condition level), the number of repeats was doubled to ensure repeatability and robustness of the results and the hermit crab's average position in the tank was adopted as the dependent variable (made possible by using behaviour tracking software). Additionally, a sex determination step was added to explore potential sex-dependent effects.

Of the 46 hermit crabs that were tested, 3 stayed hidden in their shell in three consecutive negative control experiments and were hence excluded from the data set, 1 was excluded due to a parasitic barnacle (*Peltogaster sp.*) and 4 that moved very little and did not enter any of the tank zones in 3 or more of the 8 experiments (including controls) were excluded due to assumed low health status. Of the remaining 38 hermit crabs, 18 were male and 20 were female, of which 8 were carrying eggs.

To gain an overview of the reaction of hermit crabs to PEA in different pH conditions, density plots of the average position of the hermit crabs within the tank were plotted as heatmaps (Supplementary Information, Fig. S1-S2).

Simplifying the continuous data of the average distance to the PEA source side (x-axis in heatmaps) to binomial choice data (closer than average = attraction, further than average = repulsion), there is moderate evidence that the sex of the hermit crab affects their choice of area in response to PEA (Likelihood ratio test, LRT= 3.70, n=1, p=0.054). Furthermore, a significant interaction of pH and concentration (Likelihood ratio test, LRT=9.34, n=3, p*=0.025), indicates that the dose-dependent response to PEA is significantly pH-dependent. In fact, for males, the response to PEA at the

highest concentration ($3 \cdot 10^{-3}$ mol/L) is significantly different in pH 7.7 and pH 8.1 (Fig. 2.6B, post-hoc test on estimated marginal means, $p^{**}=0.005$). 14 out of 18 male hermit crabs preferred the side closest to PEA over the side with the control cue at pH 7.7, which is significantly different from a random choice (exact binomial test, proportion=0.5, $p^*=0.03$). There is no evidence for a dose-dependent choice of females to PEA in either pH conditions (Fig. 2.6A). The date of the experiment had no significant effect in the model, which testifies the rigorousness of the methods.

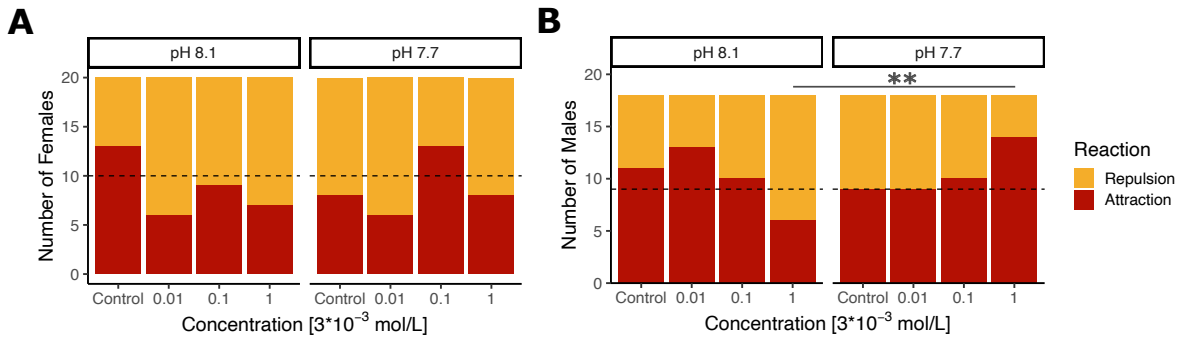


Fig. 2.6: Reaction of female (A) and male hermit crabs (B) to different concentrations of PEA in pH 8.1 and pH 7.7. PEA had no significant effect on the average attraction/repulsion of female hermit crabs in either pH condition. For male hermit crabs, however, there is a significant interaction between the effects of increasing PEA concentration and pH, resulting in a significant difference between pH 8.1 and pH 7.7 at the highest concentration (post-hoc test on estimated marginal means, $p^{**}=0.005$). The dotted line represents a random 50:50 choice.

Similarly, the average distance to the PEA source is significantly affected by the interaction of the concentration of PEA and the pH condition for male hermit crabs (Likelihood ratio test on linear mixed effect model, $LRT=14.5$, $n=3$, $p^{**}=0.002$). Hence, the pH significantly affected the concentration-dependent trend in males, whilst there was no significant effect in females (see Fig. 2.7). The post-hoc test reveals that in pH 7.7, male hermit crabs were significantly closer to the PEA source at its highest concentration than in pH 8.1.

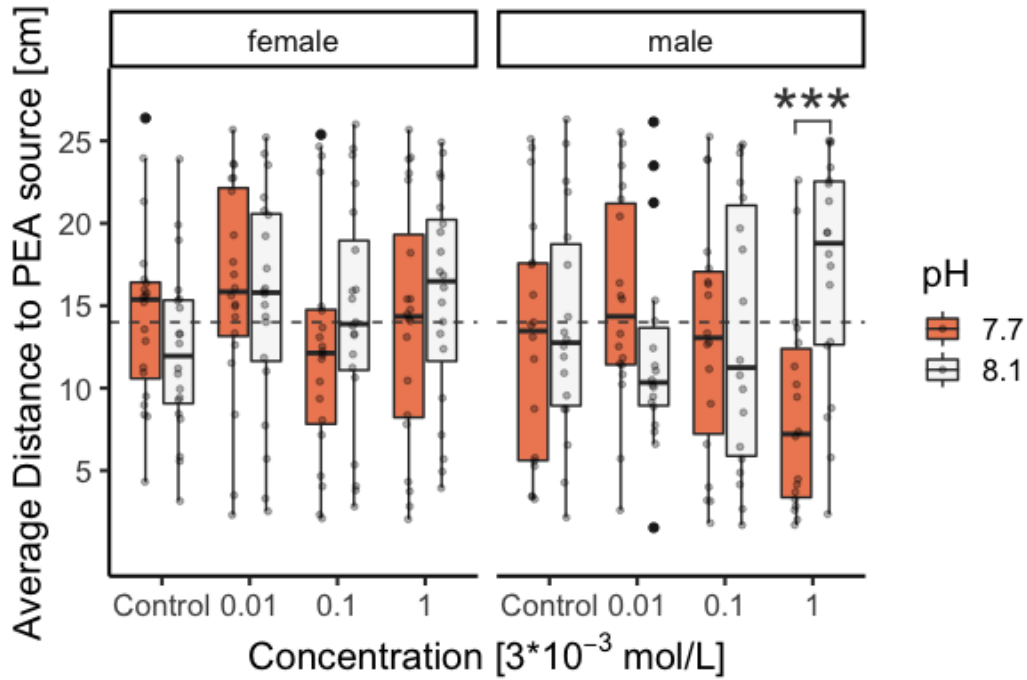


Fig. 2.7: Average distance of N=20 female and N=18 male hermit crabs to different concentrations of PEA in pH 8.1 (white) and pH 7.7 (orange). Whilst there is no evidence for a dose-dependent response in females, the response of males shows a significant interactive effect of pH and concentration. Asterisks depict the p-value in post-hoc test on estimated marginal means with $p^{***} < 0.001$. The boxplots depict the median with first and third quartile of the distribution. Whiskers extend to $1.5 \times$ the interquartile range; data beyond that range are defined as outliers and plotted individually. The boxplots are overlaid by the actual data points in semi-transparent. The dotted line represents the average position in control conditions.

The behaviour tracking software also computes other locomotion-related parameters, such as distance travelled, average acceleration and percentage of time spent active. As there is no evidence that the pH, PEA conditions or sex of the hermit crabs affects these variables, data were not further analysed. The distance travelled, average acceleration and percentage of assay time spent active of hermit crabs in response to the different pH and PEA conditions is visualised in the Supplementary Information (Fig. S3 - S5).

2.3.3 Choice Experiments in Flume

To approach my research question of the pH-dependent ecological role of PEA for hermit crabs from a different angle, I also tested the attraction/repulsion of hermit crabs in response to PEA in a flume. Hermit crabs were exposed to six in-flow concentrations of PEA and seawater (as control), both in pH 8.1 and pH 7.7.

Of the 30 animals that were tested in the flume, three had parasites (one *Peltogaster sp.* and two *Athelges paguri*) and were hence removed from the data set. Of the remaining 27 animals, 14 were male and 13 were female, of which 2 were carrying eggs.

To gain a first overview of the overall response, the choice of hermit crabs in response to different concentrations of PEA is visualised in stacked barplots (see Fig. 2.8).

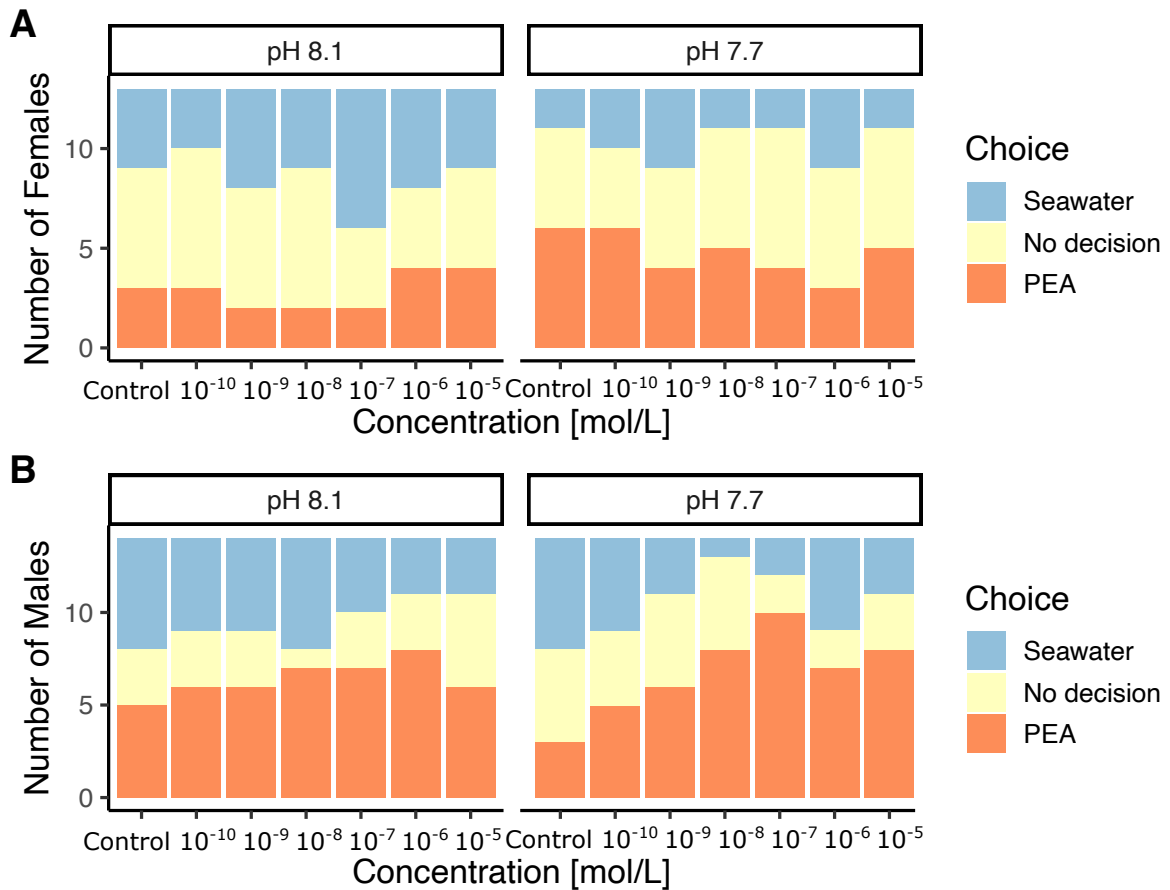


Fig. 2.8: Choice of flume side for female (A) and male hermit crabs (B) in response to different concentrations of PEA in pH 8.1 and pH 7.7. Females are overall less likely to make a decision, across all conditions (including controls). Furthermore, the bar plot gives a first indication of a dose-dependent attraction to PEA for males in pH 7.7, that peaks at a concentration of 10^{-7} mol/L.

Firstly, Fig. 2.8 suggests a general sex-specific difference in the number of animals that make a decision. Males are consistently, across all PEA concentrations (including controls) and pH conditions, more likely to cross the decision-line in the flume. Whilst 24% of all bioassays with male hermit crabs are censored (no decision reached in flume over 10 min), significantly more females (43%) failed to reach a decision (Pearson's Chi-squared test with Yates' continuity correction, $\chi^2=14.35$, $df=1$, $p^{***}=0.00015$).

To determine whether this can be attributed to a sex-specific difference in exploratory movement, I compared hermit crabs' sex-specific probability to cross the decision line to their sex-specific probability to cross the start line (data not visualised). Similarly to animals crossing the decision line, females are twice as likely to stay within the start compartment, not crossing the start line, with no apparent pH- or concentration-dependent trend. In 26% of experiments with females, the hermit crab did not cross the start line, whilst this only applies to 13% of experiments with males (Pearson's Chi-squared test with Yates' continuity correction, $\chi^2=8.76$, $df=1$, $p^{**}=0.0031$). As this tendency for more tank exploration in males compared to females is neither pH nor concentration dependent, and also observed in control conditions, this sex-specific difference in hermit crabs cannot be attributed to PEA but is a general observation.

Furthermore, Fig. 2.8 suggests that male hermit crabs are attracted to PEA at pH 7.7 in a dose-dependent manner. The choice response peaks at a PEA concentration of 10^{-7} mol/L, with 10 out of 14 male hermit crabs choosing PEA, which is significantly different to their reaction in control conditions (Pearson's Chi-squared test with Yates' continuity correction, $\chi^2=5.17$, $df = 1$, $p^* = 0.02$). However, due to the high number of experiments that ended without a decision, the concentration- and pH-dependent attraction/repulsion of hermit crabs in the flume shouldn't be analysed using a binomial model, as used previously in section 2.3.2.

33% of all bioassays in the flume ended without a decision; excluding these datapoints by focusing only on experiments where hermit crabs chose either the flume arm with seawater or PEA would skew the results. Time-to-event analysis, however, can include these datapoints as censored data (time >600 s, but no decision). Furthermore, it combines the time until the decision with the final choice of the hermit crab. This can be visualised in cumulative probability plots, whereby every step signifies a decision. A strong response is characterised by a lot of steps at an early timepoint, whereby the

time is plotted on the x-axis. The cumulative probability plots (Fig. 2.9) below, confirm a strong response of male hermit crabs to PEA, especially at pH 7.7 (Fig. 2.9D), whilst the response of males is much reduced at pH 8.1 (Fig. 2.9C) and negligible for female hermit crabs (Fig. 2.9A-B).

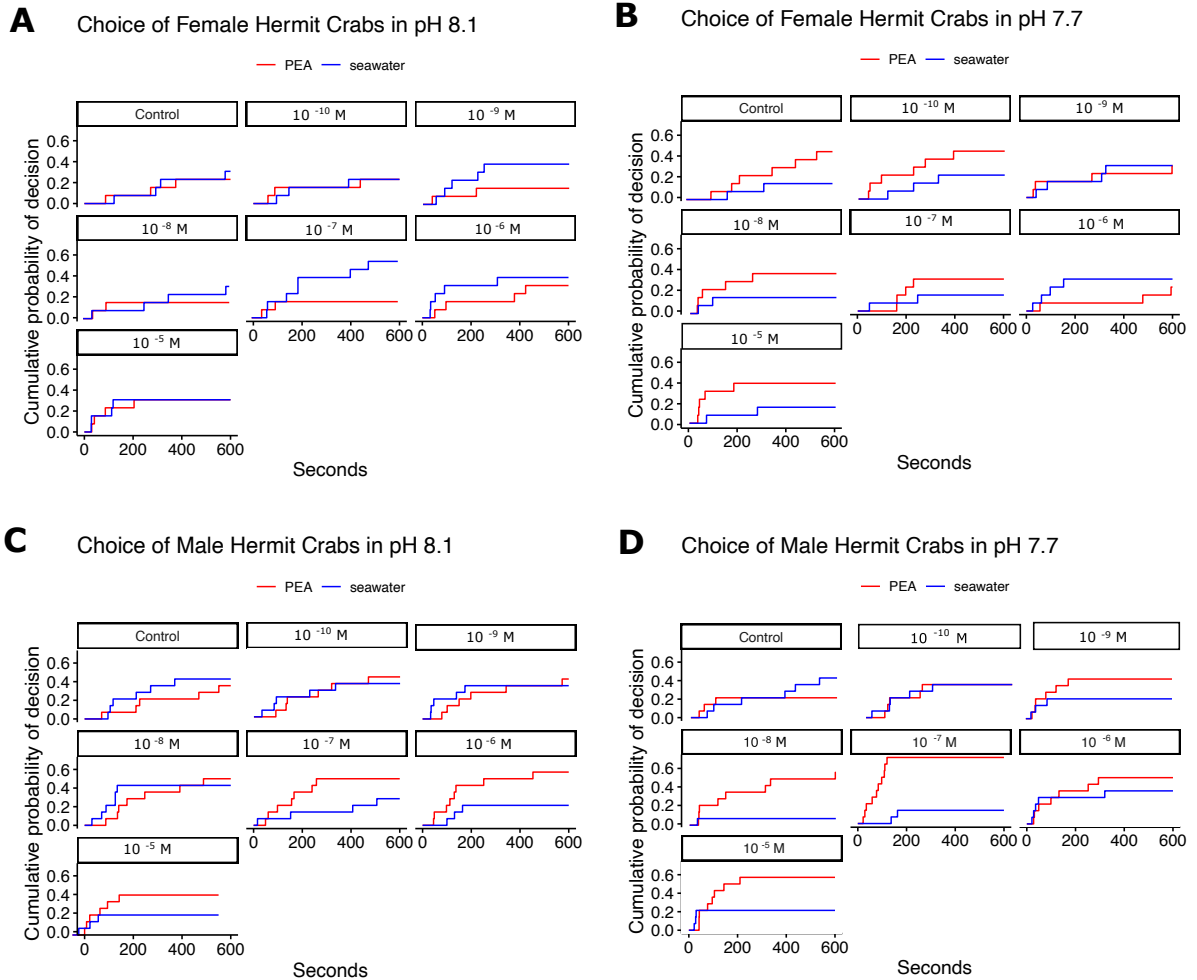


Fig. 2.9: Cumulative probability of decision for PEA (red) and seawater (blue) in flume for females (A & B) and male hermit crabs (C & D) in response to different concentrations of PEA in pH 8.1 and pH 7.7. A strong response is characterised by a lot of steps (decisions, y-axis) at an early timepoint (x-axis). Whilst A & B show no apparent dose-dependent trends for females, males (C & D) seem to choose PEA over seawater in a dose-dependent manner, with the strongest response in pH 7.7.

Considering either endpoint of the experiment (decision for seawater side (blue) as well as PEA side (red)), the ‘motivation’ of the animal to make a decision can be compared across all conditions. Thereby, the data reveals very strong evidence for the concentration (Analysis of Deviance, $\chi^2=91.42$, $df=6$, $p^{***}<0.0001$) and the sex ($\chi^2=16.34$, $df=1$, $p^{***}<0.0001$) to influence the motivation of hermit crabs to cross the decision line. Additionally, the motivation of hermit crabs to cross the decision line significantly depends on the interactive effect of concentration, pH and sex ($\chi^2=21.5183$, $df=6$, $p^{**}=0.0015$). In other words, there is strong evidence that the decision to choose a side of the flume is dose-dependent, pH- and sex-dependent.

Fig. 2.9 suggests little variation in the reaction to seawater (blue) but large differences in the decision for PEA (red) depending on the condition. Hence, a time-to-event analysis specifically focused on the decision for PEA was conducted for each pH condition to further explore the hermit crabs’ attraction to PEA. In pH 8.1, there was no evidence for the concentration of PEA to affect the animals’ decision for PEA (Analysis of Deviance between models with and without concentration as effect, $\chi^2=9.95$, $df=6$, $p=0.13$); and only sex-dependent differences were significant in pH 8.1 (Analysis of Deviance, $\chi^2=33.03$, $df=1$, $p^{***}<0.0001$). As the sex-dependent effect is not affected by the concentration of PEA, the decreased tendency of females to make any decision in the flume experiments, as observed above, is likely to have driven the sex-dependent effect.

In pH 7.7, there is very strong evidence for a positive effect of the concentration of PEA on the choice of hermit crabs for PEA (Analysis of Deviance, $\chi^2=46.25$, $df=6$, $p^{***}<0.0001$). As observed before, the animal’s sex is a significant factor for their reaction to PEA (Analysis of Deviance, $\chi^2=4.74$, $df=1$, $p^*=0.03$). Furthermore, there is reliable evidence for an interactive effect of concentration and sex (Analysis of Deviance, $\chi^2=14.78$, $df=6$, $p^*=0.02$). The hazard ratio plot (Fig. 2.10) shows that in males, the probability of making a decision for PEA was significantly increased for concentrations

10^{-7} mol/L, 10^{-6} mol/L and 10^{-5} mol/L as compared to their response in the control experiments (post-hoc test on emmeans (back transformed from log scale) with Sidak adjustment of p-values, $p^{**}=0.009$, $p^*=0.017$ and $p^*=0.02$ respectively).

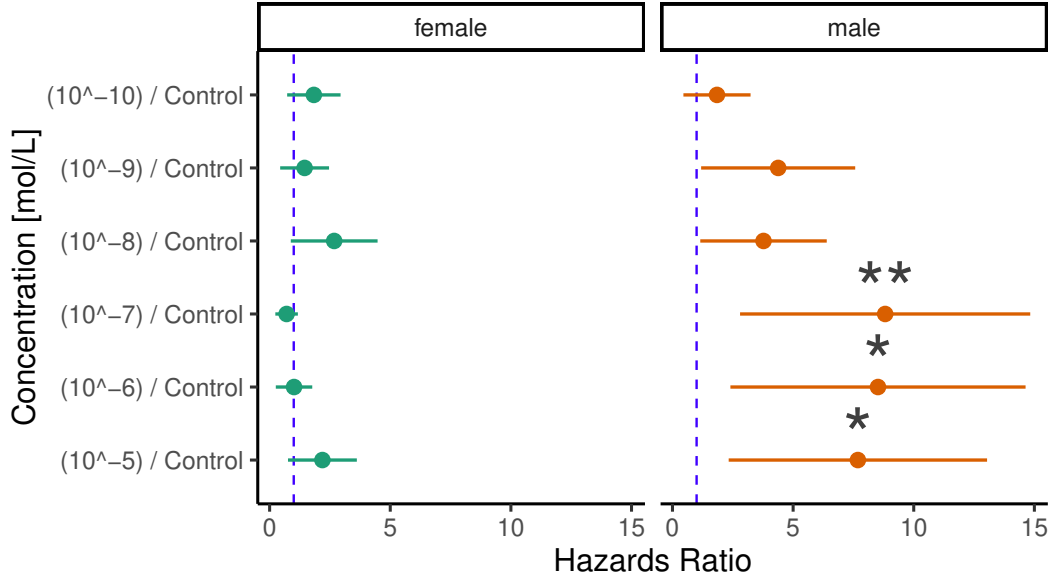


Fig. 2.10: The hermit crabs' decision probability for different concentrations of PEA in the flume at pH 7.7 relative to their response in control conditions. The asterisks depict significant differences between the control and the PEA experiment with $p^* < 0.05$ and $p^{**} < 0.01$. The hazards ratio is the outcome variable in the time-to-event analysis and represents the probability of the decision for PEA in the respective condition as compared to control. The vertical line represents a hazard ratio of 1, meaning zero change in likelihood to move towards PEA compared to control conditions. A higher hazards ratio signifies a higher likelihood for hermit crabs to move towards PEA, as compared to control conditions.

2.3.4 Seasonality

In both, the static tank (section 2.3.2) and the flume experiments (section 2.3.3), a similar sex-specific pattern in the response to PEA was observed: Males were attracted to PEA at reduced pH, and there was little evidence for a response in females. Whilst the static tank experiments were carried out with animals collected in February 2021, at

the height of their reproductive season,¹⁰⁹ the flume experiments were conducted with animals collected in August 2021, 6 months later. Although the results are not directly comparable as the experimental set-ups are different, the similar sex-specific pattern of the results suggests that the response to PEA is not seasonal.

It is important to note, that both sets of animals were acclimatised to 15°C and 12 h/12 h light/dark periods for 3 weeks prior to the experiments to create comparable conditions. The different proportion of females with eggs (40% in the static tank and 15% in flume experiments), however, suggests that the acclimation period might not have completely offset differences in the reproductive state due to seasonal differences.

2.3.5 Weight-dependent vs. Sex-dependent Effects

Male hermit crabs (without their shell) weighed 0.9 g (in static tank experiments) to 1.0 g (in flume experiments) in median, whilst female median weight was 0.7 g (in static tank experiments) to 0.6 g (in flume experiments). Although this median difference of 0.2 g (in static tank experiments) to 0.4 g (in flume experiments) (see Fig. 2.11) is significant (Welch's t-test, $t = -3.26$, $df = 28.09$, $p^{**} = 0.003$ for static tank experiment and $t = -2.84$, $df = 16.09$, $p^* = 0.012$ for flume), there is some overlap between the weight distributions of males and females. This raises the question, whether the sex-dependent effect that was observed in both the static and the flume experiment, is the result of the differences in weight between males and females. In other words: Are larger females attracted to PEA in a manner comparable to same-sized males?

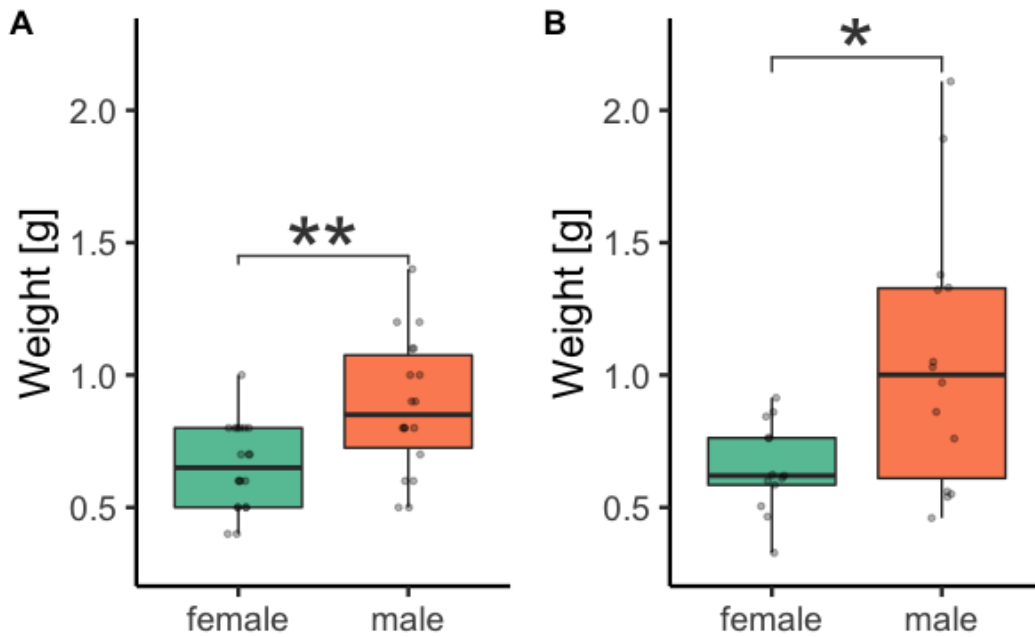


Fig. 2.11: Weight difference between female and male hermit crabs in the static tank experiment (A, see section 2.3.2) and the flume experiment (B, see section 2.3.3). The asterisks depict significant differences according to the Welch t-test, with $p^* < 0.05$ and $p^{**} < 0.01$. Boxplots depict the median with first and third quartile of the distribution. Whiskers extend to 1.5 the interquartile range. The boxplots are overlaid by the actual data points in semi-transparent.

Due to animals making a choice between the seawater and the PEA side, the flume experiment provides no continuous variable to adequately address this question. In the static tank experiments, however, the average distance to the PEA source side at the highest concentration of PEA (x-axis in heatmaps Fig. S1-S2 G & H) is a continuous measure for the hermit crab's attraction to PEA. A linear model shows that the response of hermit crabs to PEA (response to $3 \cdot 10^{-3}$ mol/L on filter paper, highest tested concentration) is pH-dependent and negatively correlated with the weight (measured without shell) of the hermit crab (linear model, adj. $R^2=0.18$, $F=9.36$ on 2 and 73 df, $p^{***}=0.0002$). Whilst the pH ($p^{**}=0.003$) and the weight ($p^{**}=0.004$) significantly affect the attraction to PEA in the linear model, there is no evidence for a sex-specific

effect (Analysis of Variance, $F=0.05$, $df=1$, $p=0.81$). Hence, heavier hermit crabs are more attracted to PEA, irrespective of their sex, whereby the pH significantly increases the attraction to PEA.

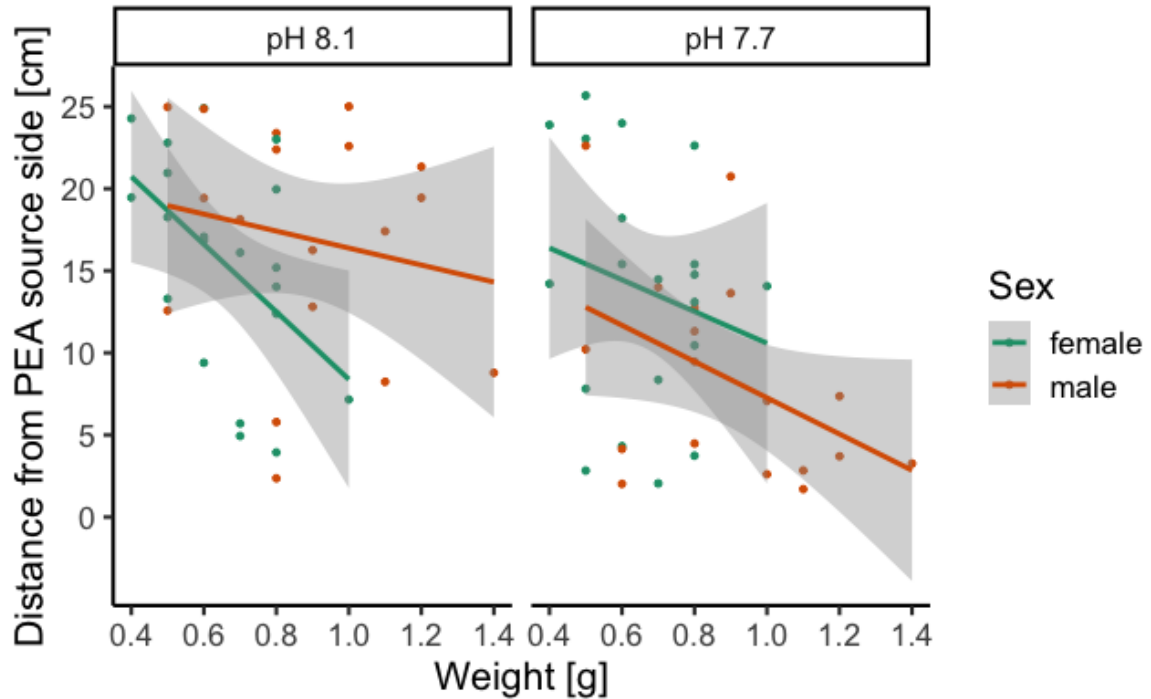


Fig. 2.12: Correlation between the attraction to PEA at the highest concentration ($200 \mu\text{L } 3 \cdot 10^{-3} \text{ mol/L}$ in 1 L) and the weight (measured without shell) of the hermit crab in pH 8.1 and pH 7.7 for females (green) and males (orange). Whilst there are no sex-specific trends in the linear model ($p=0.81$), the pH ($p^{**}=0.003$) and the weight ($p^{**}=0.004$) significantly affect the distance to the PEA source side. Shaded area represents 95 % confidence interval of the linear model.

2.3.6 pH-dependent Behavioural Effect Size Compared to Changes in Biologically Active Compound

Comparing the pH-dependency of the behavioural response to PEA (‘biological effect size’) to the abundance of PEA in the different protonation states (‘chemical effect size’) allows me to estimate whether the pH-dependent biological effect could be a consequence

of an increase in biologically active compound upon protonation of PEA. With a pK_a of 9.83,¹⁰⁵ the amino group in PEA can be protonated. The pH-dependent abundance of protonation states of PEA can be calculated using the Henderson-Hasselbalch equation (see eq. 1.7).

With respect to the ‘biological effect size’, Fig. 2.13A & C show that, when exposed to 200 μL of $3 \cdot 10^{-3}$ mol/L, hermit crabs are on average 37% closer to the PEA source side (6.4 cm median difference) at pH 7.7 than at pH 8.1 (Wilcoxon test, $W = 450$, $p^{**}=0.004$).

Using the Henderson-Hasselbalch equation (eq. 1.7), the percentage of protonated and neutral PEA can be estimated for different pH conditions (Fig. 2.13B) to compute the ‘chemical effect size’. With a pK_a of 9.83,¹⁰⁵ PEA is mostly protonated in aquatic environments. At pH 8.1 98.0% and at pH 7.7 99.3% of PEA are protonated. The difference in protonation state abundance between the two experimental pH conditions is therefore only 1.3%.

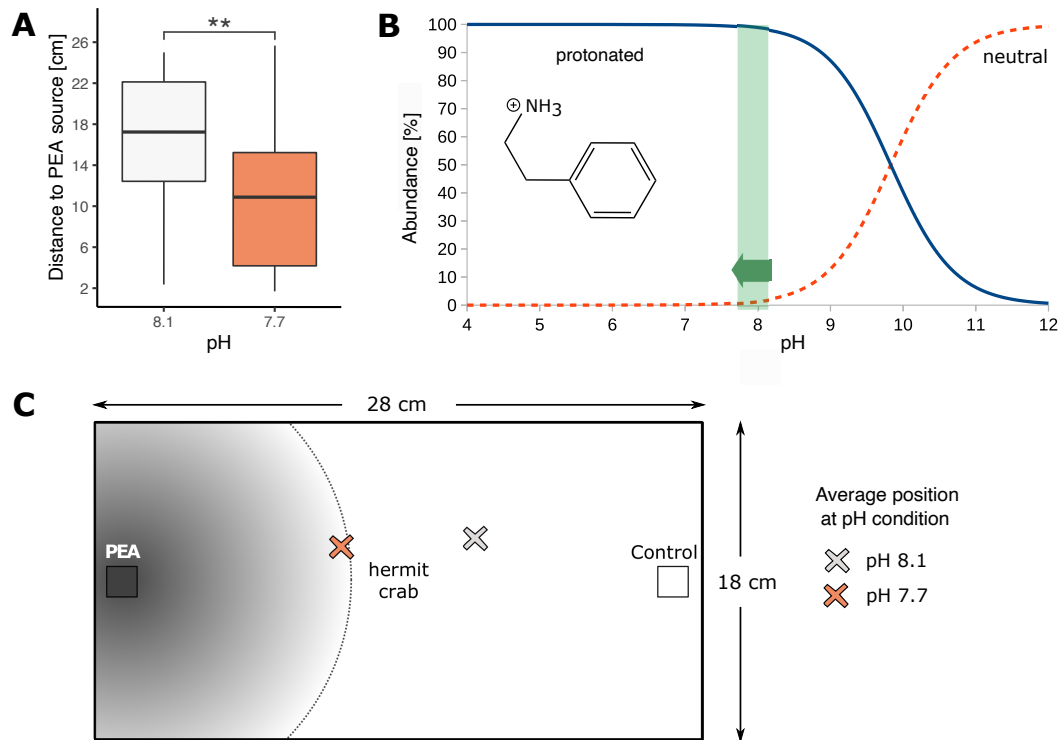


Fig. 2.13: Comparison of the effect size of the pH changing hermit crab behaviour and the protonation state of PEA respectively. (A) shows the distance to the PEA source side in the static tank experiments at the highest concentration in different pH conditions, combining the response of males and females. The asterisks indicate a significantly closer average position at pH 7.7 with $p^{**} < 0.01$. (B) is a plot of the Henderson-Hasselbalch equation for PEA to visualise the proportion of the neutral (red, dashed) and protonated (blue, solid) state present across the pH range. The pH range from 8.1 to 7.7 is shaded in green. (C) depicts a topview of the experimental tank, marking the average position of hermit crabs (data based on output from behaviour tracking software), regardless of sex, at pH 7.7 (orange) and pH 8.1 (white) in relation to the diffusion of a PEA point source. The dotted line marks the zone where a point source of 200 μL PEA at 10^{-3} mol/L reaches 10^{-7} mol/L, as extrapolated assuming spherical diffusion from the point source (filter paper).

Finally, although flume experiments and static-water tank experiments are not directly comparable, a rough estimation of the accordance of the concentration conditions in both set-ups can be achieved by assuming a spherical diffusion from the point source (filter paper) in the static-water tank experiments. The distance at which the most effective concentration of 10^{-7} mol/L in the flume (for pH 7.7, see section 2.3.3) is reached in the

static-water tank can be calculated. For the diffusion of 200 μL PEA at $3 \cdot 10^{-3}$ mol/L, a spherical diffusion leads to a concentration of 10^{-7} mol/L at a distance of 11.27 cm from the filter paper (see dotted radius in Fig. 2.13C). At pH 8.1, the average position of hermit crabs lays clearly outside the identified radius, whilst at pH 7.7, hermit crabs move, on average, within the area of the most effective concentration of PEA.

Increasing the amount of active compound on the point source by 1.3 % ($3.039 \cdot 10^{-3}$ mol/L) changes this radius by merely 0.05 cm, which is hence not visible in the figure. The ‘chemical effect size’ due to protonation of the infochemical is therefore several orders of magnitude below the ‘biological effect size’ of the pH-dependent chemically mediated movement of hermit crabs.

2.4 Discussion

This chapter explores the behavioural response of hermit crabs to PEA, assessing pH-, sex-, weight-, and season-dependent patterns; and thereby starting to explore the ecological role of PEA as an infochemical for crustaceans. Observing an attraction of hermit crabs to PEA in the very first experiment of my PhD (section 2.3.1) stands in contrast to observations with mammals and sea lampreys, which avoid the smell of PEA.^{24,25} This called for a rather uncommon approach in chemical ecology: Testing a known infochemical for its unknown ecological role. Traditionally, chemical ecologists tend to identify unknown infochemicals (see e.g. Poulin et al. (2018)⁹⁰) or test the behavioural response to unknown chemicals from animal secretion (‘conditioned water’, see Clark et al. (2020)⁴⁷ and Dixson et al. (2010)⁴⁵ for examples).

Both, the experiments in static water and flume found a weight/sex dependent attraction to PEA that was amplified in reduced pH conditions. Receiving the same results with different methods testifies the reproducibility of my findings. In the context of the

current dispute on reproducible methods in marine infodisruption research,^{47–49,52} I chose to exclude observer bias by using behaviour tracking software with blind analysis and to repeat my own experiments with variations in methods (static water and in-flow) to ensure robust results.

Section 2.3.1 shows that hermit crabs are attracted to PEA in a pH-dependent manner at the chosen concentration range. Their attraction (rather than avoidance) make it unlikely that this infochemical acts as a predator cue for hermit crabs. Similarly, opposite behavioural responses to an infochemical have also been observed for cadaverine and putrescine, which are repulsive odours for zebrafish,⁷² but have been reported to be feeding cues for goldfish.⁷³ To explore alternative hypotheses, I repeated the initial experiment with small variations and recorded additional data to explore sex and weight-dependent effects (section 2.3.2-2.3.3). Although additional qualitative behavioural observations might have been insightful, the small size of hermit crabs and partial obstruction of their body by the shell from top view (i.e. in videos used for tracking) didn't allow for unambiguous interpretations of their behaviour in the chosen set-ups. Instead, I focused on pH-dependent, sex-and weight-dependent effects on the attraction/repulsion in response to PEA.

Originally, the pH conditions for this set of experiments were chosen based on the average pH conditions in current and end-of-the-century oceans:³¹ The current average pH 8.1 of ocean surface water is known to decrease to an average of pH 7.7 by the end of the century.³¹ My decision to study pH-dependency of the response to PEA was based on my hypothesis that PEA-mediated information is disrupted by ocean acidification. Ocean acidification is known to have the potential to disrupt different steps of the chemically mediated information cascade,³⁷ but pH-dependent effects are not limited to climate change related scenarios. Hermit crabs live in intertidal environments with daily and seasonal pH fluctuations,⁸² whereby coastal diel pH extremes often exceed open-ocean

average pH changes for 2100.⁸¹ A study on seagrass habitats⁸¹ indicates that the current average diel cycle (data from 2015) of pH 8.26 during the day to pH 7.87 at night could increase in range and shift to pH 8.02 during the day and pH 7.47 at night by the end of the century. Exploring pH-dependent effects is therefore as important for today's hermit crab habitats as for our understanding of average pH-dependent effects by the end of the century.

My results show that the response of hermit crabs to PEA at the highest tested concentration was significantly increased in pH 7.7 as compared to pH 8.1 (section 2.3.1- 2.3.1). Therefore, decreasing the pH increases the potency of PEA. Although negative impacts of ocean acidification on marine animal behaviour predominate in the literature,⁵⁰ some behaviours were shown to increase under elevated CO₂ conditions, which decrease the pH (reviewed in Clements and Hunt, 2015⁵⁰). This study indicates that PEA is one of the cues that are amplified by decreased pH conditions.

When the pH is reduced from 8.1 to 7.7, the abundance of the protonated state of PEA increases by less than 2% (Fig. 2.13B), whilst the attraction of hermit crabs changes significantly (Fig. 2.13A), with animals being on average 37% closer to the PEA source at pH 7.7 as compared to pH 8.1. This indicates that the increase in abundance of protonated PEA alone cannot explain the changes in behaviour. The small change in the amount of active compound of PEA within the range of ocean acidification raises the question of the mechanism by which the pH influences the behavioural response of hermit crabs to PEA. Some animals can sense CO₂ levels in terrestrial¹²⁶ or aquatic environments¹²⁷ to locate their prey. But pH sensing in the absence of changes in CO₂ levels, has not been reported. Acute pH changes are likely to affect the sensory signalling cascades only indirectly, by altering pH sensitive residues in proteins (such as receptors or enzymes) or infochemicals.^{41,74} Chapter 4 assesses the potential mechanisms

underlying the observed pH dependency of the behavioural response of hermit crabs to PEA.

As static-water tank experiments showed a significant attraction to PEA in reduced pH conditions only (pH 7.7), but not current average pH 8.1, I set out to measure a larger concentration range for both pH conditions. Using in-flow concentrations in a flume set-up allowed me to determine the most attractive dose (threshold concentration). However, although the concentration range was increased, I again only observed a significant (sex-dependent) attraction to PEA in pH 7.7, but not in pH 8.1 (see Fig. 2.9), similarly to my results from static tank experiments. Whilst PEA evoked a clear dose-dependent attraction of male hermit crabs in pH 7.7, there was no statistical evidence for a response of the same animals in current average oceanic pH 8.1. Hence, the full behavioural response to PEA was only observed in reduced pH conditions. This indicates that the pH of the medium is a crucial aspect of the chemically mediated message of PEA: Only pH and infochemical together transmit the information to its full extent. The pH might therefore be an indicator of the authenticity of the PEA-mediated information.

The inseparability of chemical information and medium allows for several potential interpretations of the ecological role of PEA for hermit crabs. Firstly, the sex-dependent response to PEA suggests a role of PEA in reproduction. In many crustacean species, urine-borne chemicals play a crucial role in chemical communication, mediating information about conspecific properties such as sex, sexual receptivity and moult stage,¹⁵ health status,¹²⁸ motivation to fight,¹²⁹ and individual identity.¹⁰⁰ As infochemicals released with urine are carried in more acidic conditions than the surrounding seawater,⁵⁹ PEA in reduced pH conditions might be associated with urine-borne reproductive cues for hermit crabs. However, the parallels between my experiments carried out with animals from winter and summer conditions (section 2.3.2 and 2.3.3) indicate that the

response to PEA is unlikely to be seasonal and a role of PEA in reproductive behaviour is therefore less likely. Littoral hermit crabs reproduce mainly in late winter, with the height of their reproductive season in February and March,¹³⁰ which coincides with experiments in static water on sex/weight dependency (section 2.3.2). The flume experiments (section 2.3.3), however, were carried out 6 months later, during late summer, showing similar pH- and sex/weight-dependent response patterns. However, the experimental set-ups in static-water tank conditions and flume are not directly comparable. Therefore, the seasonality of the ecological role of PEA remains speculative and further experiments are required to explore whether PEA could play a role in reproductive behaviour. Section 2.3.5 showed that the observed sex-dependent effect could be explained by differences in weight between males and females. The sex-dependent response of hermit crabs to PEA therefore does not necessarily equate to a role of PEA in mediating reproductive behaviour.

Another potential interpretation of the pH- and weight-dependent attraction of hermit crabs to PEA is that PEA could be a feeding cue. As bacteria can biosynthesise PEA from organic detritus by decarboxylating phenylalanine,⁷ PEA could act as a feeding cue for scavengers. Increased CO₂ production through bacterial degradation of bioorganic matter (such as carcasses) decreases local pH. As scavengers,¹⁰⁷ *P. bernhardus* might therefore associate the combination of low pH and PEA with food. Ocean acidification is known to increase bacterial degradation activity.¹³¹ The potential pathway of pH interfering with the signal source is represented by pathway 1 in the scheme of potential mechanisms by which decreased pH can alter animal behaviour (Fig. 1.1). If PEA is indeed a feeding cue for hermit crabs, the observed amplified response of hermit crabs in low pH conditions indicates that ocean acidification could promote its availability and importance in future oceans. This is of particular interest as the efficacy of many fresh

food indicators such as amino acids and peptides have been shown to decrease with ocean acidification.^{41,44,57,102}

It is important to note that foraging is not necessarily detached from social interactions. When competition is intense, large hermit crabs are known to be more successful at scavenging than smaller animals.⁹⁹ Anticipating competition could explain the observed weight-dependent response of hermit crabs to PEA. However, Ramsay et al. 1997⁹⁹ showed that decreasing the density of hermit crabs at a feeding patch (carrion) reduced the observed size-dependent effects on the attraction to the feeding cue(s). As the field study does not include single animal experiments, it remains unclear whether the size-dependency of the attraction to feeding cues persists to a small degree in the complete absence of competition. To minimise behavioural effects due to competition, all behaviour assays in this thesis were carried out with single animals.

A third potential interpretation of the amplified response of hermit crabs to PEA at reduced pH conditions also hinges on the notion that PEA might be expelled with urine (see above for a potential role in reproductive behaviour). As discussed above, PEA being urine-borne would be indicative of a potential role of PEA in chemical communication, i.e. intra- or interspecies social interactions. Crustaceans are known to time the release of their urine with agonistic interactions, whereby the urine has been hypothesised to contain infochemicals mediating individual status information to the fight opponent.¹³² Although, crustaceans can control the release and transfer direction of urine through their gills, it is unknown whether senders can manipulate the composition of urine-borne compounds.⁹

It might seem counter-intuitive to observe the attraction of hermit crabs to an infochemical and hypothesise a potential role in agonistic interactions. However, actively seeking out an interaction or fight with conspecifics is common for crustaceans with active dominance hierarchies such as hermit crabs.^{133–135} Similarly, crayfish were found

to explore the source of the odour from a dominant male, actively moving towards the nozzle of a flume supplying the conditioned water.¹³⁶

Animals living in social groups, such as hermit crabs, mediate their social interactions by forming rank orders,¹³⁷ which are determined and maintained through agonistic behaviours.¹³⁸ The formation of rank orders in social groups can be explained by three different mechanisms. Exploring potential mechanisms by which hermit crabs form and maintain rank orders can give further indications on the potential role of PEA in agonistic interactions.

Firstly, hierarchies can be maintained through individual recognition, i.e. the ability of an individual to discriminate between conspecifics by detecting and memorising a unique set of characteristics and cues that define every individual.^{133,137} Although this mechanism is common in vertebrates,¹³⁷ it is a complex task for invertebrates.¹³³ Secondly, an individual might be able to extrapolate its rank from the outcome of previous fights, thus establishing its level of confidence.¹³⁹ Rather than focusing on the opponent, this mechanism reflects the animal's expectation of the outcome of future fights based on its own motivation to attack (e.g. cuttlefish *Sepia officinalis*¹⁴⁰). The third mechanism by which rank orders can be established is status recognition.¹³⁹ Thereby, an individual assesses the agonistic potential of an opponent based on a (chemical) signal or cue that provides information on an animal's physical ability or fighting experience (e.g. crayfish¹²⁹).

Hermit crabs (*Pagurus bernhardus*) are known to maintain active dominance hierarchies that are based on within-group experiences and visual displays.¹⁴¹ Hence, hermit crabs can recognise and distinguish between individuals.¹⁴¹ Dominance hierarchies that are based on individual recognition have only been described in few other invertebrate species (e.g. *Homarus americanus*¹⁴²). In a hermit crab species closely related to *Pagurus bernhardus*, *Pagurus longicarpus*, individual recognition proved not to entail a

memory of all social partners but rather the ability to distinguish between known and unknown cues from individuals. The evidence of formation and maintenance of dominance hierarchies in hermit crabs through individual recognition¹³³ seems to conflict with findings from Winston and Jacobson (1978),¹³⁴ who showed that *Pagurus longicarpus* recognise their opponents' aggressive state, not its individual characteristics. However, the conflict between these mechanisms is built on the premise that there can be only a single mechanism by which dominance hierarchies are formed and maintained. In fact, fashioning hermit crab models from dried exoskeletons, Hazlett (1968)¹⁴³ showed that hermit crabs use visual cues from cheliped and ambulatory leg positioning for status recognition a year before publishing his study on individual recognition in hermit crabs.¹⁴¹ This indicates that dominance hierarchies in hermit crabs might be mediated by multiple processes, namely individual recognition and status recognition, which do not have to be exclusive.

Individual status can be signalled to opponents through cheliped size.¹⁴⁴ As cheliped and body size of hermit crabs were not measured in this study to reduce handling stress, the animals' weight was used as a proxy. Cheliped size is known to be closely related to body weight in hermit crabs.¹⁴⁴ However, the relationship between weight and cheliped size is sex-dependent in *P. bernhardus*, with males having larger chelipeds than females, even when cheliped size was adjusted by body size.¹⁴⁴ Similarly, Fig 2.12 shows that in pH 7.7, the weight-dependent attraction of hermit crabs was stronger for males than for females. Although the difference was not significant, adjusting the weight by cheliped size in future experiments might close this sex-specific gap, creating a more reliable variable to explore PEA-mediated behaviour (see section 3.3.2-3.3.3 for use of cheliped-adjusted weight in shore crabs).

A potential interpretation of the pH and weight-dependent response to PEA is that PEA is involved in mediating status information to establish dominance hierarchies in

hermit crabs. Similarly to my results with *P. bernhardus* in the flume, crayfish (*Procambarus clarkii*) spend more time near the odour source of dominant individuals in a flow-through flume, irrespective of previous experience with that animal.¹³⁶ Furthermore, the response to dominant odours in *P. clarkii* was more pronounced in males, responding more aggressively (as measured by meral spread), which also correlates with my observation of a sex/weight-dependent response in *P. bernhardus*.

The parallels between the study with *P. clarkii* and my results with PEA in *P. bernhardus* raise the question whether PEA could be a transferable infochemical, applying to multiple species (see chapter 3). The ubiquity of PEA as a decarboxylation product of the amino acid phenylalanine¹⁰⁶ indicates that this small biogenic amine could be expelled with urine in many species with high protein diets. Phenylalanine is found in dietary protein and its metabolite PEA is known to be excreted with urine in mammals.²⁴ PEA levels in crustacean urine are further addressed in chapter 3.

Due to the above discussed limitations of exploring qualitative behaviours of hermit crabs in response to PEA in the established assay set up, the ecological role of PEA for hermit crabs cannot be further narrowed down. Based on the observed pH- and sex/weight-dependent attraction of hermit crabs to PEA, I conclude that PEA could be involved in mediating reproductive behaviour, it could be a feeding cue or mediate agonistic interactions. In the following chapter, I will explore parallels in the response to PEA of a distantly related crustacean species, which will also allow me to explore the presence of PEA in crustacean urine and add qualitative behavioural observations to further explore the ecological role of PEA for crustaceans (chapter 3).

2.5 Conclusion

I was able to demonstrate that PEA is an attractant for hermit crabs at an in-flow concentration of 10^{-7} mol/L, whilst being widely considered a predator cue. Thereby, the response to PEA depends on the pH within a range relevant for ocean acidification scenarios by 2100 and pH fluctuations in intertidal habitats. Interestingly, decreasing the pH amplifies the response to PEA. The modes of action of the pH on the behavioural response are yet to be explored (chapter 4), showcasing the need for cross-disciplinary research between chemistry and ecology to help unravel the underlying mechanisms of infodisruption in chemical ecology. Additionally, the observed weight/sex-dependency of the attraction of hermit crabs to PEA indicates that PEA might be involved in reproductive behaviour, foraging or mediate agonistic interactions. Further research is needed to promote our understanding of the role of PEA for crustaceans in current and future oceans. Thereby, assessing the presence of PEA in crustacean urine and describing behavioural responses beyond attraction/repulsion is key to explore a potential role of PEA in crustacean chemosensory behaviour.

CHAPTER 3

Is PEA a Transferable Infochemical?

3.1 Introduction

Although some infochemicals are species-specific, an array of chemical communication is based on transferable infochemicals (see section 1.2). To explore the transferability of the behavioural observations in hermit crabs in response to PEA to other species, I compare my previous findings with hermit crabs (chapter 2) to the response of shore crabs (*Carcinus maenas*) to PEA.

3.1.1 PEA Mediated Behaviours

Urine of carnivorous predators is known to contain much higher levels of PEA than urine of herbivores,²⁴ which in turn elicits defensive responses and avoidance in various prey, such as rodents^{24,145,146} and sea lamprey.^{25,91} Other fish, however, such as white suckers (*Catostomus commersonii*) and rainbow trout (*Oncorhynchus mykiss*) show no evidence of avoidance in a manner comparable to sea lamprey.^{147,148} Although PEA has been suggested to be used for pest control measures of sea lamprey in the Upper Great Lakes of North America,⁹¹ to the best of my knowledge, to date, no aquatic non-fish species have been tested for their behavioural response to PEA.

To assess a potential role of PEA for aquatic species, determining its sources in aquatic environments is paramount. Whilst PEA levels in urine have been measured for sev-

eral terrestrial mammals,²⁴ to date, to the best of my knowledge, the urine of aquatic species has not been tested for PEA. However, PEA is known to be present in aquatic environments through bacterial decarboxylation of the amino acid phenylalanine in decomposing or metabolised animal protein (such as carrion and animal excretions).^{106,149} Furthermore, PEA has been found in algae,^{94,150} where it is hypothesised to act as a feeding deterrent.⁹³ Although aquatic food sources, such as carrion and algae thus contain PEA, to the best of my knowledge a feeding response (or deterrence) has not yet been reported in response to PEA.

3.1.2 Shore Crabs and their Chemosensory Behaviours

Shore crabs (*Carcinus maenas*) and hermit crabs (*Pagurus bernhardus*) are both scavengers^{99,151} and often co-occur in British coastal environments.^{97,151} However, shore crabs inhabit a different ecological niche to hermit crabs: In addition to scavenging, shore crabs are also predators for a large variety of organisms.¹⁵¹ Although native to the UK, shore crabs are a very destructive invasive species in other parts of the world, including both coasts of North America, Australia, South Africa and Argentina.¹⁵¹ Their damage to aquaculture (especially oysters) and potential for further invasion secured shore crabs a place among the world's 100 worst invaders by the International Union for the Conservation of Nature (IUCN).¹⁵² Their invasive potential is in part due to their phenotypic plasticity, allowing *C. maenas* to tolerate a wide range of environmental conditions with regards to low oxygen levels, temperature and salinity.¹⁵¹

Whilst hermit crabs and shore crabs are both crustaceans, anomurans ('false crabs', e.g. hermit crabs) have probably separated from the line leading to true crabs (brachyuran, e.g. shore crabs) during the lower Jurassic period, about 200 million years ago.¹⁵³ Like hermit crabs, shore crabs are known to display a variety of chemically mediated

behaviours.^{15,154,155} Similarly to hermit crabs, the literature provides few examples of known infochemicals for shore crabs. A notable exception, however, is the sex pheromone of shore crabs. It has been identified as a bouquet of the nucleotides uridine diphosphate and uridine triphosphate, which are released by females as a by-product of chitin biosynthesis during the moulting stages.^{14,15} Hence, the mating season of *C. maenas* is synchronised with female molting (July-September in UK^{59,151}). Copulatory behaviour of males in response to the sex pheromone or female urine is marked by male crabs advancing towards the female, rising on pereopods 2 to 4, probing the softness of the female carapace with chelipeds and proceeding to cover the female with their body to claim their mate and ensure her safety after copulation.^{151,156} Thereby, large red phase males have a competitive advantage over smaller rivals.^{151,157}

Infochemicals also play a crucial role in shore crab foraging.^{155,158} To characterise feeding behaviour in crustaceans, Lee and Meyers (1996)¹⁵⁹ proposed a five phase model, whereby detection (1) is followed by orientation towards or away from the cue (feeding attractant/repellent; 2), followed by locomotion (3) and finally initiation (4) and continuation and or termination of feeding (5). Whilst feeding attractants and repellents/arrestants act from a distance (stage 1-3) and are detectable at low concentrations, iniciants, suppressants, stimulants and deterrents (stage 4 & 5) function upon direct contact of the food source with the chemoreceptors.¹⁵⁹ Thereby, feeding cues can act on distinct or multiple stages of the cascade.¹⁵⁹ Although the exact chemical nature of feeding cues is often unknown,¹⁵⁵ some amino acids and amines, such as glycine and betaine, have been identified to stimulate feeding.¹⁵⁵ Shelton and Mackie (1971)¹⁵⁸ showed that a synthetic mixture of feeding cues (containing 18 amino acids, 3 organic acids, 4 nucleotides, betaine, hypoxanthine and inosine), based on the composition of the short-necked clam *Tapes japonica*, is more attractive to *C. maenas* than its individual components. This indicates that feeding attraction is based on additive effects

of several chemical feeding cues and no single compound can reproduce the effect of a chemical feeding bouquet.

Finally, agonistic behaviours are well studied for shore crabs.^{154,160–163} As urine-borne information are known to define the course of agonistic interactions in crayfish, lobsters and spiny lobsters,^{132,164,165} infochemicals are likely to be involved in shore crab agonistic behaviours too. The frontal position of the nephropores (on top of the gill opening) allows crustaceans to send urine-borne chemical messages towards their opponent.⁹ Crayfish *Astacus leptodactylus*, for example, are known to manipulate the direction of urine release as well as its timing.¹³² Similarly, spiny lobsters (*Panulirus argus*) use urine-borne chemical signalling, paired with physical aggressive behaviour, during agonistic interactions.¹⁶⁵ This indicates that crustacean urine contains chemical information about the fighting ability or aggressiveness of the signal emitter. However, the identity of these infochemicals that mediate agonistic interactions are still unknown.

Visual agonistic displays, on the other hand, have been studied in detail: In brachyuran crabs, a visual display¹⁶⁶ is defined as a motor pattern that is associated with communicatory activities. Many features are common in agonistic displays across different crab species: The body is raised above the substrate with the merus of the walking legs held horizontally and at right angles to the carpus and propodus.¹⁶⁶ Additionally, the claws are exhibited ('cheliped display') and the body is usually oriented towards the source of disturbance, for example a predator, a rival, or a potential mate.¹⁶⁶ Game theory predicts that during an agonistic encounter, individuals compare their resource holding potential (RHP) before deciding to escalate into a fight.^{167,168} The RHP consists of a variety of interacting descriptors, including the animal's morphology (body size, weight or weapon size^{162,169}), physiology (energy reserves¹⁷⁰), and previous agonistic experience.¹⁷¹ In shore crabs, cheliped size is known to be a better indicator for the RHP (and consequently for winning a fight) than body weight.¹⁶²

3.1.3 Research Approach and Hypotheses

This chapter addresses the research question of the transferability of the sex/weight-specific response to PEA in hermit crabs to other crustacean species.

To explore the transferability of the observed sex- and pH-specific attraction of hermit crabs to PEA to other species, I compare the previous findings (chapter 2) to the response of shore crabs (*Carcinus maenas*) to PEA. To ensure comparability between the datasets with hermit crabs and shore crabs, I use the same design of static-water tank experiments as previously established, scaled up in size to accommodate the larger size of shore crabs. Hermit crabs and shore crabs often co-occur at British coasts and are hence likely to be exposed to similar environmental infochemicals. Furthermore, as the decarboxylation product of phenylalanine, an essential amino acid found in dietary protein,¹⁰⁶ PEA could be ubiquitous in animal excretions and/or food sources.²⁴ I hence hypothesise that shore crabs show a weight/sex-dependent attraction to PEA, comparable to the response observed in hermit crabs.

The chelipeds of shore crabs can be measured more reliably than for the smaller hermit crab. I hypothesise that female and male shore crabs differ significantly in their cheliped sizes as well as their weight (as observed for hermit crabs). Furthermore, I hypothesise that the claw size-adjusted body weight significantly affects the response of shore crabs to PEA, with heavier crabs being more strongly attracted to PEA.

As a predator,¹⁵¹ *C. maenas* is expected to accumulate high levels of PEA which could be released in the urine.²⁴ The larger size of shore crabs (as compared to hermit crabs) allows for the extraction of urine from shore crab gills to determine the presence of PEA in crab urine. I hypothesise that shore crabs excrete PEA in their urine. As PEA might be associated with diet,²⁴ I further expect that PEA conveys information on the signallers size or, more generally, its resource holding potential (RHP).

To enable acid-base regulation, the pH of crustacean urine is known to be below the pH of the aquatic environment,⁵⁹ which provides a potential explanation for the amplified response of hermit crabs to PEA at reduced pH if the compound is urine-borne (as discussed in section 2.4). I hence expect the response of shore crabs to PEA to be amplified in reduced pH conditions, similarly to the results in hermit crabs. The presence of PEA in shore crab urine would suggest a potential role of PEA in social interactions: agonistic behaviour or reproductive behaviour during mating season. Testing shore crabs outside their reproductive season, I therefore hypothesise that shore crabs show behavioural displays that are associated with agonistic behaviour, such as cheliped display and escape behaviour in response to PEA.

In summary, this chapter is guided by three hypotheses: 1. shore crabs and hermit crabs show comparable weight-dependent attraction to PEA, 2. shore crabs show significantly increased escape behaviour and cheliped displays in response to PEA as compared to control conditions and 3. PEA is excreted in shore crab urine. Confirming all three hypotheses, would allow me to confirm the main hypothesis for this chapter, that PEA could be a transferable infochemical mediating agonistic interactions in crustaceans.

3.2 Materials and Methods

3.2.1 Shore Crab Collection and Husbandry

Shore crabs (*Carcinus maenas*) were collected at low tide from Whitby (54.486914°N 0.612701°W), UK, using raw bacon as bait. For behavioural experiments, animals were collected on the 3rd of October 2021 and shore crabs for urine extractions were collected on the 29th of October 2021. The animals were transferred to the aquaria facilities of the University of Hull and acclimatised to pH 8.0 ± 0.1 $15 \pm 1^\circ\text{C}$, a twice weekly

feeding rhythm with thawed cooked blue mussel and a 12h/12h light/dark cycle. 48 animals used in behaviour assays were kept in natural seawater (18 tanks) and 5 animals for urine extractions in artificial seawater (2 tanks), both in circulating water systems of 1500 L with a salinity of 34-36 PSU in 60 L tanks at a density of 3-6 animals per tank. The alkalinity of the husbandry water for animals kept for behaviour assays was 130 ± 12.5 mg/L (as CaCO_3 , average \pm standard deviation). Nitrate levels, pH and salinity were checked regularly and weekly 15% water changes ensured adequate water quality.

3.2.2 Behavioural Choice Experiments with Shore Crabs

Behaviour assays were carried out with the help of Amber Jones. The behavioural response of 24 male and 24 female shore crabs to PEA was recorded on video in pH 8.1 and pH 7.7. All animals were characterised prior to the experiments by weighing them, measuring their carapace width at the widest point, by determining their dominant claw by size comparison and by measuring their dominant claw length, claw height and dactyl length (see Fig. 3.1).

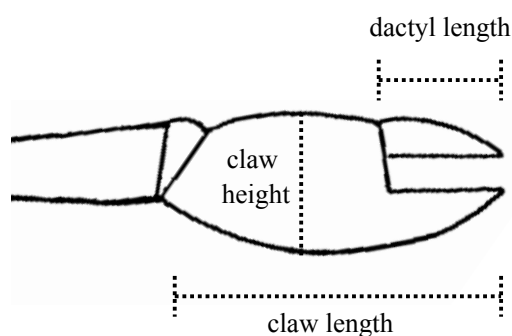


Fig. 3.1: Claw measurements in shore crabs. Image of claw is based on drawing from Wright (1968).¹⁶⁶

For identification, a number was glued to each shore crab's carapace using super glue gel (Supadec), which was left to dry completely before returning the animals to their husbandry tanks. Prior to the experiments, shore crabs were not fed for 5-7 days to standardise appetite levels. For experiments in pH 7.7 the bioassay water was adjusted in batches of 120 L using 1 mol/L hydrochloric acid (diluted from 37% hydrochloric acid, Fisher Scientific). The artificial seawater for bioassays was 17-19°C, had a salinity of 35 ± 1 PSU and the total alkalinity averaged at 133.9 ± 10.1 mg/L for pH 8.1 and 106.0 ± 2.0 mg/L for pH 7.7 (as CaCO_3 , average \pm standard deviation).

As shore crabs are considerably larger than hermit crabs, a 49 cm \times 29 cm assay tank was chosen and filled with 10 L artificial seawater (instead of 1 L for hermit crabs). To ensure comparability between the assays with hermit crabs and shore crabs, the point source for the cue was kept at 200 μL , but due to the 10-fold increased bioassay water volume, the concentration of the point source was increased 10-fold to $3 \cdot 10^{-2}$ mol/L, $3 \cdot 10^{-3}$ mol/L, $3 \cdot 10^{-4}$ mol/L and $3 \cdot 10^{-5}$ mol/L. Considering the about 1.5-fold increased tank dimensions, the cue was allowed to diffuse for 30 s instead of 20 s (as used for hermit crabs) and the assay was recorded for 3 min instead of 2 min. Preliminary experiments confirmed that streaks of a 200 μL food dye (black, 1:10 dilution, Dr. Oetker) can diffuse into about a quarter of the bioassay tank in 30 s, which is comparable to 20 s in the hermit crab bioassay tank.

Each bioassay started with an acclimation of the animal to the experimental conditions for 3 min in a separate tank. Then, the shore crab was transferred to the center of the assay tank and filter papers (1 cm^2 , Whatman No. 3), containing the cues, were dropped on either side of the tank. The animal was caged for 30 s to allow the cues to diffuse. Choosing a perforated bucket turned upside down to cage the animal instead of a cylinder (as used for hermit crabs), reduced initial flight behaviour at the beginning of the assay, as the animal could not see the experimenter's hand approaching to lift the

cage. The cues on the filter paper were either a control (left empty) or 200 μL PEA at $3 \cdot 10^{-2}$ mol/L, $3 \cdot 10^{-3}$ mol/L, $3 \cdot 10^{-4}$ mol/L and $3 \cdot 10^{-5}$ mol/L, which was prepared with 2-phenylethylamine hydrochloride (Sigma-Aldrich, 98 %) in artificial seawater, adjusted to the same pH as the assay water. The response of each shore crab to each of the 4 cues and control was tested against a control of an empty filter paper on the other side of the tank. These five experiments were repeated with each animal in pH 8.1 and pH 7.7 on consecutive days, whereby the order of the pH condition and the side of the cue was randomised for each animal. Each animal was hence exposed to 10 experiments, with 24 hours rest period after the first set of 5 experiments. The order of the experiments was also randomised to exclude effects of learning or saturation of the odour receptors.

3.2.3 Data Gathering

All assays were recorded on video, randomised and condition-blinded for analysis. As described previously, this involved trimming all videos to exclude the first frames, where a summary sheet with the experimental conditions was presented to the camera. After all videos had been analysed, information about the experimental conditions were retrieved from the original videos and analysis results and information on the experimental conditions were merged. As for hermit crabs (chapter 2), locomotion-related parameters were gathered using the behaviour tracking software LoliTrack (version 5.1.1, Loligo Systems, Denmark).

Due to the larger size of shore crabs as compared to hermit crabs and the absence of foreign shells, I was able to extend my analysis to observing qualitative behaviour of shore crabs in the videos. This required clear behavioural patterns that can be filmed from above (to reduce disturbance). Being smaller and partially hidden in their shells as viewed from above, behavioural observations based on top-view video footage would

not have been a reliable data source in hermit crabs. As for locomotion data, the visual identification of behaviours was based on condition-blinded video evidence to avoid observer bias. Without knowledge of the experimental condition or sex of the animal, the occurrence of distinct behaviours was recorded in a binary system (occurrence yes/no). To consider the potential role of PEA in feeding and agonistic behaviour, I gathered data on grabbing or probing of the cue source (both control and PEA filter paper), cheliped displays and escape behaviour. Grabbing and probing of the cue source could be indicative of feeding or reproductive behaviour. However, as *C. maenas* were collected in October, outside their reproductive season,^{151,172} reproductive behaviours can be excluded. With regard to agonistic behaviours, two forms of cheliped display can be distinguished based on the position of the chelae: In the lateral merus display the chelae are raised and extended laterally (see Fig. 3.2A), whilst in the chelae-forward display chelae are raised and extended forward¹⁶⁶ (see Fig. 3.2B). Fig. 3.2A shows the full merus display, but depending on the motivation of the crab, chelae (manus and dactyl) might be flexed and point forward or inward instead of upward.¹⁶⁶

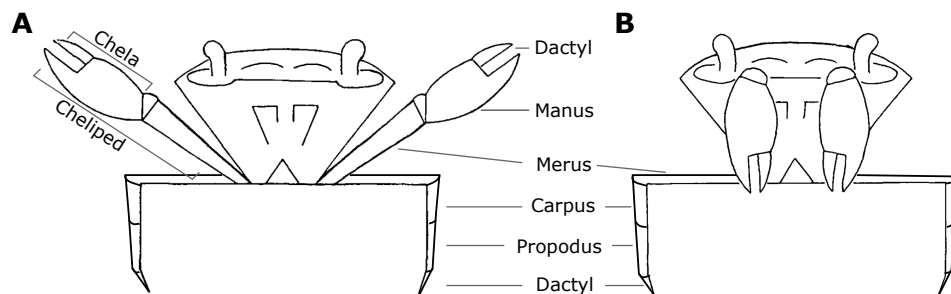


Fig. 3.2: Schematic illustration of cheliped display with selected crab anatomy, based on Wright (1968).¹⁶⁶ In the lateral merus display chelipeds are extended to the sides (A), whilst they extend to the front in the chelae-forward display (B). (A) shows the full lateral merus display. Alternatively, the chelae ('claws', manus and dactyl) can also be directed forward or point inward, depending on the motivation for the display.

Exposure of shore crabs to objects with large horizontal axes (compare cheliped display) induces the escape reaction in shore crabs.¹⁷³ Cheliped display and escape reaction are therefore considered opposite reactions.¹⁷³ For the purpose of this study, escape behaviour was defined as a retreat away from the stimulus whereby the animal extends at least two legs up the wall of the bioassay tank.

3.2.4 Data Analysis and Statistics

Using the behaviour tracking software LoliTrack (version 5.1.1, Loligo Systems, Denmark), allowed me to export several locomotion-related parameters from the videos of the behaviour assays. As the average position inside the tank has previously been insightful (section 2.3.2) it was used to visualise the attractive/repulsive effect of PEA on shore crabs using heatmaps of the tank (based on `drawcontours.R`, written by J.D. Forester¹¹⁷) for each condition and sex. Thereby the x-axis displays the distance from the cue source side rather than the length of the tank to account for the randomised side (left or right) of the cue. Additionally, the percentage of time spent active (i.e. moving) was analysed with LoliTrack, as this allows for verification of potential dose-dependent increases in escape behaviour.

All statistics were carried out with R (version 4.0.2).¹¹⁰ For data visualisation, the package `'ggplot2'`¹¹¹ was used. The average distance from the PEA source side (x-axis in heatmaps) and percentage of time spent active were analysed in linear mixed effect models (package `'lme4'`¹¹² in R), testing for significant additive and interactive effects of pH, concentration, sex and claw-size adjusted weight, whilst controlling for the paired design on the individual level (random effects).

Sex-specific differences in claw size and weight were explored using Welch's t-test. This test was chosen as it is more robust to differences in variance between groups than the Student t-test or Wilcoxon test.

Behavioural patterns, i.e. the occurrence of escape behaviour and cheliped displays, were analysed in generalised mixed effect models (binomial distribution with a logit link) with the same fixed and random effect structure as for the locomotion data.

3.2.5 Urine Extraction and Chemical Preparation of PEA

Five male shore crabs were kept in individual containers crafted from aquaria plant baskets and mesh and fed 24 h before urine extraction. Using elastic bands, the crab was fixed to a plate to expose their underside. Then, one side of their mouthpart was gently lifted and, lifting the nephropore flap with a small needle, the emerging fluid was aspirated into an eppendorf vial. To minimise the animal's stress, urine was only extracted from one side of the gills per extraction procedure.

The chemical extraction of PEA is based on a method used by Ferrero et al. (2011).²⁴ The extracted urine was immediately filtered through a 3 kDa filter to remove larger enzymes and proteins. The sample was then diluted to gain three technical repeats of 100 μ L, to determine the accuracy of the chemical extraction method. Additionally, three 100 nmol/L PEA standard solutions in 0.1 % formic acid/water underwent chemical extraction in the same way as urine samples to gain insights on PEA recovery levels.

The pH of samples was adjusted to approximately 12 by adding 1.5 μ L 5 mol/L NaOH solution (Sigma-Aldrich). PEA was then extracted five times with 170 μ L dichloromethane (>99 %, Riedel-de-Haen, Honeywell). The combined organic extracts were heated to 55°C to evaporate the solvent. After evaporating about 80 % of dichloromethane, 100 μ L

0.1 % formic acid in deionised water was added. The remaining organic solvent was then evaporated by continuing to heat the extracts to 55°C. PEA levels were measured using liquid chromatography with tandem mass spectrometry.

3.2.6 Liquid Chromatography and Tandem Mass Spectrometry of PEA

Extracts were separated and analysed by Liquid Chromatography with Tandem Mass Spectrometry (LC-MS/MS) using a C18 column (4.6 × 100 mm, Shimadzu Shimpack) on a Shimadzu LCMS-8050 instrument with 10 µL injection volume. The samples were eluted (5-min run, flow rate 0.4 mL/min) using a linear gradient (0-40 %) of solvent A (0.1 % formic acid in acetonitrile) in solvent B (0.1 % formic acid in water). A product ion scan of a 100 nmol/L PEA standard solution (focused on $m/z=122$, PEA, collision energy -35 eV) allowed the identification of $m/z=105$ and $m/z=77$ at a retention time of 1.3 to 2.3 min as reliable fragments of ionised PEA. Hence, the collision energy and cell acceleration voltage were optimised for these two product ions.

Using Multiple Reaction Monitoring, the number of ion counts for the two fragments was determined for standard solutions and PEA urine extracts. As the ratio of the ion counts for the two fragments was highly variable, the sum of the integrated areas for $m/z=105$ and $m/z=77$ was used to quantify PEA levels. Collision energies were -14 eV for $m/z=105$ and -27 eV for $m/z=77$ fragment, and cell acceleration voltage was 3 V and 2 V respectively. PEA standards in 0.1 % formic acid/ water with concentrations 100 nmol/L, 50 nmol/L, 25 nmol/L, 12.5 nmol/L and 6.25 nmol/L were run on the same day as the samples to determine PEA concentrations in urine samples based on linear regression analysis.

3.3 Results

3.3.1 Sex-specific Differences in Shore Crabs

Fig. 3.3 shows that there is no evidence for sex-specific differences in shore crab weight and carapace width (Welch's t-test, $t = -1.43$, $df = 30.38$, $p = 0.16$ and $t = -0.98$, $df = 38.70$, $p = 0.33$), but very strong evidence for sex-specific differences in claw-related measurements, such as claw height (Welch's t-test, $t = -4.5$, $df = 31.05$, $p^{****} < 0.0001$), claw length (Welch's t-test, $t = -3.9$, $df = 35.75$, $p^{***} = 0.0004$) and dactyl length (Welch's t-test, $t = -2.7$, $df = 41.23$, $p^{**} = 0.0095$). For the majority of shore crabs, the right claw was dominant (i.e. larger than the left claw, 41 out of 48). However, the proportion of left claw dominant animals was slightly higher in females (5 out of 24, compared to 2 out of 24 in males; no significant sex-specific difference, Fisher's exact test, $p = 0.42$).

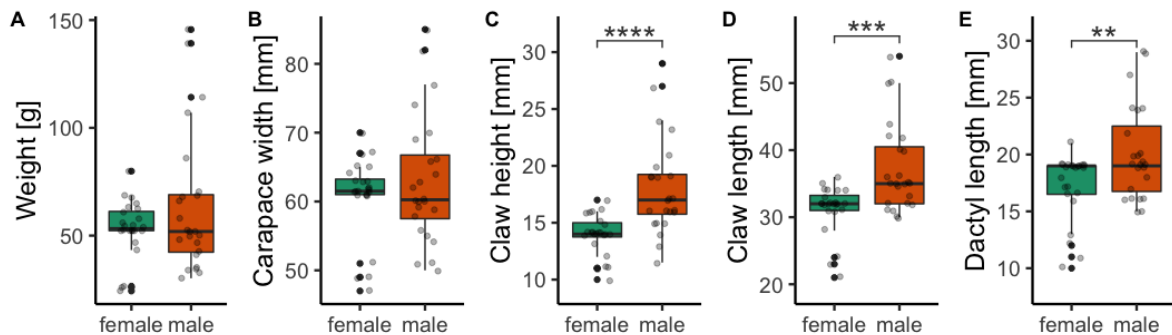


Fig. 3.3: Sex-specific measurements of shore crabs. (A) shows weight distributions, (B) shows the carapace width, (C) shows claw height, (D) the claw length and (E) the dactyl length in males and females. Asterisks depict differences in the distributions following Welch's t-tests with $p^{**} < 0.01$, $p^{***} < 0.001$ and $p^{****} < 0.0001$. Boxplots depict the median with first and third quartile of the distribution. Whiskers extend to 1.5 the interquartile range; data beyond that range are defined as outliers and plotted individually. The boxplots are overlaid by the actual data points in semi-transparent.

3.3.2 Movement of Shore Crabs in Response to PEA

As for previous experiments, heatmaps allow for a first overview of the spatial reaction (attraction/repulsion) of shore crabs to different concentrations of PEA in pH 8.1 and pH 7.7 (Supplementary Information, Fig. S6-S7). With increasing concentrations of PEA, the heatmaps display an increased likelihood of a division of the response: a group of animals being attracted, another repulsed, as shown by separate hotspots in the heatmaps. This is particularly pronounced in pH 7.7 (Fig. S7). Although this phenomenon seems strongest for male shore crabs, it can also be observed in females (see e.g. S7I). The division of the response suggests that some physiological characteristic (e.g. weight or claw size) of the shore crab besides its sex affects the animals' response to PEA. The large variance in the data and the divided response to PEA at higher concentrations, particularly in pH 7.7, makes it unsuitable for visualisation in boxplots.

As weight and claw size related measurements span a larger range for males as compared to females (Fig. 3.3), a weight or claw-size related response of shore crabs to PEA could explain the higher prevalence of the divided response in male shore crabs. To ensure comparability with experiments in hermit crabs, I chose to continue to use the animal's weight as a variable for the data analysis. However, to adjust for potential sex-specific differences in the response to PEA, the weight was adjusted by claw length (weight/claw-length ratio). As the measure 'claw length adjusted weight' (weight/ claw length ratio) is not particularly intuitive, I plotted the raw values for shore crab weight against claw length, as well as claw length and weight against the new metric of claw length adjusted weight for males and females (Supplementary Information, Fig. S8). The strong positive relationship between the weight and the weight/claw length ratio, means that big shore crabs have a large weight/claw length ratio and small/light shore crabs a low weight/claw length ratio (Fig. S8B). Similarly, although the relationship is weaker, animals with small claws have a small weight/claw length ratio, whilst animals

with large claws have a large weight/claw length ratio (Fig. S8C). Furthermore, using the new metric of weight/ claw length ratio, sex-specific differences disappear: female and male shore crabs have comparable claw-length adjusted weight, which is not the case for claw length alone (Fig. 3.3D). Additionally, sex-specific variability of weight is mitigated by adjusting weight by claw length. Fig 3.3A shows that shore crab weight spans 56 g for females and 115 g for males. Large differences in variance between groups (heteroscedasticity) can invalidate linear models.¹²⁵ Adjusting weight by claw length reduces the sex-specific variability (1.3 g/mm for females, 1.8 g/mm for males, Fig. S8), hence making the variable weight/claw length ratio more robust for statistical analysis of sex-specific effects.

Unlike in hermit crabs, shore crabs show no evidence for sex-specific effects on their response to PEA, when the claw-length adjusted weight is considered (likelihood ratio test, LRT=1.33, n=1, p=0.25). Data for males and females was hence combined in further linear mixed effect model. However, the linear mixed effect model shows a significant 3-way interaction between the concentration of PEA, the pH condition and the weight to claw length ratio (likelihood ratio test, LRT=11.89, n=4, p*=0.018). This is strong evidence that the claw-length adjusted weight of the shore crab alters pH-dependent effects on the dose-dependent response of shore crabs to PEA (see Fig. 3.4).

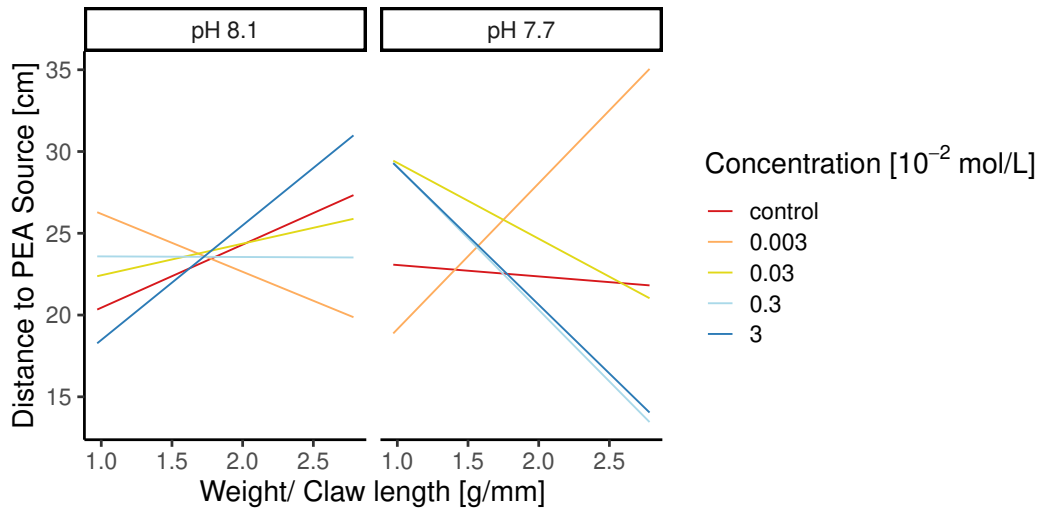


Fig. 3.4: Weight and claw length-dependent response of shore crabs to PEA. The distance to the cue depends on the pH condition, concentration and weight to claw length ratio. The strong weight/claw length-dependent effect at high PEA concentrations is reversed with the pH condition, indicating that there is a 3-way interaction between pH condition, concentration and weight/ claw length ratio.

Fig. 3.4 shows that the weight/claw length-dependent effect is strongest in pH 7.7, with opposite effects for the lowest and highest concentration: In pH 7.7, at the lowest concentration (orange), bigger shore crabs with larger claws are strongly repulsed, whilst they are attracted to PEA at the highest concentration (dark blue). Furthermore, Fig. 3.4 shows that the strong weight/claw size-dependent effect in response to high PEA concentrations reverses depending on the pH condition. The dark blue line in Fig. 3.4 shows a strong positive relationship with weight/claw length ratio in pH 8.1 and a strong negative relationship in pH 7.7. This visualises the 3-way interaction between pH condition, concentration and weight/ claw length ratio.

3.3.3 Behavioural Response of Shore Crabs to PEA

Increasing the PEA concentration doesn't just affect the attraction/repulsion of shore crabs in a weight-dependent manner, it also increases the occurrence of cheliped displays. The probability of cheliped displays significantly increases with increasing concentration of PEA (binomial mixed effect model, likelihood ratio test between model with and without factor, $LRT=9.67$, $n=4$, $p^*=0.046$). However, whilst shore crabs with low weight to claw length ratio are less likely to be attracted to PEA (Fig 3.4), they are more likely to exhibit cheliped displays (see Fig. 3.5, likelihood ratio test, $LRT=4.73$, $n=1$, $p^*=0.029$) regardless of the pH. In response to $3 \cdot 10^{-2}$ mol/L PEA (concentration of 200 μ L odour source in 10 L tank water), 25 % of shore crabs displayed their chelipeds, compared to 11 % in control conditions. Thereby, animals exhibiting cheliped display in response to PEA at $3 \cdot 10^{-2}$ mol/L are 3.2 g (median difference) lighter than animals where this behaviour was not recorded. In control conditions, the weight difference between animals that did and did not display their chelipeds is 0.3 g (median difference).

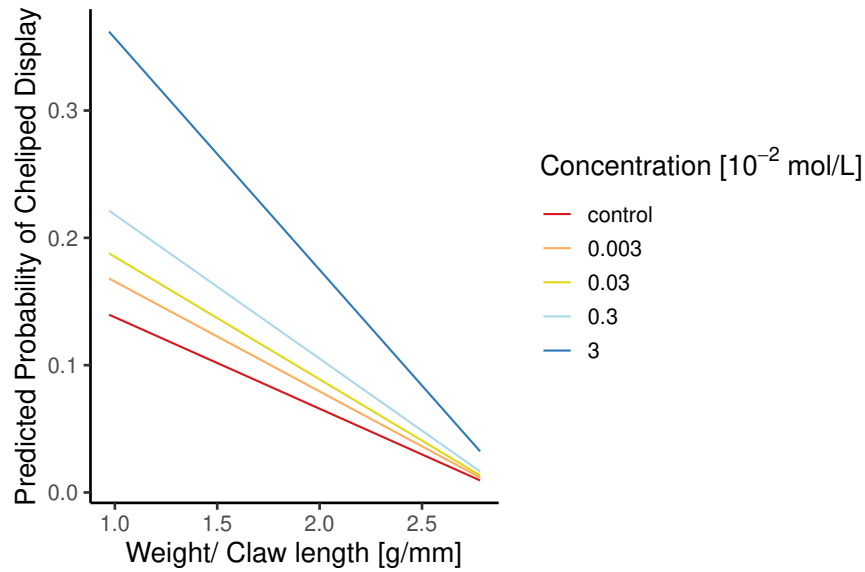


Fig. 3.5: The probability of cheliped displays increases significantly in a dose-dependent manner with decreasing weight to claw length ratio in response to PEA. The predicted probabilities are extracted from the binomial mixed effect model.

There is very strong evidence that the escape behaviour of shore crabs is dose-dependent (binomial mixed effect model, likelihood ratio test between model with and without factor, $LRT=31.47$, $n=4$, $p^{****}<0.0001$). Furthermore, there is strong evidence that the weight to claw length ratio of the shore crab affects the display of escape behaviour ($LRT=6.33$, $n=1$, $p^*=0.011$). Whilst cheliped displays were more frequent for small shore crabs at high PEA concentration, small shore crabs are more likely to display escape behaviour at low PEA concentration (Fig. 3.6). In response to $3 \cdot 10^{-5}$ mol/L PEA, 33% of shore crabs displayed escape behaviour and these individuals were 4.3 g (median difference) lighter than the animals that didn't show the same behaviour. In control conditions, 11% of animals displayed escape behaviour with a median weight difference of 0.3 g between animals that did and did not display escape behaviour. The dose- and weight-dependent probability of escape behaviour display is visualised in Fig. 3.6.

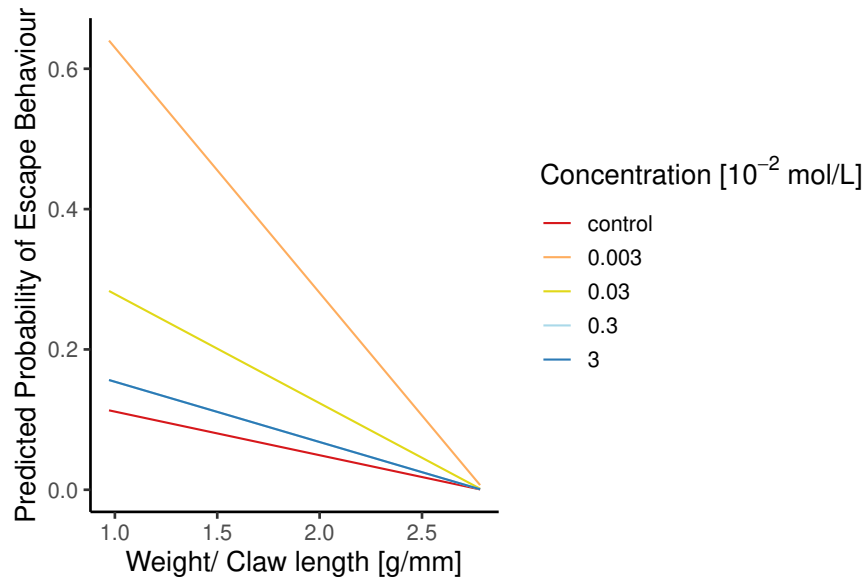


Fig. 3.6: The probability of shore crabs to display escape behaviour in response to PEA is dose-dependent and weight-dependent (claw length adjusted), whereby smaller shore crabs are more likely to show escape behaviour and the probability is highest when exposed to $3 \cdot 10^{-5}$ mol/L (concentration at odour source). The predicted probabilities are extracted from the binomial mixed effect model. The regression line for $3 \cdot 10^{-3}$ mol/L (light blue) overlaps with the regression for $3 \cdot 10^{-2}$ mol/L (dark blue).

Finally, the dose-dependent escape behaviour, which is strongest at the lowest concentration of PEA for small animals, coincides with similar observations for the active time: There is strong evidence that the active percentage of bioassay time is dose-dependent (likelihood ratio test, $LRT=47.5$, $n=4$, $p^{***}<0.0001$), irrespective of sex or weight/claw related parameters. Fig. 3.7 shows that $3 \cdot 10^{-5}$ mol/L PEA at the odour source significantly increased the percentage of active time (post-hoc test on estimated marginal means, $p^{***}<0.0001$). There is slight indication of an additive pH-dependent effect (likelihood ratio test, $LRT=3.57$, $n=1$, $p=0.058$): Shore crabs tend to be less active in pH 7.7 than in pH 8.1, regardless of the PEA concentration or the animals sex or weight. However, this effect is not significant, applying the usual significance level of $\alpha = 0.05$.

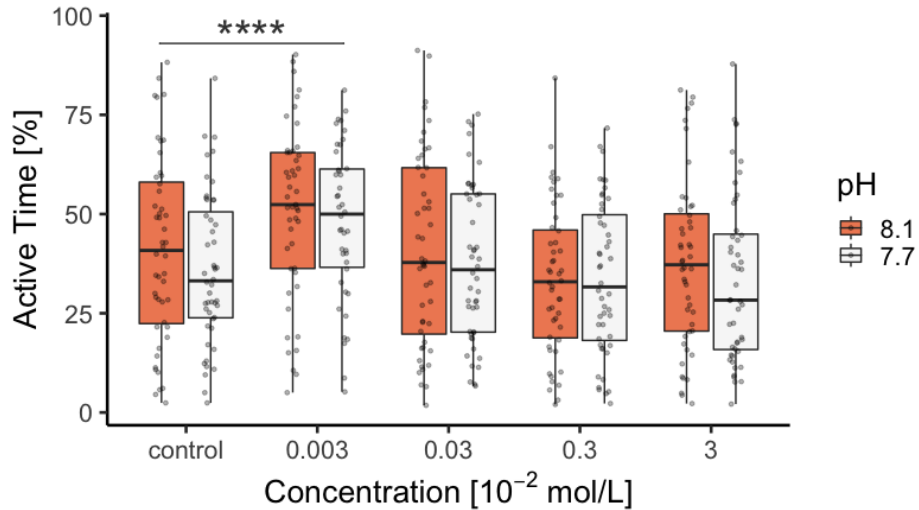


Fig. 3.7: Percentage of bioassay time spent active (moving) for 24 female and 24 male shore crabs in response to different concentrations of PEA in pH 8.1 (white) and pH 7.7 (orange). Asterisks depict the significant difference in the active time of shore crabs in response to $3 \cdot 10^{-5}$ mol/L PEA at the odour source as compared to control with $p^{***} < 0.0001$, regardless of the pH condition. The active time was also not significantly different in males and females. The boxplots are overlaid by the actual data points in semi-transparent.

Grabbing or probing of the filter paper was observed in only 8.4% (4.6% PEA and 3.8% control filter paper) of the behaviour assays with no apparent sex-, pH- or concentration-dependent trend or preference for filter papers containing PEA over empty control-side filter papers (Fig. 3.8). This behaviour was hence excluded from further analysis.

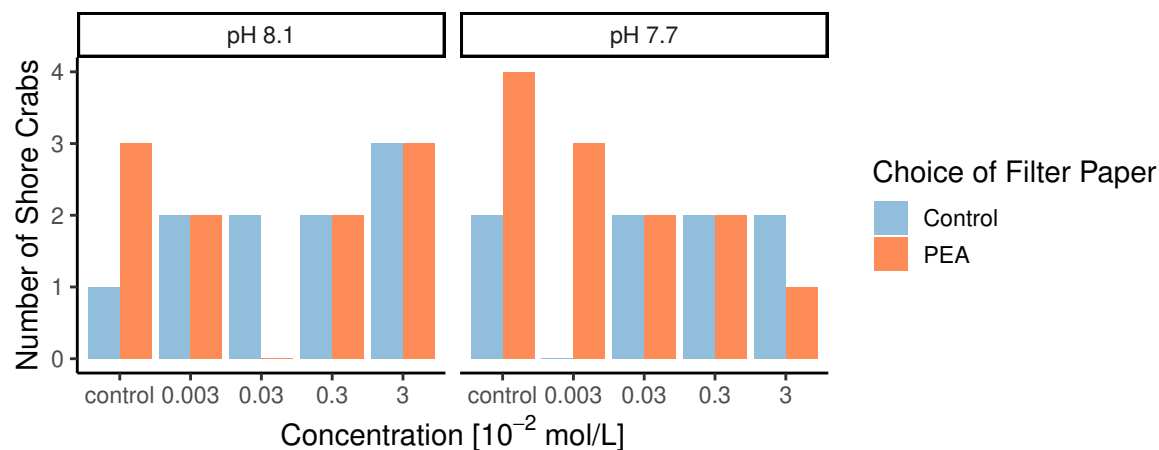


Fig. 3.8: Number of shore crabs grabbing or probing filter papers containing control or PEA in response to different concentrations of PEA in pH 8.1 and pH 7.7. In total, 48 (24 male and 24 female) shore crabs were tested for their response in all 10 conditions.

3.3.4 PEA in Shore Crab Urine

All LC-MS/MS spectra of urine samples extracted from shore crabs show clear evidence for the presence of PEA. However, based on the recovery of PEA from stock solutions, the extraction procedure has a low recovery rate (three replicates of 100 nmol/L PEA averaged at 44 ± 18 nmol/L after extraction). Furthermore, slight shifts in the retention time and split-up peaks suggest that the extraction procedure leads to chemical reactions of PEA, potentially including tautomerisation* (compare control Fig. 3.9 A-B to extraction control 3.9 C-D). As the first mass spectrometry (MS) in LC-MS/MS filters for the precursor ion (PEA) and the second mass analyser then filters for the chosen product ions with $m/z=105$ and 77 , I can be certain that all measured peaks originate from the precursor ion PEA. Hence, the split-up peaks from the different fragments can be combined for quantification. However, this only allows for the inclusion of tautomers

*Tautomers are chemical compounds that readily interconvert as they have the same structure ('structural isomers', same number of atoms for each element and the same bonds connecting them) except for a relocated hydrogen atom.¹⁷⁴

of PEA fragments. PEA reacting with urine- or extraction-borne compounds are lost in the quantification.

Dividing each of the five diluted urine sample into three technical replicates for the extraction and analysis shows high variation of PEA levels within triplicates (up to 10-fold difference, standard deviations 13-72 nmol/L), whilst the PEA solutions that underwent the same extraction procedure vary less (18 nmol/L standard deviation). Although the presence of PEA in shore crab urine is evident (see Fig. 3.9 E-F for a representative example, 2-fold diluted), its quantification is not possible with this method.

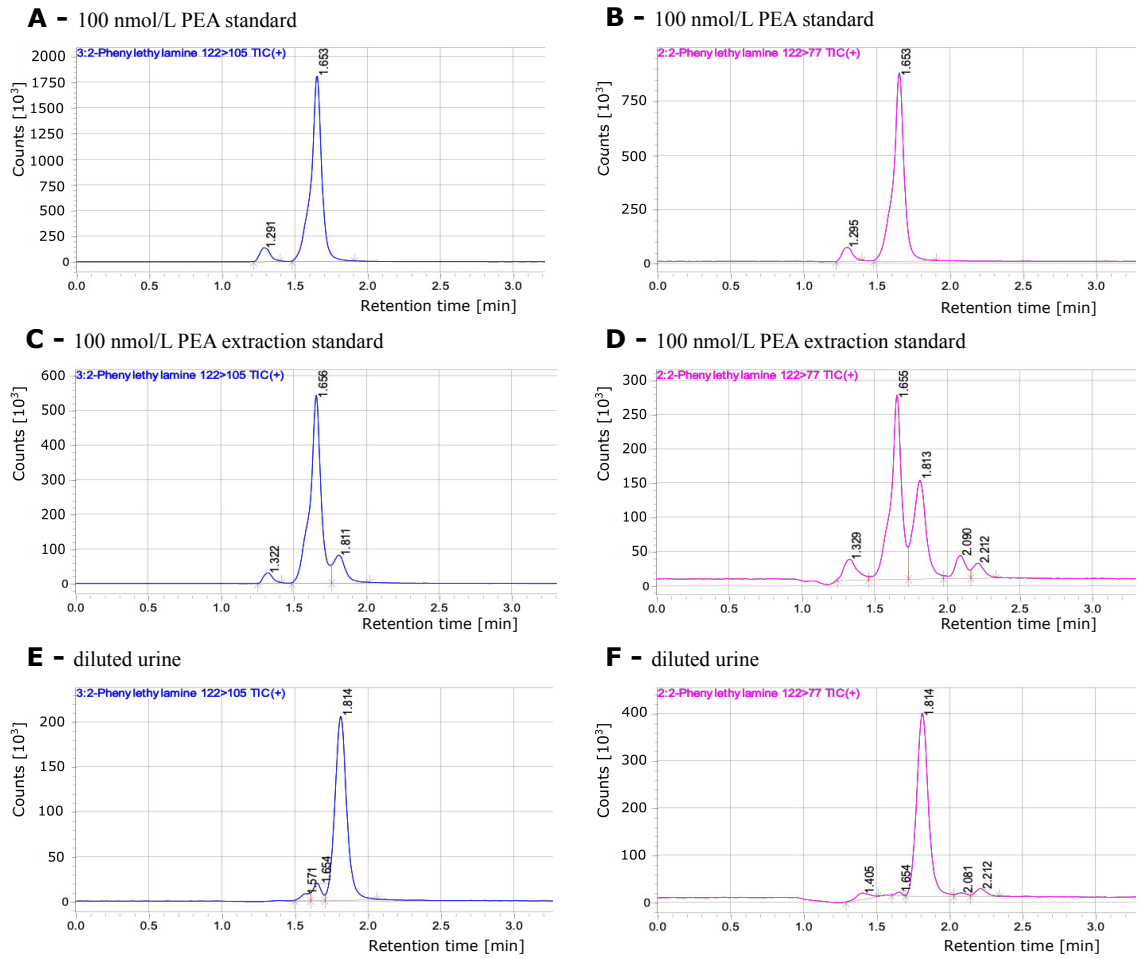


Fig. 3.9: Chromatograms of PEA fragments $m/z=105$ (A, C & E) and $m/z=77$ (B, D & F) for a 100 nmol/L PEA standard, a 100 nmol/L PEA extraction standard and a shore crab urine sample (2-fold diluted) as measured in LC-MS/MS.

3.4 Discussion

This study explores whether the observed behavioural response to PEA in hermit crabs is transferable to shore crabs. For this chapter, I repeated one of the behavioural experiments from chapter 2 with shore crabs, analysed the behavioural response of shore crabs in response to different concentrations of PEA and identified the presence of PEA in their urine.

In summary, my findings show that the PEA concentration, pH and weight/claw length ratio affect the attraction/repulsion of shore crabs to PEA. Thereby, similarly to my findings in hermit crabs, the strongest response was observed in pH 7.7, where large animals retreat from PEA at the lowest concentration and are attracted at the highest concentration (section 3.3.2). Additionally, I analysed the behavioural response of shore crabs to PEA (section 3.3.3). The results reveal no evidence for feeding-related behaviour of shore crabs in response to PEA, like grabbing or probing of the filter paper. Agonistic behaviours, on the other hand increased in response to PEA. The probability of cheliped displays increased significantly with increasing PEA concentration, whereby the strongest response was observed in crabs with a low weight/claw length ratio. PEA also induced a concentration and weight/claw length ratio dependent escape response, which was strongest at low concentration for animals with low weight/claw length ratio. Thereby, the increased occurrence of escape behaviour at low PEA concentration coincided with increased activity. Observing agonistic behaviour of shore crabs in response to PEA prompted me to explore the presence of PEA in shore crab urine (section 3.3.4). Although the mass spectrometric analysis of shore crab urine showed a high variance in PEA levels, even in technical replicates of the same urine sample, the presence of PEA in shore crab urine is evident.

Although I have to reject my hypothesis of sex-specific differences in shore crab weight (Fig 3.3A), shore crab claw measurements are significantly different in males and females (Fig 3.3B-E), which aligns with my hypothesis. Similarly to the weight distributions in this study, shore crab collections in 1973 from the same site as this study and a nearby site in North England also showed no significant sex-specific difference in shore crab weight.¹⁷⁵In hermit crabs, my findings indicated that the weight-dependent response to PEA coincides with a sex-dependent effect of PEA (section 2.3.5), presumably due to sex-specific differences in hermit crab weight and cheliped sizes. This motivated me to

adapt the previously established data analysis by using weight/claw length ratio as a variable instead of weight alone. Indeed, the weight-dependent (adjusted by cheliped size) response of shore crabs to PEA does not coincide with a sex-dependent effect (compare section 2.3.5). However, the absence of sex-specific effects in this chapter does not exclude an additional role of PEA in reproductive behaviour as the shore crabs used in this study were collected outside the reproductive season.

Shore crabs are only distantly related to hermit crabs¹⁵³ and occupy a different ecological niche,¹⁵¹ but like hermit crabs, my findings show a weight-dependent (adjusted by cheliped length) attraction to PEA for shore crabs. This aligns with my hypothesis. It is interesting to note that the spatial response (attraction/repulsion) is pH dependent and concentration dependent, whilst behavioural displays (cheliped display/escape behaviour) are only concentration dependent. This indicates that the behavioural response is a more sensitive measure for the response to PEA in crustaceans than locomotion-related parameters. This coincides with observations on feeding behaviour in crustaceans, whereby probing with the pereiopods precedes the movement towards the source of the feeding cue.¹⁵⁹

My data suggests that, when exposed to the same chemical information of PEA, small shore crabs tend to use visual displays, whilst large shore crabs move in response to the infochemical: Large shore crabs are attracted to the higher concentrations of PEA at pH 7.7 and smaller crabs are more likely to display their chelipeds. Similarly at the lowest concentration of PEA, larger animals tend to retreat from the source of PEA, whilst smaller animals display escape behaviour.

Sneddon et al (1997)¹⁶² found that during fights, the frequency of cheliped displays increases with chela length in shore crabs and winners perform significantly more displays than losers. This seems to contradict the findings of this study, where light animals with small claws (low weight/claw length ratio) are more likely to display their chelipeds,

whilst heavier crabs with larger claws (high weight/claw length ratio) tend to move towards the source of PEA instead. However, the study by Sneddon et al. (1997)¹⁶² involves actual fights between two opponents, whilst I study the response of a single animal to an infochemical associated with agonistic behaviour. My study hence focuses on pre-fight behaviour and the potential initiation of a fight.

Whilst movement towards a potential opponent indicates willingness to engage in a fight, cheliped display without locomotion is more defensive. This suggests that PEA is associated with a risk which larger animals are more likely to take due to their larger resource holding potential (RHP). Risk-benefit models, developed studying agonistic interactions in birds, indicate that animals choose a behaviour (here approaching the cue source versus visual display) depending on its costs and that the choice of behaviour reflects the individual's willingness to escalate the fight.¹⁷⁶⁻¹⁷⁸ Hence, larger animals signal their willingness to engage in a fight by approaching the source of PEA, whilst smaller animals are more likely to show a more defensive threat display. Smith et al. (1994)¹⁷⁹ shows that the probability that an agonistic interaction in velvet swimming crabs ends without visual displays is most likely for opponents with a large size difference. Thereby the large crab approaches the smaller without displaying their chelipeds, eliciting the retreat of the smaller.¹⁷⁹ With decreasing size difference between the opponents, the likelihood of displays increases.¹⁷⁹ As there are no visual opponents in my study, the shore crab relies on previous fight experience and its own RHP compared to the average opponent. Hence, bigger than average crabs (large weight/claw length ratio) approach a strong PEA source, willing to escalate the fight, and smaller than average crabs (low weight/claw length ratio) display their chelipeds defensively. This coincides with the observations on agonistic interactions by Smith et al. (1944),¹⁷⁹ assuming an average opponent.

Although body and cheliped size can predict the outcome of a fight,¹⁶² neither reliably predicts which opponent will initiate the fight.¹⁶² Thereby, the study defined the crab that first moved towards its opponent to engage in physical contact as the initiator.¹⁶² As small and large shore crabs are equally likely to initiate a fight,¹⁶² other predictors, such as urine release,¹³² could be crucial for crustacean fight initiation.

Hence, if PEA is a urine-borne infochemical mediating agonistic behaviours of crustaceans, the animals in my bioassay might have received the chemical information of an opponent initiating a fight. As body and claw size are not related to fight initiation,¹⁶² the weight/claw length-dependency of the response to PEA indicates that animals are acting in response to a perceived fight initiation rather than initiating a fight themselves by displaying their chelipeds or moving towards the source of the cue. According to cost-benefit analysis during agonistic interactions (see above, p. 93), large individuals are more likely to actively engage in a fight rather than display defensive behaviours.

In this study, agonistic behaviour is studied in the absence of a visual opponent, so information on the opponent's body or weapon size are not available to the crabs. For the animal in the experiment, the only existing information is the concentration of PEA and its own level of confidence based on previous fighting experience. The behavioural response to PEA changes from escape behaviour/retreat at the lowest concentration to cheliped display/attraction upon 1000-fold increase of the cue source concentration. Hence, I reject my hypothesis that PEA conveys information on the size or RHP of the signaller: If PEA signalled the size of the opponent, shore crabs would display their chelipeds at low concentrations and showed escape behaviour at higher concentrations, as a low concentration would indicate a smaller opponent and higher concentrations a large animal. Since the data shows the opposite trend, from escape behaviour/retreat at low concentration to cheliped display/attraction at higher concentration of PEA, PEA is more likely to convey information on the presence/absence of an opponent, whereby

a lower concentration indicates a greater distance, allowing for time to escape and avoid a conflict.

As the receiver distance is known to affect visual displays in crabs¹⁸⁰ there could be a critical distance beyond which the animal cannot yet use visual communication via displays but might already be able to detect the opponent chemically, hence allowing for time to avoid a costly fight. Urine is known to act as a threat signal, effectively deterring an opponent crustacean.^{132,165} Similarly, my study shows that shore crabs show escape behaviour/retreat at low concentrations of PEA. Furthermore, the risk-benefit model suggests that the risk of choosing a visual display (attracting attention and getting injured in the resulting fight) correlates with the estimated benefit or effectiveness of the display in deterring the opponent.^{176,177} The visual display of smaller crabs in response to high concentrations of PEA hence indicates that the potential benefit of appearing more threatening outweighs the risk of being noticed by extending their chelipeds. This further supports the hypothesis that the concentration of PEA conveys information on the distance between the opponents: When opponents are within close range the additional risk of drawing attention to oneself through visual displays is low as visual contact is inevitable.

It has been suggested that crustaceans combine the release of urine and offensive behaviours to add reliability to the chemical message for the receiver:^{132,164} Offensive behaviour alone was not effective in deterring the opponent crayfish when not accompanied by the chemical message.^{132,164} However, the identity of the infochemical(s) in urine was previously unknown. The combination of agonistic behaviour in response to PEA and evidence for its presence in shore crab urine (Fig. 3.9) suggests that PEA is one of the chemicals in crustacean urine that signals willingness to fight. Breithaupt and Eger (2002)¹³² showed that the probability of urine release is greater during fights than during non-social activities or inactivity and that eventual winners are more likely

to release urine during fights than the eventual loser. This supports the notion that urine doesn't convey information on the individual's RHP (or else a reciprocal urine release would be expected) but rather its aggressiveness, or willingness to engage in a fight. The willingness to fight cannot be gradual but is a binary choice, signalled by the absence or presence of urine or, deducing from my results, the absence/presence of PEA in acidified water. My results indicate that PEA is an infochemical that is released with urine and signals the willingness to engage in a fight, whereby the concentration conveys information on the distance of the signaller. As during spontaneous release, urine is fanned laterally (allowing for fast dilution of infochemicals), whilst it is directed towards the opponent in a forward-projecting gill current during agonistic encounters,¹³² urine release (PEA release) does not signal willingness to fight in non-aggressive situations due to hydrodynamics.

The large fluctuations in PEA extraction levels from shore crab urine do not allow for conclusions on the concentration of PEA in crustacean urine. The presence of PEA in shore crab urine, however, is evident. It is unclear whether the quantification was unsuccessful due to suboptimal extraction or LC-MS/MS conditions or PEA catabolism in shore crab urine. Whilst in vertebrates, PEA is degraded via monoamine oxidase (MAO) enzymes,¹⁸¹ the primary invertebrate degradative route for biogenic amines, including PEA, is N-acetylation and N-methylation;^{182,183} and sulfate, β -alanyl, glycosyl, and γ -glutamyl conjugations are further possible degradative routes.¹⁸⁴⁻¹⁸⁶ There is some evidence that monoamines are not metabolised via MAO in crustaceans, but the route of catabolism remains unknown.¹⁸⁶ Interestingly, a rapid degradation of PEA in shore crab urine itself supports the notion that PEA could be involved in mediating agonistic interactions, as urine-borne dominance signals used in close, near-contact, situations are expected to rapidly degrade to ensure their situation-specificity.⁸ In other words: Only fresh urine should signal the willingness to fight.

Nevertheless, further experiments are needed to explore more reliable routes of chemical extraction of PEA from crustacean urine to determine the concentration of PEA. As the catabolic mechanism is unknown, suggestions for alternative chemical extractions are difficult. Derivatisation of PEA, e.g. with dansyl chloride or o-phthalaldehyde,^{187,188} might suppress the chemical degradation during the purification step. Alternatively, Ochi (2019)¹⁸⁹ recommends the purification of biogenic amines (including PEA) from animal tissue via ion-pair solid-phase extraction using a C18 cartridge and nonafluoropentanoic acid as volatile ion-pair reagent before quantifying biogenic amine levels with LC-MS/MS. This method eliminates the need for derivatisation and pH control. A reliable quantification method for PEA in crustacean urine would allow for comparisons of PEA levels across samples from the same individual, from differently sized individuals as well as across species and sex.

3.5 Conclusion

The combined evidence from this chapter suggests that PEA is an infochemical that is used by multiple crustaceans in agonistic interactions. PEA can hence be called a transferable infochemical. The dose-dependent change in the behavioural response to PEA indicates that PEA (particularly in reduced pH conditions) conveys information on the presence of an opponent that is willing to fight. Furthermore, using mass spectrometry, PEA was identified in shore crab urine. As directional urine release is known to initiate a fight in crustaceans, PEA could be a urine-borne infochemical that is detected by crustaceans leading to the onset of agonistic interactions.

CHAPTER 4

Mechanistic Assessment of the pH-dependent Response to PEA

4.1 Introduction

Using computational chemical methods, I want to assess the potential mechanisms that drive the pH-dependent response of hermit crabs and shore crabs to PEA, as observed in the previous chapters. This chapter aims to show how computational chemistry can help unravel underlying mechanisms in chemical ecology.

Fig. 2.13 shows that the biological effect size - pH-dependent changes in the behavioural response of hermit crabs to PEA - cannot be fully explained by increased amounts of the protonated form of PEA in reduced pH conditions (chemical effect size). More specifically, whilst hermit crabs are on average 37% closer to the PEA source in reduced pH conditions (Fig. 2.13B), the amount of protonated PEA changes only marginally when the pH is decreased (Fig. 2.13B). As changes in the amount of the infochemical cannot explain the amplified response of hermit crabs, the role of conformational and charge-related changes in the infochemical and its receptor upon protonation are assessed as potential mechanisms driving the pH-dependent response.

As deduced in the general introduction (see Fig. 1.1), a decreased pH can affect the chemoreception, amongst others by altering the infochemical in water (pathway 2) and by changing the interaction with the olfactory receptor (pathway 3). These two potential

mechanisms are the focus of this chapter. Therefore, I use computational chemical methods to study pH-dependent changes in the infochemical PEA and its receptor by comparing PEA in its two protonation states, as well as their interactions with (protonated) model receptors.

In the following, I introduce the use of computational chemistry in chemical ecology, describe the basic principles of quantum chemical methods and give a brief introduction of chemoreception in crustaceans. The latter allows me to link this chapter back to my work with shore crabs and hermit crabs and to clarify my choice of receptor model.

4.1.1 Computational Chemistry in Chemical Ecological Research Questions

In most instances chemical ecology requires a thorough understanding of the behaviour of chemical systems as well as an understanding of the behaviour of animals. Acknowledging that chemical communication can be affected by changes in the environmental conditions (such as pH, see section 1.4), we are facing the question of how to study environmental effects on chemical systems. Some direct empirical measures are possible: Infochemicals¹⁹⁰ and receptors¹⁹¹ can be measured using spectroscopic approaches. However, purifying or synthesising these compounds for chemical experiments is often challenging and not always possible.

Although empirical model validations are still crucial, combining mathematical methods with fundamental laws of physics and chemistry, chemical systems can be studied in computational models.¹⁹² In chemical ecology, the discovery of natural products that are involved in chemical communication often relies on computational chemical methods to deduce the structure and stereochemistry of a new compound.^{193,194} Furthermore, quantum chemical methods have been used in chemical ecological studies to predict

increasing bioavailability of the neurotoxins saxitoxin and tetrodotoxin due to climate change⁴³ and allowed for the calculation of pH-dependent changes in the structure and electrostatic properties of signalling peptides.⁴¹

In the following, I want to briefly introduce the concept of quantum chemistry and the development of density functional theory, as it is the foundation for the computational chemistry methods in this thesis. I focus on key notions rather than their mathematical expressions.

4.1.2 Quantum Chemistry

Quantum chemistry is a field in computational chemistry that is derived from the postulates of quantum mechanics. A fundamental aspect of the theory of quantum mechanics is that equations cannot yield exact predictions, but only give probabilities.¹⁹⁵ Mathematically, a probability is found by taking the square of the absolute value of a complex number.¹⁹⁶ This is also called a ‘probability amplitude’.

Describing probability amplitudes of a quantum particle, such as an electron, in space leads to its wave function. In the wave function each point in space is associated with a probability amplitude.^{195,196} As the wave function contains information on the state (energy, spin, momentum, etc.) of a particle, it is a key variable in quantum chemistry. The Schrödinger equation allows us to relate probability amplitudes at a certain moment in time to probability amplitudes at another time point and hence describes the time-dependent development of the wave function.¹⁹⁷

However, describing a system with multiple components evolving over time would involve handling such information-dense variables, that it is mathematically not practical and approximations are made to obtain a more manageable system.¹⁹⁸ Firstly, the time variable is removed, leading to the time-independent Schrödinger equation.¹⁹⁸ Secondly,

the wave functions of nuclei and electrons are separated in the Born-Oppenheimer approximation,¹⁹⁹ allowing us to solve the electronic Schrödinger equation for a set of ‘stationary’ nuclei.¹⁹⁸ Unfortunately, even with these approximations, exact solutions to the Schrödinger equation can only be found for the simplest of systems, with two particles, e.g. the hydrogen atom.¹⁹⁸ For many-bodied problems, such as molecules, only approximate solutions can be found. In brief, quantum chemistry is the study of chemistry based on approximate solutions to the (electronic) Schrödinger equation.¹⁹⁸

The underlying physical laws necessary for the mathematical theory of a large part of physics and the whole of chemistry are thus completely known, and the difficulty is only that the exact application of these laws leads to equations much too complicated to be soluble.

– Paul A.M. Dirac (1929) ‘Quantum mechanics of many-electron systems’²⁰⁰

This proclamation was made in 1929, a year after the Dirac equation was first formulated, which allows scientists to account for special relativity in the context of quantum mechanics.²⁰¹ Unfortunately, almost a century after Dirac’s famous proclamation, ‘the exact application of these laws’ describing ‘the whole of chemistry’ are still ‘too complicated to be soluble’.²⁰⁰

However, with the aid of some further approximations, computational chemistry allows for the determination of the wave function and the corresponding energy of a quantum many-body system such as a molecule. Methods attempting to solve the electronic Schrödinger equation based on the positions of the nuclei and the number of electrons are called *ab initio* quantum chemical methods.^{198,202} Thereby, the Hartree-Fock method is the most prominent approach, whereby it is assumed that the wave function of a molecule is the product of its molecular orbitals for each electron.¹⁹⁸ This assumes that the electrons act independently, which neglects all interactions between electrons. Using

this Hartree-Fock method, the Schrödinger equation can be ‘solved’.¹⁹⁸ However, using molecular orbitals without electronic interactions, the approximate solution will always be higher than the true ground-state energy of the system.¹⁹⁸ Although this might seem like a shortcoming, relying on the systematic overestimation of the energy allows computational chemists to approach the exact solution using the variational method, which is central to the Hartree-Fock theory.¹⁹⁸

The second main approach in computational chemistry is quite different to the Hartree-Fock theory, as the central object is no longer the wave function, but the much simpler electron density distribution.¹⁹⁸ As indicated above, probability density and wave function are closely related: The probability density of finding a particle at a certain point is proportional to the square of the magnitude of the particle’s wave function at that point. Pierre Hohenberg and Walter Kohn showed that the energy of a system (as well as all other observables) can be unambiguously derived from its electron density functional.²⁰³ Although the Hohenberg-Kohn theorems have been proven true, they do not actually offer a way of calculating the energy from the electron density in practice. Hence, approximate functionals have been developed.¹⁹⁸ The most common approach in density functional theory (DFT) is to approximate the electron density as the sum of densities of the non-interacting molecular orbitals (Kohn-Sham orbitals),²⁰⁴ basically in analogy to the Hartree-Fock theory. The Kohn-Sham equation builds the basis of most DFT approaches, making it one of the most popular and versatile methods in computational chemistry.²⁰⁵

In practice, to run Kohn-Sham DFT calculations, the first step is to decide on a basis set that describes the molecular orbitals¹⁹⁸ of the chosen chemical system. This study makes use of the polarisation-consistent basis set pc-2²⁰⁶⁻²⁰⁸ for smaller systems and gaussian basis sets for larger systems.²⁰⁹ As in DFT the exact functionals for exchange and correlation of the electrons are not known (we assumed non-interacting molecular

orbitals), an exchange correlation variable needs to be added to account for the non-homogeneity of the electron density. For the purpose of this study, the functional PBE²¹⁰ and its hybrid form PBE0²¹¹ have been chosen. Hybrid forms of the exchange correlation functional include a component of the exact exchange energy based on Hartree-Fock theory.¹⁹⁸ The choice of basis sets and exchange correlation functionals is guided by the trade-off between accuracy of the result and computational cost. Including a component of the exact Hartree-Fock exchange and correlation energy for example (by choosing PBE0 over PBE), has been found to improve the calculated results,¹⁹² but it increases computational costs to such an extent that it was not a viable option for calculations in larger systems, such as receptor-ligand binding.

Usually a calculation is started with ‘initial guess’ orbitals, then the Kohn-Sham equations can be generated and solved.¹⁹⁸ This process is repeated iteratively until convergence. Thereby, one can aim to determine the energy of a system for a given set of nuclei positions or alternatively, the geometry of the chemical system can be optimised.¹⁹⁸ The optimal conformation of a molecule can be identified by finding the lowest energy (minimum). As the energy of a molecule depends on its conformation, this is often visualised via the potential energy surface.¹⁹⁸ A potential energy surface describes the energy of a system in relation to the positions of its atoms.¹⁹⁸ Assuming, for example, two geometric variables on the x- and y-axis (such as atomic angles or torsion angles), the potential energy surface can be visualised as a three dimensional surface with the total energy on the z-axis. Thereby, the optimal geometry is represented by an energy minimum and sterically hindered conformations are shown as energetic maxima (‘energy barriers’) on the potential energy surface.¹⁹⁸ The process of geometry optimisation essentially allows the system to converge towards the energy minimum (i.e. optimum).¹⁹⁸

Additionally, quantum chemistry can yield information beyond energy calculations. The dipole moment and charge distribution of a molecule can be calculated, providing valu-

able insights into electrostatic interactions between molecules.¹⁹² Also, several solvation models can be incorporated into the calculations, allowing me to evaluate the effect of the environment.¹⁹²

Most of the calculations that are carried out by computational chemists use existing programs. In this thesis, the chemical software packages ORCA,^{212,213} GAMESS²¹⁴ and CP2K²¹⁵ were used. Whilst ORCA is a general-purpose quantum chemistry software,^{212,213} that allows for flexible calculations of small systems (such as PEA/PEAH⁺ in water), larger systems (such as PEA/PEAH⁺ interacting with a receptor pocket) are better reflected by calculations in CP2K, which is designed to handle large or complex systems by creating periodic systems.²¹⁵ Periodic systems mirror a core unit cell to create an infinite environment, which is ideal for modelling e.g. large biological systems, liquids or metals.¹⁹² GAMESS was primarily designed for *ab initio* quantum chemistry calculations but also provides some DFT methods.²¹⁴ In this study, it was only used to calculate the charge distribution of PEA/PEAH⁺ via the molecular electrostatic potential.

Although computational chemical methods can provide valuable insights into chemical properties, all calculations need to be anchored in reality by comparing them to reference data or validating them with empirical measurements.¹⁹² As the conformation of a molecule is defined by the spatial arrangement of its functional groups this study uses nuclear magnetic resonance (NMR) spectroscopy for validation: NMR spectroscopy measures chemical shifts of atomic nuclei, which change depending on the proximity to functional groups.¹⁹² Hence, by calculating nuclear proton shieldings of PEA/PEAH⁺ based on my computational models and comparing them with empirically measured NMR shifts of PEA in water, I can check the accuracy of my computational methods.

4.1.3 The Conformation of PEA

PEA has only limited conformational flexibility. As the benzene ring is fixed, only the amino side chain can rotate around its first and second carbon-carbon bond (see Fig. 4.1). Rotation around the bond that connects the amino group with the benzene ring (first carbon-carbon bond) positions the entire amino side chain in relation to the ring (e.g. orthogonal to the benzene ring or in a plane with it). Rotating this first torsion angle to around 180° would position the amino side chain in a plane with the ring, which is sterically hindered: A large energy barrier can be expected and planar PEA/PEAH⁺ are unstable conformations.²¹⁶ The first carbon-carbon bond hence assumes a torsion angle of about 90° , positioning the amino side chain orthogonally to the benzene ring (see Fig. 4.1A & B). Additionally, Fig. 4.1 shows that rotating around the second carbon-carbon bond (torsion angle τ) can lead to an extended or a folded conformation of PEA. An extended geometry with a torsion angle τ of about 180° (see Fig. 4.1A) is generally termed *anti*, whilst the folded conformation with a torsion angle τ of around $\pm 60^\circ$ is called *gauche* (see Fig. 4.1B).

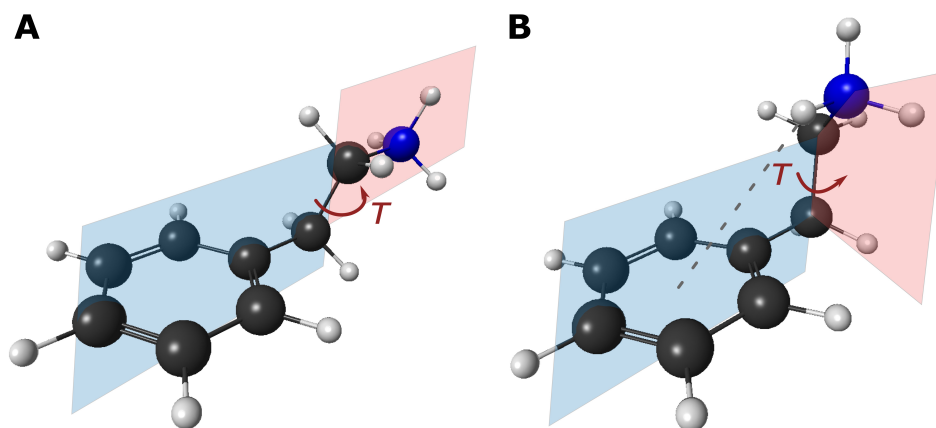


Fig. 4.1: Conformations of protonated PEA (PEAH⁺) with torsion angle τ of the amino side chain in dark red. The *anti* conformation (A) corresponds to an extended geometry with $\tau \approx 180^\circ$. The torsion angle of the folded conformation (*gauche*, B) is $\tau \approx \pm 60^\circ$ and leads to a weak π -hydrogen bond (dotted line).

To date, the conformation of PEA has mostly been studied in gas phase in the uncharged state. Rotational and infrared spectra found a strong preference for folded (*gauche*) conformations.^{216,217} Thereby, the interaction of the amino group with the conjugated electron system of the benzene ring (π -system) contributes largely to the stabilisation of this conformation^{218,219} (see dotted line in Fig. 4.1B). Studying 1:1 PEA-water clusters in gas phase, a direct interaction of PEA and water was observed.^{220,221} Infrared and rotational spectroscopy paired with *ab initio* quantum chemical calculations confirmed a *gauche* 1:1 PEA-water complex,^{222,223} showing that PEA is likely to interact with water in aqueous solutions. More recently, the hydration properties of neutral and protonated PEA were also assessed in molecular dynamics simulations, revealing, again, a conformational preference for *gauche* PEA-water clusters for both protonation states.²²⁴ As my computational calculations also cover both protonation states of PEA, I make a clear distinction in my terminology: In the following, ‘PEA’ refers only to the neutral form, whilst ‘PEAH⁺’ is the protonated state.

4.1.4 Chemoreception in Crustaceans

When an infochemical is detected, a receptor protein on a chemosensory cell binds the odour molecule, leading to a cascade of signal transductions.²²⁵ Chemosensory sensilla in crustaceans are hair-like cuticular organs that are distributed over the entire body, but cumulate on mouthparts, antenna, antennule and the tips of the walking legs (dactyl).²²⁵ Whilst in humans, olfaction and taste are the two modes of chemoreception,⁵ crustaceans possess a wide array of chemosensory sensilla and their chemoreception is broadly grouped into olfaction (due to unimodal olfactory sensilla (aesthetascs), which are innervated by olfactory sensory neurons) and distributed chemoreception (due to bimodal sensilla, innervated by chemosensory and mechanosensory neurons).²²⁵ Whilst

(long-range) olfactory sensilla are limited to the lateral flagellum of the antennule, all other chemosensory organs serve contact or short-range distributed chemoreception.²²⁵

In crustaceans, the expression of chemoreceptors has been studied in two chemosensory organs: The lateral flagellum of the antennule and the walking leg dactyl.^{226,227} Hundreds of candidate chemoreceptors for olfaction and distributed chemoreception have been identified in decapod crustaceans.²²⁷ The majority of chemoreceptors in decapods, particularly on the antennule, belong to the group of ionotropic receptors (IR).²²⁷ Their roles and functions, however, remain largely unexplored.²²⁷ Furthermore, transient receptor potential (TRP) channels likely include chemoreceptor proteins and chemoreception might additionally be aided by gustatory receptor-like (GRL) receptors in decapod crustaceans.²²⁷ Although G protein-coupled receptors (GPCRs) have been shown to function as chemoreceptor proteins in some invertebrates^{228–230} and are the classical mammalian olfactory receptors, to date, there is no evidence that GPCRs are chemoreceptors in crustaceans.²²⁷

4.1.5 Potential Receptors for PEA and their pH Dependency

Although evidence suggests that chemoreception, and olfaction in particular, is predominantly mediated by IRs in decapod crustaceans,²²⁷ the function, conformation and primary ligands of chemoreceptors in crustaceans are largely unknown.²²⁷

As the chemoreceptor of PEA in shore crabs or hermit crabs is unknown, I set out to study the pH-dependency of the interaction of PEA with the binding pocket of the human trace amine associated receptor 1 (TAAR1) instead. The endogenous ligand of TAAR1 is PEA.²³¹ Although there is no evidence for TAAR receptors acting as chemoreceptors in crustaceans, this approach allows me to provide a proof a principle in assessing potential mechanisms that drive pH-dependent chemoreception.

Many TAAR receptors act as vertebrate olfactory receptors.²³¹ Whilst TAAR4 is a known olfactory receptor and associated with a fear response in rodents,²⁴ TAAR1 mostly functions in the vertebrate brain.²³¹ However, the 3D structure and binding pocket of olfactory TAAR receptors (such as TAAR4) are not known. Therefore, I chose to work with TAAR1 instead, which is closely related to olfactory TAAR receptors²³¹ and its 3D structure is described in the literature through homology modelling.²³²

Receptor-ligand binding relies on electrostatic interactions between the receptor binding pocket and the ligand²³³ (i.e. infochemical for chemoreception). Non-uniform distributions of positive and negative charges on atoms can give molecules a dipole moment,²³⁴ which is essential for creating electrostatic attraction between molecules.²³⁴ However, changes in the protonation state of the ligand or the receptor can affect its charge distribution (or dipole) and thereby potentially its electronic binding properties.²³⁵ Protonation of the receptor has been hypothesised to be the leading cause for olfactory-disruption in the course of ocean acidification⁷⁴ and pharmacological studies show pH-dependent changes in histamine H₁ receptor binding kinetics.⁷⁵ Gillard et al. (2006)⁷⁵ deduce that whilst changes in the protonation state of histamine (ligand) would lead to under- or overestimation of the amount of reactive species, evidence for altered binding kinetics in their study, suggests that pH-dependent changes in the receptor rather than changes in the ligand are likely the cause of the pH-dependent binding properties with the H₁ receptor.⁷⁵ This study explores both potential aspects of pH-dependent changes to the receptor-ligand interaction, protonation of the ligand (PEA) and protonation of an amino acid residue within the receptor (TAAR1).

It is difficult to estimate the susceptibility to protonation of residues inside proteins, such as receptors. Amino acid pK_a values from aqueous environments are only a rough indication of the protonation state of an amino acid residue inside a protein,²³⁶ as pK_a values vary depending on their direct environment.²³⁷ The susceptibility to protonation

of residues inside the TAAR1 binding pocket is therefore unknown. Comparing average pK_a values of amino acid residues inside proteins, histidine stands out, as its pK_a value in proteins averages at near neutral pH conditions ($pK_a=6.4$), with minimum and maximum experimental observations of $pK_a=2.13-9.19$.²³⁶ This makes histidine a prime candidate for pH-dependent changes within the range relevant for marine environments. Additionally, the histidine residue Hist99 of TAAR1 is in close proximity to the binding site of the PEA ligand inside the binding pocket.²³² As this histidine residue is solvent-accessible due to its position inside the binding pocket, its pH-dependency could directly impact receptor-ligand binding properties.

The solvent accessible surface area (SASA) is known to affect the pK_a values of amino acid residues inside proteins.^{236,237} Whilst deeply or partially buried histidine residues are more likely to have extreme pK_a values (<5 and >8), histidine residues with larger SASA ($>40\%$, e.g. as part of a binding pocket) have the same average pK_a of 6.4 as deeply buried histidine residues, but they mostly range between pK_a 5.2 to 8.²³⁶ As Hist99 is part of the TAAR1 binding pocket, it is therefore likely to have a large SASA and could be pH-dependent within a range relevant for marine average pH conditions. As part of this study, I therefore assess to which extent changes in the protonation state of Hist99 could affect TAAR1-PEA and TAAR1-PEAH⁺ interactions.

4.1.6 Research Approach and Hypotheses

In this chapter I assess the potential mechanisms underlying the pH dependency of the behavioural response of crustaceans to PEA/PEAH⁺. Using quantum chemical methods verified by nuclear magnetic resonance (NMR) spectroscopy, the changes in the conformation and charge distribution of the infochemical PEA upon protonation are studied in an aqueous environment. As, using molecular dynamic simulations, Ristić

et al. (2019)²²⁴ found that both protonation states of PEA are predominantly in the *gauche* conformation, I hypothesise that my quantum chemical calculations and NMR spectra show no large changes in the conformation of PEA/PEAH⁺ upon protonation. Furthermore, I hypothesise that the charge distribution of PEAH⁺ differs significantly from its neutral state PEA, as the protonation of such a small molecule is likely to affect the magnitude of its dipole. Finally, I expect that the solvation model significantly affects the height of energy barriers and relative stabilities of the conformers for both PEA and PEAH⁺.

As (charge dependent) electrostatic interactions are an essential aspect of receptor-ligand interactions, I study the binding of PEA/PEAH⁺ with the receptor TAAR1 in further computational chemical experiments. Thereby, receptor-ligand interactions are assessed upon protonation of the ligand PEA/PEAH⁺ and of the Hist99 residue inside the TAAR1 binding pocket. As the binding pocket of TAAR1 is negatively charged, I hypothesise that it binds more strongly to the positively charged PEAH⁺ than to its neutral equivalent PEA. Consequently, I also hypothesise that protonation of the binding pocket residue Hist99 reduces the binding strength to PEAH⁺, as the protonation of Hist99 renders the binding pocket neutral. Decreasing the pH could hence have opposing effects on the receptor-ligand interaction, and the overall effect of ocean acidification on receptor-ligand binding is difficult to predict.

In addition to changes in pH, intertidal environments, the natural habitat of hermit crabs and shore crabs, also show daily and seasonal fluctuations in salinity and temperature.⁸² Temperature and salinity are known to affect the dielectric environment in a model,^{236,237} which might in turn affect the chemical properties of the in-fochemical PEA/PEAH⁺ in water and the chemoreception (receptor-ligand binding) TAAR1-PEA/PEAH⁺. Therefore, the impact of changes in temperature and salinity on PEA/PEAH⁺ and the receptor-ligand binding is assessed. As the pH can affect the

protonation state, potentially changing electrostatic interactions,²³⁴ I hypothesise that effects of temperature and salinity on PEA/PEAH⁺ and the receptor-ligand interaction are existent, but exceeded in magnitude by pH-dependent effects.

4.2 Materials and Methods

4.2.1 Computations of PEA in Water

The conformation of neutral and protonated PEA was studied using quantum chemical methods. The calculations were carried out with the supercomputer (Viper) of the University of Hull and validated by NMR spectroscopy. In a torsion angle energy scan, the total energy of geometry-optimised PEA and PEAH⁺ was calculated at different (constrained) torsion angles τ of the amino side chain in 5° intervals, which resulted in potential energy curves. In a torsion angle energy scan, the energy is typically plotted on the y-axis and the torsion angle on the x-axis, showing the energetically favourable conformations as energetic minima and energetic barrier heights (maxima) between conformations. A potential energy curve/ energy scan is essentially a cross-section of a potential energy surface (see section 4.1.2). Due to the conformation of PEA/PEAH⁺ (see Fig. 4.1), the position of the amino side chain is defined by the torsion angle τ , which is the main structural factor in the determination of energetically favoured geometries of PEA/PEAH⁺. This justifies the use of an energy scan (1 geometric dimension) rather than calculating the full potential energy surface (2 geometric dimensions).

Furthermore, the aquatic environment of PEA/PEAH⁺ has to be taken into account. Long-range and short-range interactions with water can have a large impact on the conformation of a molecule.¹⁹⁰ Therefore, the torsion angle energy scan was studied in three model environments: in gas phase, in a dielectric infinite continuum of water using the

conductor-like polarisation continuum model (CPCM, also termed ‘implicit solvation approach/environment’ in the following),^{212, 213, 238, 239} and in an implicit solvation environment that also includes the interaction of one explicit water molecule with the amino group (‘hybrid solvation model’). In implicit solvation approaches, the bulk of the solvent is represented as a structureless polarisable medium that is solely characterised by its dielectric constant ϵ .^{238, 239} Generally, computational models use a dielectric constant of 80.4 to include the aqueous background. One explicit water molecule per ionisable group in addition to the implicit solvation environment was found to improve accuracy and reliability of isotropic nuclear magnetic shielding calculations, which were used as computational model validation.¹⁹⁰

Geometry optimisations in ORCA (version 4.0.1) were performed with the PBE0 exchange correlation functional,²¹¹ using a pc-2 basis set.^{206–208} D3 dispersion correction^{240, 241} was included and the RIJ-COSX approximation²⁴² with a def2/J auxiliary basis set²⁴³ was applied. The final point energy values for each geometry optimised conformation were then plotted against the respective constrained torsion angle. To facilitate the comparison between the different environments, the total energy is shown relative to the energy in the *gauche 1* conformation for each system. The identified energetic minima were reoptimised without conformational restraints and their eigenvalues were checked for imaginary frequencies to verify whether the points of convergence were actual energetic minima rather than saddle points.

The molecular electrostatic potential (MEP) of energetically-favoured conformations (energetic minima) of PEA/PEAH⁺ was obtained using the GAMESS program (version 18/08/2016, R1)²¹⁴ with the PBE0 exchange functional in conjunction with the pc-2 basis set.^{206–208} Calculations were carried out with a polarisable solvation continuum model. Using the wxMacMolPlt program (version 7.6),²⁴⁴ a three-dimensional electron density isosurface was created with 100 grid points and a contour value of $0.1 \text{ e} \cdot \text{a}_0^{-3}$. To

visualise the MEP, the density isosurface was coloured with a maximum value of $0.9 E_h \cdot e^{-1}$ and the RGB colour scheme with red representing positive, green neutral and blue negative charge.

4.2.2 Nuclear Magnetic Resonance Spectroscopy of PEA for Model Validation

To compare the computational model to empirical measurements of nuclear magnetic resonance (NMR) ^1H shifts of PEA/PEAH⁺, isotropic nuclear magnetic shielding values of ^1H nuclei were calculated for the identified energetically favoured conformations in the hybrid solvation model, using ORCA (version 3.0.0) at the PBE0/aug-pc-2 level of theory. As for previous geometry optimisations, RIJ-COSX approximation with a def2-TZVPP/J auxiliary basis set was used. All nuclear shielding calculations were run with the Individual Gauge for Localized Orbitals method (IGLO).²⁴⁵

Solutions of 0.05 mol/L of 2-phenylethylamine hydrochloride (Sigma-Aldrich, 98 %) were used as samples for NMR spectroscopy. Solutions were prepared in 0.04 mol/L sodium phosphate buffer at pH 11.8 for PEA and pH 6.8 for PEAH⁺ containing 10 % deuterium oxide (Sigma-Aldrich) as solvent lock and tetramethylsilane (TMS, 50 μL , Sigma-Aldrich, >99.5 %) as the internal standard ($\delta_H = 0$). NMR spectra were recorded on a JEOL ECZ 400S spectrometer.

The calculated ^1H nuclear shielding constants of PEA/PEAH⁺ in the hybrid solvation model were then compared to experimentally determined ^1H NMR shifts of PEA/PEAH⁺ measured in water by plotting calculated values against experimental results and performing least-squares linear regressions for the different conformations *gauche* and *anti* for PEA and PEAH⁺.

4.2.3 Computations of Receptor Binding

The homology model for the active state of human TAAR1 was downloaded from the GPCR database.²⁴⁶ Then, 32 amino acids, known to be involved in the ligand binding site,²³² were cut out of the 3D model of the TAAR1 receptor using the molecular visualization program VMD.²⁴⁷ The position and size of the chosen binding pocket is shown in Fig. 4.2. Using Avogadro (version 1.1.1),²⁴⁸ hydrogen atoms were added to the amino acid backbone. As the amino acids of the binding pocket are in their standard protonation state (at physiological pH 7.4), all are neutral except for aspartate residue 103 (Asp103), which is negatively charged. Additionally, peptide bonds were added manually using Avogadro²⁴⁸ to cap the cutting sites of the binding pocket. Thereby, a methyl group was introduced on the amino side and a nitrogen-methyl group was added to the unbound carboxyl side. The molecular capping procedure of amino acids was adapted from the Molecular Fractionation with Conjugate Caps (MFCC) approach.²⁴⁹

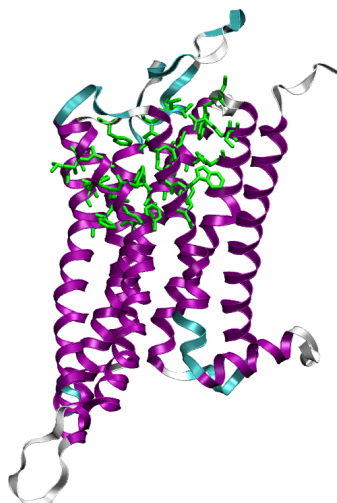


Fig. 4.2: Secondary structure of the TAAR1 receptor with alpha helices in purple, beta turns in cyan and random coils in white. The amino acids of the binding pocket are shown in green stick representation. The majority of the chosen binding pocket is part of alpha helix secondary structures. The receptor model is the homology model for the active state of human TAAR1, which was downloaded from the GPCR database²⁴⁶ and the visualisation was produced using the molecular visualization program VMD.²⁴⁷

After the preparation of the binding pocket, I used the molecular visualization program VMD²⁴⁷ to position the ligand PEA/PEAH⁺ in the center of mass of the binding pocket, facing Asp103 with its amino group, as this had previously been identified as the primary binding point.²³² Thereby, the start conformation of the ligand was the geometry-optimised *gauche 2* conformation from the implicit solvation model.

In a first computational step, all manually added methyl groups, nitrogen and hydrogen atoms were allowed to optimise using the universal force field²⁵⁰ approach in Avogadro.²⁴⁸ Keeping the ligand (PEA/PEAH⁺) and the amino acid backbone constrained, the manually added atoms were then further optimised using the PBE functional²¹⁰ with D3 dispersion correction^{240,241} and SZV-MOLOPT-GTH basis set^{209,251} in CP2K (version 6.1).^{215,252}

In the following, the binding pocket was placed inside a spherical cavity with radius 18.12 Å, outside which a dielectric continuum simulated the protein background. The size of the dielectric cavity for the TAAR1 receptor binding pocket was chosen based on the van der Waals radii of all atoms. To model the protein background, the self-consistent reaction field (SCRF) method²⁵³ with a dielectric constant of 8 was applied. Previous studies showed that the protein environment in an enzymatic reaction can be adequately represented by embedding the active site in a dielectric cavity with this dielectric constant.²⁵⁴

Then, PEA/PEAH⁺ was allowed to optimise inside the binding pocket (all binding pocket atoms constrained) using the PBE²¹⁰ functional with D3 dispersion correction^{240,241} and TZV2PX-MOLOPT-GTH basis set^{209,251} in CP2K. Thereby, the poisson solver^{255,256} was used to isolate the (40 Å)³ unit cells in the periodic system. This suppresses any potential interactions between the binding pockets from neighbouring unit cells. By default, CP2K introduces a uniform background charge to neutralise charged periodic systems.

The binding energy between the TAAR1 binding pocket and the ligand (PEA/PEAH⁺) was calculated by subtracting the energy of the binding pocket and the energy of the ligand from the energy of the TAAR1-ligand complex. Furthermore, other binding properties of PEA and PEAH⁺ were measured, such as the distance and the angle between the Asp103 amino acid residue and the ligand, and the root mean-square deviation between the backbone atomic positions of the protonated and neutral ligand upon binding. In structure based drug design and bioinformatics, the root-mean-square deviation (RMSD) between atomic positions is commonly used as a measure of difference between two superimposed molecules.²⁵⁷

To determine the effect of the protonation of PEA on receptor-ligand binding, the comparability of the start conditions for PEAH⁺ and neutral PEA is key. Hence, both

were optimised based on the same start conformation and position. For PEAH⁺ the energetically-favoured *gauche 2* conformation from calculations in the implicit solvation environment was chosen. For neutral PEA-TAAR1 binding experiments, a hydrogen atom from the PEAH⁺ amino group was removed. This ensures the same start conditions for PEA-TAAR1 as for computational experiments with PEAH⁺-TAAR1. The conformation of PEA in water was found to be very similar to PEAH⁺ in water, with $\Delta\tau = 2.2^\circ$ in the implicit solvation environment (see results below), justifying this approach as being representative for optimal geometries for PEA as well as PEAH⁺.

4.2.4 Computations of Protonated Receptor Binding

To explore the effects of receptor protonation on receptor-ligand binding, a proton was added to the Hist99 residue of the previously defined binding pocket of TAAR1, using Avogadro (version 1.1.1).²⁴⁸ The hydrogen was allowed to optimise in the absence of a ligand using the PBE²¹⁰ functional with D3 dispersion correction^{240,241} and TZV2PX-MOLOPT-GTH basis set^{209,251} in CP2K. Thereby, the rest of the binding pocket was constrained and the poisson solver^{255,256} isolated $(40 \text{ \AA})^3$ unit cells in the periodic system. As before, the binding pocket was enveloped in a dielectric continuum ($\varepsilon = 8$), allowing for a spherical cavity with the radius of 18.12 \AA for the binding pocket.

Subsequently, PEA and PEAH⁺ were added to the center of the binding pocket, occupying the same start position and conformation as for the unprotonated TAAR1 binding pocket. Constraining the entire binding pocket, including the additional histidine proton, PEA and PEAH⁺ were allowed to optimise using CP2K with the PBE²¹⁰ functional and D3 dispersion correction,^{240,241} TZV2PX-MOLOPT-GTH basis set^{209,251} and the poisson solver^{255,256} isolating $(40 \text{ \AA})^3$ unit cells in the periodic system. The protein background was again modelled using the SCRF method with $\varepsilon = 8$ and radius 18.12 \AA .

As before, the binding energy between the TAAR1 binding pocket with protonated histidine and the ligand (PEA/PEAH⁺) was calculated by subtracting the energy of the binding pocket and the energy of the ligand from the energy of the optimised TAAR1-ligand complex. Furthermore, other binding properties of PEA and PEAH⁺ were measured, such as the distance and the angle between the Asp103 amino acid residues and the ligand, and Hist99 and the ligand.

4.2.5 Reality Check: Salinity and Temperature Conditions in Field and Model

The dielectric constant (ϵ , also called relative permittivity) is a measure for the capacity of a material to store a charge.²⁵⁸ In computational chemistry, water or a protein background can be modelled implicitly by applying a background dielectric environment.^{238,239} Although a fixed value of 80.4 is usually assumed to model any aqueous background²⁵⁹ and $\epsilon = 8$ has been shown to approximate a protein background,²⁵⁴ in reality, the dielectric constant varies depending on the salinity and temperature of the environment.²⁶⁰

Effects on PEA/PEAH⁺

To explore the range of the dielectric constant that is relevant for intertidal crustacean habitats in England, the regression equation developed by Klein and Swift (1977)²⁶⁰ was used. Fig. 4.3 plots the salinities and temperatures that are relevant for British coastal waters against the dielectric constant ϵ . The sea temperature at the British coast varies between around 5 and 20°C.²⁶¹ Inhabiting a variety of environments, *P. bernhardus* and *C. maenas* can encounter salinities from 20 ppt NaCl,⁹⁷ e.g. after heavy rainfall or in estuaries, to 45 ppt after evaporation in summer in tide pools. 45 ppt has

also been used to study the chemosensory ability of crustaceans under salinity stress.²⁶² Furthermore, 15-20°C and 35ppt NaCl concentration approximates the behavioural experimental condition in this study. Fig 4.3 shows that, following the deductions described above, a range of 80.5 to 70.2 for the dielectric constant is relevant for British coastal habitats.

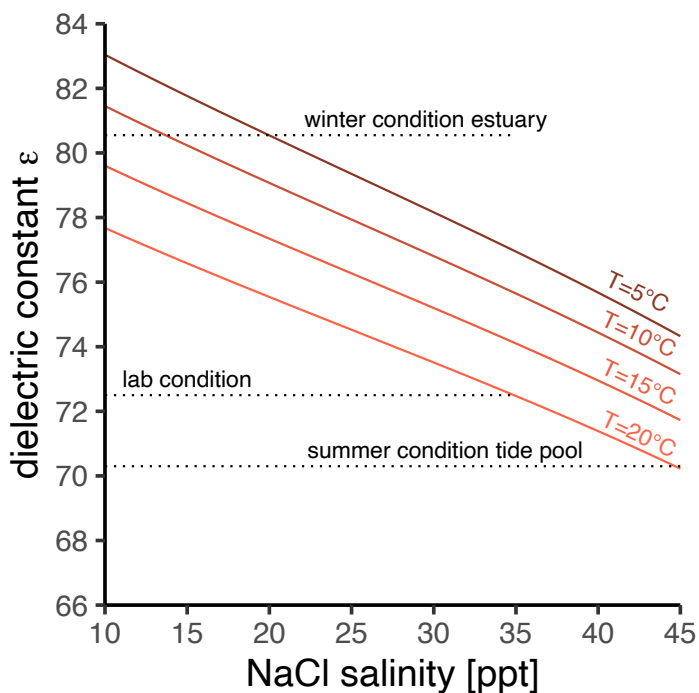


Fig. 4.3: The dielectric constant ϵ of water depends on the temperature and salinity. The dielectric constant decreases with increasing salinity and temperature. The chosen salinity and temperature range is relevant for hermit crab and shore crab habitats in Great Britain. The data is fitted using the regression equation from Klein and Swift (1977).²⁶⁰

To explore the impact of changes in the dielectric constant on PEA/PEAH⁺ due to changes in temperature and salinity, the previously optimised conformers of PEA and PEAH⁺ in the implicit solvation models ($\epsilon = 80.4$) were reoptimised in different dielectric environments within the CPCM using ORCA (version 4.0.1).^{212,213} To explore the effect of salt (NaCl) in water and changes in temperature on the quantum chemical

models of PEA and PEAH⁺, the dielectric constant $\varepsilon = 80.4$ was reduced in 3 5-point decrements, leading to a range of 80.4 - 65.4. To explicitly include the conditions during the behavioural experiments I also added the dielectric constant of 72.5 to the computational set of experiments. Geometry optimisations were performed as previously, with the PBE0 exchange correlation functional²¹¹ using a pc-2 basis set²⁰⁶⁻²⁰⁸ and RIJ-COSX approximation²⁴² with a def2/J auxiliary basis set.²⁴³ D3 dispersion correction^{240,241} was included. The energy difference between extended and folded conformation, the torsion angle τ and the dipole moment were compared to the original results obtained with $\varepsilon = 80.4$.

Effects on TAAR1-PEA/PEAH⁺

Finally, as water penetration is known to affect local structures and polarisability inside proteins (increasing the dielectric environment)²⁶³ and dissolved salt (NaCl) and increasing temperatures may decrease the dielectric constant,²⁶⁴ I also explored the effect of changes in the model dielectric environment for the receptor-ligand binding experiments. To study receptor-ligand binding properties under water and/or salt penetration, a series of computational experiments were carried out. Thereby the dielectric constant was increased from $\varepsilon = 8$ (protein background) to $\varepsilon = 10$ to explore the potential effect of water penetration and decreased to $\varepsilon = 6$ and $\varepsilon = 4$ to explore the effect of a dielectric decrement upon salt introduction or at increased temperatures. For each set of experiments PEA/PEAH⁺ was allowed to optimise inside the TAAR1 binding pocket (all binding pocket atoms constrained) using the PBE²¹⁰ functional with D3 dispersion correction^{240,241} and TZV2PX-MOLOPT-GTH basis set^{209,251} in CP2K. The TAAR1-PEA and TAAR1-PEAH⁺ binding models were compared in the four dielectric environments by determining the distance between Asp103 oxygen atom and PEA/PEAH⁺ nitrogen

atom, the hydrogen bond angle, the torsion angle of the PEA/PEAH⁺ amino side chain and the TAAR1-PEA/PEAH⁺ binding energy.

4.3 Results

4.3.1 Conformational Preference and Charge Distribution of Different Protonation States of PEA

Fig. 4.4A & B show the energy of PEA and PEAH⁺ respectively as a function of the torsion angle τ of PEA/PEAH⁺ in the three model environments: gas phase, a conductor-like polarisable continuum model (implicit solvation environment) and in the hybrid solvation environment, which is the implicit solvation environment with an explicit water molecule interacting with the PEA amino group. Energetically stable (favoured) conformations are energetic minima in the torsion angle energy scan. The 360° torsion angle energy scans reveal three energetically favoured conformations as minima for both neutral and protonated PEA and for all three model environments. An extended (*anti*) and two folded (*gauche*) conformations were found regardless of the model environment. The solvation models (blue and green in Fig 4.4) clearly change the scan profile as compared to the gas phase environment (red in Fig. 4.4) for both protonation states, PEA and PEAH⁺, with regards to the relative stabilities of the energetic minima and energy barrier heights (discussed in more detail below). The torsion angles of the energetic minima of PEA and PEAH⁺ (x-axis of Fig. 4.4) on the other hand, seem to be largely independent of the model environment.

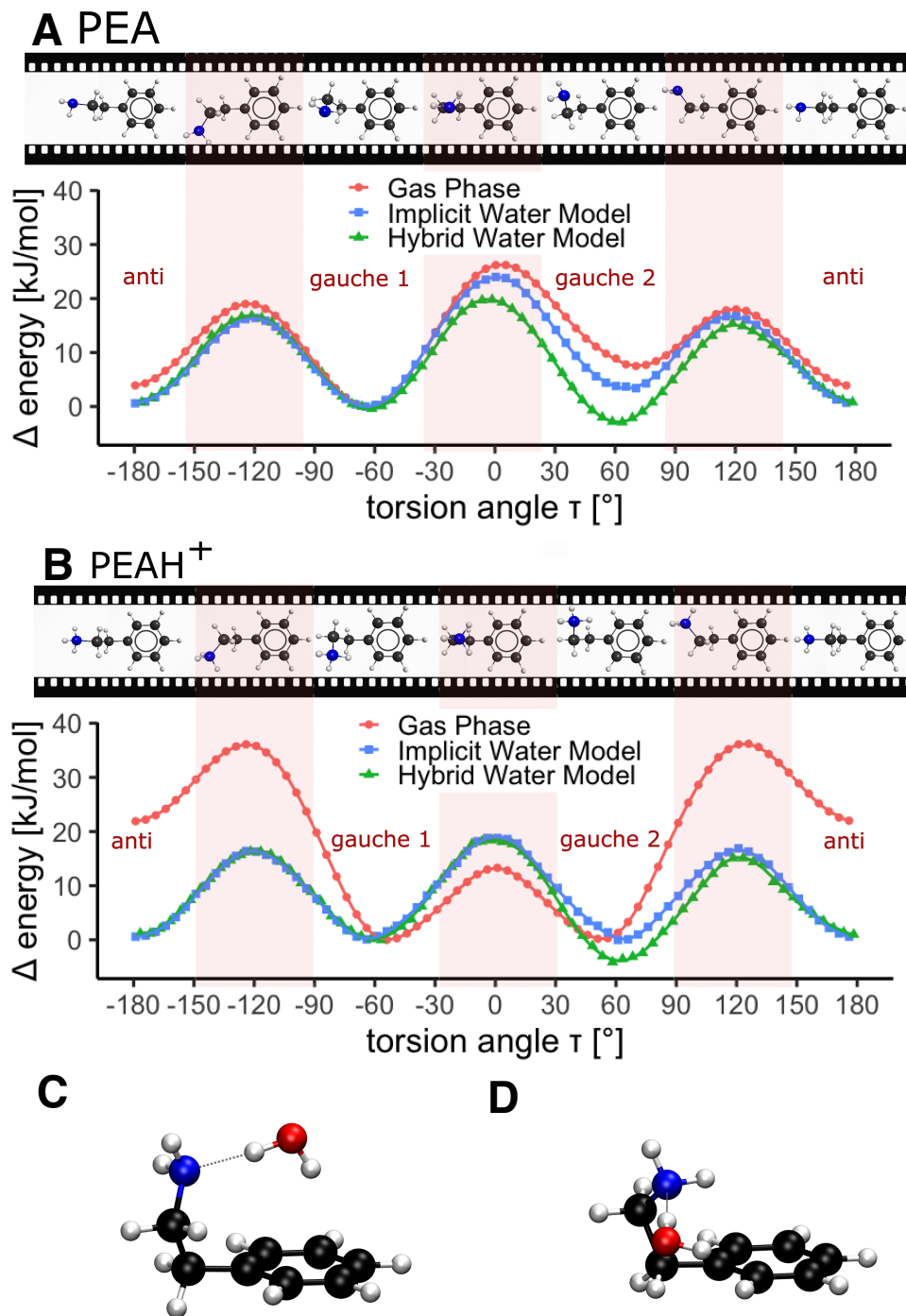


Fig. 4.4: Torsion angle energy scan of PEA and PEAH⁺ in different environments to identify energetically stable conformations. (Full caption on the following page.)

Fig. 4.4: (Continued from previous page.) Torsion angle energy scan of the amino side chain torsion angle τ of neutral (A) and protonated (B) PEA; and the conformation of folded neutral PEA in *gauche 2* (C) and *gauche 1* (D) interacting with a water molecule. Energy values are relative to the energy of the *gauche 1* conformation from the respective environment. Conformations for selected torsion angles are depicted in a filmstrip above the scan. Energetically stable (favoured) conformations are energetic minima; both protonation states show minima at an extended and two folded conformations. The potential energy curves in two solvation models (blue and green) are compared to gas phase (red circles). The implicit solvation model (blue squares) is augmented by including the interaction with one explicit water molecule (hybrid solvation model, green triangles). As only one water molecule has been added, this scan is asymmetric. Hydrogen atoms are depicted in white, carbon atoms in black, nitrogen atoms in blue and oxygen atoms in red.

The neutral PEA torsion angle energy scans (Fig. 4.4A) show an asymmetry in the relative energetic stability of the two folded conformations ($\tau_{gauche1} \approx -60^\circ$, $\tau_{gauche2} \approx +60^\circ$). This can be explained by the asymmetry of the amino group, containing two hydrogen atoms (H_N) and an electron lone pair. In the *gauche* conformation either H_N or the nitrogen lone pair are interacting with the aromatic ring, leading to different relative stabilities. The environment, however, has a clear impact on these energetic differences. The implicit solvation model stabilises the *gauche 2* conformation with lone pair- π interaction ($\tau \approx +60^\circ$), as compared to the gas phase. This effect becomes more pronounced with the inclusion of an explicit water molecule (hybrid solvation model), which even reverses the preference for the folded conformations: Whilst *gauche 1* was the energetically favoured folded conformation in gas phase and in the implicit solvation model, *gauche 2* is favoured in the hybrid solvation model. This is due to the hydrogen atoms of the water molecule forming hydrogen bonds with the nitrogen lone pair and the π -system on either side and thereby promoting the energetic stability of the *gauche 2* conformation (Fig. 4.4C). The distance between the amino group hydrogen atom closest to the benzene ring and the π -system is 3.28 Å for the *gauche 1* conformation (Fig. 4.4D)

whilst the distance between the π -system and the water hydrogen atom is 2.48 Å for *gauche 2* (Fig. 4.4C). As oxygen atoms are known to be rather weak hydrogen-bond acceptors compared to nitrogen atoms,²⁶⁵ the nitrogen lone pair of PEA interacts with the water hydrogen atom rather than PEA's H_N forming a bond with the water oxygen atom.

The torsion angle energy scan for PEAH⁺ (Fig. 4.4B) shows that solvation has a strong effect on the conformation of PEAH⁺. The difference between the gas phase model (red) and the solvation models (green and blue) are particularly pronounced in the relative energetic stability of the extended conformation ($\tau_{anti} \approx \pm 180^\circ$) and the energetic barrier height between the folded and extended conformation ($\tau_{barrier} \approx \pm 120^\circ$). The solvation models (green and blue) stabilise the *anti* conformation, decreasing their energy relative to the *gauche* conformations. Adding one explicit water molecule (hybrid solvation model, green) further decreases the relative energy of one of the folded conformations. Similarly to neutral PEA, the folded conformation where the water molecule mediates between the amino group and the aromatic ring is the energetically most stable geometry of PEAH⁺ in the hybrid solvation model (compare Fig. 4.4C for PEA). In this conformation, the distance between the hydrogen atom of the PEAH⁺-bound water molecule and the π -system is 2.39 Å, slightly smaller than for PEA (see above), which indicates a stronger bond.

Some of the torsion angle energy scans (Fig. 4.4A& B) are asymmetric, reflecting the range of potential conformations for PEA and PEAH⁺. It is important to note, however, that neutral and protonated PEA both have degenerate (i.e. same energy level) folded conformations for negative and positive torsion angles ($\tau \approx \pm 60^\circ$) as their absolute energetic minimum. By rotation around the C-N bond, the flexible amino side chain allows the molecule to lock into the same folded conformation for negative as well as positive torsion angles. This symmetry is not reflected in the above torsion angle

energy scans as computational methods only allow for the convergence towards the local energetic minimum. The global energy minimum can only be identified through understanding the chemical structure of the molecule or else a comprehensive exploration of the entire potential energy surface.

To ensure an accurate representation of the energetic minima of PEA/PEAH⁺, their conformations, as deduced from the torsion angle energy scans, were reoptimised without torsion angle constraints. The resulting energy differences between the conformations allow me to deduce that in water, the *gauche* conformation of PEA/PEAH⁺ is energetically favoured over the *anti* conformation for both protonation states (Table 4.1). The torsion angles and energy differences for the hybrid solvation model are summarised in Table 4.1, whereby the energy of the water molecule was subtracted from the total energy of the PEA/PEAH⁺-water system. It is important to note that especially the *gauche 1/gauche 2* energetic differences are very close to chemical accuracy of quantum chemical calculations (about 4 kJ/mol),²⁶⁶ making a precise conformational prediction difficult. However, the concept of chemical accuracy is a rule of thumb to estimate the accuracy of computational results as compared to empirical measures and therefore doesn't fully apply to the comparison between computational models.²⁶⁶

Table 4.1: Torsion angles τ and energy differences ΔE of the energetically favoured conformations of PEA and PEAH⁺ in solvation as determined with the hybrid solvation model. The energetic minima were optimised without geometrical constraint and the energy of the explicit water molecule was subtracted. Energy differences are shown relative to the lowest energy conformation.

	PEA		PEAH ⁺	
	ΔE [kJ/mol]	τ [°]	ΔE [kJ/mol]	τ [°]
<i>anti</i>	3.5	178.1	4.5	179.8
<i>gauche 1</i>	1.2	-60.8	3.9	-59.0
<i>gauche 2</i>	0	61.8	0	60.6

The proportion of PEA/PEAH⁺ in the different conformations is governed by the energy difference between conformations and the temperature of the system.²⁶⁷ By calculating the Boltzmann factor (eq. 4.1), the energy differences (Table 4.1) can be translated into relative populations N .²⁶⁷

$$\frac{N_{anti}}{N_{gauche}} = \frac{g_{anti}}{g_{gauche}} \cdot e^{-\frac{E_{anti}-E_{gauche}}{R \cdot T}} = \frac{1}{2} \cdot e^{-\frac{\Delta E}{R \cdot T}} \quad (4.1)$$

with g : degeneracy (number of states at energy level)

R : molar gas constant

With an annually averaged sea surface temperature of 17 °C for 2021,²⁶⁸ the ratio of extended to folded conformation is 1:9 for neutral PEA and 1:13 for PEAH⁺. Hence, decreasing the pH leads to a small increase in the proportion of the infochemical in the folded conformation.

To assess pH-dependent effects on the electrostatic properties of PEA/PEAH⁺, I studied its charge distribution in both protonation states. Both, neutral PEA and PEAH⁺ show charge separations in the amino group and C-H bonds (Fig. 4.5A & B). PEA is overall less positively charged than PEAH⁺ (red in Fig. 4.5A vs. B). The dipole moment can be used as a measure of the charge separation.²³⁴ Even in the same folded conformation, protonated and neutral PEA clearly differ in magnitude and direction of the dipole moment (red arrow in Fig. 4.5C & D). The dipole moment is 2.5D for folded neutral PEA, and 12.6D for PEAH⁺ in the same conformation.

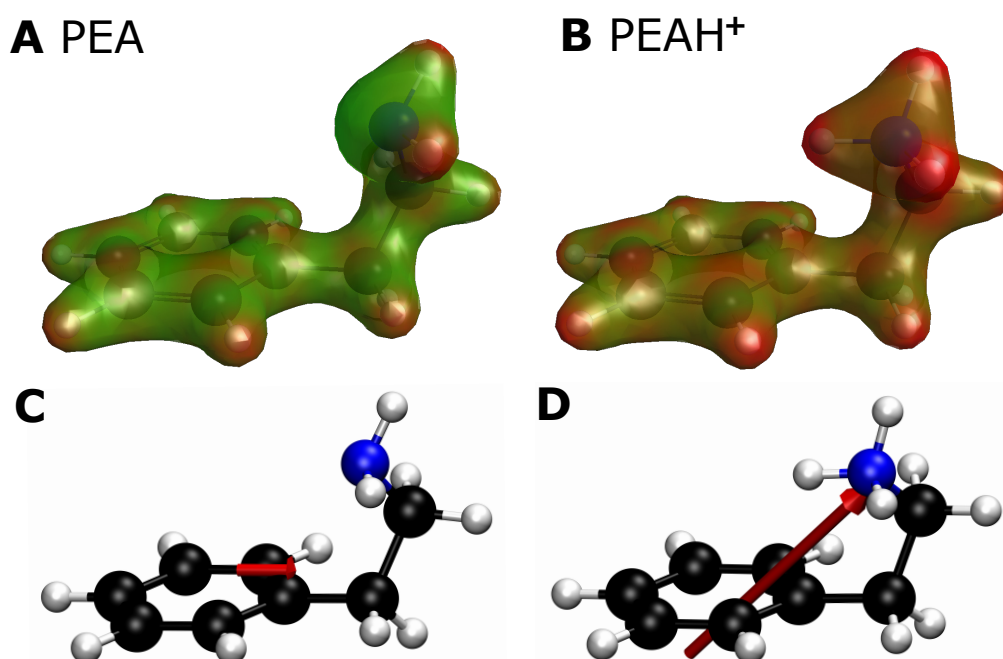


Fig. 4.5: Charge distributions (A & B) and dipole moment (C & D) of folded PEA in the implicit solvation model in the neutral (A & C) and protonated state (B & D). Electron density isosurfaces (A & B) are colour-coded according to the molecular electrostatic potential with blue representing negative, green neutral and red positive charge. The 30% transparency of the electron density surface shows the conformation of the molecule underneath with hydrogen atoms in white, carbon atoms in black and nitrogen atoms in blue. The dipole moment (C & D) is represented by a red arrow pointing from negative to positive charge.

4.3.2 Computational Model Validation

^1H chemical shieldings of the computational PEA/PEAH⁺ models were calculated to determine whether the computationally identified global energetic minimum *gauche* conformation coincides with the empirically measured conformation of PEA/PEAH⁺ in water. In the following, I assess the correlation of the experimental nuclear magnetic resonance (NMR) ^1H shifts of PEA/PEAH⁺ in water with the calculated ^1H chemical shieldings for the different conformations of PEA/PEAH⁺ using linear regressions.

Due to the symmetry of the aromatic ring of PEA/PEAH⁺ and the free rotation about single bonds (fast exchange rate) only 4 carbon-bound ^1H shifts can be measured experimentally (see Fig. 4.6 for naming of PEA/PEAH⁺ carbons). Hence, the corresponding calculated shieldings were averaged to facilitate comparability: The calculated shieldings of the two hydrogen atoms bound to C_1 and C_2 were averaged to $\text{C}_1\text{-H}$ and $\text{C}_2\text{-H}$ respectively and the shieldings of the hydrogen atoms bound to C_{ar1} and C_{ar2} were averaged to $\text{C}_{ar1}\text{-H}$ and $\text{C}_{ar2}\text{-H}$ (see Fig. 4.6). As the protons bound to nitrogen were only observed in the low pH NMR experiments (PEAH⁺) they were excluded from the linear model. Furthermore, H_N are known to be problematic in NMR shielding calculations as they are highly affected by hydrogen bridge networks.²⁶⁹

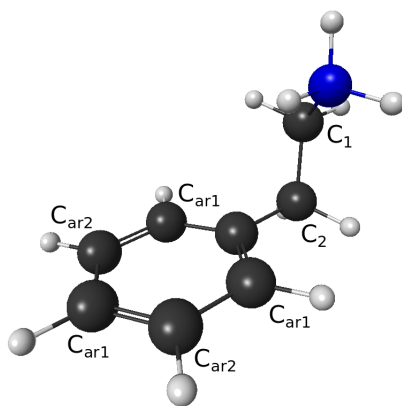


Fig. 4.6: Structure and naming of the carbons in PEA/PEAH⁺ to assign experimental ¹H NMR shifts to the calculated shieldings for both protonation states. Carbon atoms are shown in black, the nitrogen atom is blue and hydrogen atoms are white.

Fig. 4.7 shows a negative linear correlation between experimental ¹H shifts and calculated nuclear shieldings for extended (*anti*, black) as well as folded (*gauche*, red) conformations of PEA and PEAH⁺. Due to the symmetry of the fully protonated amino group in PEAH⁺, the *gauche* conformation of PEAH⁺ is the same at $\tau \approx -60^\circ$ and $\tau \approx +60^\circ$, whilst there are two different *gauche* conformations for PEA: (*gauche 1* with the amino group electron lone pair pointing away from the benzene ring and *gauche 2* with the lone pair pointing towards it, compare also section 4.3.1). In the following, I am aiming to determine, which computational model best aligns with the experimental findings. Calculated nuclear shieldings are absolute values whilst the experimental shifts are measured relative to the (pH-insusceptible) reference compound TMS, which explains the negative relationship between experimental and calculated values. The experimental ¹H shift of TMS is zero, whilst their ¹H shielding was calculated to be 31.3 ppm.

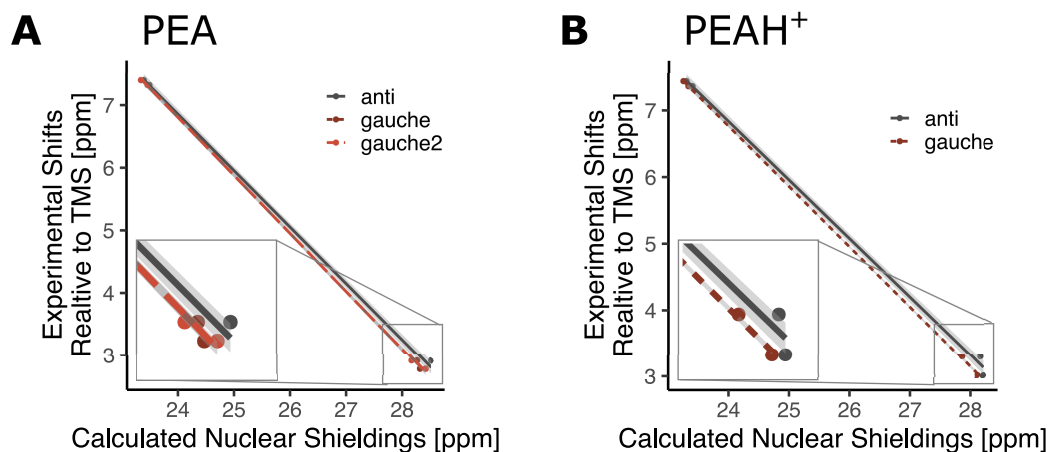


Fig. 4.7: Calculated nuclear proton shieldings as a function of the experimental ^1H NMR shifts for the different conformations of neutral PEA (A) and PEAH^+ (B). The 95% confidence interval is shown in gray (narrow for both). The amino protons were only measurable for PEAH^+ and thus excluded from the linear regression analysis. Magnified inset window shows the protons of the PEA/ PEAH^+ ethyl groups ($\text{C}_{1/2}\text{-H}$).

The two folded conformations (*gauche*) of neutral PEA are not separable in the linear regressions (see Fig. 4.7A). However, the folded and extended conformation show slightly different linear fits for both protonation states (see red vs black in Fig. 4.7A & B). To measure the correlation between experimental NMR shifts and calculated shieldings, the accuracy of the fit can be determined. As the calculated values are absolute but the experimental shifts are measured relative to TMS, the calculated ^1H NMR shielding for TMS (31.3 ppm) would be the x-axis intercept if the computational model fully coincided with the experimental observations. In reality, depending on the fit of the linear regression, the projected ^1H NMR shift for TMS deviates from $y(31.3 \text{ ppm})=0 \text{ ppm}$. The ‘accuracy’ of the model can be defined as the chemical shift that corresponds to the calculated TMS shielding ($y(31.3 \text{ ppm})$) based on the respective linear regression¹⁹⁰ (see also TMS-H, last row in Table 4.2). A perfect model fit would have the accuracy 0 ppm: The calculated TMS proton shielding (31.3 ppm) would coincide with the experimental NMR measurement where TMS was used as a reference (i.e. set to zero). Estimating

the accuracy of the fit of the experimental findings with the computational models is one way of validating the quantum chemical calculations.

With an accuracy of 0.03 ppm, the *gauche* conformations of neutral PEA fit the experimental values better than the *anti* conformation (accuracy 0.27 ppm). Likewise for PEAH⁺, the *gauche* conformation of PEAH⁺ reaches an accuracy of 0.14 ppm whilst the accuracy of the computational model of PEAH⁺ in the *anti* conformation is only 0.40 ppm. Based on the accuracy, the folded conformation aligns best with experimental findings of the conformation for both protonation states of PEA in water.

Additionally, the scattering of values in the linear model can give valuable information on the goodness of fit. The 95 % confidence intervals (gray band in Fig. 4.7) of the linear models of the folded conformations (*gauche*) are narrow for both protonation states. However, less scattering in higher calculated nuclear shieldings leads to narrower confidence intervals for the *gauche* conformations, indicating a better fit of these computational models with the experimental results. The linear models of the *gauche* conformations reach a coefficient of determination of R²=99.99 % for protonated and R²=99.97 % for neutral PEA, whilst the *anti* conformations have an R²=99.86 % and R²=99.89 % respectively. I conclude that PEA and PEAH⁺ in the *gauche* conformation show the best fit with the experimental data. This coincides with the conclusion based on the accuracy of the models (see above).

Although Fig. 4.7 indicates that the linear regressions for the *gauche* and *anti* models overlap for lower calculated nuclear shieldings (protons of the benzene ring, C_{ar}-H in Fig. 4.6), they separate towards higher calculated shieldings (protons of the amino side chain, C_{1/2}-H in Fig. 4.6). The accuracy of the fit was measured at 31.3 ppm (calculated ¹H TMS shielding), where the models for the *gauche* and *anti* conformations are notably different. Hence, the difference between folded (*gauche*) and extended (*anti*) conformation of PEA and PEAH⁺ is reflected mainly in higher calculated nuclear shieldings,

corresponding to chemical proton shifts of the side chain (C₁-H and C₂-H in Fig. 4.6). Applying the linear regression equation (eq. 4.2), the calculated nuclear shieldings (σ) were transformed into chemical shifts (δ) to enable a direct comparison (Table 4.2).

$$\delta = a \cdot \sigma + b \quad (4.2)$$

$$\text{for PEA : } a_{anti} \approx -0.90, \quad b_{anti} \approx 28.55 \text{ ppm}$$

$$a_{gauche} \approx -0.93, \quad b_{gauche} \approx 29.12 \text{ ppm}$$

$$a_{gauche2} \approx -0.93, \quad b_{gauche2} \approx 29.10 \text{ ppm}$$

$$\text{for PEAH}^+ : a_{anti} \approx -0.88, \quad b_{anti} \approx 27.96 \text{ ppm}$$

$$a_{gauche} \approx -0.91, \quad b_{gauche} \approx 28.53 \text{ ppm}$$

Table 4.2: Comparison of experimental ^1H shifts (δ) with calculated shifts (δ) of protonated and neutral PEA in water. Computationally determined shieldings (σ) were averaged for each of the four experimentally determined shifts and transformed into shifts following linear regression equation 4.2. The naming of the PEA/PEAH $^+$ -carbons is visualised in Fig. 4.6. The last row (TMS-H) shows the calculated chemical shifts for TMS based on the respective linear regression (‘accuracy’).

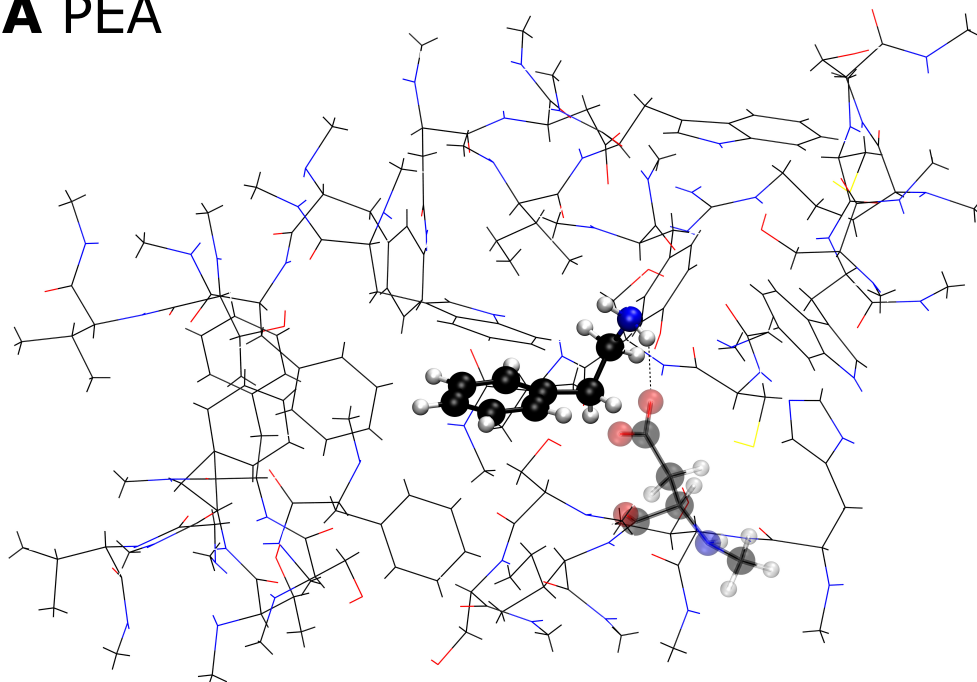
	neutral PEA [ppm]				PEAH $^+$ [ppm]		
	experimental δ	calculated δ			experimental δ	calculated δ	
		<i>anti</i>	<i>gauche 1</i>	<i>gauche 2</i>		<i>anti</i>	<i>gauche</i>
C $_1$ -H	2.91	2.80	2.86	2.96	3.30	3.18	3.27
C $_2$ -H	2.78	2.89	2.82	2.72	3.02	3.13	3.04
C $_{ar1}$ -H	7.32	7.32	7.31	7.31	7.37	7.36	7.37
C $_{ar2}$ -H	7.40	7.41	7.42	7.42	7.44	7.45	7.44
TMS-H	0	0.27	0.03	0.03	0	0.40	0.14

In summary, ^1H NMR spectroscopy verifies the computational findings: A comparison of the accuracies as well as the linear model fits confirm that the identified global energetic minima (PEA and PEAH $^+$ in the *gauche* conformation) fit best with the experimental values. Although models for *gauche 1* and *gauche 2* in PEA were not separable based on this method, my findings confirm that the folded conformation is the energetically favoured conformation for PEA and PEAH $^+$ in water.

4.3.3 An Increased PEA Dipole Increases Receptor-Ligand Binding

Computational binding experiments of PEA/PEAH⁺ with the TAAR1 binding pocket show that the protonation state of the ligand affects the binding properties. Although both binding experiments were initiated with the same conformation and location of the ligand (PEA/PEAH⁺) inside the binding pocket, their orientation and conformation differs upon binding to TAAR1 (see Fig. 4.8A vs. B). In the following, I describe how protonation of PEA changes different characteristics of receptor-ligand binding.

A PEA



B PEAH⁺

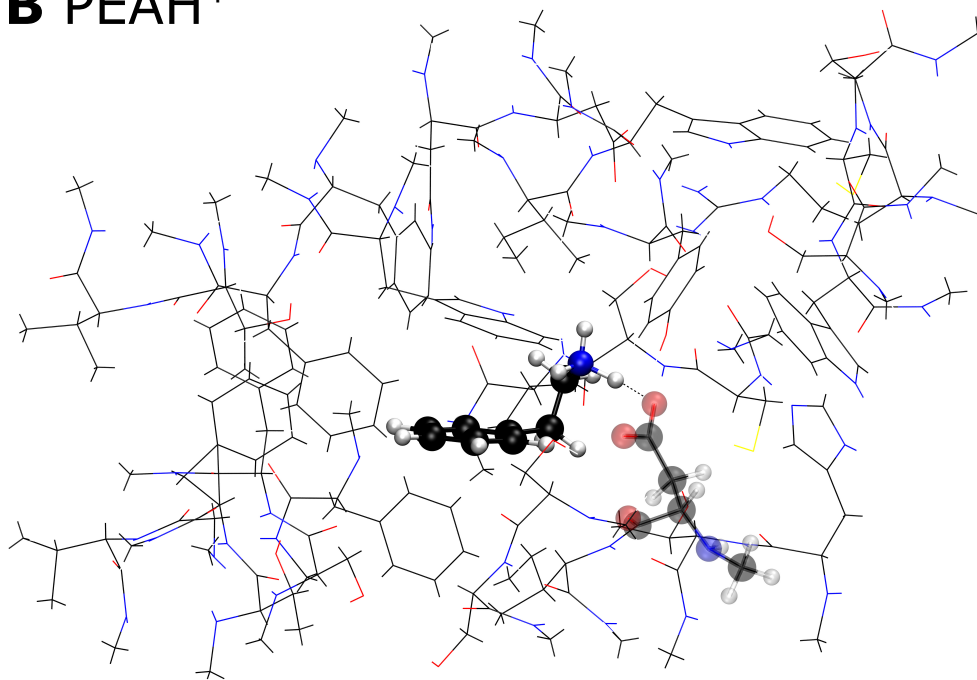


Fig. 4.8: Conformation of neutral (A) and protonated PEA (B) inside the TAAR1 receptor pocket. (Full caption on the following page.)

Fig. 4.8: (Continued from previous page.) Conformation of neutral (A) and protonated PEA (B) inside the TAAR1 receptor pocket. PEA/PEAH⁺ and the amino acid residue Asp103 (semi-transparent) are shown as ball-and-stick model, whilst the rest of the binding pocket is stylised as lines. Carbon atoms are shown in black, oxygen atoms in red, nitrogen in blue and hydrogen atoms in white.

Although the geometry optimisation of PEA and PEAH⁺ started with the same conformation of the backbone atoms (excluding hydrogens, RMSD=0 Å), the root-mean-square deviation (RMSD) between the backbone atomic positions of superimposed protonated and neutral PEA after binding is 2.1 Å. This shows that PEA and PEAH⁺ undergo substantially different conformational changes upon binding to TAAR1. The final torsion angle τ of the amino group side chain (see Fig. 4.1 for illustration of torsion angle) of neutral PEA is 82.9° whilst PEAH⁺ adopts a torsion angle of 66.5° inside the binding pocket. Both hence adopt very different conformations upon binding as compared to their non-complexed state (e.g. in water, compare section 4.3.1), $\tau = 61.8^\circ$ and 60.6° respectively.

Furthermore, PEAH⁺ establishes a strong hydrogen bond with the negatively charged Asp103 (Fig. 4.8B) whilst neutral PEA only maintains a weak link (Fig. 4.8A). The distance between the closest amino group hydrogen atom of PEA/PEAH⁺ and the negatively charged carboxyl group of Asp103 is 2.2 Å for neutral PEA whilst it is 1.4 Å for PEAH⁺ (see dotted lines in Fig. 4.8A & B). The distance between the PEA nitrogen atom and the aspartate oxygen atom is 3.1 Å for neutral PEA and 2.5 Å for PEAH⁺. Also, the angle of the hydrogen bond between PEA and aspartate increases upon protonation from 147.2° to 169.8°, another measure for a stronger hydrogen bond between TAAR1 and PEAH⁺ compared to PEA.

The resulting binding energy of PEAH⁺ with the TAAR1 binding pocket is -549 kJ/mol and -102 kJ/mol for neutral PEA. As both binding energies are negative, the com-

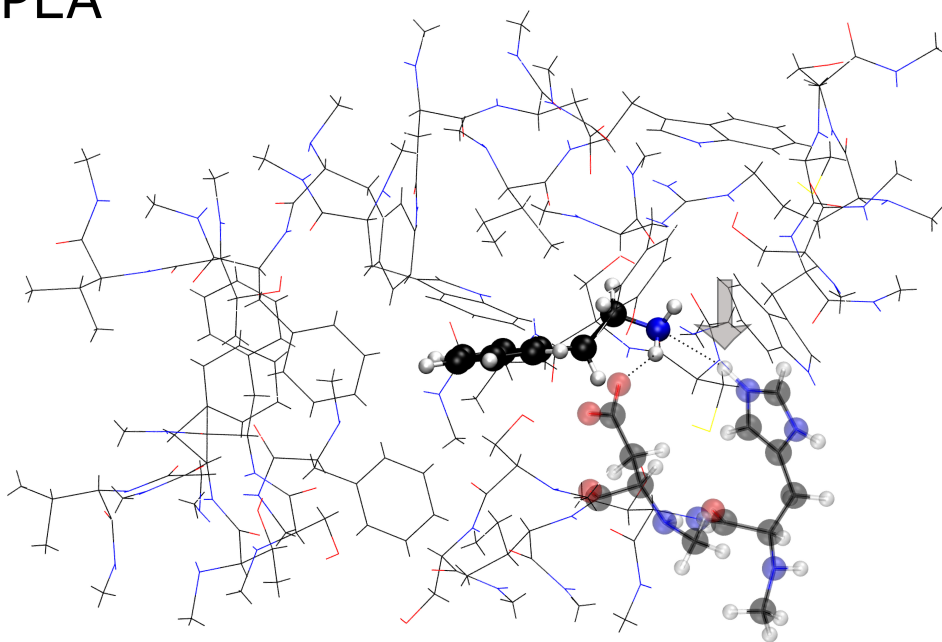
plexed state (bound to the TAAR1 receptor) is energetically favoured for both PEA and PEAH^+ over the non-complexed state. This confirms that PEA/ PEAH^+ could bind spontaneously to TAAR1. Furthermore, with a difference of 447 kJ/mol between the binding of TAAR1-PEA and TAAR1- PEAH^+ , the receptor-ligand binding becomes over 5 times stronger upon protonation of PEA.

4.3.4 A Protonated Receptor Binding Pocket Residue Decreases Receptor-Ligand Binding

Section 4.3.3 showed that decreasing the pH (protonation of the ligand PEA to PEAH^+) can increase receptor-ligand binding. However, changes in the pH could also affect residues of the receptor, which might in turn change receptor-ligand binding. As the aspartate residue Asp103 is negatively charged, the protonation of histidine residue Hist99 effectively neutralises the TAAR1 binding pocket.

Similar to findings in the unprotonated TAAR1 binding pocket (section 4.3.3), Fig. 4.9 shows substantial differences in receptor-ligand binding of PEA and PEAH^+ with TAAR1 when a histidine residue inside the TAAR1 binding pocket was protonated (gray arrow in Fig. 4.9). Furthermore, protonation of the histidine residue of TAAR1 changes the binding properties of both PEA and PEAH^+ (compare Fig. 4.8A vs. 4.9A and 4.8B vs. 4.9B). In the following, I describe the differences between the binding properties of PEA and PEAH^+ inside TAAR1 with protonated Hist99 and compare these to the binding properties of the unprotonated TAAR1 binding pocket.

A PEA



B PEAH⁺

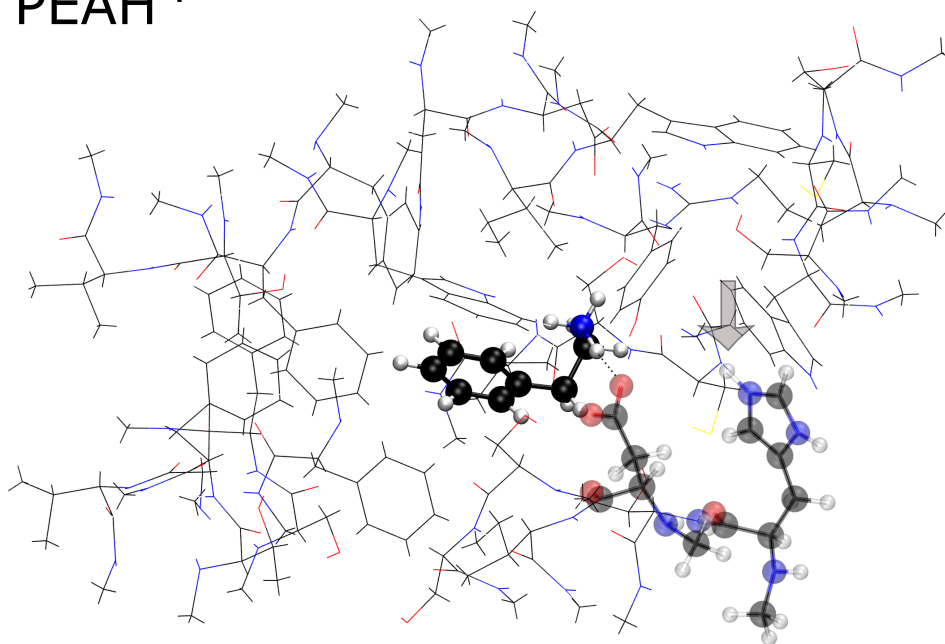


Fig. 4.9: Conformation of neutral (A) and protonated PEA (B) inside the TAAR1 receptor pocket with protonated histidine residues. (Full caption on following page.)

Fig. 4.9: (Continued from previous page.) Conformation of neutral (A) and protonated PEA (B) inside the TAAR1 receptor pocket with protonated histidine residue. PEA (opaque), Asp103 and protonated Hist99 (both semi-transparent) are shown as ball-and-stick models, whilst the rest of the binding pocket is stylised as lines. Carbon atoms are shown in black, oxygen atoms in red, nitrogen in blue and hydrogen atoms in white. A gray arrow points towards the added proton on the histidine residue.

With a torsion angle τ of 145.2° for the amino group side chain of PEA, neutral PEA adopts an almost extended (*anti*) conformation when binding to TAAR1 with protonated histidine residue, whilst PEAH^+ remains in the folded conformation (torsion angle of 58.9°). For comparison, the respective torsion angles in the energetically favoured non-complexed states were 61.8° (PEA) and 60.6° (PEAH^+ , both *gauche*) and 82.9° and 66.5° respectively inside the unprotonated TAAR1 binding pocket (see section 4.3.3). This indicates large changes in the conformation of the ligand, especially for neutral PEA, inside the receptor upon protonation of the histidine residue.

Whilst PEA forms a weak hydrogen bond between its nitrogen atom and the histidine hydrogen (distance 2.64 \AA) in addition to its bond to the aspartate residue (distance 1.9 \AA for $\text{H}_\text{N} \dots \text{O}_\text{Asp}$, see dotted lines in Fig 4.9A), the main point of receptor-ligand interaction for PEAH^+ remains the negatively charged carboxyl group of Asp103 (dotted line in Fig 4.9B). The distance between the PEAH^+ nitrogen atom and the histidine hydrogen is 5.15 \AA , revealing no evidence for an interaction of PEAH^+ with the protonated histidine residue, whilst the distance for $\text{H}_\text{N} \dots \text{O}_\text{Asp}$ remains at 1.4 \AA (as for unprotonated Hist99 in TAAR1, compare Fig. 4.8B). The distance between the PEA nitrogen atom and the aspartate oxygen atom is now 2.8 \AA for neutral PEA and remains at 2.5 \AA for PEAH^+ , with respective hydrogen bond angles of 145.7° and 154.0° .

Comparing these binding properties with section 4.3.3 indicates that the binding affinity of PEAH^+ to TAAR1 decreases, whilst the binding affinity of neutral PEA is strengthened by the protonation of the the histidine residue in TAAR1.

With a receptor binding energy of -127 kJ/mol for PEA and -376 kJ/mol for PEAH^+ , PEAH^+ -receptor binding is 249 kJ/mol stronger than PEA-receptor binding when the Hist99 residue of TAAR1 is protonated. This implies a 3-fold difference in binding affinity upon protonation of the ligand, whilst the binding was 5 times stronger upon protonation in the unprotonated binding pocket (section 4.3.3). Notably, the binding affinity of PEAH^+ with its receptor decreases by 173 kJ/mol , from -549 kJ/mol to -376 kJ/mol , upon protonation of the histidine residue inside the TAAR1 binding pocket, whilst the binding affinity of PEA increases by merely 25 kJ/mol .

4.3.5 Reality Check: Salinity and Temperature Conditions in Field and Model

Effects on PEA/ PEAH^+

To explore the effect of salt (NaCl) in water or increasing temperatures on the quantum chemical models of PEA and PEAH^+ , I conducted a set of computational experiments, whereby the dielectric constant was reduced in 3 5-point decrements, leading to a range of 80.4 - 65.4 for environmentally relevant conditions at the British coast. To explicitly include the conditions during the behavioural experiments I also added the dielectric constant of 72.5 to the computational set of experiments. The previously identified energetic minima of PEA and PEAH^+ were re-optimised in the implicit solvation model, applying different values for the dielectric constant.

As Fig 4.10 shows, the energy difference ΔE between the (energetically preferred) folded and extended conformation is stable for PEA over the examined range of dielectric constants, whilst it varies slightly for PEAH⁺. The energy difference between the folded and extended conformation ΔE_{PEAH^+} ranges between 0 and 2 kJ/mol, depending on the dielectric constant. However, no trend between ΔE and ϵ is apparent. Although changes in salinity and temperature lead to slight changes in energy difference and hence the population of energetically preferred conformations, the conformation of PEA and PEAH⁺ itself was unaffected by changes in the dielectric constant (maximum difference in amine side chain torsion angle for PEAH⁺ $\Delta\tau = 0.16^\circ$) and also the dipole moment remained unchanged within an accuracy of ± 0.05 D.

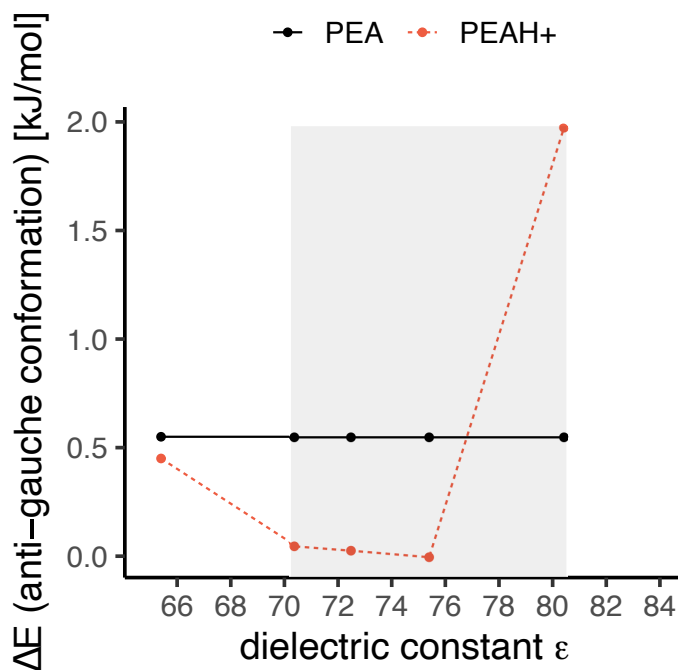


Fig. 4.10: The dielectric constant ϵ of water depends on the temperature and salinity and may in turn affect the energy difference between conformers. The energy difference between extended (*anti*) and folded (*gauche*) PEA and PEAH⁺ is shown at different dielectric constants within the implicit solvation model. The range of the dielectric constant relevant for British coastal waters is shaded in gray.

Effects on TAAR1-PEA/PEAH⁺

To explore potential effects of salt and water penetration into TAAR1 on the receptor-ligand binding properties, a series of computational experiments were carried out, whereby the dielectric constant was increased from $\varepsilon = 8$ (protein background) to $\varepsilon = 10$ to explore the potential effect of water penetration and decreased to $\varepsilon = 6$ and $\varepsilon = 4$ to explore the effect of a dielectric decrement upon salt introduction.

The bond length between the Asp103 oxygen and PEA/PEAH⁺ nitrogen remains at 3.10 Å and 2.52 Å respectively within all model environments. Similarly, the H-bond angle between Asp103 and the amino group of PEA/PEAH⁺ remains the same across all dielectric constants with an accuracy of $\pm 0.1^\circ$. The torsion angle of the ligand varies slightly, by $\Delta\tau_{max} = 1.4^\circ$ for both PEA and PEAH⁺, without an apparent trend with the dielectric constant.

Whilst ligand conformation and location change only marginally within the explored range of the dielectric constant, the dielectric environment can affect the receptor-ligand binding energy. Fig. 4.11 shows that whilst the binding affinity of PEA to TAAR1 varies only slightly ($\Delta E = 0.6$ kJ/mol), the binding affinity between PEAH⁺ and TAAR1, is weakened with increasing dielectric constant ($\Delta E = 12.1$ kJ/mol from $\varepsilon = 4$ to $\varepsilon = 10$). Introducing water into TAAR1 might therefore reduce its binding affinity to PEAH⁺, whilst the addition of salt increases it. In $\varepsilon = 4$, PEAH⁺ binds 5.47 times stronger to TAAR1 than PEA. The ratio decreases to 5.35 times in $\varepsilon = 10$.

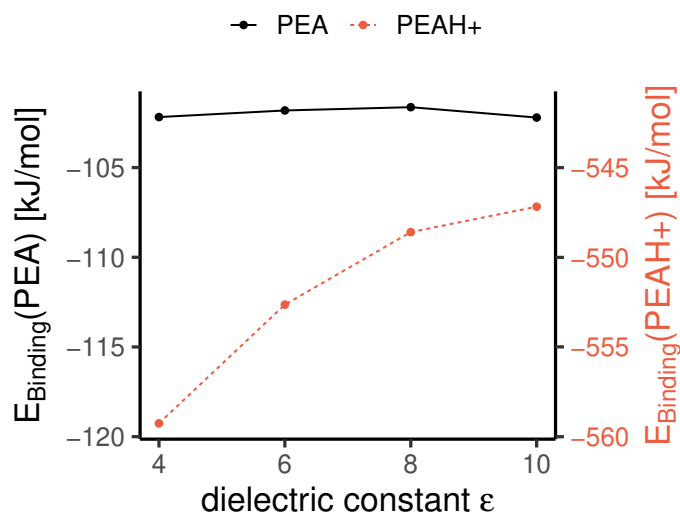


Fig. 4.11: The binding energy of PEA/PEAH⁺ with TAAR1 depends on the dielectric constant of the protein environment, which might be affected by water and salt ion penetration.

4.4 Discussion

This chapter assesses the potential mechanisms underlying the pH dependency of the behavioural response of hermit crabs and shore crabs to PEA/PEAH⁺, which has been described in chapter 2 and 3. Firstly, quantum chemical calculations validated by NMR spectroscopy confirmed my hypothesis that the changes in the conformation of PEA compared to PEAH⁺ in water are small (see Fig. 4.4A vs. B and Table 4.1). Finding PEA and PEAH⁺ predominantly in the *gauche* conformation aligns with molecular dynamics results by Ristić et al (2019).²²⁴ Considering the small change in the protonation state of PEA within the range of ocean acidification (1.3%, see Fig. 2.13B), it was in any case unlikely that conformational changes could account for the change in animal behaviour as the proportion of bioactive compound changes only marginally. This stands in contrast to a study on peptide infochemicals,⁴¹ where conformational

changes upon protonation of the infochemical were deemed responsible for changes in animal behaviour. Peptides, however, are considerably larger than PEA/PEAH⁺ and hence possess more conformational flexibility.

Whilst the protonation of PEA induces only small conformational changes in the infochemical, the dipole of PEA increases more than 5-fold upon protonation, substantially changing its direction and magnitude (see Fig. 4.5). Literature values for PEA/PEAH⁺ dipole are scarce. Melandri et al. (2010)²²² report a dipole of 3.64 D for the folded PEA-water complex, where the water molecule builds a hydrogen bridge with the benzene ring (similar to Fig. 4.4C), whilst I found a dipole of 2.5 D for the same conformation. However, my calculations for the dipole moment excluded the water molecule, whilst it is included in the *ab initio* calculations by Melandri et al.

Similarly to my results, changes to the charge distribution of peptide infochemicals upon protonation have been deemed responsible for a pH-dependent behaviour in shore crabs.⁴¹ As (charge-dependent) electrostatic interactions are crucial for receptor-ligand interactions, I used further computational proof-of-concept experiments, to study the binding of PEA/PEAH⁺ with the receptor TAAR1. Thereby, I considered changes in the receptor-binding properties both, due to the protonation of the ligand PEA and due to protonation of Hist99, a residue inside the TAAR1 binding pocket (see section 4.3.3 and 4.3.4). As the binding pocket of TAAR1 is negatively charged, it binds more strongly to the positively charged PEAH⁺, as compared to PEA. However, whilst protonating PEA substantially increases the binding affinity between the ligand and its receptor ($\Delta E = 447$ kJ/mol), protonation of a receptor pocket residue slightly increases the binding strength of neutral PEA, whilst reducing the binding strength of PEAH⁺ ($\Delta E_{\text{PEA}} = 25$ kJ/mol and $\Delta E_{\text{PEAH}^+} = -173$ kJ/mol respectively). As hypothesised, decreasing the pH could hence have opposing effects on the receptor-ligand interaction and the overall pH-dependent effect on receptor-ligand binding is difficult to estimate.

PEAH⁺ is the most abundant form of PEA in marine environments (see Henderson-Hasselbalch eq 1.7, with 98.0% of PEA in the protonated state (PEAH⁺) in average marine pH 8.1). As I observe a stronger receptor binding affinity of PEAH⁺ as compared to neutral PEA, PEAH⁺ is likely to be the bioactive protonation state. In many cases, only one protonation state of a compound is bioactive and even specific bioactive conformations have been observed.^{270,271} Thereby, the bioactive form is not necessarily the most abundant.^{270,271} Whilst in some cases, specific bioactive conformations have been observed,^{270,271} according to the ‘induced fit’ theory both receptor and ligand change their conformation to adopt the complementary shapes required for binding.^{272,273} For dopamine, for example, which is similar to PEA in its chemical structure (see chapter 5), the amino group acts as the anchoring point to bind to the D2 receptor.²⁷⁴ Similarly to dopamine-D2 binding²⁷⁴ as well as studies on PEAH⁺-TAAR1 binding,²³² my findings show that the amino group of the ligand binds to the aspartate residue inside the binding pocket. In dopamine-D2 receptor binding, the initial ‘anchoring’ is followed by a rapid rearrangement of the ligand conformation.²⁷⁴ If the molecular dynamics of the PEA/PEAH⁺-TAAR1 binding mechanism are similar to dopamine-D2, the original conformation of PEA/PEAH⁺ in water might be arbitrary for its receptor binding, putting further emphasis on the dipole moment, which remains crucial for the electrostatic interactions in receptor-ligand binding.

With the over 5-fold lower receptor binding strength of PEA as compared to PEAH⁺, it is possible that the binding affinity of neutral PEA to its receptor is not strong enough to elicit downstream signal transduction. Studies on the effects of ligand protonation on receptor binding are rare as most studies assume stable pH conditions. However, Radic et al. (1997) demonstrated the importance of electrostatic interactions for protein-ligand interactions by comparing the association and dissociation rates of acetylcholinesterase inhibitors.²³⁵ Binding with the cationic inhibitor *m*-trimethylammoniotrifluoroaceto-

phenone was 50-fold faster and unbinding 10-fold slower than with a neutral analogue where a positively charged nitrogen was exchanged for a carbon atom in the trimethylammonium group.²³⁵ Similarly, my calculations indicate that protonation of PEA might be an essential prerequisite to ensure a biological response. In comparison with the strong increase in receptor-ligand binding upon ligand protonation (447kJ/mol), the observed decrease in receptor affinity for PEAH⁺ upon protonation of the histidine residue inside the receptor binding pocket is less pronounced (-173kJ/mol). Changes in pH have been shown to affect the binding properties of receptor-ligand interactions.^{75,275} However, the direction, magnitude and binding properties affected are different for different receptor-ligand systems.⁷⁵ Hence, general conclusions regarding changes in association or dissociation constants of receptor-ligand interactions depending on pH are not possible and every system has to be evaluated anew.

A major aspect for the uncertainty of pH-dependent effects on PEA/PEAH⁺-TAAR1 binding is that the susceptibility of the histidine residue (Hist99) to protonation is unknown.²³⁶ Future research should aim to also calculate or experimentally determine pK_a values within the receptor's binding pocket to determine the relative population of protonation states for residues that are protonated within the pH range of ocean acidification (see Alexov et al. (2011)²⁷⁶ and Pahari et al. (2018)²⁷⁷ for potential methods).

Finally, as hypothesised, the computational models of PEA and PEAH⁺ are clearly affected by solvation effects (Fig. 4.4, gas phase calculations vs. solvation models). For PEA, solvation effects reverse the relative energetic preference of *gauche 1* (H_N facing benzene ring) and *gauche 2* (amino electron lone pair facing benzene ring) due to the hydrogen bond bridge between the amino group and benzene ring (see Fig. 4.4A and C vs D). For the symmetric PEAH⁺, on the other hand, this is not possible as *gauche 1* and *gauche 2* are identical. Different energetic minima for *gauche 1* and *gauche 2* in the hybrid solvation model in Fig. 4.4B are a remnant of the computational method -

rotation around the C-N bond dissolves the energy differences. The energy barriers for PEAH⁺ between the *gauche* and *anti* conformation, however, are substantially lower when the aqueous background is taken into account and the *anti* conformation gains relative energetic stability (see Fig. 4.4B).

Research into quantum chemical models of ecologically relevant systems is under-represented. However, to investigate infochemicals in aquatic environments, it is crucial to improve our understanding of environmentally realistic computational chemical models. My findings on the importance of solvation effects is in line with a study on solvation representation in nuclear shielding calculations, showing that the accuracy of the nuclear shielding calculations for molecules in water is significantly improved by incorporating an implicit solvation model, and even further improved when an explicit water molecule per ionisable group is added.¹⁹⁰ Similarly, infrared photodissociation spectroscopy identifies a stable structure of monohydrated PEAH⁺, whereby the position of the water molecule (external hydration or insertion between the amino group and the phenyl ring) is temperature-dependent.²²³

To improve our understanding of the applicability of quantum chemical methods for environmentally-relevant systems, it is crucial to consider all aspects of environmental variability effects. As the habitat of hermit crabs and shore crabs is an environment of extremes,⁸² salinity- and temperature-dependent effects were also considered but found to have only minor influences on the infochemical in water or its receptor-ligand interaction (see Fig. 4.3B for PEA/PEAH⁺ and Fig. 4.11 for TAAR1-PEA/PEAH⁺). Keeping the perspective of this study in mind, the ratio between the binding energy of PEA and PEAH⁺ with TAAR1 is crucial to improve the understanding of pH-dependent effects on PEA-mediated behaviour. Although the binding energy of PEAH⁺ with TAAR1 increases by 12 kJ/mol within the range of 4-10 for the dielectric constant, I still observe a five-fold increase upon protonation irrespective of the dielectric environment: The

binding energy of PEAH^+ with TAAR1 is 5.47-times stronger in $\varepsilon = 4$ than for PEA, whilst it is 5.35-times stronger in $\varepsilon = 10$. Although $\Delta E = 12.1 \text{ kJ/mol}$ is clearly above chemical accuracy,²⁶⁶ pH-dependent effects dominate the TAAR1-PEA/ PEAH^+ system for British coastal environments, as compared to smaller salinity- and temperature-dependent effects.

Another key aspect for environmentally-relevant quantum chemical calculations is the correct representation of the solvation. Modelling water explicitly (hybrid solvation model) allows for short-range interactions with the aqueous background, potentially changing the conformation of the molecule, particularly for small compounds. My PEAH^+ hybrid solvation model coincides with findings of Bouchet et al. (2016),²²³ where the same distance between the water hydrogen atom and the benzene π -system (2.39 Å) of PEAH^+ was identified at the energetic minimum at absolute zero. In contrast to Bouchet et al. (2016),²¹⁸ my quantum chemical calculations rely solely on the electronic energy to find energetic minima, which approximates the properties of a chemical compound at absolute zero. As customary in quantum chemical calculations, my model omits all other energetic contribution to the enthalpy, including kinetic energy. Furthermore, temperature-dependent entropy effects, the second component of the Gibbs free energy, are also not included in my energy calculations. Hence, to correctly represent solvation effects, future calculations should consider adding corrections to represent the Gibbs free energy, rather than the electronic energy. Although the interactions with water might be slightly affected by temperature-dependent effects, the energy difference between the conformers (based on the electronic energy, Table 4.1), is comparable to calculations at room temperature (considering Gibbs free energy, based on calculations by Bouchet et al. (2016)²²³).

4.5 Conclusion

In this chapter I used quantum chemical methods to investigate potential mechanistic explanation for the increased attraction of crustaceans to PEA at reduced pH conditions. I considered different routes of pH dependency: the conformation of the infochemical in water, its charge distribution, changes to its receptor interaction depending on the infochemical's protonation state and the interaction of the infochemical with the receptor in different protonation states. The magnitude and direction of the different pH-dependent effects varies and the overall effect is difficult to estimate, not least because the pK_a values of residues inside the receptor binding pocket are only estimated based on the literature and the minimum receptor-ligand binding affinity that leads to signal transduction and translation is unknown. However, my results indicate that decreasing the pH can amplify PEA/PEAH⁺-dependent chemical communication, mainly by protonating the infochemical and thereby substantially increasing its receptor binding affinity, which could lead to the observed amplification in the behavioural response. Additionally, I estimated salinity and temperature-dependent effects within my calculations to ensure their validity for the reality of marine coastal environments. However, within my system, pH is the dominant driver that determines the conformation, charge and binding of PEA/PEAH⁺. The dipole moment of PEA increases considerably upon protonation, which leads to a much stronger binding affinity. I conclude that the observed pH-dependent response of hermit crabs and shore crabs to PEA (chapter 2 and 3) could be the result of changes in receptor-ligand affinity upon protonation of the infochemical.

CHAPTER 5

Similar Chemistry - Same Function?

5.1 Introduction

Most receptors can bind an array of different molecules.²⁷⁸ On my journey to explore the ecological role of PEA for chemical communication in crustaceans, I came across the notion that the behavioural response that I observed in response to PEA might be elicited by PEA binding to the endogenous receptor of a ligand similar to PEA, rather than a PEA-specific receptor.

As the prevalence of PEA in marine environments was unclear prior to my mass-spectrometric analysis of PEA in shore crab urine (see chapter 3), PEA could be a non-native ligand for crustaceans. This led me to explore whether PEA could be so similar to another compound that it binds to its receptor, effectively mimicking it. Chemically, PEA ($C_8H_{12}N$) is similar to the neurotransmitter dopamine ($C_8H_{12}NO_2$) in its composition (see Fig. 5.1).

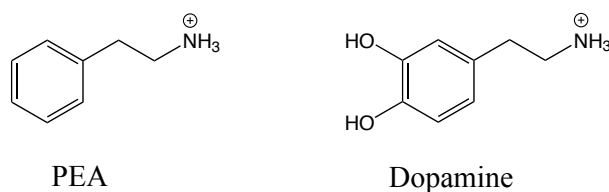


Fig. 5.1: Chemical structure of PEA and dopamine.

In this chapter I explore the chemical similarity between the two compounds and whether they have the same biological role for crustaceans. In the following, I give an introduction into the characteristics and reactivity of dopamine in water (section 5.1.2) and the biological role of dopamine for crustacean behaviour according to the literature (section 5.1.3) to draw parallels to my findings with PEA.

But first of all, what is *similar* in chemistry?

5.1.1 The Similarity Concept in Chemistry

Structural similarity of chemicals is a key concept in toxicology and drug design. The main reason for the strong interest of researchers in similarity is the ‘lock and key’ concept for receptor binding, which hypothesises that only a certain key (ligand) can open a lock (i.e. bind to the receptor).²⁷⁹ Defining a similarity measure allows researchers to assess if chemicals could have comparable biochemical activity, and hence bind to the same receptor. Indeed, analysing databases shows that common substructural fragments lead to similar biological activities.^{280,281} However, similarity is difficult to measure²⁷⁹ and often based on intuitive judgement of experts. A common definition of chemical similarity is that the topological description of the atoms in both compounds and their connecting bonds must contain a sufficiently large number of common features.^{279,282} In other words, most chemists would describe two compounds as ‘similar’ if the structure of their backbone and their functional groups are comparable.

Although a lot of research in toxicology and drug discovery is based on the concept of similarity, in some instances, minor modifications in the structure of a molecule can drastically change its biochemical activity. This is known as the similarity paradox.²⁸³ Although distance measures in chemical space are a crucial aspect of similarity assess-

ment, similarity cannot be judged based on chemical similarity alone.²⁸² A similarity in the properties and biological activity of the compounds is paramount.²⁸²

5.1.2 Characteristics and Reactivity of Dopamine in Water compared to PEA

Chemically, both PEA and dopamine are monoamines (although PEA is traditionally often referred to as a trace amine) and both are known neurotransmitters across the animal kingdom.²⁸⁴ Structurally, both PEA and dopamine consist of a benzene ring with an amino group. Unlike PEA, however, dopamine also has two hydroxy groups, binding to the benzene ring. Hence, PEA and dopamine share only 1 out of 3 functional groups.

As a key neurotransmitter, protonated dopamine has been addressed extensively in computational studies:^{274,285–287} The first comprehensive computational study of protonated dopamine in aqueous solution generated conformers in solution and gas-phase by rotation about the four main torsion angles.²⁸⁷ They found two folded and one extended conformation in gas-phase and in solution.²⁸⁷ This is in line with my previous results on PEA, which is structurally very similar to dopamine and also has three stable conformers in solution (see section 4.3.1). Furthermore, the neighbouring hydroxy groups of dopamine were found to build intramolecular hydrogen bonds that are close to coplanar with the benzene ring.²⁸⁷ A more recent study by Tosso et al. (2020)²⁸⁶ confirms the coplanar conformation of the hydroxy groups and identifies the *gauche* conformations (folded amino group) as energetic minima. Whilst protonated dopamine has been studied in detail, studies on other protonation states of dopamine are scarce.

Dopamine has four protonation states. The three deprotonation steps, from fully protonated dopamine (charge +1) to neutral or zwitterionic forms (charge 0), to deprotonated

states (charge -1), to the fully deprotonated dopamine (charge -2) are shown as rows in Fig 5.2. The dissociation constants of dopamine for these three deprotonation steps ($K_1 - K_3$ in Fig. 5.2) can be observed experimentally.^{288,289} However, whilst the acid dissociation constants are known, the microscopic speciation is unclear.^{290,291} In other words: Does protonated dopamine form mainly neutral dopamine or are the zwitterionic species more stable? This question can be addressed computationally, by determining relative stabilities of the tautomers of neutral/zwitterionic dopamine. Tautomers are chemical compounds that readily interconvert as they have the same structure ('structural isomers', same number of atoms for each element and the same bonds connecting them) except for a relocated hydrogen atom.¹⁷⁴ Chemical compounds in the same row in Fig. 5.2 are tautomers.

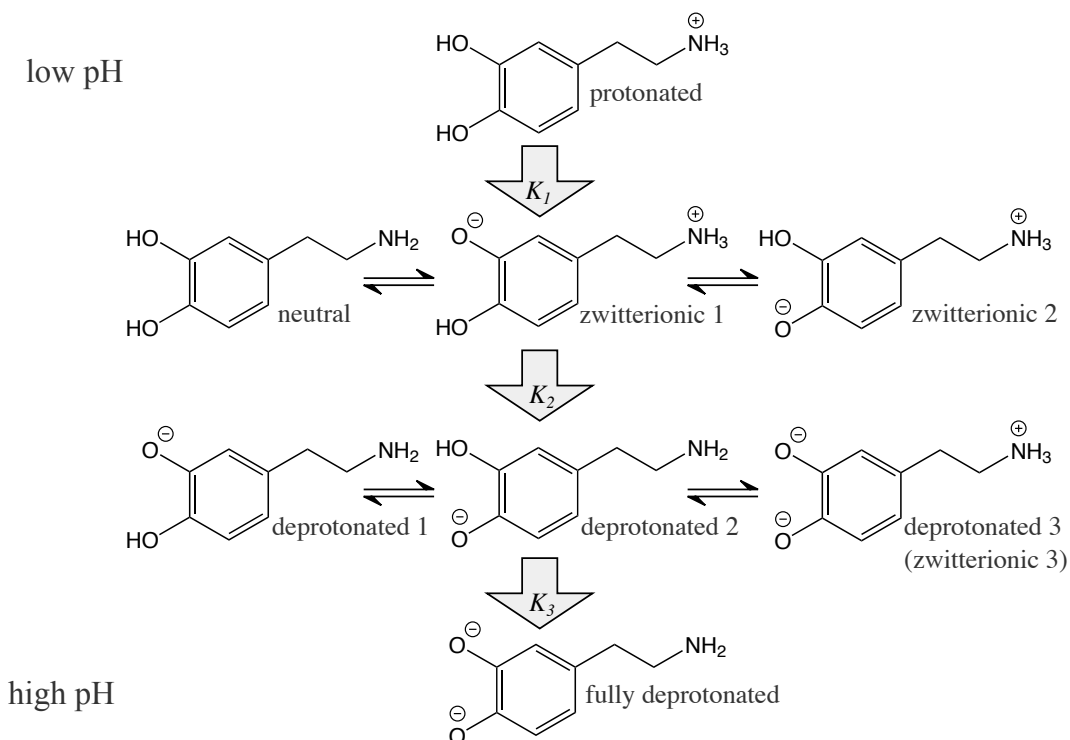


Fig. 5.2: Deprotonation scheme of dopamine adapted from Ishimitsu et al.²⁸⁸ The first deprotonation step is controlled by the equilibrium constant K_1 , with microspeciation into three potential forms, one neutral and two zwitterionic states. The second deprotonation step (K_2) leads to the formation of deprotonated forms of dopamine (overall charge -1). Further increase of the pH leads to the formation of fully deprotonated dopamine (charge -2, controlled by K_3).

Whilst PEA is thought to not undergo spontaneous reactions when dissolved in water, dopamine oxidises in water, leading to the formation of reactive oxygen species (ROS) and quinones, which are cytotoxic and genotoxic.²⁹² Toxicity due to dopamine oxidation spans a range of contexts, including marine environments and health: In the Northwest Pacific, green tide blooms of dopamine-producing macroalgae *U. obscura* lead to increased environmental levels of toxic oxidation products of dopamine.²⁹³ Furthermore, some neurological diseases such as Parkinson's and schizophrenia have been associated with neurotoxicity due to oxidation products of dopamine.^{292,294} Fig. 5.3 shows a sim-

plified pathway of dopamine oxidation that ultimately forms black and brown coloured insoluble melanins.

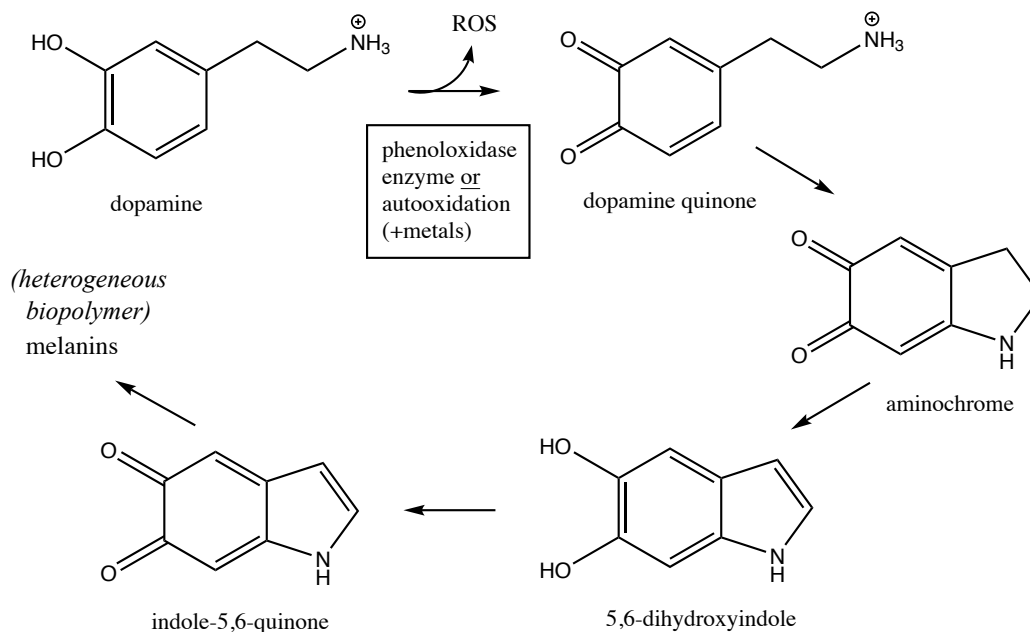


Fig. 5.3: Simplified pathway of dopamine oxidation. Modified from Stokes et al. (1999)²⁹² and Yang et al. (2014).²⁹⁵

Fig. 5.3 shows that the first step of the oxidation pathway is the deprotonation of the hydroxy groups, forming a quinone. Energetically, this deprotonation step heavily depends on the electron density in the adjacent benzene ring.²⁹⁶ The electron density on the benzene ring might in turn be affected by the protonation states of the functional groups that bind to the ring. Characterising dopamine in the different protonation states is therefore crucial to improve our understanding of the pH-dependency of the oxidation reaction of dopamine to allow for the comparison to PEA, which was studied in different protonation states (see chapter 4).

5.1.3 The Role of Dopamine in Crustacean Behaviour

Dopamine and other monoamines are widely distributed in crustacean nervous systems, where they mediate a wide array of physiological roles.²⁹⁷ In many crustaceans, internal levels of monoamine neurotransmitters are associated with decision making during aggressive interactions.^{135,163} In hermit crabs (*Pagurus bernhardus*), high dopamine levels indicate aggression and are positively correlated with the motivation to initiate a fight.¹³⁵ Congruously, dopamine levels drop when a defending hermit crab surrenders in a shell fight.¹³⁵ Similarly in shore crabs (*Carcinus maenas*), dopamine levels are higher post-fight in winners compared to losers.¹⁶³

In fighting hermit crabs, the attacker's motivation to fight can also be studied by applying a novel stimulus mid-fight that causes a startle response.¹³⁵ The attacking hermit crab withdraws into its shell in response to an impact upon its shell. The duration until reappearance from the shell is known to be inversely proportional to the attacker's motivation to fight, independent of the animal's size.²⁹⁸ Briffa & Elwood (2007)¹³⁵ found a negative correlation between the startle response duration and the dopamine concentration in haemolymph, indicating that high levels of dopamine are associated with a high motivation to fight in attackers, whilst there is no relationship with other monoamines. Similarly, in shore crabs, the escalatory behaviour and hence the intensity of the fight correlates with dopamine levels of the attacker,¹⁶³ supporting the notion that dopamine is associated with the motivation to fight in crustaceans.

Furthermore, dopamine levels decrease in the course of a fight in crustaceans.^{135,163,299} After fighting, dopamine levels in haemolymph as well as the expression of dopamine receptor 2 (DA2) mRNA levels in the haemolymph, eyestalk, cranial ganglia and thoracic ganglia in Chinese mitten crabs (*Eriocheir sinensis*) show a significant decrease.²⁹⁹ As the changes in dopamine and dopamine receptor concentrations were accompanied

by changes in cyclic adenosine monophosphate (cAMP) and protein kinase A (PKA) concentrations in the circulating system, these pathways might be involved in agonistic behaviour of *E. sinensis* and potentially other crustaceans. These findings coincide with a study in crayfish (*Procambarus clarkii*), showing that the cAMP-PKA signalling pathway is essential for mediating effects of previous winning or losing on agonistic behaviour in subsequent fights.³⁰⁰

Many studies have focused on the role of dopamine and other monoamine neurotransmitters on agonistic behaviours in crustaceans (see above). However, there is also some evidence suggesting that courtship behaviour is mediated by dopamine levels.³⁰¹ Injection of dopamine initiated a courtship display posture in the blue crab, *Callinectes sapidus*, and the distribution of dopamine-like immunoreactivity across the nervous system supports the notion that internal dopamine levels could be involved in mediating reproduction-related behaviours in crustaceans.³⁰¹

Although the above examples reveal functional relationships between internal dopamine levels and the regulation of behaviours in crustaceans, it is unclear to what extent this translates to the behavioural reaction to external exposure to said compounds, particularly at the low concentrations relevant for olfactory-mediated behaviours. A study on crayfish on decision-making during fights, where the animal was infused in serotonin,³⁰² indicates that monoamines might indeed be able to diffuse from the surrounding water into the animal to bind to internal receptors. However, generally only small uncharged molecules can diffuse freely across cell membranes.³⁰³ As serotonin ($pK_a = 10.16$ ³⁰⁴) as well as PEA (see section 2.3.6) and dopamine (see section 5.3.1) are $> 90\%$ in the protonated state (and hence charged) in pH 7-8, their passive diffusion across cell membranes is unlikely.³⁰³ Hence, external receptors, facilitated diffusion or active transport across the semi-permeable lipid bilayer of cell membranes is a prerequisite for monoamines in the surrounding water to elicit any of the above mentioned behaviours in crustaceans.

5.1.4 Research Approach and Hypotheses

For this chapter, selected experiments from the previous chapters were repeated with dopamine to determine similarities between PEA and dopamine, based on chemical structure, chemical reactions and biological response.

Firstly, I determine the protonation states of dopamine that are relevant for marine environments. Acid dissociation constants from the literature and the Henderson-Hasselbalch equation are used to study pH-dependent abundance of dopamine in the different protonation states. Based on this, I determine which protonation states of dopamine should be the focus of my computational experiments.

As structurally, both PEA and dopamine consist of a benzene ring with an amino-ethyl group, I hypothesise that, similarly to PEA, computational experiments find dopamine in all protonation states predominantly in the folded (*gauche*) conformation in water, with comparable torsion angles of the amino side chain for PEA and dopamine.

However, PEA and dopamine share only 1 out of 3 functional groups (dopamine having two hydroxy groups in addition to the amine group). This is a substantial difference in the chemical structure, particularly for such a small molecule, which leads to differences in chemical reactivity. The different chemical reactivity is reflected in the tendency of dopamine to oxidise in water, whilst PEA is stable in water (see section 5.1.2). This adds complexity to the comparison of PEA and dopamine, as not only the different protonation states of dopamine need to be assessed computationally but also their contribution to oxidation reaction kinetics.

To improve understanding of the pH-dependency of the oxidation reaction, I compare computational models of the relevant protonation states of dopamine in water. As the reaction pathway suggests a rate-limiting step that depends on the electron density in the benzene ring (see section 5.1.2), I hypothesise that decreasing the pH (increasing

the proportion of protonated dopamine) hampers the oxidation by decreasing the electron density in the benzene ring. Additionally, as an aqueous environment is known to stabilise zwitterionic states (as opposed to the neutral tautomer) in amino acids,³⁰⁵ I hypothesise that, in a computational solvation model, zwitterionic dopamine is energetically preferred to neutral dopamine.

As my results indicate that PEA is associated with chemically mediated agonistic behaviour in reduced pH conditions (see chapter 2-3) and the literature suggests that internal dopamine levels are increased when crustaceans are motivated to initiate a fight (section 5.1.3), a biological analogy between PEA and dopamine seems plausible. I therefore hypothesise that exposure to dopamine induces comparable pH and sex-specific behavioural responses in hermit crabs as observed in response to PEA. To ensure comparability, I used the same static-water tank experimental set-up as in chapter 2.

5.2 Materials and Methods

5.2.1 Determination of Relevant Protonation States of Dopamine

To determine which protonation states of dopamine are relevant for marine environments, acid dissociation constants were retrieved from the literature and, applying the Henderson-Hasselbalch equation (eq. 1.7), the pH-dependent abundance was calculated and visualised.

5.2.2 Computations of Dopamine

Geometry optimisations were performed with ORCA (version 4.1.2)^{212,213} using the PBE0 exchange correlation functional²¹¹ with a pc-2 basis set.^{206–208} D3 dispersion correction^{240,241} was included and the RIJ-COSX approximation was applied with a def2/J auxiliary basis set.²⁴³ All eigenvalues of the identified energetic minima were checked for imaginary frequencies.

In a first step, the protonation states relevant for the pH range of marine environments, were optimised in a dielectric infinite continuum of water using the CPCM approach^{238,239} implemented in ORCA (implicit solvation model, compare also section 4.3.1). Subsequently, dopamine was modelled in a hybrid solvation environment, adding one explicit water molecule per ionisable group (3 in total) to the implicit solvation environment.

The conformation *gauche 1* was defined as folded over the proximal hydroxy (OH) group and *gauche 2* as folded towards the distal OH group. The zwitterionic state 1 is deprotonated at the proximal OH group, whereas the zwitterionic state 2 of dopamine is deprotonated at the distal OH group. The terminology is visualised in Fig. 5.4.

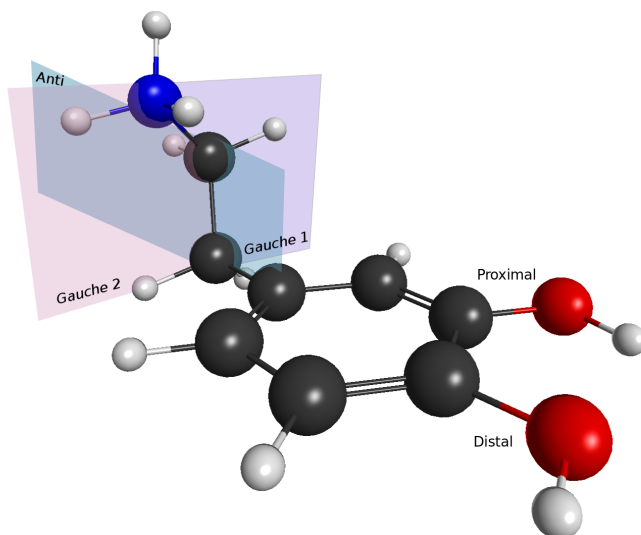


Fig. 5.4: Protonated dopamine in a *gauche 2* conformation, folded towards the distal hydroxy (OH) group. The other OH group, closer to the amino side chain, is termed ‘proximal’. For the *anti* conformation, the amino side chain assumes an extended conformation (along blue sheet) and in the *gauche 1* conformation dopamine is folded over the proximal OH group (along purple sheet). Carbon atoms are in black, oxygen atoms in red, nitrogen in blue and hydrogen atoms are shown in white.

To promote understanding of potential changes in electrostatic interactions with the surrounding environment, such as enzymes and receptors, the dipole moment was calculated for the energetic minima of each protonation state based on the implicit solvation model. The implicit solvation model (rather than the hybrid solvation model) was chosen for dipole moment calculations as the dipole of the water molecules would otherwise contribute to the calculated dopamine dipole moment.

Finally, the ^1H nuclear magnetic shieldings of dopamine in the hybrid solvation model were calculated and compared to experimental NMR measurements in water. Isotropic nuclear magnetic shielding values of ^1H nuclei were calculated using ORCA (version 4.2.0) at the PBE0/aug-pc-2 level of theory. RIJ-K approximation with a def2/JK auxiliary basis set³⁰⁶ was used. For all nuclear shielding calculations the Gauge Including

Atomic Orbitals (GIAO) method³⁰⁷⁻³⁰⁹ was applied. The resulting nuclear shielding constants were compared to experimentally determined chemical shifts.

5.2.3 NMR Spectroscopy of Dopamine

Samples for NMR measurement were prepared with dopamine (3-hydroxytyramine hydrochloride, Sigma-Aldrich, 98 %) at pH 6.8 and pH 9.8 to ensure a high percentage of dopamine in the respective protonation state. Dopamine was measured at 0.05 mol/L in 0.04 mol/L sodium phosphate buffer to stabilise the pH during measurements. As solvent lock, 10 % deuterium oxide (Sigma-Aldrich) was included. ¹H NMR spectra were recorded on a JEOL ECZ 400S spectrometer with Tetramethylsilane (TMS, 50 µL, Sigma-Aldrich, >99.5 %) $\delta_H = 0$ as the internal standard.

5.2.4 Behavioural Choice Experiments with Hermit Crabs

To directly compare the behavioural response of hermit crabs to PEA and dopamine, the data collection with the two neurotransmitter-like compounds was paired. Hence, the response of the same animals to PEA and dopamine was recorded on the same day (compare sections 2.2.1- 2.2.2 - ‘Behaviour Tracking and Sex-specific Effects’ for details on animal collection, husbandry and behavioural experiments with PEA). In the following, I describe again the methods for behaviour experiments with dopamine, which are the same as for PEA.

The light level was reduced during behaviour assays (around 45 lux, Mini Light Meter DT-86, CEM instruments) to diminish the impact of visual stimuli. For the experiments in pH 7.7, the pH of the artificial seawater was adjusted in batches of 10 L to 7.7 ± 0.05 , using 1 mol/L hydrochloric acid (diluted from 37 % hydrochloric acid, Fisher Scientific). The total alkalinity of the artificial seawater was determined in weekly random samples

and averaged at 116.4 ± 8.9 mg/L for pH 8.1 and 100.6 ± 3.4 mg/L for pH 7.7 (as CaCO_3 , average \pm standard deviation).

At the beginning of the experiment, a hermit crab was placed in a separate tank filled with artificial seawater ($18 \pm 1^\circ\text{C}$, 35 ± 1 PSU, pH 8.1 or 7.7) and allowed to acclimatise to the experimental conditions for up to 3 min. After acclimatisation, the animal was transferred to the centre of the bioassay tank ($28 \text{ cm} \times 18 \text{ cm}$), which was filled with 1 L artificial seawater of the respective pH and left to acclimatise to the tank conditions for 30 s, whilst being caged in the center of the tank. This was enough for most of the animals to emerge from their shells. Subsequently, a filter paper (1 cm^2 , Whatman No. 3) was introduced on both sides of the tank. On one side of the tank the filter paper contained 200 μL dopamine at $3 \cdot 10^{-5}$ mol/L, $3 \cdot 10^{-4}$ mol/L or $3 \cdot 10^{-3}$ mol/L or was left blank as a control. The test solutions were prepared with dopamine (3-hydroxytyramine hydrochloride, Sigma-Aldrich, 98 %) in artificial seawater of the respective experimental pH. The cue side was randomised for each individual and to exclude potential effects of learning and memory, the order of the experiments was randomised.

After the cue on the filter paper was allowed to diffuse for 20 s, the cage was lifted and the movement of the animal was recorded on video for 2 min. All videos were analysed blindly using the behaviour tracking software LoliTrack (version 5.1.1, Loligo Systems, Denmark). Blind analysis involved trimming all videos to exclude the first frames, where a summary sheet with the experimental conditions was presented to the camera. This removed all potential unconscious bias from the analysis, as I was unable to deduce the experimental conditions from the videos. After finishing the analysis, information about the experimental conditions were retrieved from the untrimmed videos and analysis results and information on the experimental conditions were merged. Animals that stayed hidden in their shell for 3 consecutive negative control experiments were deemed unfit and excluded from the experiment. The hermit crabs were returned to their

housing tanks (in individual containers) for at least 2 h to recover after a maximum of 7 consecutive assays (about 30 min). The sex and weight of the hermit crabs was determined after all behavioural experiments were completed (see section 2.2.3). As the experiments with dopamine ran alongside those with PEA, the same animals as for chapter 2 were used.

5.2.5 Data Analysis and Statistics

Using the behaviour tracking software LoliTrack (version 5.1.1, Loligo Systems, Denmark) digitalised the movement patterns of hermit crabs in response to dopamine. As the average hermit crab position inside the tank has previously been insightful to evaluate differences in the behavioural response (section 2.3.2), it was again used to visualise the attractive/repulsive effect of dopamine on hermit crabs through heatmaps of the tank (based on `drawcontours.R`, written by J.D. Forester¹¹⁷) for each condition and sex. Thereby the x-axis displays the distance from the cue source side rather than the length of the tank to account for the randomised side (left or right) of the cue.

All statistics were carried out with R (version 4.0.2).¹¹⁰ For data visualisation the package ‘`ggplot2`’¹¹¹ was used. As in previous chapters 2 and 3, the average distance from the cue source side (x-axis in heatmaps) was analysed in linear mixed effect models (package ‘`lme4`’¹¹² in R), testing for significant additive and interactive effects of pH, concentration and sex whilst controlling for the paired design on the individual level (random effects).

5.3 Results

5.3.1 Protonation States of Dopamine

The acid dissociation constants pK_a give insight on the pH-dependent protonation state of dopamine (see Fig 5.2 for the chemical structure, naming and respective dissociation constants for all protonation states of dopamine). The three ionisable groups of dopamine (an amino, a proximal and a distal hydroxy group) can change their protonation state, resulting in a fully protonated form of dopamine, two zwitterionic and a neutral forms, three deprotonated form and a fully deprotonated form of dopamine. The respective dissociation constants pK_a for the three deprotonation steps are $pK_{a1}=9.1$, $pK_{a2}=10.5$ and $pK_{a3}=12.0$ respectively.^{288,289} The (by-)products of dopamine oxidation (see Fig. 5.2) have pK_a values outside the pH range relevant for marine environments and can therefore be regarded as pH-stable.

Fig. 5.5 shows the pH-dependent abundance of dopamine in the different protonation states. This was calculated based on the pK_a values, applying the Henderson-Hasselbalch equation (eq. 1.7).

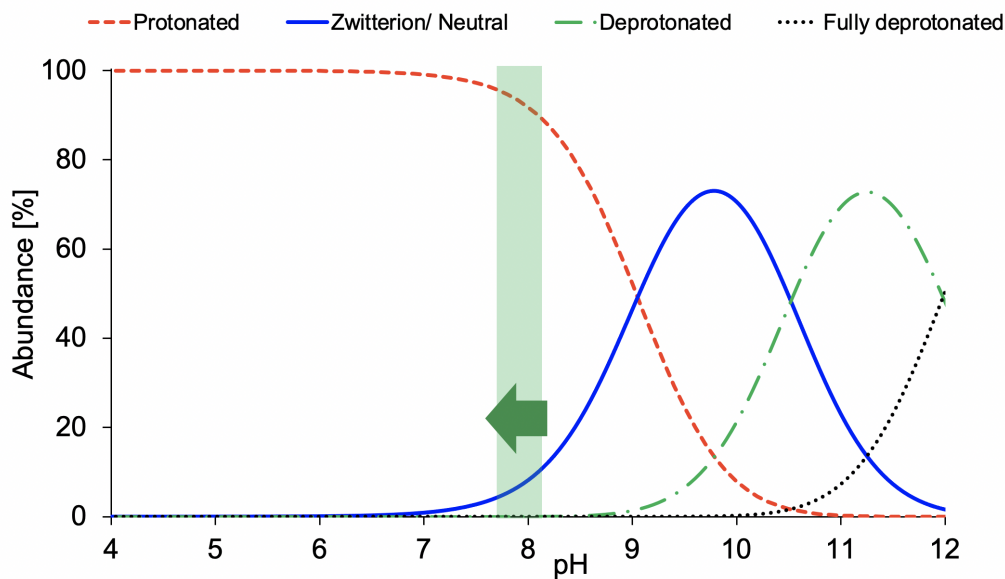


Fig. 5.5: pH-dependent abundance of dopamine in different protonation states, based on the Henderson-Hasselbalch equation and $pK_{a1}=9.1$, $pK_{a2}=10.5$ and $pK_{a3}=12.0$.^{288,289} The dissociation constants refer to the (de)protonation of the amino group, proximal and distal hydroxy group respectively.²⁸⁹ The pH range relevant for ocean acidification scenarios (pH 8.1 - pH 7.7) is shaded in green, with the direction of change visualised with an arrow.

Fig 5.5 shows that a decrease in pH from 8.1 to 7.7 (shaded green) entails an increase in the abundance of protonated dopamine by 5.8% (red in Fig. 5.5) and a respective decrease in the zwitterionic/neutral form (blue in Fig. 5.5). Changes in the abundance of deprotonated and fully deprotonated dopamine (green and black in Fig. 5.5) are negligible. Considering the pH range relevant for marine ecosystems, I hence focus on computational models for protonated and neutral/zwitterionic forms of dopamine.

5.3.2 Conformational Preference and Charge Distribution of Different Protonation States of Dopamine

My computational chemical calculations show that the choice of solvation model has a large effect on the energetically favoured tautomer of dopamine in the zwitterionic/neutral state. Calculations using the implicit solvation model lead to the conclusion that protonated dopamine mainly forms neutral dopamine upon deprotonation, with an energy difference of 11.4 kJ/mol between the most stable zwitterionic form and the energetically preferred neutral state (all in *gauche 2*, see Table 5.1).

Table 5.1: Energy differences ΔE between the different energetically stable conformations of dopamine in the protonated and zwitterionic/neutral form, as determined with the implicit solvation model. The energetic minima were optimised without geometric constraint. Energy differences are shown relative to the lowest energy conformation for the respective tautomer. The energetically preferred conformation for each tautomer is highlighted in bold. The dipole moment reflects the charge separation of the dopamine molecule.

	protonated		neutral		zwitterion 1		zwitterion 2	
ΔE [kJ/mol] /								
Dipole [D]	ΔE	Dipole	ΔE	Dipole	ΔE	Dipole	ΔE	Dipole
<i>anti</i>	1.4	18.7	0.8	3.8	17.5	31.3	16.6	29.1
<i>gauche 1</i>	0.9	13.6	2.7	2.0	14.0	24.1	12.2	21.8
<i>gauche 2</i>	0.0	16.2	0.0	3.3	12.6	24.4	11.4	23.5

However, Table 5.2 shows that in a more realistic water model (including a water molecule per ionisable group, hybrid solvation model), the zwitterionic state 2 (*gauche 1*) is actually energetically favoured by 10.0 kJ/mol rather than neutral dopamine (*gauche 2*). This indicates that zwitterionic dopamine is the energetically preferred tautomer in water.

As the energetically preferred tautomer of neutral/zwitterionic dopamine changes depending on the solvation model, the solvation model has a substantial effect on the dipole moment of dopamine. With protonated dopamine predominantly in the *gauche 2* conformation, the dipole moment is 16.2 D as opposed to 13.6 D in the hybrid solvation environment (*gauche 1*). Furthermore, applying a simpler implicit solvation model, the dipole moment of neutral/zwitterionic dopamine in its energetically favoured tautomer is 3.3 D, (neutral dopamine in *gauche 2*) whilst it is 21.8 D (zwitterionic, *gauche 1*) in the more realistic (hybrid) solvation environment.

Table 5.2: Energy differences ΔE between the different energetically stable conformations of dopamine in the protonated and zwitterionic/neutral form, as determined with the more realistic (hybrid) solvation model. The energetic minima were optimised without geometric constraint and the energy of the explicit water molecules was subtracted. Energy differences are shown relative to the lowest energy conformation for the respective tautomer. The energetically preferred conformation for each tautomer is highlighted in bold. The dipole moment reflects the charge separation of the dopamine molecule (excluding water molecules).

	protonated		neutral		zwitterion 1		zwitterion 2	
ΔE [kJ/mol] /	ΔE	Dipole	ΔE	Dipole	ΔE	Dipole	ΔE	Dipole
<i>anti</i>	2.1	18.7	11.6	3.8	11.9	31.3	10.8	29.1
<i>gauche 1</i>	0.0	13.6	10.1	2.0	8.8	24.1	0.0	21.8
<i>gauche 2</i>	0.4	16.2	10.0	3.3	7.8	24.4	7.2	23.5

Table 5.2 shows that in a more realistic solvation model, dopamine is predominantly found in the *gauche* conformation in all protonation states. In most cases, however, with the exception of zwitterion 2, the energy difference between the extended (*anti*) and folded (*gauche*) conformation is very small and below the accuracy of quantum chemical calculations (about 4 kJ/mol).²⁶⁶

The torsion angles of the different conformations of dopamine in the hybrid solvation model are summarised in Table 5.3. The general order of magnitude of dopamine torsion angles is comparable to PEA ($\approx \pm 60^\circ$ for *gauche* and $\approx \pm 180^\circ$ for *anti*). However, absolute torsion angle values of protonated dopamine are on average about 1° below the respective dihedral angles of PEAH⁺ (see Table 4.1), whilst the absolute torsion angle values for neutral dopamine are on average about 1° above the respective PEA dihedral angles (see Table 4.1). Furthermore, zwitterionic dopamine has smaller torsion angles for the folded conformation as compared to neutral dopamine. As a smaller torsion angle folds the side chain more centrally over the benzene ring, this indicates a stronger association of the amino group with the benzene ring and the hydroxy groups.

Table 5.3: Torsion angles of the amino side chain for dopamine in protonated, neutral and zwitterionic 1 and 2 state. The energetically preferred conformation for each protonation state is highlighted in bold.

Torsion angle [°]	protonated	neutral	zwitterion 1	zwitterion 2
<i>anti</i>	178.2	179.7	178.8	179.1
<i>gauche 1</i>	-58.1	-62.1	-56.9	-47.5
<i>gauche 2</i>	57.8	61.8	56.8	56.9

Fig. 5.6 depicts the energetically favoured conformations of neutral dopamine and the two zwitterionic dopamine forms in the hybrid solvation model, which includes a water molecule per ionisable group. The hydrogen atoms of the hydroxy groups, which are bound to the benzene ring at meta and para position (proximal and distal OH group), are coplanar with the benzene ring (see also Fig. 5.7). The water molecules form a concise structure with dopamine in the zwitterionic state 2 (Fig. 5.6C), folded over the proximal hydroxy group (*gauche 1*). In neutral and zwitterionic state 1, however, my quantum chemical calculations reveal an open composition, where the addition of water molecules does not form a fixed frame (Fig. 5.6A-B). The lower number of bonds account for these conformations being less energetically stable. In conclusion, in water, the energetically preferred tautomer of dopamine is zwitterionic 2, which is predominantly in the *gauche 1* conformation.

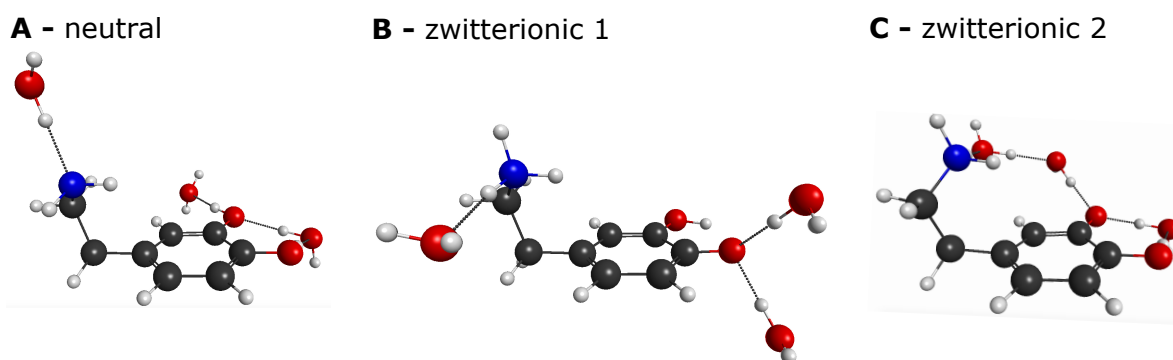


Fig. 5.6: Neutral and zwitterionic dopamine in their preferred conformations in the hybrid solvation model, which includes a water molecule per ionisable group. (A) is neutral dopamine in *gauche 2*, (B) is zwitterionic form 1 of dopamine in *gauche 2* and (C) is the energetically preferred tautomer of neutral/zwitterionic dopamine: zwitterion 2 in *gauche 1*.

Table 5.2 shows that in the hybrid solvation model, the dipole of dopamine decreases upon protonation, from 21.8 D to 13.6 D, when zwitterionic dopamine in *gauche 1* forms protonated dopamine in *gauche 1*. In Fig. 5.7 the dipole is visualised as a red arrow for the energetically preferred conformer for each tautomer. Whilst neutral dopamine

(Fig. 5.7B) only has a small dipole moment, the zwitterionic forms have a large dipole (see Fig. 5.7C& D), as the overall neutral charge is split into a positively charged amino group and negatively charged hydroxy group. The different dipoles of neutral and zwitterionic dopamine underscore the relevance of determining the most stable tautomer of neutral/zwitterionic dopamine. Protonated dopamine (Fig. 5.7A) also has a large charge separation due to the protonated amino side chain. The direction of the dipole moment, however, is markedly different from the dipoles of the neutral and zwitterionic forms.

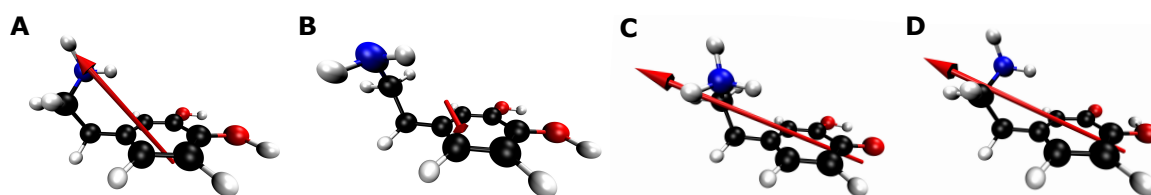


Fig. 5.7: The energetically preferred conformations of dopamine and their dipoles in protonated (A), neutral (B) and the two zwitterionic states (B & C). The dipoles (red arrows) visualise the size and direction of the charge separation. Dopamine is depicted in the energetically preferred conformation for each protonation state, as determined in the hybrid solvation model, which is *gauche 1* for protonated (A) and zwitterionic 2 (D) and *gauche 2* for neutral (B) and zwitterionic 1 (D).

In the following, I apply the above observations on energetically preferred tautomers and conformers and their respective dipole moments to the dopamine oxidation reaction (see Fig. 5.3) to determine the pH dependency of the oxidation reaction. In the first step of the dopamine oxidation, the hydroxy groups with the benzene ring are rearranged to a fully conjugated dicarbonyl (dione) structure, forming of quinone²⁹⁵ (see Fig. 5.3). This first oxidation step is rate-determining for the reaction kinetics.^{294,310} As the kinetics of this structural rearrangement depends on the electron density in the benzene ring, the protonation and tautomerisation state of dopamine affects the speed of oxidation: A stronger electron withdrawing functional group at the aromatic ring

(NH_3^+ in protonated and zwitterionic dopamine instead of NH_2 in neutral dopamine) destabilises intermediate radicals and hence hampers the oxidation.²⁹⁵ Protonation of dopamine therefore hinders its oxidation. A deprotonated hydroxy group on the other hand (zwitterionic dopamine) increases the electron density in the benzene ring, which stabilises intermediate radicals. Additionally, as only one hydroxy group is deprotonated when zwitterionic dopamine forms quinone, the reduction potential is reduced as compared to the protonated/neutral state.²⁹⁵ Due to these structural effects, the oxidation of dopamine is highly pH-dependent.²⁹⁴

5.3.3 Computational Model Validation

To validate my quantum chemical calculations, I prepared samples of dopamine at pH 6.8 and pH 9.8 to measure protonated and neutral/zwitterionic dopamine in NMR spectroscopy. However, adjusting the pH of the dopamine solution to pH 9.8 reliably resulted in rapid oxidation of dopamine, evidenced by a tinge of reddish-brown within the first minute. The sample darkened rapidly, and a brown precipitation was observed. Whilst this confirms my deduction (see section 5.3.2) that increasing the pH accelerates the oxidation reaction (as the dark precipitate was likely melanin) it also rendered one of the two experiments unfeasible with the established methods.

The computational model can therefore only be validated using the protonated form of dopamine (pH 6.8), which stayed colourless. The absence of contamination in the NMR spectra (see Fig. 5.8A) confirms that the solution was protonated dopamine without traces of oxidation for the duration of the experiment.

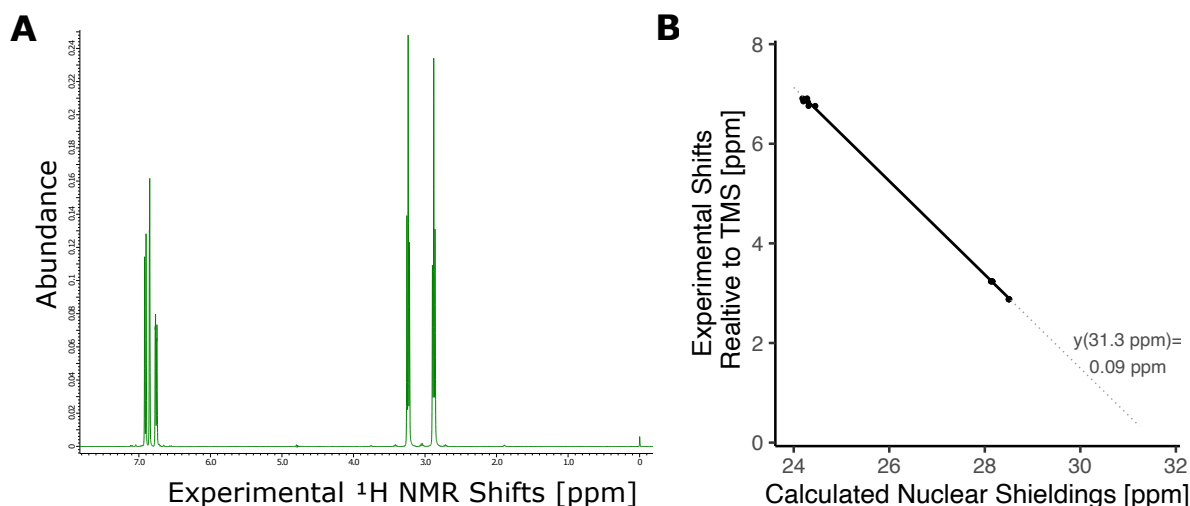


Fig. 5.8: ^1H NMR spectrum of protonated dopamine (A) and correlation of experimental shifts with calculated NMR shieldings of dopamine in *gauche* conformation (B). The dotted line is the extended trendline of the fit and shows that the estimated experimental shift for the calculated ^1H nuclear shielding of TMS (31.3 ppm) is 0.09 ppm, close to zero.

The experimental results correlate well with the calculated nuclear shieldings of protonated dopamine in *gauche 1* conformation, which was found to be the energetic minimum (Fig 5.8B). However, the difference between ^1H nuclear shieldings for *gauche 1* and *gauche 2* was too small to be separable in their comparison to the experimental ^1H NMR shifts. As the calculated energy difference between the two *gauche* conformations is very small ($\Delta E = 0.4 \text{ kJ/mol}$, see Table 5.2) they are likely to be equally populated and the NMR sample likely contained a mix of both conformers.

As the nuclear shieldings are absolute values and the experimental NMR shifts are measured relative to the ^1H NMR shift of TMS (i.e. set to zero), the deviation from zero of the estimated experimental shift for the nuclear shielding of TMS (31.3 ppm) is a quality criterion ('accuracy'). This value was 0.24 ppm for the *anti* conformation of protonated dopamine, whilst it was 0.09 ppm for both *gauche* conformations. Being close to zero testifies that the calculated *gauche* conformation is in good correlation with exper-

imental findings. This indicates that protonated dopamine in water is predominantly in the *gauche* conformation, confirming that the folded conformation (*gauche*) is the energetic minimum.

5.3.4 Behavioural Response of Hermit Crabs to Dopamine

As the experiments were paired (carried out with the same animals on the same days), the response of hermit crabs to dopamine can be directly compared to their response to PEA (see chapter 2).

To gain an overview of the reaction of hermit crabs to dopamine in different pH conditions, the average position of all hermit crabs within the tank were plotted as heatmaps for the respective conditions (Supplementary Information, Fig. S9-S10).

Fig. S9 shows that whilst in pH 8.1 dopamine does not attract or repulse male hermit crabs, it seems to be mildly attractive to female hermit crabs (see Fig. S9G). This effect, however, is not reproduced at pH 7.7 (Fig. S10, see also Fig. 5.9).

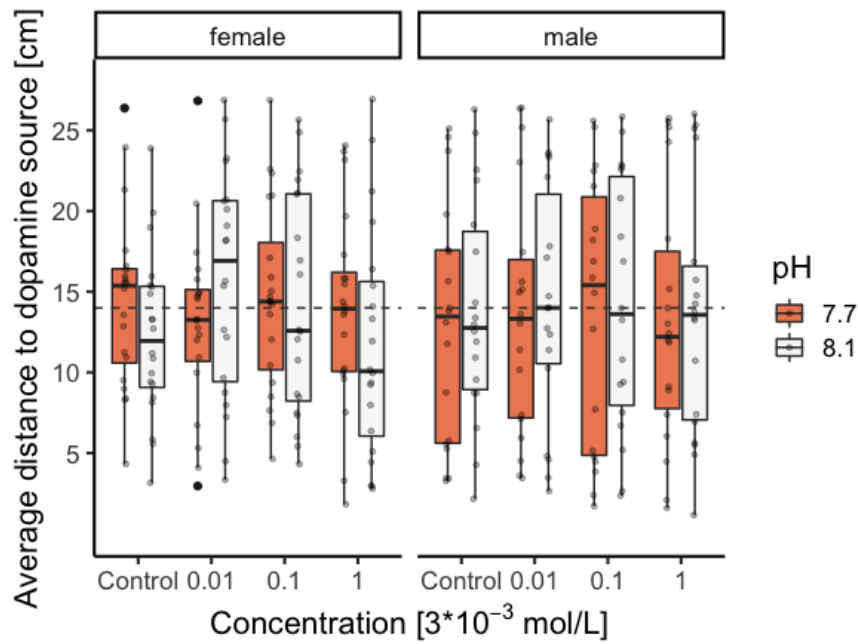


Fig. 5.9: Average Distance of N=20 female and N=18 male hermit crabs to different concentrations of dopamine in pH 8.1 (white) and pH 7.7 (orange). There is no evidence for a dose-dependent response or an interactive effect of pH and concentration. The boxplots are overlaid by the actual data points in semi-transparent. The dotted line represents the average position in control conditions.

A linear mixed effect analysis based on the average distance of hermit crabs to the cue (see also x-axis in heatmaps) shows no evidence for concentration-, pH or sex-specific effects (see Table 5.4). The absence of any clear trends in the average distance of hermit crabs to the dopamine source is also visualised in Fig. 5.9. Similarly, no other outcome variable, such as distance travelled, acceleration or active time, shows a significant concentration-, pH or sex-dependent trend (see Supplementary Information, Fig. S11-S13).

Table 5.4: Details of linear mixed effect analysis of the spatial response of hermit crabs to dopamine reveal no evidence for concentration, pH or sex-dependent effects of dopamine on hermit crabs movement with the chosen experimental set-up and concentration range. The table summarises the number of parameters (npar), the Akaike information criterion (AIC), likelihood ratio test (LRT) and p-value for the different fixed factors.

	npar	AIC	LRT	p
3-way interaction: concentration * pH * sex	3	2057	1.54	0.67
2-way interaction: concentration * pH	3	2046	1.82	0.61
effect of sex	1	2043	0.004	0.95
effect of concentration	3	2041	1.59	0.66
effect of pH	1	2043	0.007	0.93

5.4 Discussion

This chapter aims to determine whether dopamine and PEA are similar - structurally, chemically and biologically, as olfactory cues for crustaceans. There are a lot of parallels between PEA and dopamine: As biogenic monoamines, their chemical structures are based on a benzene ring with a flexible amino side chain; both are known neurotransmitters²⁸⁴ and both exist in marine environments, excreted by algae.¹⁵⁰ Furthermore, both PEA and dopamine are associated with agonistic behaviour in crustaceans (see chapter 2-3 for PEA and published studies for dopamine^{135,163,299}). However, my results indicate that PEA mediates agonistic behaviour upon external exposure (as infochemical), whilst published studies on dopamine focus on internal levels of the neurotransmitter. Hence, I set out to evaluate whether dopamine and PEA are so similar that the internal role of dopamine in agonistic behaviours of crustaceans could translate to an olfactory-mediated response comparable to my previous observations with PEA.

After comparing structural features of the compounds PEA and dopamine, I assessed their chemical similarities and finally their biological similarity is studied by repeating a behavioural experiment with hermit crabs and PEA from chapter 2 using dopamine. In a first step, the susceptibility of dopamine to pH fluctuations was determined by means of pK_a values of the different protonation states. Based on the Henderson-Hasselbalch equation, the pH-dependent abundance of the different protonation states was assessed (see Fig. 5.5). Dopamine has two additional functional groups (hydroxy groups) compared to PEA, resulting in four protonation states for dopamine instead of two for PEA. With $pK_{a1} = 9.1$, the first dissociation constant of dopamine, which defines the pH-dependent conversion from the protonated to the zwitterionic/neutral state, is lower for dopamine than for PEA ($pK_a = 9.83$, see also Fig 2.13B). Dopamine is hence more susceptible to protonation than PEA at a pH range relevant for marine

environments. Modelling average ocean acidification scenarios (pH 8.1 - pH 7.7), the abundance of protonated dopamine increases by 5.8%, whilst protonated PEA increases by 1.3% within the same pH range.

My computational models suggest that dopamine is predominantly in the *gauche* conformation, regardless of the protonation state. However, the energy difference to the *anti* conformation is, with the notable exception of the zwitterionic 2 state, small (see Table 5.2). This is in contrast to a conformational study from the 1980s of dopamine in D₂O solution, which measured the pH dependency of coupling constants in NMR experiments³¹¹ as an indicator of torsion angles and found that *anti* and *gauche* conformations are equally populated at pH 9.0 with the *gauche* conformation increasing in abundance with decreasing pH. My quantum chemical calculations, on the other hand, indicate that the *gauche* conformation of zwitterionic 2 clearly dominates in high pH conditions (pH 9-10.5) and the energy difference to the *anti* conformation decreases with decreasing pH (protonated dopamine, pH<9; compare Fig. 5.5 and Table 5.2). However, using D₂O rather than H₂O as the solvent increases hydrogen bonds of dopamine with the surrounding solvent, as deuterium is less electronegative than hydrogen due to its higher mass. Stronger hydrogen bonds with the solvent might have led to the increased observation of dopamine in the *anti* conformation as compared to my calculations. Furthermore, other, more recent studies are in agreement with my findings on the *gauche* conformation as the global minimum for dopamine in water.^{274, 286} I can therefore confirm my hypothesis that, similarly to PEA, dopamine is mainly found in the folded conformation, regardless of the protonation state.

Although both PEA and dopamine are predominantly found in the *gauche* conformation, the torsion angles of the amino side chain are slightly different (compare Table 5.3 and Table 4.1). Bioassays and NMR measurements with acetylcholin analogues (biogenic amines like dopamine and PEA) binding to the M₂ muscarinic acetylcholine receptor

(G-protein coupled receptor like the PEA receptor TAAR1 and dopamine receptor D2), suggest that the torsion angle of the ligand can affect receptor binding.³¹² However, computational studies with dopamine indicate that the amino group functions as an anchor in receptor binding and a rapid rearrangement of the dopamine conformation upon binding, potentially rendering the exact conformation of dopamine in solution less important for binding.²⁷⁴

In contrast to PEA, dopamine undergoes a decrease in its dipole moment when the pH is decreased. Whilst protonating PEA to PEAH⁺ entails a 5-fold increase in the dipole moment and a substantial change in the direction of the charge separation (see Fig. 4.5), protonating the zwitterionic state 2 of dopamine (the energetically-preferred tautomer of zwitterionic/neutral dopamine) leads to a 60% reduction in the dipole strength (see Table 5.2) accompanied by small changes in the dipole direction (see Fig. 5.7). This constitutes a major difference between dopamine and PEA. In the previous chapter (chapter 4), the pH-dependent behavioural response of crustaceans to PEA has been mainly attributed to pH-dependent changes in the receptor-ligand binding affinity, which heavily depends on electrostatic interactions. With the pH affecting the dipole moment of PEA and dopamine in a contrasting manner, dopamine receptor binding is unlikely to be equally pH-dependent. Hence, dopamine might not evoke a pH-dependent behavioural response as observed for PEA.

Due to the chemical reactivity of dopamine, the increased abundance of protonated dopamine at reduced pH conditions entails more than just structural and charge-related changes in the molecule itself (as observed for PEA). In contrast to PEA, dopamine oxidises in water.^{292,295} The first step of the reaction is the oxidation of the hydroxy groups on the benzene ring to form a dicarbonyl structure (see Fig. 5.3). This step is pH-dependent as the rearrangement of the conjugated system of delocalised electrons requires high electron density in the benzene ring.^{294,295} Protonation of a functional group

binding to the benzene ring has an electron-withdrawing effect²⁹⁵ and therefore hampers the oxidation reaction, whilst electron-donating properties of a functional group (e.g. deprotonated hydroxyl group in zwitterionic dopamine) increases the oxidation rate. My computational finding that the energetically preferred tautomer of neutral/zwitterionic dopamine is the zwitterionic 2 state therefore aligns with the increased oxidation rate at reduced pH. The increased oxidation rate of dopamine at increased pH was observed during the preparation of dopamine solutions for NMR spectroscopy (see section 5.3.3). The dopamine solution at pH 9.8 oxidised so quickly that NMR measurement of zwitterionic/neutral dopamine was not possible, whilst the dopamine solution at pH 6.8 stayed unoxidised (see clean spectra in Fig. 5.8A).

In the northeast Pacific the green alga *Ulvaria obscura* produces dopamine at concentrations ranging up to 5% of the alga's dry mass.^{313,314} Therefore, the pH-dependent oxidation reaction of dopamine has environmental relevance in the face of ocean acidification. Dopamine exudates have been shown to work as anti-herbivore defence for the alga³¹⁴ and are also known to affect larval development in several invertebrates.^{315,316} Histochemical studies show that dopamine is stored in acidic vesicles in the cells of *U. obscura*,¹⁵⁰ which hampers the oxidation reaction until the alga is stranded at low tide. Upon rehydration by the incoming tide, dopamine is released into the surrounding water.²⁹³ During green tides, which are vast blooms of green macroalgae (such as *U. obscura*), concentrations of dopamine can reach up to 1340 $\mu\text{mol/L}$ at the northeast Pacific coast.²⁹³

Green tide events have been increasing in scale and frequency over the last decades.³¹⁷ The pH dependency of dopamine oxidation, as deduced above, leads to a slower oxidation rate under more acidic conditions. With a slower oxidation of dopamine under ocean acidification scenarios, the immediate dopamine concentration in *U. obscura* exudates could increase, simultaneously decreasing the amount of cyto- and genotoxic

reaction products such as quinones and reactive oxygen species (ROS). By shifting pH ranges and increasing the amplitude of diurnal and seasonal pH fluctuations,^{81,87} ocean acidification could thereby allow more time for the dilution of the reaction products whilst stabilising dopamine itself. This would lead to a shift in the aspects related to *U. obscura* toxicity. The toxicity and general effects of dopamine itself would gain importance under ocean acidification scenarios whilst the concentration of toxic reaction products would be reduced.

Whilst my comparisons of the chemistry of dopamine and PEA have produced parallels as well as distinct differences (see above), the reaction of hermit crabs to the two biogenic amines as external cues is not comparable (compare section 5.3.4 and 2.3.2). Although there is some evidence that neurotransmitters can be involved in aquatic chemical communication for microorganisms,³¹⁸ to date, to the best of my knowledge, there is no evidence that dopamine acts as an infochemical for crustaceans. This coincides with the absence of concentration-, sex- or pH-dependent trends of dopamine from a point source on locomotion-related parameters for hermit crabs in my study (see Fig. 5.9 and Table 5.4). Although both PEA and dopamine are associated with agonistic behaviours in crustaceans, I have to reject my hypothesis that exposure to dopamine induces a comparable pH and sex-specific behavioural response as observed for PEA.

Although there is some evidence of an attraction of female hermit crabs to the highest concentration of dopamine ($3 \cdot 10^{-3}$ mol/L) at pH 8.1 (see Fig. S9G), this effect was not statistically significant in the linear mixed effect model. Furthermore, it was not observed in a dose-dependent manner and wasn't replicated in experiments in pH 7.7 or with males. It is possible, however, that the high number of different groups (the model evaluated concentration, sex and pH as fixed factors) masked an actual pH- and sex-specific effect.

The animals used for this experiment were collected during their reproductive season and copulatory-type behaviour was observed during the three-week acclimation period. Although no reproduction-associated behaviours were observed anymore at the time of data collection, it cannot be excluded that the weak attractive effect of dopamine on females is a remnant of dopamine-mediated reproductive behaviour. In blue crabs, elevated internal dopamine levels were suggested to play a role in courtship display behaviour,³⁰¹ which female crabs might be able to perceive chemically as well as visually. However, different experimental set-ups and husbandry conditions would be needed for further investigations on the potential role of dopamine in reproduction-related chemical communication. Finally, as chapter 2 and 3 revealed no indication of PEA attracting female crustaceans, this does not constitute a similar biological role of dopamine and PEA. I conclude that PEA and dopamine do not have the same biological function in olfactory-mediated behaviour of crustaceans within the observed concentration range.

5.5 Conclusion

Whilst, as biogenic amines, dopamine and PEA are similar in some aspects of their chemical structure (benzene ring with amino side chain) and they are both primarily found in the folded conformation, I also observed distinct differences between PEA and dopamine on the level of the chemical structure and reactivity: For one, dopamine oxidises in water whilst PEA is stable in water. Secondly, decreasing the pH increases the dipole moment of PEA substantially, whilst it slightly decreases the dipole moment of dopamine. This means that dopamine and PEA are unlikely to exhibit similar pH-dependency in their receptor-ligand interactions, as the ligand's dipole moment is a crucial aspect of receptor-ligand electrostatic interactions. Finally, the biological reactivity is a key component of the similarity concept.²⁸² For the purpose of this study,

rejecting the similarity of PEA and dopamine on the biological level is the critical factor in rejecting the notion that PEA and dopamine are similar. Behavioural experiments with hermit crabs revealed no comparable olfactory-mediated response for dopamine and PEA within the tested concentration range. I therefore reject the hypothesis that PEA and dopamine are similar. I conclude that the observed behavioural response of hermit crabs and shore crabs to PEA as an infochemical (see chapter 2-3) is not the result of PEA mimicking dopamine.

CHAPTER 6

Summary and Discussion

This thesis aims to determine the ecological role of the infochemical PEA for crustaceans and assess potential mechanisms of its pH-dependency. Whilst PEA is a predator cue for mammals,²⁴ my findings show that crustaceans are attracted to this infochemical in a weight and pH-dependent manner (see chapters 2-3).

My results suggest that PEA attracts heavy shore crabs and hermit crabs in decreased pH conditions in a comparable manner. Additionally, behavioural displays of shore crabs suggest that PEA might be used to signal willingness to fight. During agonistic encounters such as fights, crustaceans are known to direct their urine towards their opponent via a gill current.^{132,165} Analysing shore crab urine via tandem mass spectrometry, my results provide clear evidence for PEA in shore crab urine (see section 3.3.4). This indicates that PEA is a urine-borne compound mediating agonistic behaviours in shore crabs. Previously, the chemical compound(s) in urine responsible for the agonistic response of the opponent receiving the gill current, were unknown.^{132,165} My thesis identifies PEA as a component of this urine-borne chemical signal in shore crabs. Comparable sex- and pH-specific movement patterns of hermit crabs and shore crabs in response to PEA furthermore suggests that the infochemical PEA might have a similar role for crustaceans other than shore crabs. However, further studies of behavioural displays of other crustaceans in response to PEA and quantifications of PEA levels in other crustacean urine are needed for clear conclusions on a potential transferable role of PEA for crustaceans. Furthermore, it is possible, that other compounds also con-

tribute to the chemical bouquet that signals willingness to fight through urine, whereby species-specific compounds are likely.

As this study focuses on the effects of PEA in single-animal experiments, staged fights with crustaceans exposed to PEA could improve our understanding of the role of PEA in agonistic interactions. Future experiments with two crustaceans could explore potential species-specificity of the intra- or even interspecific role of PEA for the timing and intensity of the onset of a fight. Additionally, refining the extraction methods for PEA from crustacean urine could allow for further insights into potentially varying PEA levels in winners and losers, male and female crustaceans, of different sizes, species or diets.

In chapter 4, I assess potential mechanisms for the pH-dependent response to PEA, as observed for hermit crabs and shore crabs in chapters 2 and 3. Protonation state abundance curves (Fig. 2.13B) suggest that with an acid dissociation constant of $pK_a=9.83$,¹⁰⁵ only 1.3% of PEA changes its protonation state when the pH is reduced from pH 8.1 to 7.7. Hence, the increased attraction of crustaceans to PEA at pH 7.7 as compared to pH 8.1 cannot be explained by an increased the abundance of the protonated form of PEA (PEAH⁺) alone. Furthermore, my computational findings, validated by NMR spectroscopy, suggest that the chemical conformation of PEA changes only marginally upon protonation. However, my calculations also reveal that the protonation of PEA leads to large changes in its charge distribution (Fig. 4.5) which cause an increased affinity to proof-of-concept receptor TAAR1 (Fig. 4.3.3). Hence, small changes in the protonation state could lead to large changes in the electrostatic interactions between receptor and ligand, potentially causing the amplified response of crustaceans to PEA in reduced pH conditions.

Drawing on methods from all previous chapters, I then compared, in chapter 5, the chemical compounds dopamine and PEA and the responses they elicit as infochemicals for hermit crabs to determine whether PEA and dopamine are ‘similar’. As they are

both monoamines, known to act as neurotransmitters across the animal kingdom,²⁹³ dopamine and PEA have some common structural features. However, my findings also suggest distinct differences, particularly concerning chemical reactivity and dipole moment. Unlike PEA, dopamine does not elicit an attraction (or repulsion) of hermit crabs within the tested concentration range and no pH-dependent response patterns were observed. This indicates that PEA does not mimic dopamine as an infochemical for crustaceans. Furthermore, I conclude that the exact structure and dipole moment of PEA matters for chemoreception in crustaceans. Whilst TAAR1 is known to bind dopamine (although with lower potency than PEA),³¹⁹ the (unknown) crustacean PEA receptor doesn't seem to bind dopamine. Hence, the observed response of crustaceans to PEA cannot be attributed to PEA binding to an (unknown) dopamine receptor. Having addressed structural, chemical and behavioural aspects, I conclude that PEA and dopamine are not similar.

Exploring potential mechanisms of the amplified response of hermit crabs and shore crabs to PEA at decreased pH, my work is also relevant in the context of research on chemical communication under climate change ('infodisruption'). Climate change is associated with a combination of increasing temperature, increasing CO₂ levels and decreasing pH (in aquatic conditions).³⁷ All these stressors can impact the chemical communication cascade, but little is known about interactive effects of the different climate change stressors.³⁷ In addition to changes in pH, realistic climate change scenarios should therefore also consider changes in temperature and CO₂ levels. Having a mechanistic focus, this study cannot capture the breadth of potential climate change effects on PEA-mediated communication: Whilst climate change encompasses long-term average changes in temperature, CO₂ levels and pH, my study only addresses pH-dependent changes with relatively short acclimation times to the new pH environment. Secondly, my chosen study species, hermit crabs and shore crabs, live in intertidal habitats, where

temperature and pH fluctuate daily,⁸² rendering the average pH decrease of pH 8.1 to 7.7 by the end of the century³¹ less momentous than changes to the range and amplitude of these pH fluctuations as expected due to climate change.^{81,87} Nevertheless, using the same pH range as previous studies on infodisruption^{41,47,79} ensures comparability of my results with the literature. Most studies on chemical communication under ocean acidification report decreased potency of the infochemical in reduced pH (via increased CO₂) conditions.^{41,57,102,108,320} A review by Clements and Hunt (2015)⁵⁰ suggests that the impact of reduced pH (high CO₂) conditions on animal behaviour varies depending on species, ecosystem, and behaviour. The stronger response of hermit crabs and shore crabs to PEA in end-of-the-century pH conditions is a rare example of an amplifying effect of ocean acidification on animal behaviour.

To exclude potential physiological effects of high CO₂ conditions, I chose to manipulate the pH using hydrochloric acid rather than increasing CO₂ levels. It is difficult to estimate potential differences between CO₂- and acid-induced pH decrease in the response of crustaceans to PEA. An increased attraction of hermit crabs and shore crabs to PEA under high CO₂ conditions, as observed for low pH conditions, is likely, but physiological costs of an increased CO₂ environment¹⁰² might attenuate the effect size. As I conclude in chapter 3 that PEA is a urine-borne infochemical, the pH-manipulation via hydrochloric acid approaches the environmental conditions in urine better than increased CO₂ levels.

In addition to excluding CO₂-dependent effects, temperature-dependent effects, as expected in the face of climate change, were largely excluded in this study. Although temperature- (and salinity-) dependent effects through changes to the dielectric environment were considered - and deemed to be small - in the computational models of PEA/PEAH⁺ and PEA-TAAR1/PEAH⁺-TAAR1 (section 4.3.5), temperature-dependent effects were only briefly discussed in behavioural experiments (section 2.3.4).

Future studies could explore seasonal/temperature-dependent effects of the role of PEA in chemically mediated behaviour of crustaceans. Likewise, future computational experiments could also incorporate further temperature-dependent aspects. Acid dissociation and tautomerisation constants, for example, which were used to calculate the abundance of PEA and dopamine in different pH conditions (Fig. 2.13B and 5.5), are often treated as non-varying values, but are in fact temperature-dependent and usually listed for 25°C.^{105,289,290} As a rough approximation, the pK_a value of amino functional groups is known to increase by about 0.02 units for each 1°C temperature decrease.³²¹ With an average ocean surface temperature of 17°C,²⁶⁸ the actual dissociation constants are hence likely to be slightly higher than the officially listed values ($pK_a \approx 9.97$ rather than 9.83 for PEA^{105,321} and 9.26 rather than 9.1 for dopamine^{288,289,321}), which stabilises the protonated states of dopamine and PEA in average marine environments.

In turn, increasing oceanic surface water temperatures through climate change, decreases the dissociation constants.^{43,290} Increasing temperatures hence shift the abundance curves of PEA and dopamine towards lower pH ranges, making infochemicals more susceptible to protonation. Potential interactive effects of temperature and pH underscore the complexity of realistic studies on climate change: The combined effect of increasing temperature and ocean acidification on infochemicals in water is likely to be different than what can be gauged in single factor studies.

Finally, the recent discussion regarding reproducible methods and results in marine infodisruption research on coral reef fishes^{47-49,52} might have created doubts whether ocean acidification can affect chemical communication. However, my results add to the ample evidence^{37,50} suggesting that the direction and magnitude of pH-dependent effects on chemically mediated behaviour depends on the study species and observed behaviour.

CHAPTER 7

Conclusion

In the course of this thesis, I demonstrate that PEA is an attractant for hermit crabs and shore crabs, whilst being widely associated with predator avoidance. As PEA evokes a comparable response in the two distantly related crustaceans, it can be called a ‘transferable’ infochemical. Agonistic displays of shore crabs in response to PEA, the weight/sex- and pH-dependency of the response and evidence for PEA in shore crab urine lead me to conclude that PEA is a urine-borne infochemical that mediates agonistic interactions in crustaceans. Furthermore, the dose-dependency of the behavioural response suggests that PEA (in reduced pH) indicates the presence of an opponent that is willing to fight. Mechanistically, the pH-dependency of the observed response in hermit crabs and shore crabs could be explained by the strongly increased dipole of PEA upon protonation, which substantially increases its receptor binding affinity. However, my quantum chemical calculations further reveal that protonation of the receptor could, in turn, slightly weaken receptor-ligand electrostatic interactions. I hence conclude that the magnitude of pH-dependent effects on chemoreception of PEA is difficult to estimate. Finally, the comparison of PEA and dopamine shows that the exact structure and charge distribution of PEA is key for its biological function for crustaceans. Despite some chemical similarities between the neurotransmitter dopamine and PEA, they have distinct biological roles for crustaceans.

References

- ¹ Grand View Research. Perfume market size, share & trends analysis report by product (mass, premium), by end user (men, women), by distribution channel (offline, online), by region, and segment forecasts, 2019–2025. 2019. 1
- ² A. Altundag, O. Saatci, D.E.T. Sanli, O.A. Duz, A.N. Sanli, O. Olmuscelik, D. Temirbekov, S.G. Kandemirli, and A.B. Karaaltin. The temporal course of COVID-19 anosmia and relation to other clinical symptoms. *Eur Arch Oto-Rhino-L*, 278(6) pages 1891–1897, 2021. DOI 10.1007/s00405-020-06496-5. 1
- ³ Z.M. Patel. Olfactory loss and olfactory training. *JAMA Otolaryngol Head Neck Surg*, 147(9) pages 840–840, 2021. DOI 10.1001/jamaoto.2021.1507. 1
- ⁴ T.D. Wyatt. *Pheromones and animal behaviour: communication by smell and taste*. Cambridge University Press, 2003. 1, 2, 3
- ⁵ T.D. Wyatt. *Pheromones and animal behavior: chemical signals and signatures*. Cambridge University Press, 2014. 1, 3, 106
- ⁶ M. Dicke and M. W. Sabelis. Infochemical terminology: based on cost-benefit analysis rather than origin of compounds? *Functional ecology*, pages 131–139, 1988. DOI 10.2307/2389687. 1, 3
- ⁷ T.D. Wyatt. Proteins and peptides as pheromone signals and chemical signatures. *Anim Behav*, v.97 pages 273–280, 2014. DOI 10.1016/j.anbehav.2014.07.025. 1, 2, 3, 5

- ⁸ M.E. Hay. Crustaceans as powerful models in aquatic chemical ecology. In T. Breithaupt and M. Thiel, editors, *Chemical communication in crustaceans*, pages 41–62. Springer, 2010. DOI 10.1007/978-0-387-77101-4_3. 2, 21, 96
- ⁹ M. Thiel and T. Breithaupt. Chemical communication in crustaceans: research challenges for the twenty-first century. In T. Breithaupt and M. Thiel, editors, *Chemical communication in crustaceans*, pages 3–22. 2010. DOI 10.1007/978-0-387-77101-4_1. 2, 62, 70
- ¹⁰ T. Wyatt. *Pheromones and animal behaviour: chemical signals and signatures*, chapter Animals in a chemical world, pages 1–48. Cambridge University Press, Cambridge, 2014. 2
- ¹¹ R.T. Cardé, A.M. Cardé, A.S. Hill, and W.L. Roelofs. Sex pheromone specificity as a reproductive isolating mechanism among the sibling species *Archips argyrospilus* and *A. mortuanus* and other sympatric tortricine moths (Lepidoptera: Tortricidae). *J Chem Ecol*, 3(1) pages 71–84, 1977. DOI 10.1007/BF00988135. 2
- ¹² C. Löfstedt. Moth pheromone genetics and evolution. *Philos Trans R Soc B Biol Sci*, 340(1292) pages 167–177, 1993. DOI 10.1098/rstb.1993.0055. 2
- ¹³ J.A. Byers. Chemical constraints on the evolution of olfactory communication channels of moths. *J Theor Biol*, 235(2) pages 199–206, 2005. DOI 10.1016/j.jtbi.2005.01.003. 2
- ¹⁴ J.D. Hardege, H.D. Bartels-Hardege, N. Fletcher, J.A. Terschak, M. Harley, M.A. Smith, L. Davidson, D. Hayden, C.T. Müller, and M. and others Lorch. Identification of a female sex pheromone in *Carcinus maenas*. *Mar Ecol Prog Ser*, v.436 pages 177–189, 2011. DOI <https://doi.org/10.3354/meps09226>. 2, 69

- ¹⁵ N. Fletcher, J.A. Terschak, H.D. Bartels-Hardege, R. Bublitz, P. Schirmacher, and J.D. Hardege. A pheromone bouquet controls the reproductive behaviour of the male shore crab, *Carcinus maenas*. *Aquat Ecol*, pages 1–9, 2021. DOI 10.1007/s10452-021-09930-w. 2, 60, 69
- ¹⁶ B.D. Wisenden. The cue–signal continuum: a hypothesized evolutionary trajectory for chemical communication in fishes. *Fish pheromones and related cues*, pages 149–158, 2014. DOI 10.1002/9781118794739.ch7. 3
- ¹⁷ J.A. Byers. Earwigs (*Labidura riparia*) mimic rotting-flesh odor to deceive vertebrate predators. *Sci Nat*, 102(7) pages 1–10, 2015. DOI 10.1007/s00114-015-1288-1. 3
- ¹⁸ J. Henneken, J.Q.D. Goodger, T.M. Jones, and M.A. Elgar. The potential role of web-based putrescine as a prey-attracting allomone. *Anim Behav*, v.129 pages 205–210, 2017. DOI 10.1016/j.anbehav.2017.05.024. 3
- ¹⁹ K.A. Anderson and A. Mathis. Friends in low places: Responses of a bethic stream fish to intra-prey-guild alarm cues. *Ethology*, 122(12) pages 954–962, 2016. DOI 10.1111/eth.12563. 3
- ²⁰ A.S. Mathuru, C. Kibat, W.F. Cheong, G. Shui, M.R. Wenk, R.W. Friedrich, and S. Jesuthasan. Chondroitin fragments are odorants that trigger fear behavior in fish. *Current Biology*, 22(6) pages 538–544, 2012. DOI 10.1016/j.cub.2012.01.061. 4, 14
- ²¹ A.E. Faulkner, I.E. Holstrom, S.A. Molitor, M.E. Hanson, W.R. Shegrud, J.C. Gillen, S.J. Willard, and B.D. Wisenden. Field verification of chondroitin sulfate as a putative component of chemical alarm cue in wild populations of fathead minnows (*Pimephales promelas*). *Chemoecology*, 27(6) pages 233–238, 2017. DOI 10.1007/s00049-017-0247-z. 4

- ²² T.J. Hara. Feeding behaviour in some teleosts is triggered by single amino acids primarily through olfaction. *J Fish Biol*, 68(3) pages 810–825, 2006. DOI 10.1111/j.0022-1112.2006.00967.x. 4, 14
- ²³ E. Lari, D. Steinkey, R.J. Steinkey, and G.G. Pyle. *Daphnia magna* increase feeding activity in the presence of four amino acids. *J Plankton Res*, 40(5) pages 537–543, 2018. DOI 10.1093/plankt/fby038. 4
- ²⁴ D.M. Ferrero, J.K. Lemon, D. Fluegge, S.L. Pashkovski, W.J. Korzan, S.R. Datta, M. Spehr, M. Fendt, and S.D. Liberles. Detection and avoidance of a carnivore odor by prey. *PNAS*, 108(27) pages 11235–11240, 2011. DOI 10.1073/pnas.1103317108. 4, 5, 17, 20, 21, 23, 57, 65, 67, 68, 71, 78, 108, 184
- ²⁵ I. Imre, R.T. di Rocco, C.F. Belanger, G.E. Brown, and N.S. Johnson. The behavioural response of adult *Petromyzon marinus* to damage-released alarm and predator cues. *J Fish Biol*, 84(5) pages 1490–1502, 2014. DOI 10.1111/jfb.12374. 4, 14, 17, 21, 57, 67
- ²⁶ C.F. Halbgewachs, T.A. Marchant, R.C. Kusch, and D.P. Chivers. Epidermal club cells and the innate immune system of minnows. *Biol J Linn Soc*, 98(4) pages 891–897, 2009. DOI 10.1111/j.1095-8312.2009.01328.x. 4
- ²⁷ M.R. Brown. The amino-acid and sugar composition of 16 species of microalgae used in mariculture. *J Exp Mar Biol Ecol*, 145(1) pages 79–99, 1991. DOI 10.1016/0022-0981(91)90007-J. 5
- ²⁸ W.E.S. Carr, J.C. Netherton, III, R.A. Gleeson, and C.D. Derby. Stimulants of feeding behavior in fish: analyses of tissues of diverse marine organisms. *Biol Bull*, 190(2) pages 149–160, 1996. DOI 10.2307/1542535. 5
- ²⁹ J. Maynard Smith and D. Harper. *Animal signals*. Oxford University Press, 2003. 5

- ³⁰ E.N. Barata, R.M. Serrano, A. Miranda, R. Nogueira, P.C. Hubbard, and A.V.M. Canário. Putative pheromones from the anal glands of male blennies attract females and enhance male reproductive success. *Anim Behav*, 75(2) pages 379–389, 2008. DOI 10.1016/j.anbehav.2007.05.018. 5
- ³¹ J.G. Canadell, P.M.S. Monteiro, M.H. Costa, L. Cotrim da Cunha, P.M. Cox, A.V. Eliseev, S. Henson, M. Ishii, S. Jaccard, C. Koven, A. Lohila, P.K. Patra, S. Piao, J. Rogelj, S. Syampungani, S. Zaehle, and K. Zickfeld. *Climate Change 2021: The Physical Science Basis. Contribution of Working Group I to the Sixth Assessment Report of the Intergovernmental Panel on Climate Change*, chapter Global Carbon and other Biogeochemical Cycles and Feedbacks, pages 673–816. Cambridge University Press, 2021. DOI 10.1017/9781009157896.007. 6, 7, 22, 23, 58, 187
- ³² S.C. Doney, V.J. Fabry, R.A. Feely, and J.A. Kleypas. Ocean acidification: the other CO₂ problem. *Ann Rev Mar Sci*, 2009. DOI 10.1146/annurev.marine.010908.163834. 6
- ³³ R.G. Bates and A.K. Vijh. Determination of pH: theory and practice. *J Electrochem Soc*, 120(8) page 263C, 1973. 6
- ³⁴ S. Solomon, D. Qin, M Manning, Z. Chen, M. Marquis, K.B. Averyt, M. Tignor, and H.L. Miller, editors. *Climate Change 2007: The Physical Science Basis. Contribution of Working Group I to the Fourth Assessment Report of the Intergovernmental Panel on Climate Change*, page 996. Cambridge University Press, 2007. 7
- ³⁵ L. Bopp, L. Resplandy, J.C. Orr, S.C. Doney, J.P. Dunne, M. Gehlen, Halloran P., C. Heinze, T. Ilyina, R. Seferian, J. Tjiputra, and M. Vichi. Multiple stressors of ocean ecosystems in the 21st century: projections with CMIP5 models. *Biogeosciences*, v.10 pages 6225–6245, 2013. DOI 10.5194/bg-10-6225-2013. 7

- ³⁶ J.C. Orr, V.J. Fabry, O. Aumont, L. Bopp, S.C. Doney, R.A. Feely, A. Gnanadesikan, N. Gruber, A. Ishida, F. Joos, et al. Anthropogenic ocean acidification over the twenty-first century and its impact on calcifying organisms. *Nature*, 437(7059) pages 681–686, 2005. 7
- ³⁷ C.C. Roggatz, M. Saha, S. Blanchard, P. Schirrmacher, P. Fink, F. Verheggen, and J.D. Hardege. Becoming nose-blind: Climate change impacts on chemical communication. *Glob Chang Biol*, 2022. DOI 10.1111/gcb.16209. 7, 8, 16, 20, 58, 186, 188
- ³⁸ M. Lürling. Infodisruption: pollutants interfering with the natural chemical information conveyance in aquatic systems. In C. Brönmark and L.A. Hansson, editors, *Chemical ecology in aquatic systems*, pages 250–264. Oxford University Press. 7
- ³⁹ C. Brönmark and L.A. Hansson. Chemical ecology in aquatic systems - an introduction. In C. Brönmark and L.A. Hansson, editors, *Chemical ecology in aquatic systems*. Oxford University Press. 7
- ⁴⁰ E.A.F. Christensen, T. Norin, I. Tabak, M. van Deurs, and J.W. Behrens. Effects of temperature on physiological performance and behavioral thermoregulation in an invasive fish, the round goby. *J Exp Biol*, 224(1) page jeb237669, 2021. DOI 10.1242/jeb.237669. 8
- ⁴¹ C.C. Roggatz, M. Lorch, J.D. Hardege, and D.M. Benoit. Ocean acidification affects marine chemical communication by changing structure and function of peptide signalling molecules. *Glob Chang Biol*, 22(12) pages 3914–3926, 2016. DOI 10.1111/gcb.13354. 8, 9, 11, 22, 23, 59, 62, 100, 143, 144, 187

- ⁴² M. Lürling and M. Scheffer. Info-disruption: pollution and the transfer of chemical information between organisms. *Trends Ecol Evol*, 22(7) pages 374–379, 2007. DOI 10.1016/j.tree.2007.04.002. 8
- ⁴³ C.C. Roggatz, N. Fletcher, D.M. Benoit, A.C. Algar, A. Doroff, B. Wright, K.C. Wollenberg Valero, and J.D. Hardege. Saxitoxin and tetrodotoxin bioavailability increases in future oceans. *Nat Clim Chang*, 9(11) pages 840–844, 2019. DOI 10.1038/s41558-019-0589-3. 8, 100, 188
- ⁴⁴ Z. Velez, C.C. Roggatz, D.M. Benoit, J.D. Hardege, and P.C. Hubbard. Short-and medium-term exposure to ocean acidification reduces olfactory sensitivity in gilthead seabream. *Front Physiol*, v.10 page 731, 2019. DOI 10.3389/fphys.2019.00731. 8, 11, 62
- ⁴⁵ D.L. Dixson, P.L. Munday, and G.P. Jones. Ocean acidification disrupts the innate ability of fish to detect predator olfactory cues. *Ecol Lett*, 13(1) pages 68–75, 2010. DOI 10.1111/j.1461-0248.2009.01400.x. 8, 9, 57
- ⁴⁶ P.L. Munday, D.L. Dixson, J.M. Donelson, G.P. Jones, M.S. Pratchett, G.V. Devitsina, and K.B. Døving. Ocean acidification impairs olfactory discrimination and homing ability of a marine fish. *PNAS*, 106(6) pages 1848–1852, 2009. DOI 10.1073/pnas.0809996106. 8, 9
- ⁴⁷ T.D. Clark, G.D. Raby, D.G. Roche, S.A. Binning, B. Speers-Roesch, F. Jutfelt, and J. Sundin. Ocean acidification does not impair the behaviour of coral reef fishes. *Nature*, 577(7790) pages 370–375, 2020. DOI 10.1038/s41586-019-1903-y. 8, 9, 23, 57, 58, 187, 188
- ⁴⁸ P.L. Munday, D.L. Dixson, M.J. Welch, D.P. Chivers, P. Domenici, M. Grosell, R.M. Heuer, G.P. Jones, M.I. McCormick, M. Meekan, et al. Methods matter in repeating

- ocean acidification studies. *Nature*, 586(7830) pages E20–E24, 2020. DOI 10.1038/s41586-020-2803-x. 8, 9, 58, 188
- ⁴⁹ T.D. Clark, G.D. Raby, D.G. Roche, S.A. Binning, B. Speers-Roesch, F. Jutfelt, and J. Sundin. Reply to: Methods matter in repeating ocean acidification studies. *Nature*, 586(7830) pages E25–E27, 2020. DOI 10.1038/s41586-020-2804-9. 8, 9, 58, 188
- ⁵⁰ J.C. Clements and H.L. Hunt. Marine animal behaviour in a high CO₂ ocean. *Mar Ecol Prog Ser*, v.536 pages 259–279, 2015. DOI 10.3354/meps11426. 8, 59, 187, 188
- ⁵¹ D.P. Chivers, M.I. McCormick, G.E. Nilsson, P.L. Munday, S.-A. Watson, M.G. Meekan, M.D. Mitchell, K.C. Corkill, and M.C.O. Ferrari. Impaired learning of predators and lower prey survival under elevated CO₂: a consequence of neurotransmitter interference. *Glob Chang Biol*, 20(2) pages 515–522, 2014. DOI 10.1111/gcb.12291. 9
- ⁵² J.C. Clements, J. Sundin, T.D. Clark, and F. Jutfelt. Meta-analysis reveals an extreme “decline effect” in the impacts of ocean acidification on fish behavior. *PLoS biology*, 20(2) page e3001511, 2022. DOI 10.1371/journal.pbio.3001511. 9, 58, 188
- ⁵³ L. Feugere, L. Angell, J. Fagents, R. Nightingale, K. Rowland, S. Skinner, J.D. Hardege, H. Bartels-Hardege, and K.C. Wollenberg Valero. Behavioural stress propagation in benthic invertebrates caused by acute ph drop-induced metabolites. *Front Mar Sci*, v.8, 2021. DOI 10.3389/fmars.2021.773870. 10
- ⁵⁴ A. Boullis, F. Francis, and F. Verheggen. Aphid–hoverfly interactions under elevated CO₂ concentrations: oviposition and larval development. *Physiol Entomol*, 43(3) pages 245–250, 2018. DOI 10.1111/phen.12253. 10

- ⁵⁵ A. Boullis, S. Blanchard, C. Detrain, G. Lognay, and F. Verheggen. Elevated CO₂ concentration impact the semiochemistry of aphid honeydew without cascade effect on an aphid predator. *Insects*, 9(2) page 47, 2018. DOI 10.3390/insects9020047. 10
- ⁵⁶ G.E. Brown, J.C. Adrian, Jr., M.G. Lewis, and J.M. Tower. The effects of reduced pH on chemical alarm signalling in ostariophysan fishes. *Can J Fish Aquat Sci*, 59(8) pages 1331–1338, 2002. DOI 10.1139/f02-104. 11
- ⁵⁷ C.S. Porteus, P.C. Hubbard, T.M. Uren Webster, R. van Aerle, A.V.M. Canário, E.M. Santos, and R.W. Wilson. Near-future CO₂ levels impair the olfactory system of a marine fish. *Nat Clim Chang*, 8(737) pages 737–743, 2018. DOI 10.1038/s41558-018-0224-8. 11, 22, 62, 187
- ⁵⁸ G.E. Nilsson, D.L. Dixon, P. Domenici, M.I. McCormick, C. Sørensen, S.-A. Watson, and P.L. Munday. Near-future carbon dioxide levels alter fish behaviour by interfering with neurotransmitter function. *Nat Clim Chang*, 2(3) pages 201–204, 2012. DOI 10.1038/nclimate1352. 11, 15
- ⁵⁹ M.G. Wheatly and R.P. Henry. Extracellular and intracellular acid-base regulation in crustaceans. *J Exp Zool*, 263(2) pages 127–142, 1992. DOI 10.1002/jez.1402630204. 11, 60, 69, 72
- ⁶⁰ J.B. Claiborne, S.L. Edwards, and A.I. Morrison-Shetlar. Acid–base regulation in fishes: cellular and molecular mechanisms. *J Exp Zool*, 293(3) pages 302–319, 2002. DOI 10.1002/jez.10125. 11
- ⁶¹ J.I. Spicer, A. Raffo, and S. Widdicombe. Influence of CO₂-related seawater acidification on extracellular acid–base balance in the velvet swimming crab *Necora puber*. *Mar Biol*, 151(3) pages 1117–1125, 2007. DOI 10.1007/s00227-006-0551-6. 11

- ⁶² J.N. Brönsted. Einige Bemerkungen über den Begriff der Säuren und Basen. *Recueil des Travaux Chimiques des Pays-Bas*, 42(8) pages 718–728, 1923. DOI 10.1002/recl.19230420815. 11
- ⁶³ T.M. Lowry. The uniqueness of hydrogen. *Journal of the Society of Chemical Industry*, 42(3) pages 43–47, 1923. DOI 10.1002/jctb.5000420302. 11
- ⁶⁴ L. J. Henderson. Concerning the relationship between the strength of acids and their capacity to preserve neutrality. *American Journal of Physiology-Legacy Content*, 21(2) pages 173–179, 1908. DOI 10.1152/ajplegacy.1908.21.2.173. 11, 12
- ⁶⁵ K. Hasselbalch. Die Berechnung der Wasserstoffzahl des Blutes aus der freien und gebundenen Kohlensäure und die Sauerstoffbindung des Blutes als Funktion der Wasserstoffzahl. *Biochem Z*, v.78 page 113, 1917. 12
- ⁶⁶ S.F. Cummins and J.H. Bowie. Pheromones, attractants and other chemical cues of aquatic organisms and amphibians. *Natural Product Reports*, 29(6) pages 642–658, 2012. DOI 10.1039/c2np00102k. 14
- ⁶⁷ J.D. Hardege, H. Bartels-Hardege, C.T. Müller, and M. Beckmann. Peptide pheromones in female *Nereis succinea*. *Peptides*, 25(9) pages 1517–1522, 2004. DOI 10.1016/j.peptides.2003.11.029. 14
- ⁶⁸ D. Rittschof and J.H. Cohen. Crustacean peptide and peptide-like pheromones and kairomones. *Peptides*, 25(9) pages 1503–1516, 2004. DOI 10.1016/j.peptides.2003.10.024. 14
- ⁶⁹ K.V. Parra, J.C. Adrian Jr, and R. Gerlai. The synthetic substance hypoxanthine 3-N-oxide elicits alarm reactions in zebrafish (*Danio rerio*). *Behav Brain Res*, 205(2) pages 336–341, 2009. DOI 10.1016/j.bbr.2009.06.037. 14

- ⁷⁰ J. He, Q. Dai, Y. Qi, Z. Wu, Q. Fang, P. Su, M. Huang, J.G. Burgess, C. Ke, and D. Feng. Aggregation pheromone for an invasive mussel consists of a precise combination of three common purines. *iScience*, v.19 pages 691–702, 2019. DOI 10.1016/j.isci.2019.08.022. 14
- ⁷¹ K. von Frisch. Zur Psychologie des Fisch-schwarmes. *Naturwissenschaften*, v.26 pages 601–606, 1938. DOI 10.1007/BF01590598. 14
- ⁷² A. Hussain, L.R. Saraiva, D.M. Ferrero, G. Ahuja, V.S. Krishna, S.D. Liberles, and S.I. Korsching. High-affinity olfactory receptor for the death-associated odor cadaverine. *PNAS*, 110(48) pages 19579–19584, 2013. DOI 10.1073/pnas.1318596110. 14, 58
- ⁷³ S.H. Rolen, P.W. Sorensen, D. Mattson, and J. Caprio. Polyamines as olfactory stimuli in the goldfish *Carassius auratus*. *J Exp Biol*, 206(10) pages 1683–1696, 2003. DOI 10.1242/jeb.00338. 14, 58
- ⁷⁴ A.J. Tierney and T. Atema. Amino acid chemoreception: effects of pH on receptors and stimuli. *J Chem Ecol*, 14(1) pages 135–141, 1988. DOI 10.1007/BF01022537. 15, 59, 108
- ⁷⁵ M. Gillard and P. Chatelain. Changes in pH differently affect the binding properties of histamine H1 receptor antagonists. *Eur J Pharmacol*, 530(3) pages 205–214, 2006. DOI 10.1016/j.ejphar.2005.11.051. 15, 108, 146
- ⁷⁶ E. Di Luccio, Y. Ishida, W.S. Leal, and D.K. Wilson. Crystallographic observation of pH-induced conformational changes in the *Amyeloidis transitella* pheromone-binding protein atrapbp1. *PLoS One*, 8(2), 2013. DOI 10.1371/journal.pone.0053840. 15

- ⁷⁷ J. Yin, Y.M. Choo, H. Duan, and W.S. Leal. Selectivity of odorant-binding proteins from the southern house mosquito tested against physiologically relevant ligands. *Front Physiol*, 6(56), 2015. DOI 10.3389/fphys.2015.00056. 15
- ⁷⁸ A.O.H.C. Leduc, P.L. Munday, G.E. Brown, and M.C.O. Ferrari. Effects of acidification on olfactory-mediated behaviour in freshwater and marine ecosystems: a synthesis. *Philos Trans R Soc B Biol Sci*, 368(1627) pages 20120447–20120447, 2013. DOI 10.1098/rstb.2012.0447. 15
- ⁷⁹ Z. Velez, R.A. Costa, W. Wang, and P.C. Hubbard. Independent effects of seawater pH and high P_{CO_2} on olfactory sensitivity in fish: possible role of carbonic anhydrase. *J Exp Biol*, 224(6) page jeb238485, 2021. DOI 10.1242/jeb.238485. 15, 23, 187
- ⁸⁰ C.E. Cornwall, C.D. Hepburn, C.M. McGraw, K.I. Currie, C.A. Pilditch, K.A. Hunter, P.W. Boyd, and C.L. Hurd. Diurnal fluctuations in seawater pH influence the response of a calcifying macroalga to ocean acidification. *Proc Royal Soc B Biol Sci*, 280(1772) page 20132201, 2013. DOI 10.1098/rspb.2013.2201. 16, 22
- ⁸¹ S. R. Pacella, C. A. Brown, G. G. Waldbusser, R. G. Labiosa, and B. Hales. Seagrass habitat metabolism increases short-term extremes and long-term offset of CO_2 under future ocean acidification. *PNAS*, 115(15) pages 3870–3875, 2018. DOI 10.1073/pnas.1703445115. 16, 22, 59, 181, 187
- ⁸² K. Wolfe, H.D. Nguyen, M. Davey, and M. Byrne. Characterizing biogeochemical fluctuations in a world of extremes: A synthesis for temperate intertidal habitats in the face of global change. *Glob Chang Biol*, 26(7) pages 3858–3879, 2020. DOI 10.1111/gcb.15103. 16, 22, 58, 110, 147, 187
- ⁸³ J.-P. Truchot. Problems of acid-base balance in rapidly changing intertidal environments. *Am Zool*, 28(1) pages 55–64, 1988. DOI 10.1093/icb/28.1.55. 16

- ⁸⁴ C.D. Santos, A.C. Miranda, J.P. Granadeiro, P.M. Lourenço, S. Saraiva, and J.M. Palmeirim. Effects of artificial illumination on the nocturnal foraging of waders. *Acta Oecologica*, 36(2) pages 166–172, 2010. DOI 10.1016/j.actao.2009.11.008. 16
- ⁸⁵ B.D. Özpolat, N. Randel, E.A. Williams, L.A. Bezares-Calderón, G. Andreatta, G. Balavoine, P.Y. Bertucci, D.E.K. Ferrier, M.C. Gambi, E. Gazave, et al. The nereid on the rise: Platynereis as a model system. *EvoDevo*, 12(1) pages 1–22, 2021. DOI 10.1186/s13227-021-00180-3. 16
- ⁸⁶ S. Morris and A.C. Taylor. Diurnal and seasonal variation in physico-chemical conditions within intertidal rock pools. *Estuar Coast Shelf Sci*, 17(3) pages 339–355, 1983. DOI 10.1016/0272-7714(83)90026-4. 16
- ⁸⁷ P. Landschützer, N. Gruber, D. C. E. Bakker, I. Stemmler, and K. D. Six. Strengthening seasonal marine CO₂ variations due to increasing atmospheric CO₂. *Nat Clim Chang*, 8(2) pages 146–150, 2018. DOI 10.1038/s41558-017-0057-x. 16, 181, 187
- ⁸⁸ M. A. Hahn, C. Effertz, L. Bigler, and E. von Elert. 5 α -cyprinol sulfate, a bile salt from fish, induces diel vertical migration in daphnia. *eLife*, v.8 page e44791, 2019. DOI 10.7554/eLife.44791. 20
- ⁸⁹ J.H. Cohen and R.B. Forward Jr. Ctenophore kairomones and modified aminosugar disaccharides alter the shadow response in a larval crab. *J Plankton Res*, 25(2) pages 203–213, 2003. DOI 10.1093/plankt/25.2.203. 20
- ⁹⁰ R.X. Poulin, S. Lavoie, K. Siegel, D.A. Gaul, M.J. Weissburg, and J. Kubanek. Chemical encoding of risk perception and predator detection among estuarine invertebrates. *PNAS*, 115(4) pages 662–667, 2018. DOI 10.1073/pnas.1713901115. 20, 57

- ⁹¹ R.T. Di Rocco, I. Imre, N.S. Johnson, and G.E. Brown. Behavioural response of adult sea lamprey (*Petromyzon marinus*) to predator and conspecific alarm cues: evidence of additive effects. *Hydrobiologia*, 767(1) pages 279–287, 2016. DOI 10.1007/s10750-015-2508-6. 21, 67
- ⁹² M.J. Siefkes. Use of physiological knowledge to control the invasive sea lamprey (*Petromyzon marinus*) in the laurentian great lakes. *Conservation Physiology*, 5(1), 2017. DOI 10.1093/conphys/cox031. 21
- ⁹³ T.A. Smith. Phenethylamine and related compounds in plants. *Phytochemistry*, 16(1) pages 9–18, 1977. DOI 10.1016/0031-9422(77)83004-5. 21, 23, 68
- ⁹⁴ M. Steiner and T. Hartmann. The occurrence and distribution of volatile amines in marine algae. *Planta*, 79(2) pages 113–121, 1968. DOI 10.1007/BF00390154. 21, 68
- ⁹⁵ A. Percot, A. Yalçın, V. Aysel, H. Erdugan, B. Dural, and K.C. Güven. β -phenylethylamine content in marine algae around turkish coasts. *Botanica Marina*, 52(1) pages 87–90, 2009. DOI 10.1515/BOT.2009.031. 21
- ⁹⁶ B.A. Hazlett. The behavioral ecology of hermit crabs. *Annu Rev Ecol System*, 12(1) pages 1–22, 1981. 21
- ⁹⁷ I. Lancaster. *Pagurus bernhardus* (l.) - an introduction to the natural history of hermit crabs. *Field Studies*, v.7 pages 189–238, 1988. 21, 23, 35, 68, 118
- ⁹⁸ M.E. Laidre and A.L. Greggor. Swarms of swift scavengers: ecological role of marine intertidal hermit crabs in california. *Mar Biol*, 162(5) pages 969–977, 2015. DOI 10.1007/s00227-015-2639-3. 21
- ⁹⁹ K. Ramsay, M.J. Kaiser, and R.N. Hughes. A field study of intraspecific competition for food in hermit crabs (*Pagurus bernhardus*). *Estuar Coast Shelf Sci*, 44(2) pages 213–220, 1997. DOI 10.1006/ecss.1996.0213. 21, 24, 62, 68

- ¹⁰⁰ F. Gherardi and J. Tiedemann. Chemical cues and binary individual recognition in the hermit crab *Pagurus longicarpus*. *Journal of Zoology*, 263(1) pages 23–29, 2004. DOI 10.1017/S0952836904004807. 21, 60
- ¹⁰¹ D. Rittschof and B.A. Hazlett. Behavioural responses of hermit crabs to shell cues, predator haemolymph and body odour. *J Mar Biolog Assoc UK*, 77(3) pages 737–751, 1997. DOI 10.1017/S002531540003616X. 21
- ¹⁰² K.L. de la Haye, J.I. Spicer, S. Widdicombe, and M. Briffa. Reduced pH sea water disrupts chemo-responsive behaviour in an intertidal crustacean. *J Exp Mar Biol Ecol*, v.412 pages 134–140, 2012. DOI 10.1016/j.jembe.2011.11.013. 21, 24, 62, 187
- ¹⁰³ F. Gherardi and E. Tricarico. Chemical ecology and social behavior of anomura. In T. Breithaupt and M. Thiel, editors, *Chemical communication in crustaceans*, pages 297–312. Springer, 2010. 21, 22
- ¹⁰⁴ E. Rosen, B. Schwarz, and A. R. Palmer. Smelling the difference: hermit crab responses to predatory and nonpredatory crabs. *Anim Behav*, 78(3) pages 691–695, 2009. DOI 10.1016/j.anbehav.2009.05.035. 22
- ¹⁰⁵ D.R. Lide, editor. *CRC Handbook of Chemistry and Physics*. CRC Press LLC, 81st edition edition, 2000. 23, 24, 55, 185, 188
- ¹⁰⁶ A. Marcobal, B. De Las Rivas, J.M. Landete, L. Tabera, and R. Munoz. Tyramine and phenylethylamine biosynthesis by food bacteria. *Crit Rev Food Sci Nutr*, 52(5) pages 448–467, 2012. DOI 10.1080/10408398.2010.500545. 23, 65, 68, 71
- ¹⁰⁷ T.D. Nickell and P.G. Moore. The behavioural ecology of epibenthic scavenging invertebrates in the clyde sea area: laboratory experiments on attractions to bait in moving water, underwater tv observation in situ and general conclusions. *J Exp Mar Bio Ecol*, 159(1) pages 15–35, 1992. DOI 10.1016/0022-0981(92)90255-9. 23, 61

- ¹⁰⁸ K.L. de la Haye, J.I. Spicer, S. Widdicombe, and M. Briffa. Reduced sea water pH disrupts resource assessment and decision making in the hermit crab *Pagurus bernhardus*. *Anim Behav*, 82(3) pages 495–501, 2011. DOI 10.1016/j.anbehav.2011.05.030. 24, 187
- ¹⁰⁹ I. Lancaster. Reproduction and life history strategy of the hermit crab *Pagurus bernhardus*. *J Mar Biol Ass UK*, 70(1) pages 129–142, 1990. DOI doi.org/10.1017/S0025315400034251. 27, 37, 52
- ¹¹⁰ R Core Team. *R: A Language and Environment for Statistical Computing*. R Foundation for Statistical Computing, Vienna, Austria, 2020. Online at <https://www.R-project.org/>. 37, 77, 164
- ¹¹¹ H. Wickham. *ggplot2: Elegant Graphics for Data Analysis*. Springer-Verlag New York, 2016. Online at <https://ggplot2.tidyverse.org>. 37, 77, 164
- ¹¹² D. Bates, M. Mächler, B. Bolker, and S. Walker. Fitting linear mixed-effects models using lme4. *J Stat Softw*, 67(1) pages 1–48, 2015. DOI 10.18637/jss.v067.i01. 37, 39, 77, 164
- ¹¹³ V.A. Brown. An introduction to linear mixed-effects modeling in r. *Adv Methods Pract Psychol Sci*, 4(1) page 2515245920960351, 2021. DOI 10.1177/2515245920960351. 38
- ¹¹⁴ X.A. Harrison, L. Donaldson, M.E. Correa-Cano, J. Evans, D.N. Fisher, C.E.D. Goodwin, B.S. Robinson, D.J. Hodgson, and R. Inger. A brief introduction to mixed effects modelling and multi-model inference in ecology. *PeerJ*, v.6 page e4794, 2018. DOI 10.7717/peerj.4794. 38
- ¹¹⁵ T. Hothorn, F. Bretz, and P. Westfall. Simultaneous inference in general parametric models. *Biom J*, 50(3) pages 346–363, 2008. 38

- ¹¹⁶ R. V. Lenth. *emmeans: Estimated Marginal Means, aka Least-Squares Means*, 2021. R package version 1.6.0, Online at <https://CRAN.R-project.org/package=emmeans>. 38
- ¹¹⁷ J.D. Forester. Plotting contours. Published under cc licence on <https://quantitative-ecology.blogspot.com/2008/03/plotting-contours.html>, 2008. 39, 77, 164
- ¹¹⁸ T. Therneau. *A Package for Survival Analysis in R. R package version 3.2-11*. Springer-Verlag New York, 2021. Online at <https://CRAN.R-project.org/package=survival>. 40
- ¹¹⁹ T. Therneau and P.M. Grambsch. *Modeling Survival Data: Extending the Cox Model*. Springer-Verlag New York, 2000. 40
- ¹²⁰ A. Kassambara, M. Kosinski, and P. Biecek. *survminer: Drawing Survival Curves using 'ggplot2'*, 2021. R package version 0.4.9, Online at <https://CRAN.R-project.org/package=survminer>. 40
- ¹²¹ B. Gray. *cmprsk: Subdistribution Analysis of Competing Risks*, 2020. R package version 2.2-10, Online at <https://CRAN.R-project.org/package=cmprsk>. 40
- ¹²² J. Landes, S.C. Engelhardt, and F. Pelletier. An introduction to event history analyses for ecologists. *Ecosphere*, 11(10) page e03238, 2020. DOI 10.1002/ecs2.3238. 40, 41
- ¹²³ V.S. Pankratz, M. De Andrade, and T.M. Therneau. Random-effects cox proportional hazards model: General variance components methods for time-to-event data. *Genet Epidemiol*, 28(2) pages 97–109, 2005. DOI 10.1002/gepi.20043. 40, 41
- ¹²⁴ T. Therneau. *coxme: Mixed Effects Cox Models*, 2020. R package version 2.2-16, Online at <https://CRAN.R-project.org/package=coxme>. 40

- ¹²⁵ P. Dalgaard. *Introductory statistics with R*. Springer, second edition edition, 2008. DOI 10.1007/978-0-387-79054-1. 41, 82
- ¹²⁶ J. Hu, C. Zhong, C. Ding, Q. Chi, A. Walz, P. Mombaerts, H. Matsunami, and M. Luo. Detection of near-atmospheric concentrations of CO₂ by an olfactory subsystem in the mouse. *Science*, 317(5840) pages 953–957, 2007. DOI 10.1126/science.1144233. 59
- ¹²⁷ J. Caprio, M. Shimohara, T. Marui, S. Harada, and S. Kiyohara. Marine teleost locates live prey through pH sensing. *Science*, 344(6188) pages 1154–1156, 2014. DOI 10.1126/science.12526. 59
- ¹²⁸ M. Yao, J. Rosenfeld, S. Attridge, S. Sidhu, V. Aksenov, and C.D. Rollo. The ancient chemistry of avoiding risks of predation and disease. *Evol Biol*, 36(3) pages 267–281, 2009. DOI 10.1007/s11692-009-9069-4. 60
- ¹²⁹ F. Gherardi and W.H. Daniels. Dominance hierarchies and status recognition in the crayfish *Procambarus acutus acutus*. *Can J Zool*, 81(7) pages 1269–1281, 2003. DOI 0.1139/Z03-107. 60, 63
- ¹³⁰ R.W. Elwood and A. Stewart. Reproduction in the littoral hermit crab *Pagurus bernhardus*. *Ir Nat' J*, 22(6) pages 252–255, 1987. 61
- ¹³¹ J. Piontek, M. Lunau, N. Händel, C. Borchard, M. Wurst, and A. Engel. Acidification increases microbial polysaccharide degradation in the ocean. *Biogeosciences*, 7(5) pages 1615–1624, 2010. DOI 10.5194/bg-7-1615-2010. 61
- ¹³² T. Breithaupt and P. Eger. Urine makes the difference: chemical communication in fighting crayfish made visible. *J Exp Biol*, 205(9) pages 1221–1231, 2002. DOI 10.1242/jeb.205.9.1221. 62, 70, 94, 95, 96, 184

- ¹³³ F. Gherardi and J. Tiedemann. Binary individual recognition in hermit crabs. *Behav Ecol Sociobiol*, 55(6) pages 524–530, 2004. DOI 10.1007/s00265-003-0734-9. 62, 63, 64
- ¹³⁴ M.L. Winston and S. Jacobson. Dominance and effects of strange conspecifics on aggressive interactions in the hermit crab *Pagurus longicarpus* (say). *Anim Behav*, v.26 pages 184–191, 1978. DOI 10.1016/0003-3472(78)90018-0. 62, 64
- ¹³⁵ M. Briffa and R.W. Elwood. Monoamines and decision making during contests in the hermit crab *Pagurus bernhardus*. *Anim Behav*, 73(4) pages 605–612, 2007. DOI 10.1016/j.anbehav.2006.06.008. 62, 156, 177
- ¹³⁶ R.A. Zulandt Schneider, R.W.S. Schneider, and P.A. Moore. Recognition of dominance status by chemoreception in the red swamp crayfish, *Procambarus clarkii*. *J Chem Ecol*, 25(4) pages 781–794, 1999. DOI 10.1023/A:1020888532513. 63, 65
- ¹³⁷ W.C. Allee, O. Park, A.E. Emerson, T. Park, and K.P. Schmidt. *Principles of animal ecology*. Number Edn 1. WB Saundere Co. Ltd., 1949. 63
- ¹³⁸ J. Herberholz. *Nervous Systems and Control of Behavior*, volume 3, chapter Neurobiology of social status in crustaceans, pages 457–483. Oxford University Press Oxford, 2014. 63
- ¹³⁹ C.J. Barnard and T. Burk. Dominance hierarchies and the evolution of individual recognition. *J theor Biol*, 81(1) pages 65–73, 1979. DOI 10.1016/0022-5193(79)90081-X. 63
- ¹⁴⁰ J.G. Boal. Absence of social recognition in laboratory-reared cuttlefish, *Sepia officinalis* l. (mollusca: Cephalopoda). *Anim Behav*, 52(3) pages 529–537, 1996. DOI 10.1006/anbe.1996.0195. 63

- ¹⁴¹ B.A. Hazlett. Individual recognition and agonistic behaviour in *Pagurus bernhardus*. *Nature*, 222(5190) pages 268–269, 1969. DOI 10.1038/222268a0. 63, 64
- ¹⁴² C. Karavanich and J. Atema. Individual recognition and memory in lobster dominance. *Anim Behav*, 56(6) pages 1553–1560, 1998. DOI 10.1006/anbe.1998.0914. 63
- ¹⁴³ B.A. Hazlett. Communicatory effect of body position in *Pagurus bernhardus* (L.) (Decapoda, Anomura). *Crustaceana*, pages 210–214, 1968. 64
- ¹⁴⁴ S. Doake, M. Scantlebury, and R.W. Elwood. The costs of bearing arms and armour in the hermit crab *Pagurus bernhardus*. *Anim Behav*, 80(4) pages 637–642, 2010. DOI 10.1016/j.anbehav.2010.06.023. 64
- ¹⁴⁵ C.R. Maestas-Olguin, M.M. Parish, and N.S. Pentkowski. Coyote urine, but not 2-phenylethylamine, induces a complete profile of unconditioned anti-predator defensive behaviors. *Physiol Behav*, v.229 page 113210, 2021. DOI 10.1016/j.physbeh.2020.113210. 67
- ¹⁴⁶ A. Villalobos, F. Schlyter, G. Birgersson, P. Koteja, and M. Löf. Fear effects on bank voles (rodentia: Arvicolinae): testing for repellent candidates from predator volatiles. *Pest Management Science*, 78(4) pages 1677–1685, 2022. DOI 0.1002/ps.6787. 67
- ¹⁴⁷ E.J. Jordbro, R.T. Di Rocco, I. Imre, N.S. Johnson, and G.E. Brown. White sucker *Catostomus commersonii* respond to conspecific and sea lamprey *Petromyzon marinus* alarm cues but not potential predator cues. *J Great Lakes Res*, 42(4) pages 849–853, 2016. DOI 10.1016/j.jglr.2016.04.003. 67
- ¹⁴⁸ N. Stratton, I. Imre, R. Di Rocco, and G. Brown. Effect of potential sea lamprey (*Petromyzon marinus*) repellents on the distribution of juvenile rainbow trout

- (*Oncorhynchus mykiss*) in a laboratory environment. *UTSC's Journal of Natural Sciences*, 2(1) pages 23–35, 2021. DOI 10.33137/jns.v2i1.34652. 67
- ¹⁴⁹ A. Arulkumar, S. Paramithiotis, and S. Paramasivam. Biogenic amines in fresh fish and fishery products and emerging control. *Aquaculture and Fisheries*, 8(4) pages 431–450, 2023. DOI 10.1016/j.aaf.2021.02.001. 68
- ¹⁵⁰ K.L. Van Alstyne, R.L. Ridgway, and T.A. Nelson. Neurotransmitters in marine and freshwater algae. In A. Ramakrishna and V.V. Roshchina, editors, *Neurotransmitters in Plants*, pages 35–54. CRC Press, 2019. DOI 10.1201/b22467-3. 68, 177, 180
- ¹⁵¹ A.M. Young and J.A. Elliott. Life history and population dynamics of green crabs (*Carcinus maenas*). *Fishes*, 5(1) page 4, 2019. DOI 10.3390/fishes5010004. 68, 69, 71, 76, 92
- ¹⁵² S. Lowe, M. Browne, S. Boudjelas, and M. De Poorter. *100 of the world's worst invasive alien species: a selection from the global invasive species database*, volume 12. Invasive Species Specialist Group Auckland, 2000. 68
- ¹⁵³ M.F. Glaessner. *Decapoda, Part R, Arthropoda 4*, chapter Treatise on Invertebrate Paleontology. Geological Society of America, 1969. 68, 92
- ¹⁵⁴ N. Fletcher and J.D. Hardege. The cost of conflict: agonistic encounters influence responses to chemical signals in the european shore crab. *Anim Behav*, 77(2) pages 357–361, 2009. DOI 10.1016/j.anbehav.2008.10.007. 69, 70
- ¹⁵⁵ D. Hayden, A. Jennings, C. Müller, D. Pascoe, R. Bublitz, H. Webb, T. Breithaupt, L. Watkins, and J. Hardege. Sex-specific mediation of foraging in the shore crab, *Carcinus maenas*. *Horm Behav*, 52(2) pages 162–168, 2007. DOI 10.1016/j.yhbeh.2007.03.004. 69

- ¹⁵⁶ J.D. Hardege, A. Jennings, D. Hayden, C.T. Müller, D. Pascoe, M.G. Bentley, and A.S. Clare. Novel behavioural assay and partial purification of a female-derived sex pheromone in *Carcinus maenas*. *Marine Ecology Progress Series*, v.244 pages 179–189, 2002. DOI 10.3354/meps244179. 69
- ¹⁵⁷ G.I. Van Der Meeren. Sex-and size-dependent mating tactics in a natural population of shore crabs *carcinus maenas*. *J Anim Ecol*, pages 307–314, 1994. DOI 10.2307/5549. 69
- ¹⁵⁸ R.G.J. Shelton and A.M. Mackie. Studies on the chemical preferences of the shore crab, *Carcinus maenas* (l.). *J Exp Mar Biol Ecol*, 7(1) pages 41–49, 1971. DOI 10.1016/0022-0981(71)90003-7. 69
- ¹⁵⁹ P.G. Lee and S.P. Meyers. Chemoattraction and feeding stimulation in crustaceans. *Aquac Nutr*, 2(3) pages 157–164, 1996. DOI 10.1111/j.1365-2095.1996.tb00055.x. 69, 92
- ¹⁶⁰ G.I. Sekkelsten. Effect of handicap on mating success in male shore crabs *Carcinus maenas*. *Oikos*, pages 131–134, 1988. DOI 10.2307/3565635. 70
- ¹⁶¹ L.U. Sneddon, F.A. Huntingford, and A.C. Taylor. The influence of resource value on the agonistic behaviour of the shore crab, *Carcinus maenas* (l.). *Mar Freshw Behav Physiol*, 30(4) pages 225–237, 1997. DOI 10.1080/10236249709379027. 70
- ¹⁶² L.U. Sneddon, F.A. Huntingford, and A.C. Taylor. Weapon size versus body size as a predictor of winning in fights between shore crabs, *Carcinus maenas* (l.). *Behav Ecol Sociobiol*, 41(4) pages 237–242, 1997. DOI 10.1007/s002650050384. 70, 92, 93, 94

- ¹⁶³ L.U. Sneddon, A.C. Taylor, F.A. Huntingford, and D.G. Watson. Agonistic behaviour and biogenic amines in shore crabs *Carcinus maenas*. *J Exp Biol*, 203(3) pages 537–545, 2000. DOI 10.1242/jeb.203.3.537. 70, 156, 177
- ¹⁶⁴ T. Breithaupt and J. Atema. The timing of chemical signaling with urine in dominance fights of male lobsters (*Homarus americanus*). *Behav Ecol Sociobiol*, 49(1) pages 67–78, 2000. DOI 10.1007/s002650000271. 70, 95
- ¹⁶⁵ S. Shabani, M. Kamio, and C.D. Derby. Spiny lobsters use urine-borne olfactory signaling and physical aggressive behaviors to influence social status of conspecifics. *J Exp Biol*, 212(15) pages 2464–2474, 2009. DOI 10.1242/jeb.026492. 70, 95, 184
- ¹⁶⁶ H.O. Wright. Visual displays in brachyuran crabs: field and laboratory studies. *American Zoologist*, 8(3) pages 655–665, 1968. DOI 10.1093/icb/8.3.655. 70, 73, 76
- ¹⁶⁷ M. Enquist and O Leimar. Evolution of fighting behaviour: decision rules and assessment of relative strength. *J Theor Biol*, 102(3) pages 387–410, 1983. DOI 10.1016/0022-5193(83)90376-4. 70
- ¹⁶⁸ J. Maynard Smith. *Evolution and the Theory of Games*. Cambridge university press, 1982. 70
- ¹⁶⁹ S. E. Riechert. Games spiders play. III: cues underlying context-associated changes in agonistic behaviour. *Anim Behav*, 32(1) pages 1–15, 1984. DOI 10.1016/S0003-3472(84)80318-8. 70
- ¹⁷⁰ B. Hazlett, D. Rubenstein, and D. Rittschof. Starvation, energy reserves, and aggression in the crayfish *Orconectes virilis* (hagen, 1870) (decapoda, cambaridae). *Crustaceana*, pages 11–16, 1975. 70
- ¹⁷¹ K.E. Thorpe. *Behavioural and physiological studies of Fighting in the velvet swimming crab, Necora puber (L.)*. PhD thesis, University of Glasgow, 1994. 70

- ¹⁷² M.G. Wheatly. The provision of oxygen to developing eggs by female shore crabs (*Carcinus maenas*). *J Mar Biol Assoc UK*, 61(1) pages 117–128, 1981. DOI 10.1017/S0025315400045951. 76
- ¹⁷³ K. Jensen. On the agonistic behaviour in *Carcinus maenas* (L.)(Decapoda). *Ophelia*, 10(1) pages 57–61, 1972. DOI 10.1080/00785326.1972.10430102. 77
- ¹⁷⁴ J. Clayden, N. Greeves, and S. Warren. *Organic chemistry*. Oxford university press, 2012. 88, 153
- ¹⁷⁵ A. McVean. The incidence of autotomy in *Carcinus maenas* (L.). *J Exp Mar Biol Ecol*, 24(2) pages 177–187, 1976. DOI 10.1016/0022-0981(76)90102-7. 91
- ¹⁷⁶ Magnus Enquist. Communication during aggressive interactions with particular reference to variation in choice of behaviour. *Animal Behaviour*, 33(4) pages 1152–1161, 1985. DOI 10.1016/S0003-3472(85)80175-5. 93, 95
- ¹⁷⁷ M. Enquist, E. Plane, and J. Röed. Aggressive communication in fulmars (*Fulmarus glacialis*) competing for food. *Anim Behav*, 33(3) pages 1007–1020, 1985. DOI 10.1016/S0003-3472(85)80035-X. 93, 95
- ¹⁷⁸ J.R. Waas. The risks and benefits of signalling aggressive motivation: a study of cave-dwelling little blue penguins. *Behav Ecol Sociobiol*, 29(2) pages 139–146, 1991. DOI 10.1007/BF00166489. 93
- ¹⁷⁹ I.P. Smith, F.A. Huntingford, R.J.A. Atkinson, and A.C. Taylor. Strategic decisions during agonistic behaviour in the velvet swimming crab, *Necora puber* (L.). *Anim Behav*, 47(4) pages 885–894, 1994. DOI 10.1006/anbe.1994.1120. 93
- ¹⁸⁰ M.J. How, J.M. Hemmi, J. Zeil, and R. Peters. Claw waving display changes with receiver distance in fiddler crabs, *Uca perplexa*. *Anim Behav*, 75(3) pages 1015–1022, 2008. DOI 10.1016/j.anbehav.2007.09.004. 95

- ¹⁸¹ H-Y.T. Yang and N.H. Neff. β -phenylethylamine: a specific substrate for type B monoamine oxidase of brain. *J Pharmacol Exp Ther*, 187(2) pages 365–371, 1973. 96
- ¹⁸² S.A. Dewhurst, S.G. Croker, K. Ikeda, and R.E. McCaman. Metabolism of biogenic amines in drosophila nervous tissue. *Comp Biochem Physiology B: Comp Biochem*, 43(4) pages 975–981, 1972. DOI 10.1016/0305-0491(72)90241-6. 96
- ¹⁸³ H. Verlinden, R. Vleugels, E. Marchal, L. Badisco, W. Pflüger, H.-J. and Blenau, and J. V. Broeck. The role of octopamine in locusts and other arthropods. *J Insect Physiol*, 56(8) pages 854–867, 2010. DOI 10.1016/j.jinsphys.2010.05.018. 96
- ¹⁸⁴ T. Roeder. Tyramine and octopamine: Ruling behavior. *Annu Rev Entomol*, v.50 pages 447–77, 2005. DOI 10.1146/annurev.ento.50.071803.130404. 96
- ¹⁸⁵ T.R.F. Wright. The genetics of biogenic amine metabolism, sclerotization, and melanization in *Drosophila melanogaster*. *Adv Genet*, v.24 pages 127–222, 1987. DOI 10.1016/S0065-2660(08)60008-5. 96
- ¹⁸⁶ B. D. Sloley. Metabolism of monoamines in invertebrates: the relative importance of monoamine oxidase in different phyla. *Neurotoxicology*, 25(1-2) pages 175–183, 2004. DOI 10.1016/S0161-813X(03)00096-2. 96
- ¹⁸⁷ S. Sentellas, Ó. Núñez, and J. Saurina. Recent advances in the determination of biogenic amines in food samples by (U)HPLC. *J Agric Food Chem*, 64(41) pages 7667–7678, 2016. DOI 10.1021/acs.jafc.6b02789. 97
- ¹⁸⁸ S. Hernández-Cassou and J. Saurina. Derivatization strategies for the determination of biogenic amines in wines by chromatographic and electrophoretic techniques. *J Chromatogr B*, 879(17-18) pages 1270–1281, 2011. DOI 10.1016/j.jchromb.2010.11.020. 97

- ¹⁸⁹ N. Ochi. Simultaneous determination of eight underivatized biogenic amines in salted mackerel fillet by ion-pair solid-phase extraction and volatile ion-pair reversed-phase liquid chromatography-tandem mass spectrometry. *J Chromatogr A*, v.1601 pages 115–120, 2019. DOI 10.1016/j.chroma.2019.06.027. 97
- ¹⁹⁰ C.C. Roggatz, M. Lorch, and D.M. Benoit. Influence of solvent representation on nuclear shielding calculations of protonation states of small biological molecules. *J Chem Theory Comput*, 14(5) pages 2684–2695, 2018. DOI 10.1021/acs.jctc.7b01020. 99, 111, 112, 130, 147
- ¹⁹¹ R. Puthenveetil and O. Vinogradova. Solution nmr: A powerful tool for structural and functional studies of membrane proteins in reconstituted environments. *J Biol Chem*, 294(44) pages 15914–15931, 2019. DOI 10.1074/jbc.REV119.009178. 99
- ¹⁹² F. Jensen. *Introduction to computational chemistry*. John wiley & sons, 2007. 99, 103, 104
- ¹⁹³ Z-H. Chen, Y-W. Guo, and X-W. Li. Recent advances on marine mollusk-derived natural products: chemistry, chemical ecology and therapeutical potential. *Nat Prod Rep*, 40(3) pages 509–556, 2023. DOI 10.1039/D2NP00021K. 99
- ¹⁹⁴ B. Khatri Chhetri, S. Lavoie, A. M. Sweeney-Jones, N. Mojib, V. Raghavan, K. Gagaring, B. Dale, C. W. McNamara, K. Soapi, C. L. Quave, et al. Peyssonosides A–B, unusual diterpene glycosides with a sterically encumbered cyclopropane motif: structure elucidation using an integrated spectroscopic and computational workflow. *J Org Chem*, 84(13) pages 8531–8541, 2019. DOI 10.1021/acs.joc.9b00884. 99
- ¹⁹⁵ M. Born. Physical aspects of quantum mechanics. *Nature*, 119(2992) pages 354–357, 1927. DOI 10.1038/119354a0. 100

- ¹⁹⁶ M. Born. Zur Quantenmechanik der Stoßvorgänge [on the quantum mechanics of collisions]. *Zeitschrift für Physik*, pages 803–827, 1926. DOI 10.1007/BF01397184. 100
- ¹⁹⁷ E. Schrödinger. An undulatory theory of the mechanics of atoms and molecules. *Physical review*, 28(6) page 1049, 1926. DOI 10.1103/PhysRev.28.1049. 100
- ¹⁹⁸ J. Harvey. *Computational chemistry*. Oxford Chemistry Primers, 2018. 100, 101, 102, 103
- ¹⁹⁹ M. Born and R. Oppenheimer. Zur Quantentheorie der Molekeln [on the quantum theory of molecules], 1927. DOI 10.1002/andp.19273892002. 101
- ²⁰⁰ P.A.M. Dirac. Quantum mechanics of many-electron systems. *Proceedings of the Royal Society of London. Series A, Containing Papers of a Mathematical and Physical Character*, 123(792) pages 714–733, 1929. DOI 10.1098/rspa.1929.0094. 101
- ²⁰¹ P.A.M. Dirac. The quantum theory of the electron. *Proceedings of the Royal Society of London. Series A, Containing Papers of a Mathematical and Physical Character*, 117(778) pages 610–624, 1928. DOI 10.1098/rspa.1928.0023. 101
- ²⁰² R.A. Friesner. *Ab initio* quantum chemistry: Methodology and applications. *PNAS*, 102(19) pages 6648–6653, 2005. DOI 10.1073/pnas.0408036102. 101
- ²⁰³ P. Hohenberg and W. Kohn. Inhomogeneous electron gas. *Phys rev*, 136(3B) page B864, 1964. DOI 10.1103/PhysRev.136.B864. 102
- ²⁰⁴ W. Kohn and L.J. Sham. Self-consistent equations including exchange and correlation effects. *Phys rev*, 140(4A) page A1133, 1965. DOI 10.1103/PhysRev.140.A1133. 102
- ²⁰⁵ A.J. Cohen, P. Mori-Sánchez, and W. Yang. Challenges for density functional theory. *Chemical reviews*, 112(1) pages 289–320, 2012. DOI 10.1021/cr200107z. 102

- ²⁰⁶ F. Jensen. Polarization consistent basis sets: principles. *J Chem Phys*, v.115 pages 9113–9125, 2001. DOI 10.1063/1.1413524. 102, 112, 120, 160
- ²⁰⁷ F. Jensen. Polarization consistent basis sets. II. estimating the Kohn-Sham basis set limit. *J Chem Phys*, v.116 pages 7372–7379, 2002. DOI 10.1063/1.1465405. 102, 112, 120, 160
- ²⁰⁸ F. Jensen. Polarization consistent basis sets. III. the importance of diffuse functions. *J Chem Phys*, v.117 pages 9234–9240, 2002. DOI 10.1063/1.1515484. 102, 112, 120, 160
- ²⁰⁹ J. VandeVondele and J. Hutter. Gaussian basis sets for accurate calculations on molecular systems in gas and condensed phases. *J Chem Phys*, 127(11) page 114105, 2007. DOI 10.1063/1.2770708. 102, 115, 116, 117, 120
- ²¹⁰ J.P. Perdew, K. Burke, and M. Ernzerhof. Generalized gradient approximation made simple. *Phys Rev Lett*, 77(18) page 3865, 1996. DOI 10.1103/PhysRevLett.77.3865. 103, 115, 116, 117, 120
- ²¹¹ C. Adamo and V. Barone. Toward reliable density functional methods without adjustable parameters: The PBE0 model. *J Chem Phys*, 110(13) pages 6158–6170, 1999. DOI 10.1063/1.478522. 103, 112, 120, 160
- ²¹² F. Neese. The ORCA program system. *WIREs Comput Mol Sci*, 2(1) pages 73–78, 2012. DOI 10.1002/wcms.81. 104, 112, 119, 160
- ²¹³ F. Neese. Software update: the orca program system, version 4.0. *WIREs Comput Mol Sci*, 8(1) page e1327, 2018. DOI 10.1002/wcms.1327. 104, 112, 119, 160
- ²¹⁴ M.W. Schmidt, K.K. Baldridge, J.A. Boatz, S.T. Elbert, M.S. Gordon, J.H. Jensen, S. Koseki, N. Matsunaga, K.A. Nguyen, and S. Su. General atomic and molecular

- electronic structure system. *J Comput Chem*, 14(11) pages 1347–1363, 1993. DOI 10.1002/jcc.540141112. 104, 112
- ²¹⁵ J. Hutter, M. Iannuzzi, F. Schiffmann, and J. VandeVondele. cp2k: atomistic simulations of condensed matter systems. *WIREs Comput Mol Sci*, 4(1) pages 15–25, 2014. DOI 10.1002/wcms.1159. 104, 115
- ²¹⁶ P. D. Godfrey, L. D. Hatherley, and R. D. Brown. The shapes of neurotransmitters by millimeter-wave spectroscopy: 2-phenylethylamine. *J Am Chem Soc*, 117(31) pages 8204–8210, 1995. DOI 10.1021/ja00136a019. 105, 106
- ²¹⁷ J.C. López, V. Cortijo, S. Blanco, and J.L. Alonso. Conformational study of 2-phenylethylamine by molecular-beam fourier transform microwave spectroscopy. *Phys Chem Chem Phys*, 9(32) pages 4521–4527, 2007. DOI 10.1039/B705614A. 106
- ²¹⁸ A. Bouchet, M. Schütz, B. Chiavarino, M.E. Crestoni, S. Fornarini, and O. Dopfer. IR spectrum of the protonated neurotransmitter 2-phenylethylamine: dispersion and anharmonicity of the NH_3^+ - π interaction. *Phys Chem Chem Phys*, 17(39) pages 25742–25754, 2015. DOI 10.1039/C5CP00221D. 106, 148
- ²¹⁹ B. Chiavarino, M.E. Crestoni, M. Schütz, A. Bouchet, S. Piccirillo, V. Steinmetz, O. Dopfer, and S. Fornarini. Cation- π interactions in protonated phenylalkylamines. *J Phys Chem A*, 118(34) pages 7130–7138, 2014. DOI 10.1021/jp505037n. 106
- ²²⁰ J.A. Dickinson, M.R. Hockridge, R.T. Kroemer, E.G. Robertson, J.P. Simons, J. McCombie, and M. Walker. Conformational choice, hydrogen bonding, and rotation of the $s_1 \leftarrow s_0$ electronic transition moment in 2-phenylethyl alcohol, 2-phenylethylamine, and their water clusters. *J Am Chem Soc*, 120(11) pages 2622–2632, 1998. DOI 10.1021/ja972104o. 106

- ²²¹ M.R. Hockridge and E.G. Robertson. Hydrated clusters of 2-phenylethyl alcohol and 2-phenylethylamine: Structure, bonding, and rotation of the $s_1 \leftarrow s_0$ electronic transition moment. *J Phys Chem A*, pages 3618–3628, 1999. DOI 10.1021/jp9900077. 106
- ²²² S. Melandri, A. Maris, B.M. Giuliano, L.B. Favero, and W. Caminati. The free jet microwave spectrum of 2-phenylethylamine-water. *Phys Chem Chem Phys*, 12(35) page 10210, 2010. DOI 10.1039/c003513k. 106, 144
- ²²³ A. Bouchet, M. Schütz, and O. Dopfer. Competing insertion and external binding motifs in hydrated neurotransmitters: Infrared spectra of protonated phenylethylamine monohydrate. *Chem Phys Chem*, 17(2) pages 232–243, 2016. DOI 10.1002/cphc.201500939. 106, 147, 148
- ²²⁴ Miroslav M Ristić, Milena Petković, Branislav Milovanović, Jelena Belić, and Mihajlo Etinski. New hybrid cluster-continuum model for pka values calculations: Case study of neurotransmitters' amino group acidity. *Chemical Physics*, v.516 pages 55–62, 2019. DOI 10.1016/j.chemphys.2018.08.022. 106, 110, 143
- ²²⁵ E. Hallberg and M. Skog. Chemosensory sensilla in crustaceans. In T. Breithaupt and M. Thiel, editors, *Chemical communication in crustaceans*, pages 103–121. 2010. DOI 10.1007/978-0-387-77101-4_6. 106, 107
- ²²⁶ M.T. Kozma, M. Schmidt, H. Ngo-Vu, S.D. Sparks, A. Senatore, and C.D. Derby. Chemoreceptor proteins in the caribbean spiny lobster, *Panulirus argus*: expression of ionotropic receptors, gustatory receptors, and trp channels in two chemosensory organs and brain. *PloS one*, 13(9) page e0203935, 2018. DOI 10.1371/journal.pone.0203935. 107

- ²²⁷ M.T. Kozma, H. Ngo-Vu, Y.Y. Wong, N.S. Shukla, S.D. Pawar, A. Senatore, M. Schmidt, and C.D. Derby. Comparison of transcriptomes from two chemosensory organs in four decapod crustaceans reveals hundreds of candidate chemoreceptor proteins. *PLoS one*, 15(3) page e0230266, 2020. DOI 10.1371/journal.pone.0230266. 107
- ²²⁸ R.E. Roberts, C.A. Motti, K.W. Baughman, N. Satoh, M.R. Hall, and S.F. Cummins. Identification of putative olfactory g-protein coupled receptors in crown-of-thorns starfish, *Acanthaster planci*. *BMC genomics*, 18(1) pages 1–15, 2017. DOI 10.1186/s12864-017-3793-4. 107
- ²²⁹ C.B. Albertin, O. Simakov, T. Mitros, Z.Y. Wang, J.R. Pungor, E. Edsinger-Gonzales, S. Brenner, C.W. Ragsdale, and D.S. Rokhsar. The octopus genome and the evolution of cephalopod neural and morphological novelties. *Nature*, 524(7564) pages 220–224, 2015. DOI 10.1038/nature14668. 107
- ²³⁰ S.F. Cummins, D. Erpenbeck, Z. Zou, C. Claudianos, L.L. Moroz, G.T. Nagle, and B.M. Degnan. Candidate chemoreceptor subfamilies differentially expressed in the chemosensory organs of the mollusc *Aplysia*. *BMC biology*, 7(1) pages 1–20, 2009. DOI 10.1186/1741-7007-7-28. 107
- ²³¹ S. D. Liberles. Trace amine-associated receptors: ligands, neural circuits, and behaviors. *Curr Opin Neurobiol*, v.34 pages 1–7, 2015. DOI 10.1016/j.conb.2015.01.001. 107, 108
- ²³² E. Cichero, S. Espinoza, R.R. Gainetdinov, L. Brasili, and P. Fossa. Insights into the structure and pharmacology of the human trace amine-associated receptor 1 (*hTAAR1*): Homology modelling and docking studies. *Chem Biol Drug Des*, 81(4) pages 509–516, 2013. DOI 10.1111/cbdd.12018. 108, 109, 114, 115, 145

- ²³³ D.E. Leckband, J.N. Israelachvili, F.J. Schmitt, and W. Knoll. Long-range attraction and molecular rearrangements in receptor-ligand interactions. *Science*, 255(5050) pages 1419–1421, 1992. DOI 10.1126/science.1542789. 108
- ²³⁴ T.R. Gilbert, R.V. Kirss, N. Foster, and G. Davies. *Chemistry: The science in context*. WW Norton & Company, 2013. 108, 111, 127
- ²³⁵ Z. Radić, P.D. Kirchhoff, D.M. Quinn, J.A. McCammon, and P. Taylor. Electrostatic influence on the kinetics of ligand binding to acetylcholinesterase distinctions between active center ligands and fasciculin. *J Biol Chem*, 272(37) pages 23265–23277, 1997. DOI 10.1074/jbc.272.37.23265. 108, 145, 146
- ²³⁶ S. Pahari, L. Sun, and E. Alexov. PKAD: a database of experimentally measured pK_a values of ionizable groups in proteins. *Database*, 2019. DOI 10.1093/database/baz024. 108, 109, 110, 146
- ²³⁷ C.N. Schutz and A. Warshel. What are the dielectric "constants" of proteins and how to validate electrostatic models? *Proteins*, 44(4) pages 400–417, 2001. DOI 10.1002/prot.1106. 108, 109, 110
- ²³⁸ V. Barone and M. Cossi. Quantum calculation of molecular energies and energy gradients in solution by a conductor solvent model. *J Phys Chem A*, 102(11) pages 1995–2001, 1998. DOI 10.1021/jp9716997. 112, 118, 160
- ²³⁹ M. Cossi, N. Rega, G. Scalmani, and V. Barone. Energies, structures, and electronic properties of molecules in solution with the C-PCM solvation model. *J Comput Chem*, 24(6) pages 669–681, 2003. DOI 10.1002/jcc.10189. 112, 118, 160
- ²⁴⁰ S. Grimme, J. Antony, S. Ehrlich, and H. Krieg. A consistent and accurate ab initio parametrization of density functional dispersion correction (DFT-D) for the 94

- elements H-Pu. *J Chem Phys*, 132(15) page 154104, 2010. DOI 10.1063/1.3382344. 112, 115, 116, 117, 120, 160
- ²⁴¹ S. Grimme, S. Ehrlich, and L. Goerigk. Effect of the damping function in dispersion corrected density functional theory. *J Comput Chem*, 32(7) pages 1456–1465, 2011. DOI 10.1002/jcc.21759. 112, 115, 116, 117, 120, 160
- ²⁴² F. Neese, F. Wennmohs, A. Hansen, and U. Becker. Efficient, approximate and parallel hartree-fock and hybrid dft calculations. a “chain-of-spheres” algorithm for the hartree-fock exchange. *Chem Phys*, 356(1-3) pages 98–109, 2009. DOI 10.1016/j.chemphys.2008.10.036. 112, 120
- ²⁴³ F. Weigend. Accurate coulomb-fitting basis sets for H to Rn. *Phys Chem Chem Phys*, 8(9) pages 1057–1065, 2006. DOI 10.1039/B515623H. 112, 120, 160
- ²⁴⁴ B.M. Bode and M.S. Gordon. Macmolplt: a graphical user interface for gamess. *J Mol Graph Model*, 16(3) pages 133–138, 1998. DOI 10.1016/S1093-3263(99)00002-9. 112
- ²⁴⁵ W. Kutzelnigg, U. Fleischer, and M. Schindler. The IGLO-method: ab-initio calculation and interpretation of NMR chemical shifts and magnetic susceptibilities. In *Deuterium and shift calculation*, pages 165–262. Springer, 1990. 113
- ²⁴⁶ G. Pándy-Szekeres, C. Munk, T.M. Tsonkov, S. Mordalski, K. Harpsøe, A.S. Hauser, A.J. Bojarski, and D.E. Gloriam. GPCRdb in 2018: adding GPCR structure models and ligands. *Nucleic Acids Res*, 46(D1) pages D440–D446, 2018. DOI 10.1093/nar/gkx1109. 114, 115
- ²⁴⁷ W. Humphrey, A. Dalke, and K. Schulten. VMD – Visual Molecular Dynamics. *J Mol Graph*, v.14 pages 33–38, 1996. DOI 10.1016/0263-7855(96)00018-5. 114, 115

- ²⁴⁸ D. Hanwell, M. D.E. Curtis, D.C. Lonie, T. Vandermeersch, E. Zurek, and G.R. Hutchison. Avogadro: An advanced semantic chemical editor, visualization, and analysis platform. *J Cheminform*, 4(1) page 17, 2012. DOI 10.1186/1758-2946-4-17. 114, 115, 117
- ²⁴⁹ D.W. Zhang and J.Z.H. Zhang. Molecular fractionation with conjugate caps for full quantum mechanical calculation of protein–molecule interaction energy. *J Chem Phys*, 119(7) pages 3599–3605, 2003. DOI 10.1063/1.1591727. 114
- ²⁵⁰ A.K. Rappé, C.J. Casewit, K.S. Colwell, W.A. Goddard III, and W.M. Skiff. UFF, a full periodic table force field for molecular mechanics and molecular dynamics simulations. *J Am Chem Soc*, 114(25) pages 10024–10035, 1992. DOI 10.1021/ja00051a040. 115
- ²⁵¹ M. Krack. Pseudopotentials for H to Kr optimized for gradient-corrected exchange-correlation functionals. *Theor Chem Acc*, 114(1-3) pages 145–152, 2005. DOI 0.1007/s00214-005-0655-y. 115, 116, 117, 120
- ²⁵² J. VandeVondele, M. Krack, F. Mohamed, M. Parrinello, T. Chassaing, and J. Hutter. Quickstep: Fast and accurate density functional calculations using a mixed gaussian and plane waves approach. *Comput Phys Commun*, 167(2) pages 103–128, 2005. DOI 10.1016/j.cpc.2004.12.014. 115
- ²⁵³ M.W. Wong, M.J. Frisch, and K.B. Wiberg. Solvent effects. 1. the mediation of electrostatic effects by solvents. *J Am Chem Soc*, 113(13) pages 4776–4782, 1991. DOI 10.1021/ja00013a010. 116
- ²⁵⁴ P.E.M. Siegbahn and F. Himo. Recent developments of the quantum chemical cluster approach for modeling enzyme reactions. *J Biol Inorg Chem*, 14(5) pages 643–651, 2009. DOI 10.1007/s00775-009-0511-y. 116, 118

- ²⁵⁵ P.E. Blöchl. Electrostatic decoupling of periodic images of plane-wave-expanded densities and derived atomic point charges. *J Chem Phys*, 103(17) pages 7422–7428, 1995. DOI 10.1063/1.470314. 116, 117
- ²⁵⁶ G.J. Martyna and M.E. Tuckerman. A reciprocal space based method for treating long range interactions in ab initio and force-field-based calculations in clusters. *J Chem Phys*, 110(6) pages 2810–2821, 1999. DOI 10.1063/1.477923. 116, 117
- ²⁵⁷ P.G. Francoeur, T. Masuda, J. Sunseri, A. Jia, R.B. Iovanisci, I. Snyder, and D.R. Koes. Three-dimensional convolutional neural networks and a cross-docked data set for structure-based drug design. *J Chem Inf Model*, 60(9) pages 4200–4215, 2020. DOI 10.1021/acs.jcim.0c00411. 116
- ²⁵⁸ S.E. Braslavsky. Glossary of terms used in photochemistry, (IUPAC recommendations 2006). *Pure Appl Chem*, 79(3) pages 293–465, 2007. DOI 10.1351/pac200779030293. 118
- ²⁵⁹ Frank Neese et al. Orca. *An ab initio, density functional and semiempirical program package version, v.2* page 19, 2009. 118
- ²⁶⁰ L. Klein and C Swift. An improved model for the dielectric constant of sea water at microwave frequencies. *IEEE Trans Antennas Propag*, 25(1) pages 104–111, 1977. DOI 10.1109/TAP.1977.1141539. 118, 119
- ²⁶¹ World sea temperature. World sea temperatures based on daily satellite readings provided by the NOAA. seatemperature.org/europe/united-kingdom, 2020. accessed 10-02-2021. 118
- ²⁶² E Ross and D Behringer. Changes in temperature, pH, and salinity affect the sheltering responses of caribbean spiny lobsters to chemosensory cues. *Sci Rep*, 9(1) pages 1–11, 2019. DOI 10.1038/s41598-019-40832-y. 119

- ²⁶³ C. A. Fitch, D. A. Karp, K. K. Lee, W. E. Stites, E. E. Lattman, and E. B. García-Moreno. Experimental pK_a values of buried residues: Analysis with continuum methods and role of water penetration. *Biophys J*, 82(6) pages 3289–3304, 2002. DOI 10.1016/S0006-3495(02)75670-1. 120
- ²⁶⁴ J. B. Hasted, D. M. Ritson, and C. H. Collie. Dielectric properties of aqueous ionic solutions. parts i and ii. *J Chem Phys*, 16(1) pages 1–21, 1948. DOI 10.1063/1.174664516. 120
- ²⁶⁵ H.-J. Böhm, S. Brode, U. Hesse, and G. Klebe. Oxygen and nitrogen in competitive situations: Which is the hydrogen-bond acceptor? *Chem Eur J*, 2(12) pages 1509–1513, 1996. DOI 10.1002/chem.19960021206. 124
- ²⁶⁶ K.N. Houk and F. Liu. Holy grails for computational organic chemistry and biochemistry. *Acc Chem Res*, 50(3) pages 539–543, 2017. DOI 10.1021/acs.accounts.6b00532. 125, 148, 169
- ²⁶⁷ D.A. McQuarrie. *Statistical Mechanics*. University Science Books, 2000. 126
- ²⁶⁸ National Centers for Environmental Information NOAA. State of the climate: Monthly global climate report for annual 2021. <https://www.ncei.noaa.gov/access/monitoring/monthly-report/global/202113>, 2022. accessed 26-07-2022. 126, 188
- ²⁶⁹ A. Frank, I. Onila, H.M. Möller, and T.E. Exner. Toward the quantum chemical calculation of nuclear magnetic resonance chemical shifts of proteins. *Proteins*, 79(7) pages 2189–2202, 2011. DOI 10.1002/prot.23041. 128
- ²⁷⁰ P.G. De Benedetti. Protonation states and conformational ensemble in ligand-based qsar modeling. *Curr Pharm Des*, 19(23) pages 4323–4329, 2013. DOI 10.2174/1381612811319230014. 145

- ²⁷¹ H.-J. Böhm and G. Klebe. What can we learn from molecular recognition in protein–ligand complexes for the design of new drugs? *Angew Chem*, 35(22) pages 2588–2614, 1996. DOI 10.1002/anie.199625881. 145
- ²⁷² John A Thoma and DE Koshland Jr. Competitive inhibition by substrate during enzyme action. evidence for the induced-fit theory. *Journal of the American Chemical Society*, 82(13) pages 3329–3333, 1960. DOI 10.1021/ja01498a025. 145
- ²⁷³ J.A. Yankeelov Jr and D.E. Koshland Jr. Evidence for conformation changes induced by substrates of phosphoglucomutase. *Journal of Biological Chemistry*, 240(4) pages 1593–1602, 1965. DOI 10.1016/S0021-9258(18)97476-4. 145
- ²⁷⁴ S.A. Andujar, R.D. Tosso, F.D. Suvire, E. Angelina, N. Peruchena, N. Cabedo, D. Cortes, and R.D. Enriz. Searching the “biologically relevant” conformation of dopamine: a computational approach. *J Chem Inf Model*, 52(1) pages 99–112, 2011. DOI 10.1021/ci2004225. 145, 152, 178, 179
- ²⁷⁵ U.M. D’Souza and P.G. Strange. pH dependence of ligand binding to d₂ dopamine receptors. *Biochemistry*, 34(41) pages 13635–13641, 1995. DOI 10.1021/bi00041a044. 146
- ²⁷⁶ E. Alexov, E.L. Mehler, N. Baker, A.M. Baptista, Y. Huang, F. Milletti, J.E. Nielsen, D. Farrell, T. Carstensen, M.H.M. Olsson, et al. Progress in the prediction of pKa values in proteins. *Proteins*, 79(12) pages 3260–3275, 2011. DOI 10.1002/prot.23189. 146
- ²⁷⁷ S. Pahari, L. Sun, S. Basu, and E. Alexov. DelPhiPKa: Including salt in the calculations and enabling polar residues to titrate. *Proteins*, 86(12) pages 1277–1283, 2018. DOI 10.1002/prot.25608. 146

- ²⁷⁸ B. Srinivasan. A guide to enzyme kinetics in early drug discovery. *The FEBS Journal*, 2022. DOI 10.1111/febs.16404. 150
- ²⁷⁹ N. Nikolova and J. Jaworska. Approaches to measure chemical similarity—a review. *QSAR & Combinatorial Science*, 22(9-10) pages 1006–1026, 2003. DOI 10.1002/qsar.200330831. 151
- ²⁸⁰ R.P. Sheridan. The most common chemical replacements in drug-like compounds. *J Chem Inf Comput Sci*, 42(1) pages 103–108, 2002. DOI 10.1021/ci0100806. 151
- ²⁸¹ R.P. Sheridan. Finding multiactivity substructures by mining databases of drug-like compounds. *J Chem Inf Comput Sci*, 43(3) pages 1037–1050, 2003. DOI 10.1021/ci030004y. 151
- ²⁸² V.J. Gillet, D.J. Wild, P. Willett, and J. Bradshaw. Similarity and dissimilarity methods for processing chemical structure databases. *Comput J*, 41(8) pages 547–558, 1998. DOI 10.1093/comjnl/41.8.547. 151, 152, 182
- ²⁸³ J. Bajorath. Virtual screening in drug discovery: Methods, expectations and reality. *Curr Drug Discov*, v.2 pages 24–28, 2002. 151
- ²⁸⁴ R.R. Gainetdinov, M.C. Hoener, and M.D. Berry. Trace amines and their receptors. *Pharmacol Rev*, 70(3) pages 549–620, 2018. DOI 10.1124/pr.117.015305. 152, 177
- ²⁸⁵ S.K. Callear, A. Johnston, S.E. McLain, and S. Imberti. Conformation and interactions of dopamine hydrochloride in solution. *J Chem Phys*, 142(1) page 01B601_1, 2015. DOI 10.1063/1.4904291. 152
- ²⁸⁶ R.D. Tosso, O. Parravicini, M.N.C. Zarycz, E. Angelina, M. Vettorazzi, N. Peruchena, S. Andujar, and R.D. Enriz. Conformational and electronic study of dopamine interacting with the D2 dopamine receptor. *J Comput Chem*, 41(21) pages 1898–1911, 2020. DOI 10.1002/jcc.26361. 152, 178

- ²⁸⁷ P.I. Nagy, G. Alagona, and C. Ghio. Theoretical studies on the conformation of protonated dopamine in the gas phase and in aqueous solution. *Journal of the American Chemical Society*, 121(20) pages 4804–4815, 1999. DOI 10.1021/ja981528v. 152
- ²⁸⁸ T. Ishimitsu, S. Hirose, and H. Sakurai. Microscopic acid dissociation constants of 3, 4-dihydroxyphenethylamine (dopamine). *Chemical and Pharmaceutical Bulletin*, 26(1) pages 74–78, 1978. DOI 10.1248/cpb.26.74. 153, 154, 165, 166, 188
- ²⁸⁹ A.E. Sanchez-Rivera, S. Corona-Avendano, G. Alarcon-Angeles, A. Rojas-Hernández, M.T. Ramirez-Silva, and M.A. Romero-Romo. Spectrophotometric study on the stability of dopamine and the determination of its acidity constants. *Spectrochimica Acta Part A: Molecular and Biomolecular Spectroscopy*, 59(13) pages 3193–3203, 2003. DOI 10.1016/S1386-1425(03)00138-0. 153, 165, 166, 188
- ²⁹⁰ P.I. Nagy, G. Völgyi, and K. Takács-Novák. Tautomeric and conformational equilibria of tyramine and dopamine in aqueous solution. *Mol Phys*, 103(11-12) pages 1589–1601, 2005. DOI 10.1080/00268970500075370. 153, 188
- ²⁹¹ S. Corona-Avendano, G. Alarcon-Angeles, G.A. Rosquete-Pina, A. Rojas-Hernandez, A. Gutierrez, M.T. Ramírez-Silva, M. Romero-Romo, and M. Palomar-Pardave. New insights on the nature of the chemical species involved during the process of dopamine deprotonation in aqueous solution: theoretical and experimental study. *The Journal of Physical Chemistry B*, 111(7) pages 1640–1647, 2007. DOI 10.1021/jp0637227. 153
- ²⁹² A.H Stokes, T.G. Hastings, and K.E. Vrana. Cytotoxic and genotoxic potential of dopamine. *J Neurosci Res*, 55(6) pages 659–665, 1999. DOI 10.1002/(SICI)1097-4547(19990315)55:6<659::AID-JNR1>3.0.CO;2-C. 154, 155, 179

- ²⁹³ K.L. Van Alstyne, K.J. Anderson, A.K. Winans, and S.-A. Gifford. Dopamine release by the green alga *Ulvaria obscura* after simulated immersion by incoming tides. *Mar Biol*, 158(9) pages 2087–2094, 2011. DOI 10.1007/s00227-011-1716-5. 154, 180, 186
- ²⁹⁴ N. Umek, B. Geršak, N. Vintar, M. Šoštarič, and J. Mavri. Dopamine autoxidation is controlled by acidic pH. *Front Mol Neurosci*, page 467, 2018. DOI 10.3389/fnmol.2018.00467. 154, 171, 172, 179
- ²⁹⁵ J. Yang, M.A.C. Stuart, and M. Kamperman. Jack of all trades: versatile catechol crosslinking mechanisms. *Chem Soc Rev*, 43(24) pages 8271–8298, 2014. DOI 10.1039/c4cs00185k. 155, 171, 172, 179, 180
- ²⁹⁶ C. Iuga, J.R. Alvarez-Idaboy, and A. Vivier-Bunge. Ros initiated oxidation of dopamine under oxidative stress conditions in aqueous and lipidic environments. *J Phys Chem B*, 115(42) pages 12234–12246, 2011. DOI 10.1021/jp206347u. 155
- ²⁹⁷ A.J. Tierney, T. Kim, and R. Abrams. Dopamine in crayfish and other crustaceans: distribution in the central nervous system and physiological functions. *Microsc Res Tech*, 60(3) pages 325–335, 2003. DOI 10.1002/jemt.10271. 156
- ²⁹⁸ R.W. Elwood, K.E. Wood, M.B. Gallagher, and J.T.A. Dick. Probing motivational state during agonistic encounters in animals. *Nature*, 393(6680) pages 66–68, 1998. DOI 10.1038/29980. 156
- ²⁹⁹ X.-Z. Yang, Y.-Y. Pang, G.-Y. Huang, M.-J. Xu, C. Zhang, L. He, J.-H. Lv, Y.-M. Song, X.-Z. Song, and Y.-X Cheng. The serotonin or dopamine by cyclic adenosine monophosphate-protein kinase a pathway involved in the agonistic behaviour of chinese mitten crab, *Eriocheir sinensis*. *Physiol Behav*, v.209 page 112621, 2019. DOI 10.1016/j.physbeh.2019.112621. 156, 177

- ³⁰⁰ Y. Momohara, H. Minami, A. Kanai, and T. Nagayama. Role of cAMP signalling in winner and loser effects in crayfish agonistic encounters. *Eur J Neurosci*, 44(2) pages 1886–1895, 2016. DOI 10.1111/ejn.13259. 157
- ³⁰¹ D.E. Wood and C.D. Derby. Distribution of dopamine-like immunoreactivity suggests a role for dopamine in the courtship display behavior of the blue crab, *Callinectes sapidus*. *Cell Tissue Res*, 285(2) pages 321–330, 1996. DOI 10.1007/s004410050649. 157, 182
- ³⁰² R. Huber and A. Delago. Serotonin alters decisions to withdraw in fighting crayfish, *Astacus astacus*: the motivational concept revisited. *J Comp Physiol A*, 182(5) pages 573–583, 1998. DOI 10.1007/s003590050204. 157
- ³⁰³ D. Voet, J.G. Voet, and C.W. Pratt. *Fundamentals of biochemistry*. Number QD415 V63. Wiley New York, 2002. 157
- ³⁰⁴ K. Mazák, V. Dóczy, J. Kökösi, and B. Noszál. Proton speciation and microspeciation of serotonin and 5-hydroxytryptophan. *Chem Biodivers*, 6(4) pages 578–590, 2009. DOI 10.1002/cbdv.200800087. 157
- ³⁰⁵ J.H. Jensen and M.S. Gordon. On the number of water molecules necessary to stabilize the glycine zwitterion. *J Am Chem Soc*, 117(31) pages 8159–8170, 1995. DOI 10.1021/ja00136a013. 159
- ³⁰⁶ F. Weigend. Hartree-fock exchange fitting basis sets for H to Rn. *J Comput Chem*, 29(2) pages 167–175, 2008. 161
- ³⁰⁷ F. London. Théorie quantique des courants interatomiques dans les combinaisons aromatiques. *Phys Radium*, 397(8), 1937. 162
- ³⁰⁸ R. Ditchfield. Molecular orbital theory of magnetic shielding and magnetic susceptibility. *The Journal of Chemical Physics*, 56(11) pages 5688–5691, 1972. 162

- ³⁰⁹ T. Helgaker, M. Jaszuński, and K. Ruud. Ab initio methods for the calculation of NMR shielding and indirect spin-spin coupling constants. *Chemical Reviews*, 99(1) pages 293–352, 1999. 162
- ³¹⁰ J. Li and B.M. Christensen. Effect of pH on the oxidation pathway of dopamine and dopa. *J Electroanal Chem*, 375(1-2) pages 219–231, 1994. DOI 10.1016/0022-0728(94)03389-7. 171
- ³¹¹ P. Šolmajer, D. Kocjan, and T. Šolmajer. Conformational study of catecholamines in solution. *Zeitschrift für Naturforschung C*, 38(9-10) pages 758–762, 1983. DOI 10.1515/znc-1983-9-1016. 178
- ³¹² H. Furukawa, T. Hamada, M.K. Hayashi, T. Haga, Y. Muto, H. Hirota, S. Yokoyama, K. Nagasawa, and M. Ishiguro. Conformation of ligands bound to the muscarinic acetylcholine receptor. *Mol Pharmacol*, 62(4) pages 778–787, 2002. DOI 10.1124/mol.62.4.778. 179
- ³¹³ R.D. Tocher and J.S. Craigie. Enzymes of marine algae: II. isolation and identification of 3-hydroxytyramine as the phenolase substrate in *Monostroma fuscum*. *Can J Bot*, 44(5) pages 605–608, 1966. DOI 10.1139/b66-072. 180
- ³¹⁴ K.L. Van Alstyne, A.V. Nelson, J.R. Vyvyan, and D.A. Cancilla. Dopamine functions as an antiherbivore defense in the temperate green alga *Ulvaria obscura*. *Oecologia*, 148(2) pages 304–311, 2006. DOI 10.1007/s00442-006-0378-3. 180
- ³¹⁵ Y.R. Vázquez, K.L. Van Alstyne, and B.L. Bingham. Exudates of the green alga *Ulvaria obscura* (Kützinger) affect larval development of the sand dollar *Dendraster excentricus* (eschscholtz) and the pacific oyster *Crassostrea gigas* (thunberg). *Mar Biol*, 164(10) page 194, 2017. DOI 10.1007/s00227-017-3228-4. 180

- ³¹⁶ K.L. Van Alstyne, E.L. Harvey, and M. Cataldo. Effects of dopamine, a compound released by the green-tide macroalga *Ulvaria obscura* (Chlorophyta), on marine algae and invertebrate larvae and juveniles. *Phycologia*, 53(2) pages 195–202, 2014. DOI 10.2216/13-237.1. 180
- ³¹⁷ N.-h. Ye, X.-w. Zhang, Y.-z. Mao, C.-w. Liang, D. Xu, J. Zou, Z.-m. Zhuang, and Q.-y. Wang. ‘green tides’ are overwhelming the coastline of our blue planet: taking the world’s largest example. *Ecol Res*, 26(3) pages 477–485, 2011. DOI 10.1007/s11284-011-0821-8. 180
- ³¹⁸ A.V. Oleskin and A.L. Postnov. Neurotransmitters as communicative agents in aquatic ecosystems. *Moscow Univ Biol Sci Bull*, 77(1) pages 6–12, 2022. DOI 10.3103/S0096392522010035. 181
- ³¹⁹ B. Borowsky, N. Adham, K.A. Jones, R. Raddatz, R. Artymyshyn, K.L. Ogozalek, M.M. Durkin, P.P. Lakhlani, J.A. Bonini, S. Pathirana, et al. Trace amines: identification of a family of mammalian g protein-coupled receptors. *PNAS*, 98(16) pages 8966–8971, 2001. DOI 10.1073/pnas.151105198. 186
- ³²⁰ A. Durant, E. Khodikian, and C.S. Porteus. Ocean acidification alters foraging behaviour in dungeness crab through impairment of the olfactory pathway. *Global Change Biology*, 2023. DOI 10.1111/gcb.16738. 187
- ³²¹ J.C. Reijenga, L.G. Gagliardi, and E. Kenndler. Temperature dependence of acidity constants, a tool to affect separation selectivity in capillary electrophoresis. *J Chromatogr A*, 1155(2) pages 142–145, 2007. DOI 10.1016/j.chroma.2006.09.084. 188

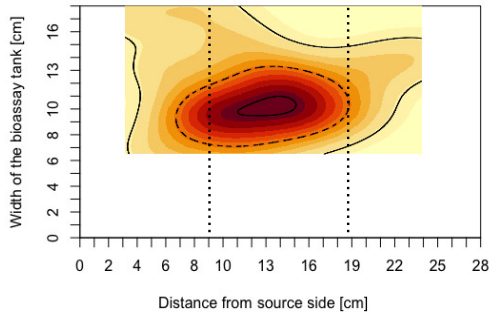
Supplementary

Movement Pattern of Hermit Crabs in Response to PEA

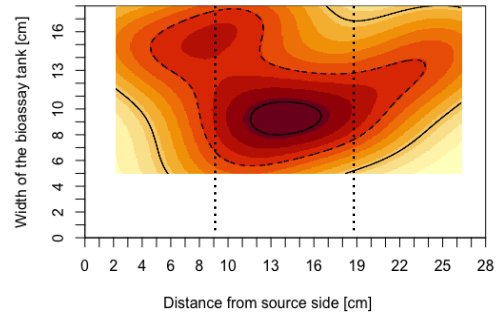
Fig. S1-S2 show that the virtual tank division into thirds, as used for the analysis of ‘first insights’ into the response of hermit crabs to PEA (section 2.3.1), can adequately reflect the response of hermit crabs, as the hermit crabs’ most likely average position can shift from the third closest or furthest away from the cue (Fig. S1H compared with Fig. S2H).

Heatmaps of the response of hermit crabs to PEA indicate sex- and pH -specific patterns. Males seem to react more strongly than females, whereby the most notable response is the attraction of male hermit crabs to PEA at pH 7.7 (Fig. S2H). Thereby, the average distance to the PEA source (x-axis) is significantly shorter than in the respective control experiment (Wilcoxon signed rank test, $V=127$, $p^*=0.037$).

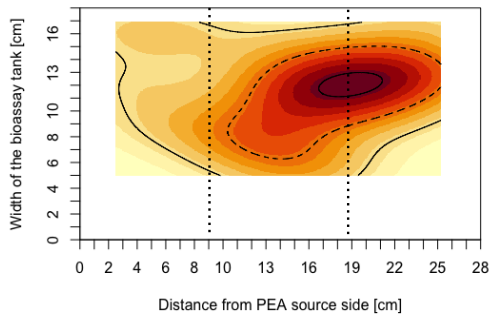
A - Control Female



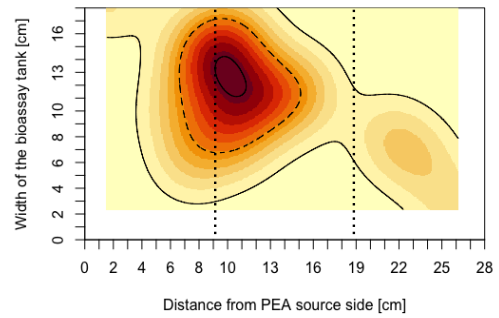
B - Control Male



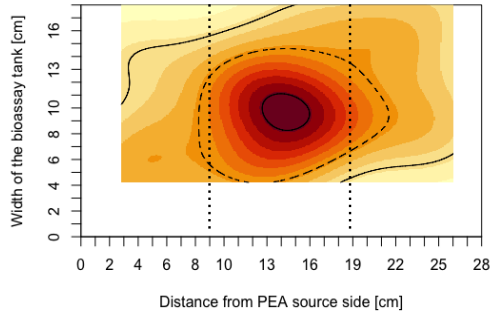
C - PEA 3 10⁻⁵ M Female



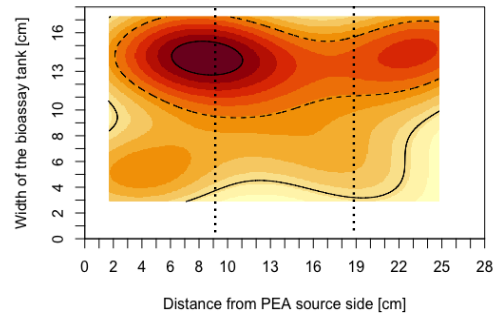
D - PEA 3 10⁻⁵ M Male



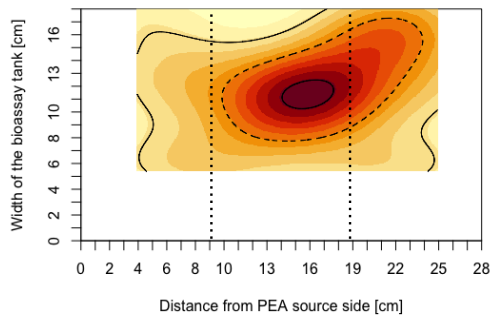
E - PEA 3 10⁻⁴ M Female



F - PEA 3 10⁻⁴ M Male



G - PEA 3 10⁻³ M Female



H - PEA 3 10⁻³ M Male

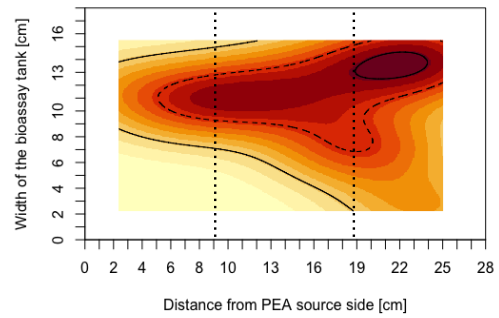
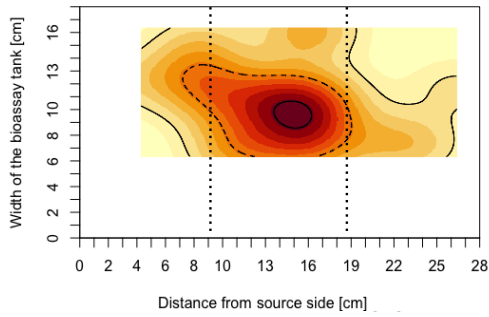


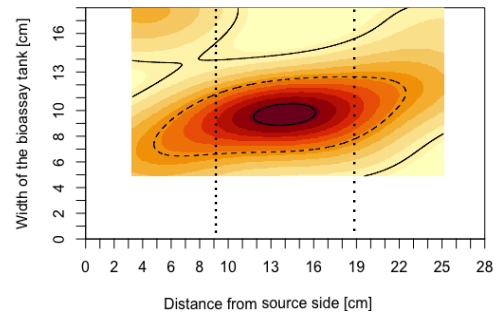
Fig. S1: Heatmaps of combined spatial response of hermit crabs to PEA at pH 8.1. (Full caption on the following page.)

Fig. S1: (Continued from previous page.) The combined spatial distribution of the hermit crabs' likelihood of average position within the tank at pH 8.1 in response to PEA at different concentrations (rows) and divided by sex (columns). N=20 for females and N=18 for males. The density distribution is plotted in a gradient from yellow (low) to dark red (high) with the solid outer contour line representing the 95% density level, the dashed line the 50% mark and the inner solid line is the 5% density level. The likelihood distribution was calculated only within the range of the x-y-coordinates actually taken by hermit crabs for each condition, which accounts for the blank areas within the tank. The dotted lines visualise the virtual tank division into thirds from the previous set of experiments ('first insights', see Fig. 2.1).

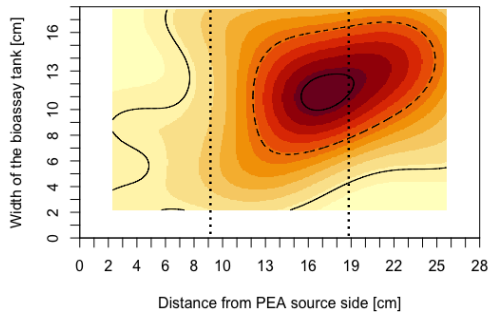
A - Control Female



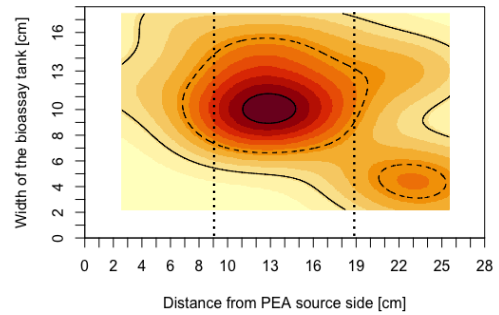
B - Control Male



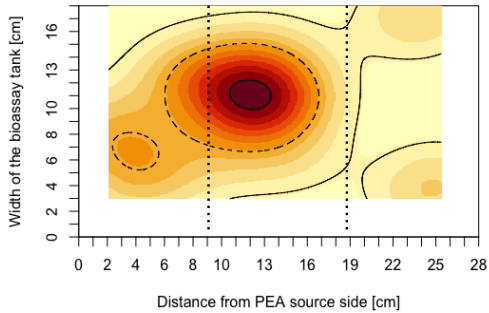
C - PEA 3 10⁻⁵ M Female



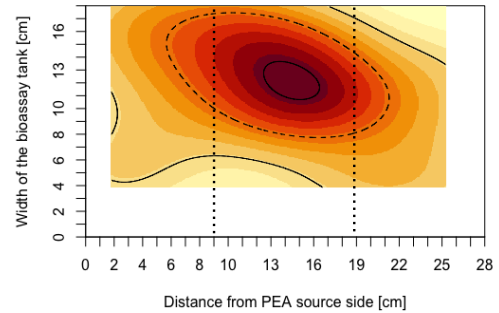
D - PEA 3 10⁻⁵ M Male



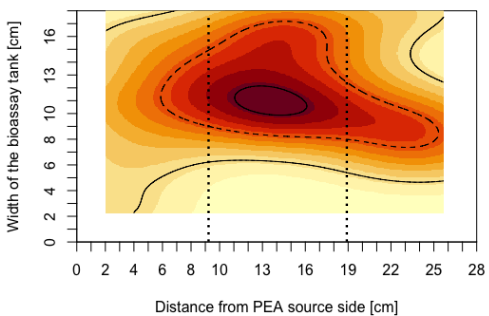
E - PEA 3 10⁻⁴ M Female



F - PEA 3 10⁻⁴ M Male



G - PEA 3 10⁻³ M Female



H - PEA 3 10⁻³ M Male

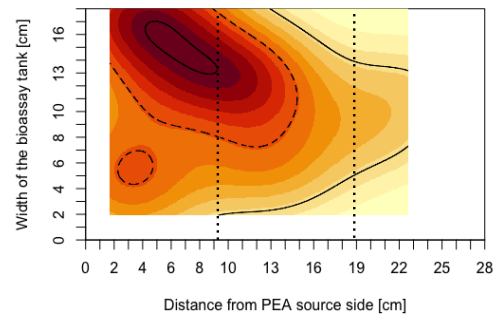


Fig. S2: Heatmaps of combined spatial response to PEA at pH 7.7. (Full caption on the following page.)

Fig. S2: (Continued from previous page.) The combined spatial distribution of the hermit crabs' likelihood of average position within the tank at pH 7.7 in response to PEA at different concentrations (rows) and divided by sex (columns). N=20 for females and N=18 for males. The density distribution is plotted in a gradient from yellow (low) to dark red (high) with the solid outer contour line representing the 95% density level, the dashed line the 50% mark and the inner solid line is the 5% density level. The likelihood distribution was calculated only within the range of the x-y-coordinates actually taken by hermit crabs for each condition, which accounts for the blank areas within the tank. The dotted lines represent the into thirds from the previous set of experiments ('first insights', see Fig. 2.1).

Further Locomotion-related Measures of Hermit Crab

Assays with PEA

The movement pattern of hermit crabs and shore crabs was analysed using the behaviour tracking software LoliTrack, which computes several locomotion-related parameters. Using the software for the first time in the context of the response to PEA (chapter 2), I had to determine which variables might best reflect the response of hermit crabs to PEA. As the first insights experiments (section 2.3.1) suggested a dose-dependent attraction to PEA, I focused on the average position of animals inside the experimental tank, distance travelled, average acceleration and active time.

Whilst the average position inside the experimental tank best reflects the previous variable (percentage of time near PEA, see section 2.3.1), the other three variables focus on changes in excitement or search behaviour. Fig. S3 - S5 visualise that there is no evidence that the pH, PEA concentration or sex of the hermit crabs affects the distance travelled, average acceleration or active time. Hence, the data was not considered for further analysis.

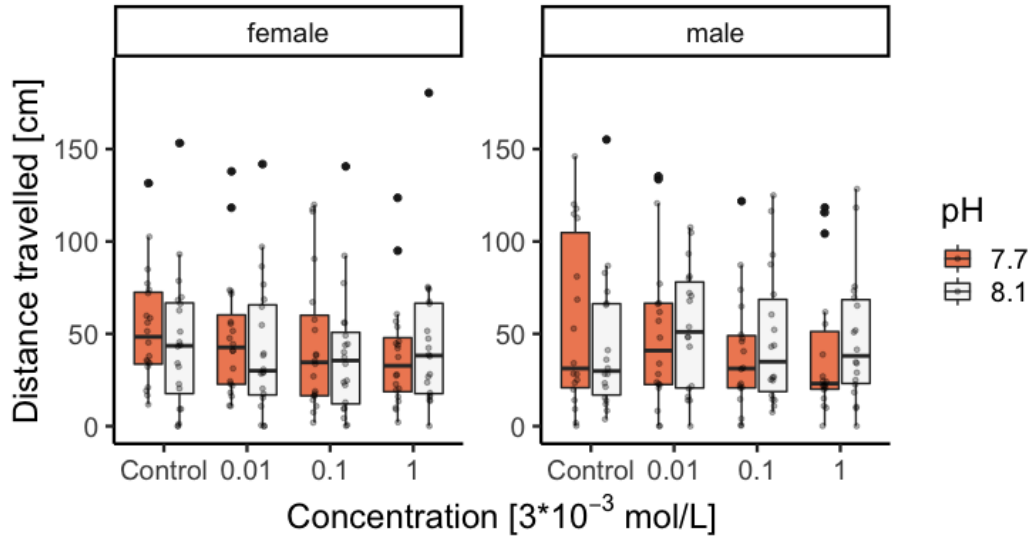


Fig. S3: Distance travelled by hermit crabs during experimental assay in static water conditions in response to different pH conditions and concentrations of PEA.

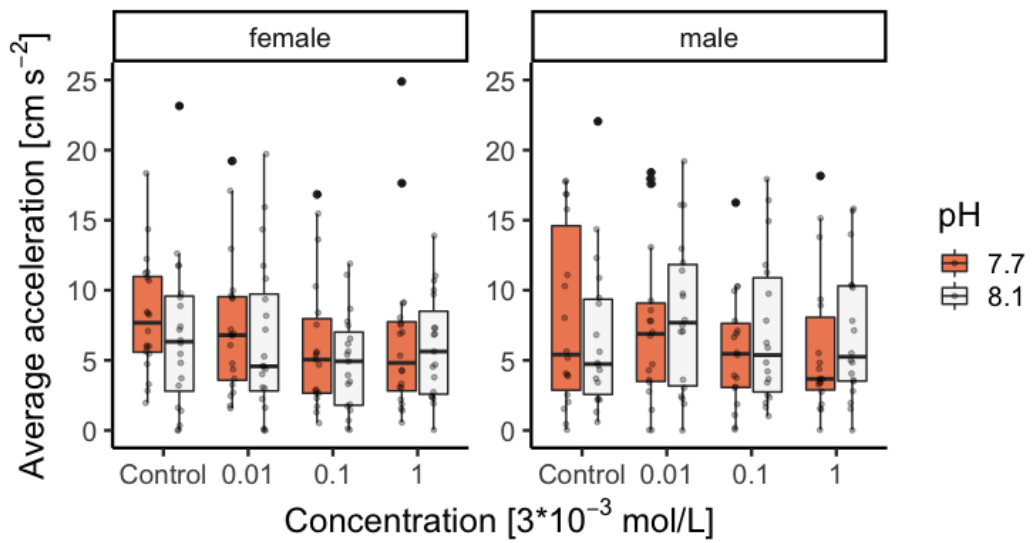


Fig. S4: Average acceleration of hermit crabs during experimental assay in static water conditions in response to different pH conditions and concentrations of PEA.

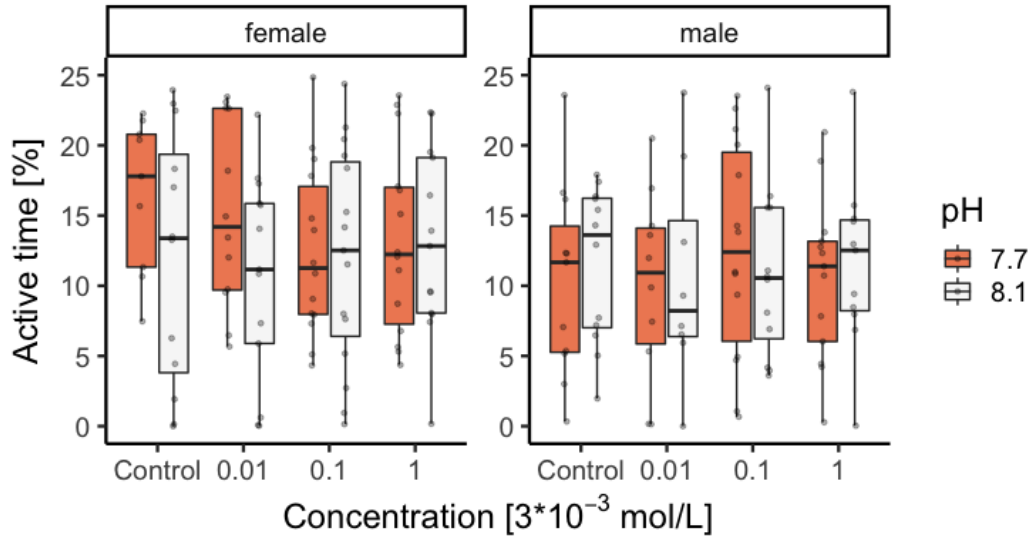
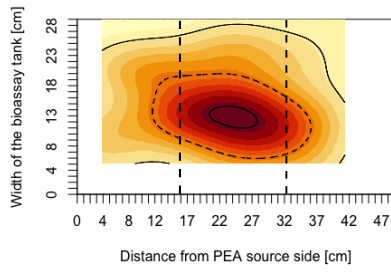


Fig. S5: Percentage of bioassay time spent active/moving by hermit crabs during experimental assay in static water conditions in response to different pH conditions and concentrations of PEA.

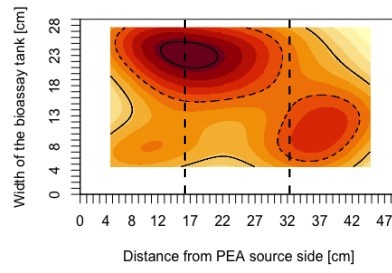
Movement Pattern of Shore Crabs in Response to PEA

Heatmaps of the movement patterns of shore crabs in response to different concentrations of PEA give indication for pH- and sex- dependent response (Fig. S9-S10). The division of the response, as indicated by distinct hotspots of the average position, suggests that a physiological characteristic other than the animals' sex affects its response to PEA.

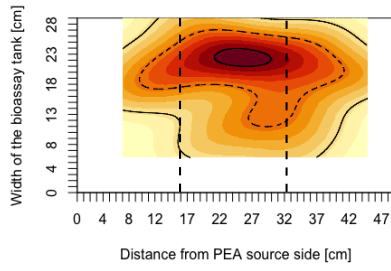
A - control female



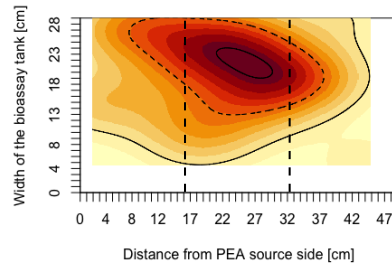
B - control male



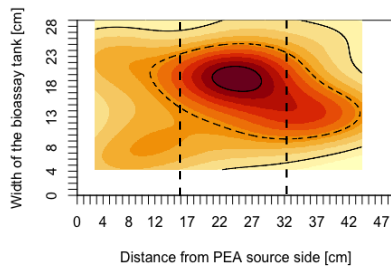
C - PEA 3 10⁻⁵ M female



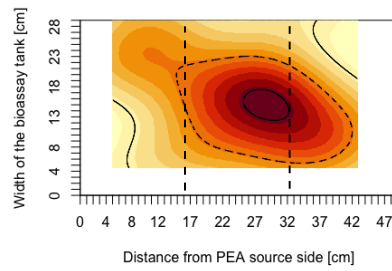
D - PEA 3 10⁻⁵ M male



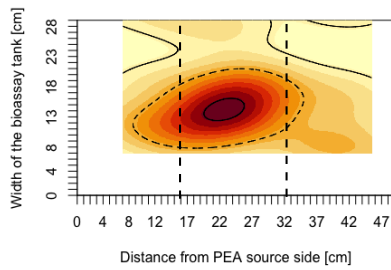
E - PEA 3 10⁻⁴ M female



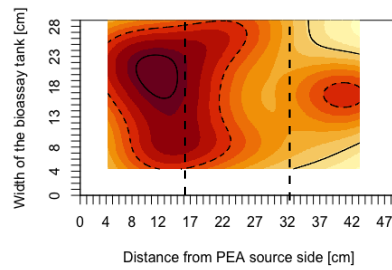
F - PEA 3 10⁻⁴ M male



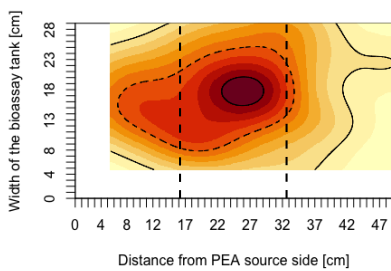
G - PEA 3 10⁻³ M female



H - PEA 3 10⁻³ M male



I - PEA 3 10⁻² M female



J - PEA 3 10⁻² M male

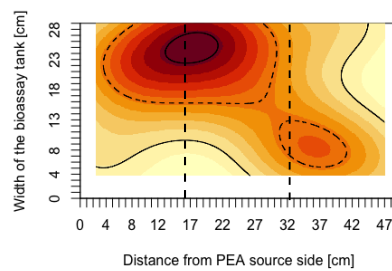
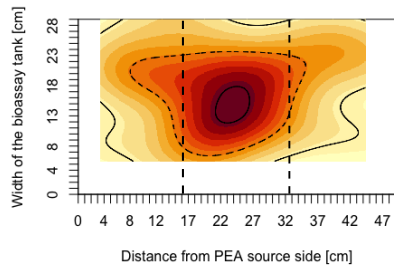


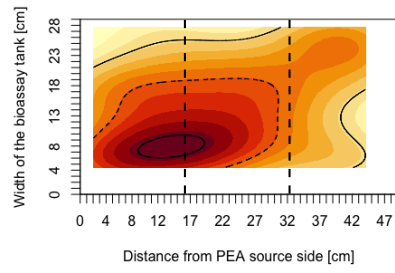
Fig. S6: Heatmaps of combined spatial response of shore crabs to PEA at pH 8.1. (Full caption on the following page.)

Fig. S6: (Continued from previous page.) The combined spatial distribution of the shore crabs' likelihood of average position within the tank at pH 8.1 in response to PEA at different concentrations (rows) and divided by sex (columns). $N=24$ for females and males respectively. The density distribution is plotted in a gradient from yellow (low) to dark red (high) with the solid outer contour line representing the 95% density level, the dashed line the 50% mark and the inner solid line is the 5% density level. The likelihood distribution was calculated only within the range of the x-y-coordinates actually taken by shore crabs for each condition, which accounts for the blank areas within the tank. The dotted lines represent the virtual tank division into thirds (see Fig. 2.1).

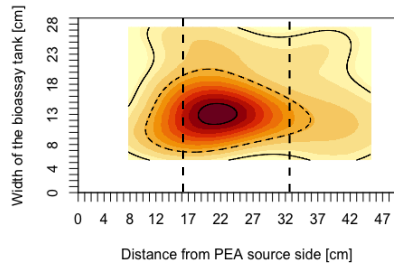
A - control female



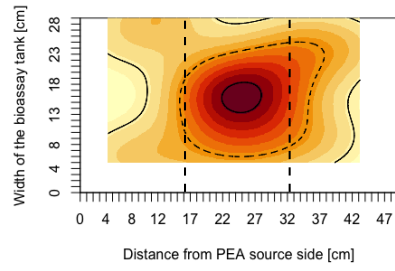
B - control male



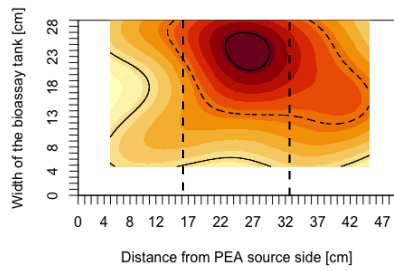
C - PEA 3 10⁻⁵ M female



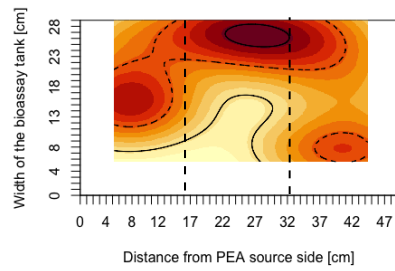
D - PEA 3 10⁻⁵ M male



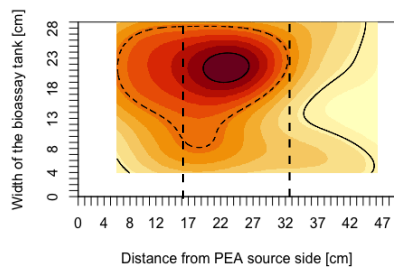
E - PEA 3 10⁻⁴ M female



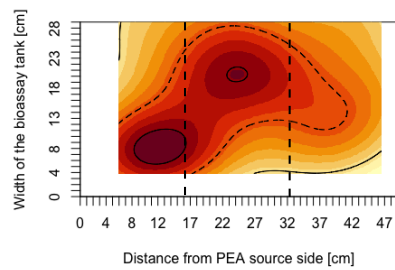
F - PEA 3 10⁻⁴ M male



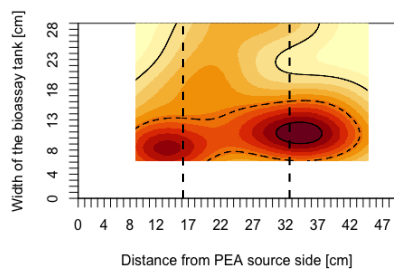
G - PEA 3 10⁻³ M female



H - PEA 3 10⁻³ M male



I - PEA 3 10⁻² M female



J - PEA 3 10⁻² M male

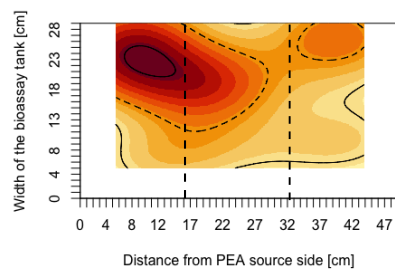


Fig. S7: Heatmaps of combined spatial response of shore crabs to PEA at pH 7.7. (Full caption on the following page.)

Fig. S7: (Continued from previous page.) The combined spatial distribution of the shore crabs' likelihood of average position within the tank at pH 7.7 in response to PEA at different concentrations (rows) and divided by sex (columns). $N=24$ for females and males respectively. The density distribution is plotted in a gradient from yellow (low) to dark red (high) with the solid outer contour line representing the 95% density level, the dashed line the 50% mark and the inner solid line is the 5% density level. The likelihood distribution was calculated only within the range of the x-y-coordinates actually taken by shore crabs for each condition, which accounts for the blank areas within the tank. The dotted lines represent the virtual tank division into thirds (see Fig. 2.1).

Relationship between Weight and Claw Length in Shore Crabs

To further explore the relationship between weight and claw length of shore crabs, I plotted the weight against claw length, as well as the new measure weight/claw length ratio against weight and against claw length (Fig. S8). There is a positive relationship between weight and claw length (Pearson's correlation, $cor=0.88$, $p^{***}<0.001$, Fig. S8A), which translates to a strong positive relationship between weight and the weight/claw length ratio (Pearson's correlation, $cor=0.92$, $p^{***}<0.001$, Fig. S8B), whilst the correlation of claw length and weight/claw length ratio is weaker (Pearson's correlation, $cor=0.66$, $p^{***}<0.001$, Fig. S8B).

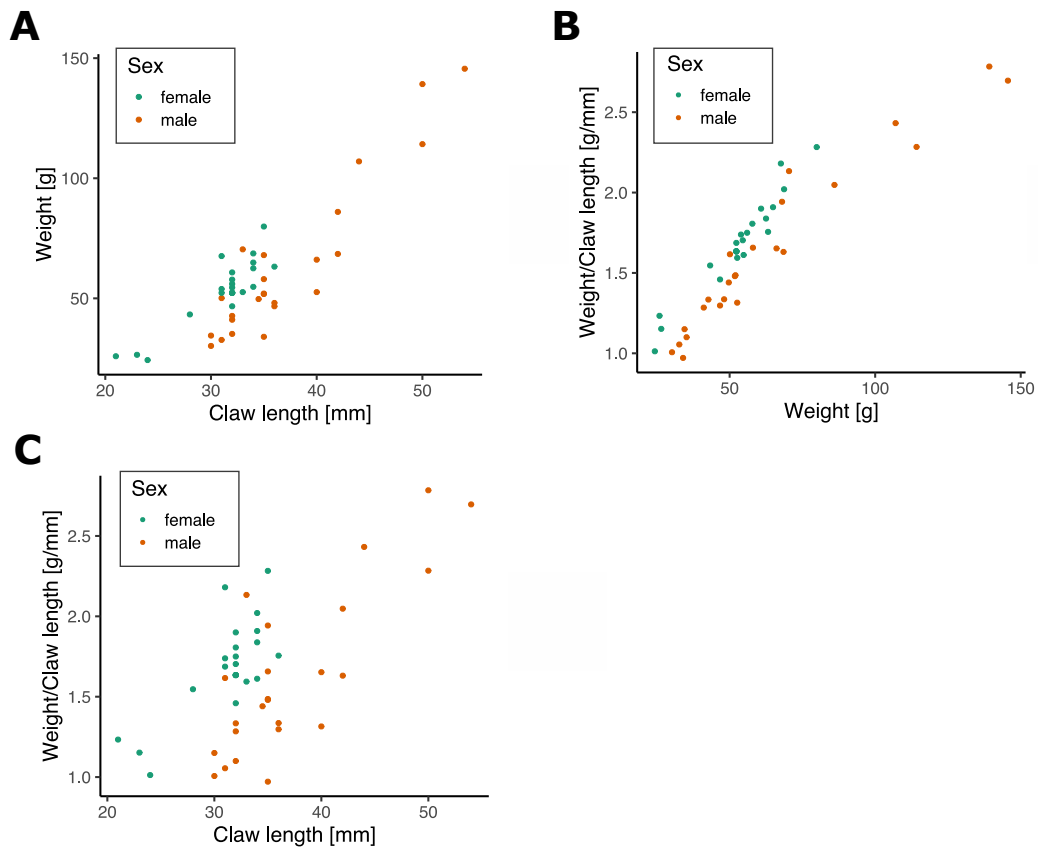


Fig. S8: Weight and claw length in female and male shore crabs. (A) shows the positive relationship of weight and claw length. (B) relates the new measure weight/ claw length ratio to the shore crab weight, whilst (C) relates it to the claw length.

Movement Pattern of Hermit Crabs in Response to Dopamine

Heatmaps of the movement patterns of hermit crabs in response to different concentrations of dopamine give no indication of sex-, pH or concentration-dependent differences (Fig. S9-S10).

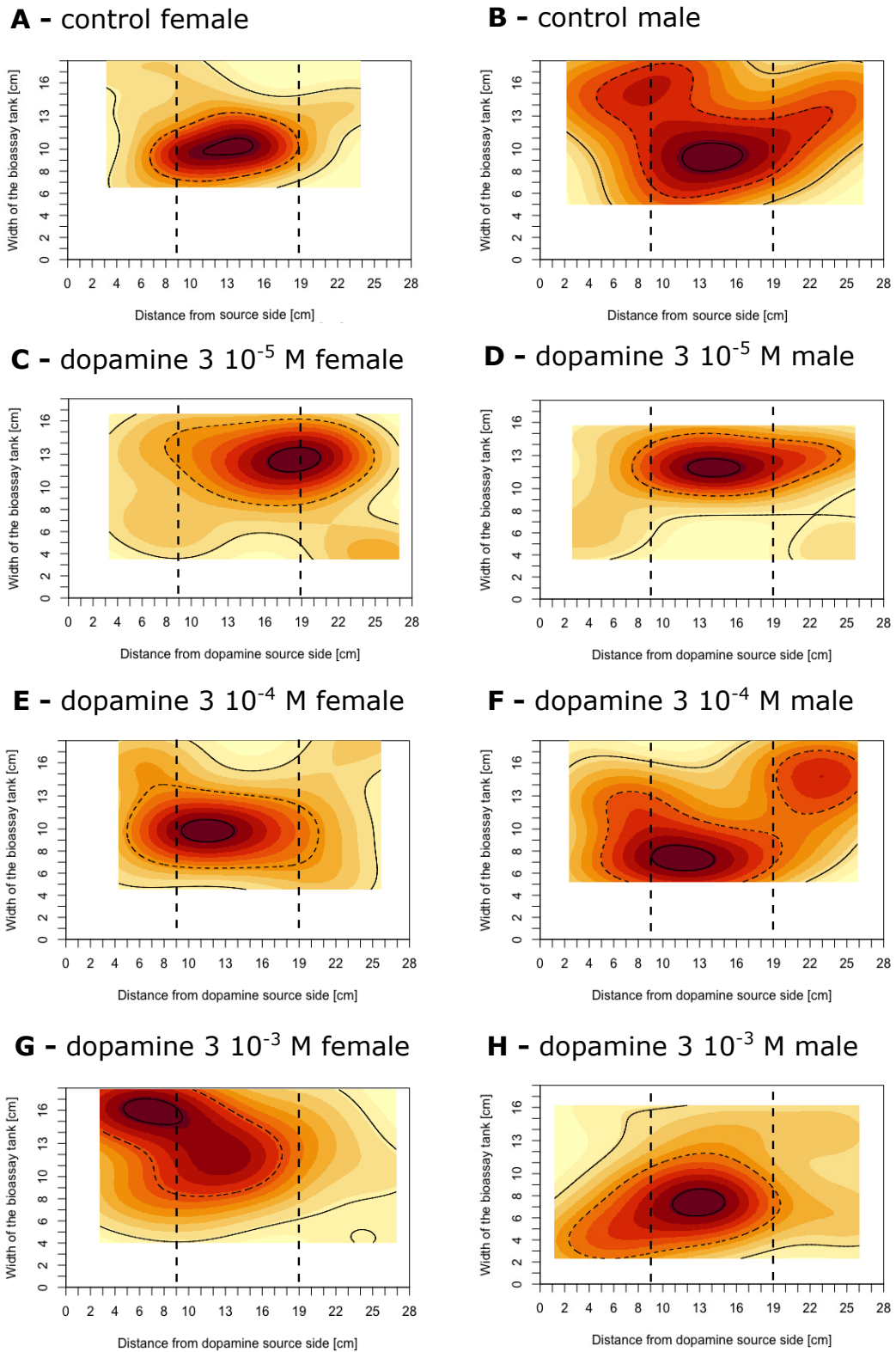
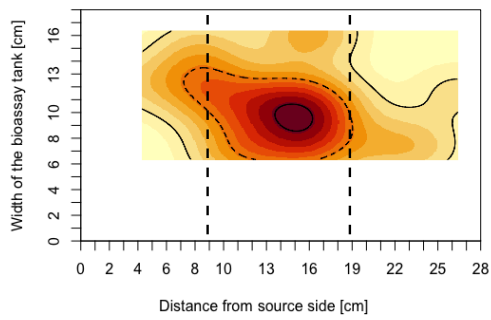


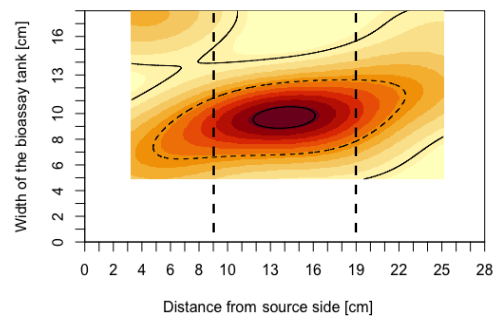
Fig. S9: Heatmaps of combined spatial response of hermit crabs to dopamine at pH 8.1. (Full caption on the following page.)

Fig. S9: (Continued from previous page.) The combined spatial distribution of the hermit crab's likelihood of average position within the tank at pH 8.1 in response to dopamine at different concentrations (rows) and divided by sex (columns). $N=20$ for females and $N=18$ for males. The density distribution is plotted in a gradient from yellow (low) to dark red (high) with the solid outer contour line representing the 95% density level, the dashed line is the 50% mark and the inner solid line is the 5% density level. The likelihood distribution was calculated only within the range of the x-y-coordinates actually taken by hermit crabs for each condition, which accounts for the blank areas within the tank. The dotted lines represent the virtual tank division into thirds (see Fig. 2.1).

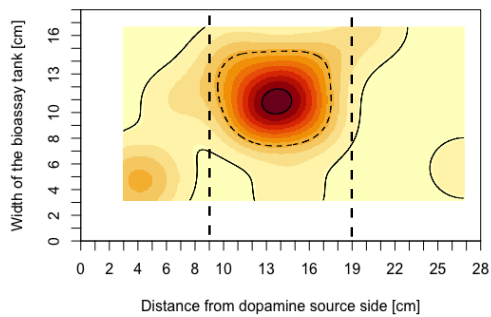
A - control female



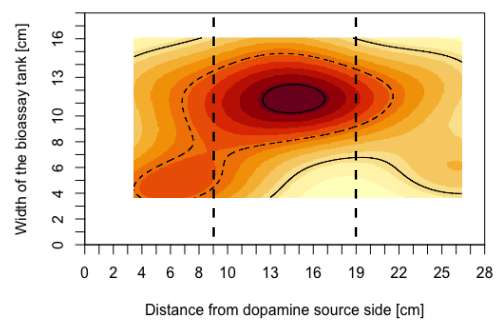
B - control male



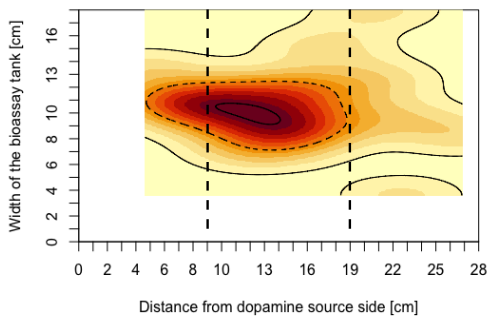
C - dopamine 3×10^{-5} M female



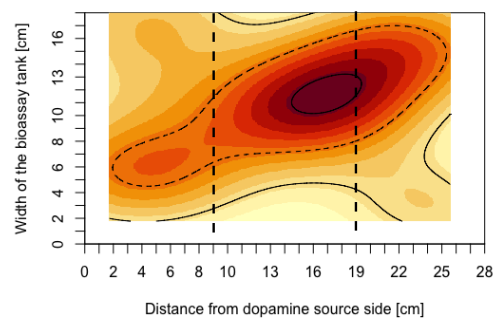
D - dopamine 3×10^{-5} M male



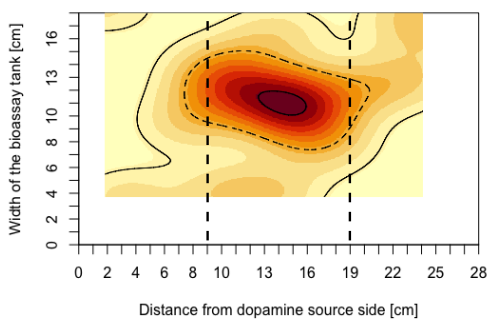
E - dopamine 3×10^{-4} M female



F - dopamine 3×10^{-4} M male



G - dopamine 3×10^{-3} M female



H - dopamine 3×10^{-3} M male

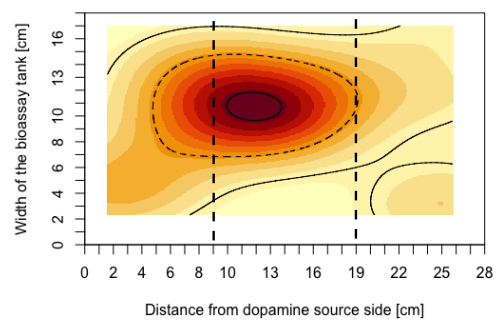


Fig. S10: Heatmaps of combined spatial response of hermit crabs to dopamine at pH 7.7. (Full caption on the following page.)

Fig. S10: (Continued from previous page.) The combined spatial distribution of the hermit crab's likelihood of average position within the tank at pH 7.7 in response to dopamine at different concentrations (rows) and divided by sex (columns). N=20 for females and N=18 for males. The density distribution is plotted in a gradient from yellow (low) to dark red (high) with the solid outer contour line representing the 95% density level, the dashed line is the 50% mark and the inner solid line is the 5% density level. The likelihood distribution was calculated only within the range of the x-y-coordinates actually taken by hermit crabs for each condition, which accounts for the blank areas within the tank. The dotted lines represent the virtual tank division into thirds (see Fig. 2.1).

Further Locomotion-related Measures of Hermit Crab

Assays with Dopamine

Similarly to the distance travelled, average acceleration and active time of hermit crabs in response to PEA in static water conditions (see Fig. S3-S5), the hermit crabs' response to dopamine also shows no significant concentration-, sex- or pH-dependent changes in response to dopamine. Although Fig. S11-S13 indicate a small trend for less mobility of female hermit crabs with increasing concentrations of dopamine, which is reflected across all three variables (distance travelled, average acceleration, active time), there is not sufficient statistical evidence to support this observation.

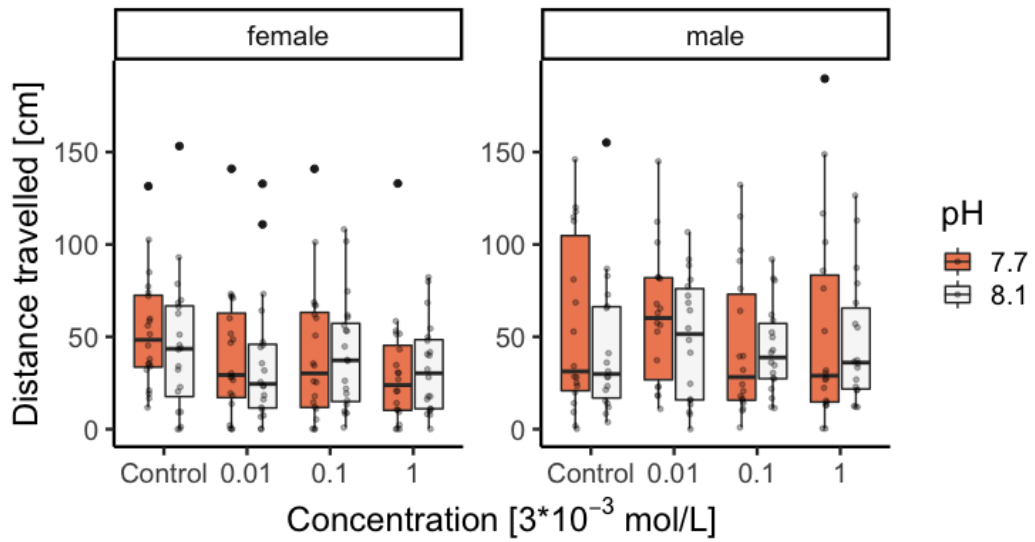


Fig. S11: Distance travelled by hermit crabs during experimental assay in static water conditions in response to different pH conditions and concentrations of dopamine.

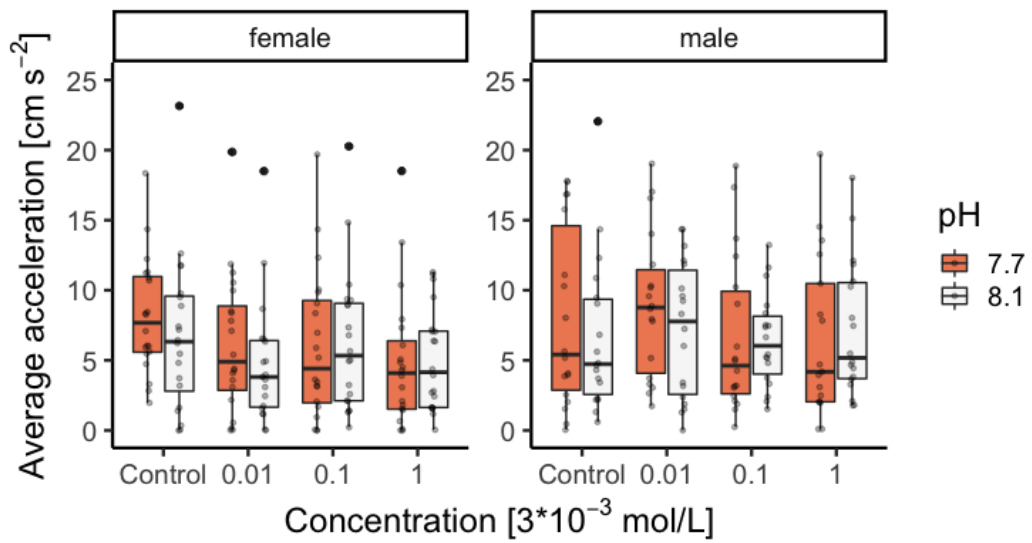


Fig. S12: Average acceleration of hermit crabs during experimental assay in static water conditions in response to different pH conditions and concentrations of dopamine.

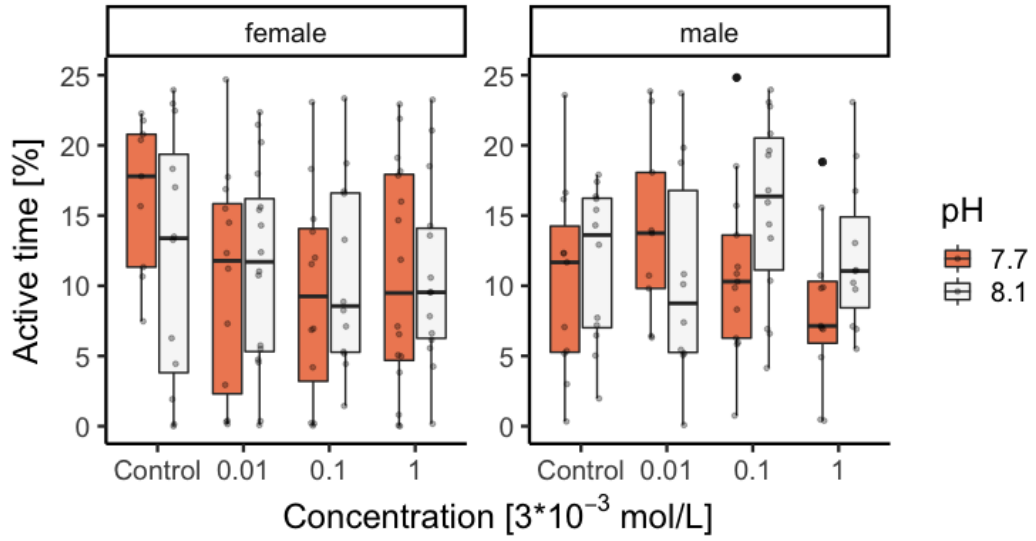


Fig. S13: Percentage of bioassay time spent active/moving by hermit crabs during experimental assay in static water conditions in response to different pH conditions and concentrations of dopamine.